Université de Strasbourg

École Doctorale des Sciences de la Vie et de la Santé STRASBOURG

ÉCOLE DOCTORALE DES SCIENCES DE LA VIE ET DE LA SANTÉ

IGBMC, UMR 7104/U1258

THÈSE présentée par :

Théo HECQUET

soutenue le : 29 novembre 2024

pour obtenir le grade de : **Docteur de l'université de Strasbourg**

Discipline/Spécialité : Biologie cellulaire et moléculaire

Multiscale characterization of *Caenorhabditis elegans* models of Human cytoplasmic actin variants hints at their pathophysiological mechanisms

THÈSE dirigée par :

Dr. REYMANN Anne-Cécile CR, IGBMC, Strasbourg, France

RAPPORTEURS :

Dr. BERTRAND Vincent DR, IBDM, Marseille, France

Dr. PACQUELET Anne CR, IGDR, Rennes, France

AUTRES MEMBRES DU JURY :

Dr. GODIN Juliette DR, IGBMC, Strasbourg, France

INVITE :

Dr. COLIN Alexandra CR, CEA, Grenoble, France

Table of contents:

Chapter 1: The actin cytoskeleton 12

Chapter introduction - Actin and the cytoskeleton 13

The Actin filaments – Discovery and assembly 14

Actin-binding proteins and actin networks 16

Formins and Filopodium 16

The Arp2/3 complex and lamellipodium 18

Myosin and the actin cortex 20

The G-/F-actin homeostasis, a finely tuned cellular challenge 25

Interlude on human actin isotypes 29

The Cytoplasmic actins 30

Lookalikes from different parents 30

What controls these differences? 33

Chapter conclusion 35

Chapter 2: Non-Muscle Actinopathies 38

Chapter Introduction – The mutated cytoskeleton. 40

Non-Muscle Actinopathies – Discovery and genetic causes 41

Phenotypic variability 43

Hypothesis on actin variant pathogenicity 45

Chapter conclusion 49

Chapter 3: *Caenorhabditis elegans* 52

Chapter introduction 54

A brief history of *C. elegans* 55

Actin in *C. elegans*, state-of-the-art 57

Genetic structure and expression 57

Null variants 60

Isoactin switching 60

C. elegans embryonic development 62

Egg activation, symmetry breaking, and first-cell division 63

Eggshell formation 63

Completion of meiosis 64

Symmetry breaking and polarity establishment 65
Maintenance and the first cell division 67
Gastrulation 69
Ventral enclosure 71
Elongation 73
Bean to 1.8-fold stage 74
1.8 to 4-fold 75
Ready to hatch? 76
Conclusion on the embryonic development of *C. elegans*: 76
Post-embryonic development 77
Nervous system 78
General information on C. elegans' nervous system 78
Neurogenesis 79
Neuronal models of cell migration and asymmetric division - The Q neuroblasts 80
Neuronal models of dendritic process – The PVD neurons 82
Hermaphrodite Gonadogenesis 84
Chapter conclusion 88
Chapter 4: Thesis project and scientific questions 90
Chapter 5: Multiscale characterization of *C. elegans act-2* variants 96
Chapter 6: Neuronal gene expression pattern 98
Introduction and experimental procedure 100
Results 102
Chapter 7: Remaining open questions from phenotypic characterization 110
Chapter introduction 112
Why do two null *act-2* alleles cause different phenotypes? 113
Can we identify the pathophysiological mechanisms of studied actin variants? 119
Actin aggregates 119
Haploinsufficiency 121
Impaired actin dynamics 123

R196H and R196C 123
R147S 125
T203M and T120I 126
L65V 128
Why do we observe such variance in our results? 129
Chapter conclusion 130
Chapter 8: *act-2* as a Human cytoplasmic actin counterpart 132
Chapter Introduction 134
Could *act-2* be an ortholog of ACTB or ACTG1? 134
Protein localization 134
mRNA 139
DNA 140
Correlation with Human actin variants phenotypes 140
Conclusion 140
Are the phenotypes observed in *C. elegans* specific to *act-2*? 141
Chapter conclusion 142
Chapter 9: Conclusion 144

List of abbreviations:

ABP = Actin-Binding Proteins

ADP = Adenosine DiPhosphate

ATP = Adenosine TriPhosphate

BWCFF = Baraitser-Winter cerebrofrontofacial syndrome

DV = Dorsal and Ventral epidermal cells

EMS = Ethyl Methane Sulfonate

F-Actin = Filamentous Actin

FH = Formin-Homology domains

G-Actin = Globular Actin

INDEL = insertion-deletion

LECA = Last Eukaryotic Common Ancestor

LoF = Loss of Function

NMA = Non-Muscle Actinopathies

NPS= Nucleation Promoting Factors

PAR proteins = abnormal embryonic PARtitioning of cytoplasm

PTM = Post-translational modifications

Pi = Inorganic Phosphate

WASP = Wiskott-Aldrich syndrome

WAVE = WASP-family verprolin-homologous

WT = Wild-Type

bp = base pair

List of figures:

Figure 1 : Cytoskeleton organization inside a fibroblast.

Figure 2: Structures of the actin monomer.

Figure 3 : Actin polymerization and recycling cycle.

Figure 4 : Formin-dependent elongation mechanism.

Figure 5: Roles of filopodia.

Figure 6: Arp2/3-dependent actin polymerization.

Figure 7: Actin in lamellipodia.

Figure 8: Myosin movement in relation to actin filaments

Figure 9: Myosin regulation.

Figure 10: The actin cortex.

Figure 11: The contractile ring.

Figure 12: Parameters contributing to bleb formation.

Figure 13: Nuclear actin transport.

Figure 14: The six mammalian actin isoforms.

Figure 15: β and γ actin structures.

Figure 16: Differential localization of ACTB and ACTG1.

Figure 17: Distribution of ACTB and ACTG1 pathogenic variants within Non Muscle Actinopathies.

Figure 18: How an actin variant could impact the association of an actin monomer with an actin-binding protein.

Figure 19: How an actin variant could induce haploinsufficiency.

Figure 20: Actin variant with impaired polymerization dynamics.

Figure 21: Actin variant forming actin rods.

Figure 22: *Caenorhabditis elegans* anatomy.

Figure 23: Sydney Brenner's lineage.

Figure 24: The *act-123* locus.

Figure 25: Nucleotide sequences alignment *act-1, act-2*, and *act-3*.

Figure 26: Amino acid sequences alignment of *C. elegans'* actin proteins.

Figure 27: Embryonic development of *C. elegans* at 22°C.

Figure 28: Schematic of the layers of the *C. elegans* eggshell.

Figure 29: Global contraction model for polar body formation.

Figure 30: Symmetry breaking of the *C. elegans'* zygote.

Figure 31: *C. elegans'* pronuclei migration.

Figure 32: A C. elegans zygote with established anteroposterior polarity.

Figure 33: Timeline of events in the C. elegans early embryo

Figure 34: *C. elegans'* gastrulation

Figure 35: *C. elegans'* ventral cleft closure.

Figure 36: *C. elegans'* ventral enclosure.

Figure 37: *C. elegans* elongation.

Figure 38: Actin during the first stage of *C. elegans'* elongation.

Figure 39: Actin during the second stage of *C. elegans'* elongation.

Figure 40: Life cycle of *C. elegans* at 22°C.

Figure 41: Overall organization of the *C. elegans* nervous system

Figure 42: Examples of asymmetric divisions during neurogenesis

Figure 43: Q progenitors' development.

Figure 44: Mechanisms of Q.p and Q.a asymmetrical division.

Figure 45: The PVD menorah.

Figure 46: The *C. elegans* hermaphrodite gonad.

Figure 47: The *C. elegans* hermaphrodite gonad development.

Figure 48: Proto-rachis formation.

Figure 49: NeuroPAL neural reporters' table.

Figure 50: Neural reporter expression for variants L65V and R196C.

Figure 51: Neural reporter expression for variants G74S, R147S, and *rey021*.

Figure 52: Neural reporter expression for variants T120I and R196H.

Figure 53: Neural reporter expression between variants T120I and R196H.

Figure 54: Schematic *act-2* representation.

Figure 55: Activity-dependent bulk endocytosis pathway.

Figure 56: Muscles of variants L65V and R196H.

Figure 57: ACTB R183W variant in cultured cells.

Figure 58: Single animal RT-qPCR of actin coding genes of variants L65V, R196C, and R196H.

Figure 59: Male pronuclear migration.

Figure 60: Heatmap of phenotypes observed in gonads of homozygotes *act-2* variants.

Figure 61: Actin binding proteins interacting with actin's R147 residue.

Figure 62: Heatmap of phenotypes observed in embryos of homozygotes act-2 variants.

Figure 63: Calmodulin roles in actin regulation.

Figure 64: *act-2*p::GFP::ACT-2 expression.

Figure 65: Progeny number and embryonic lethality of ACT-2$^{\alpha}$, ACT-2$^{\alpha}$; Nb::mKate2, *rey021,* and WT animals.

Figure 66: ACT-2$^{\alpha}$; Nb::mKate2 expression during C. elegans' development.

Figure 67: ACT-2α; Nb::mKate2 is absent in the zygotic contractile ring.

Figure 68: Ribosome profiling of *act-1*, *act-2*, and *act-3*.

Figure 69: Progeny number and embryonic lethality of the T120I variant in different actin isotypes.

Table 1: Summary of mentioned symptoms for ACTB variants R183W, R196C, R196H and R196S.

Table 2: Summary of altered expression pattern for each analyzed actin variant.

Introduction

Chapter 1:
The actin cytoskeleton

Chapter introduction - Actin and the cytoskeleton

Actin is part of the cytoskeleton, an intricate network of filaments within every cell in all three domains of life (Eubacteria, Archae, and Eukaryota) (Wickstead and Gull, 2011). Evolutionary studies suggest that the last eukaryotic common ancestor (LECA) already possessed actin microfilaments (abbreviated as 'filaments', **Figure 1**), one of the cytoskeleton's components (Velle et al., 2024). Actin filaments form complex networks inside all cells thanks to different regulatory proteins. Evolutionary studies show that actin evolved from the LECA with minimal structural changes. However, the loss and addition of actin regulators, as well as the development of actin isotypes through gene duplications, have been crucial for generating phenotypic diversity. Indeed, this allowed the creation of specialized networks associated with specific functions within various cell types (Velle et al., 2024).

In addition to actin, metazoan's cytoskeleton is composed of two other types of filaments: microtubules (Pollard and Goldman, 2018; Borisy et al., 2016; Gudimchuk and McIntosh, 2021; Janke and Magiera, 2020, **Figure 1**) and intermediate filaments (Leduc and Etienne-Manneville, 2015; Sobo et al., 2024, **Figure 1**). While all of these fibers have specific functions associated with particular structures within the cell, they are also known to interact and impact each other's dynamics (Pimm and Henty-Ridilla, 2021; Pradeau-Phélut and Etienne-Manneville, 2024).

Protégé par le droit à l'image
doi: 10.1101/cshperspect.a030288

Figure 1: Cytoskeleton organization.

The Actin filaments – Discovery and assembly

Actin filaments were discovered in 1942 by Ilona Banga and Albert Szent-György by comparing two myosin extracts performed over different durations (Banga and Szent-Györgyi, 1942). The first extract prepared using the typical 20-minute protocol was viscous, whereas one left overnight became gelatinous. The authors realized that they could reversibly change the viscosity of the gelatinous solution by adding adenosine triphosphate (ATP). This observation led them to propose that the second extract contained not only myosin but an additional component, which they called actin (Banga and Szent-Györgyi, 1942). Soon after, Brúnó F. Straub purified actin and realized that this protein exists in two forms: monomeric, or globular, and polymerized, or filamentous (Straub, 1942; Straub, 1943). He respectively named them G-Actin and F-Actin, nomenclatures we still use today.

In most cells, actin is the most abundant protein, present in the µM order of magnitude (Pollard, 2016; Pollard et al., 2000), co-existing in its globular and filamentous states. Actin proteins oscillate between these two forms, as actin filaments are highly dynamic, with a rapid turnover rate on the scale of tens of seconds *in vivo* (Pollard, 2016). The monomeric form of actin (G-actin) is a small (42kDa) ATPase of weak activity composed of four subdomains surrounding the nucleotide-binding cleft that can additionally bind the cations Mg^{2+} or Ca^{2+} (**Figure 2**, Oosterheert et al., 2022; Pollard, 2016). Because of the monomers' structure, the actin filament is polar, exhibiting a fast-growing barbed end (or '+' end) and a slow-growing pointed end (or '–' end) (Pollard, 2016).

Protégé par le droit à l'image
doi: 10.1101/cshperspect.a018226

Figure 2: Structures of the actin monomer.

Actin polymerization into filaments (F-Actin) requires three distinct steps: nucleation, stabilization, and elongation. The *de novo* nucleation of an actin filament is unfavorable. Indeed, during this process, ATP-bound G-Actin is assumed to form a trimer called a seed or nucleus (**FIGURE 3**). However, seeds are unstable and dissociate rapidly (POLLARD, 2016). Therefore, their formation is often helped by actin-binding proteins (ABP, see 'ACTIN BINDING PROTEINS AND ACTIN NETWORKS').

The second step of polymerization involves stabilizing this nucleus by adding a fourth actin monomer. This initiates elongation, where G-Actins rapidly add to the stabilized nucleus (**FIGURE 2**). Of importance, these actin subunits are mostly bound to ATP as they have a 3-fold higher association constant than adenosine diphosphate- (ADP) bound G-actins (POLLARD ET AL., 2000). Upon polymerization, the actin subunits slightly change their conformations, which increases their ATPase activity, leading to the hydrolyzation of ATP into ADP and inorganic phosphate (Pi) in a scale of seconds (BLANCHOIN AND POLLARD, 2002). This again changes the subunits' conformations, slightly weakening their interactions with each other. Therefore, ADP-bound actin is less stable and more prone to depolymerization than ATP-bound actin (POLLARD ET AL., 2000). Then, the inorganic phosphate is slowly released. Consequently, the + end is enriched in ATP-bound subunits, the – end in ADP-bound subunits, while ADP+Pi-bound subunits are present along the filament (POLLARD, 2016). Depolymerization can happen spontaneously by the dissociation of monomers, preferentially at the minus end, or with the help of actin-severing proteins. The resulting free ADP-bound G-Actins are then recycled into ATP-bound monomers that are thus able to be incorporated again into filaments (**FIGURE 3**).

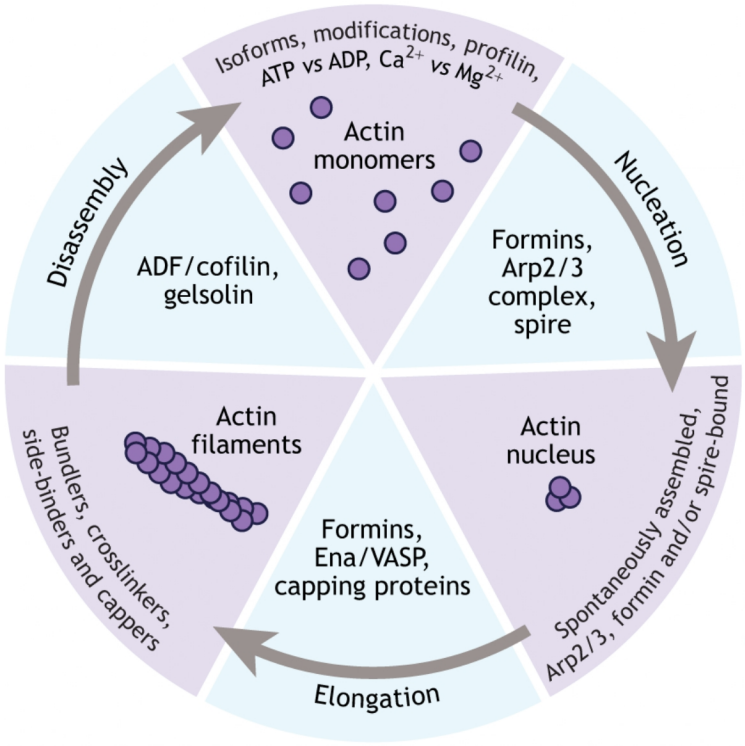

Figure 3: Actin polymerization and recycling cycle. Figure and legend extracted from Velle et al., 2024.

Actin-binding proteins and actin networks

Actin dynamics are tightly regulated by actin-binding proteins (ABP). To date, 357 genes encode for proteins observed in human actin filaments (THE HUMAN CELL IN ACTIN FILAMENTS - THE HUMAN PROTEIN ATLAS, accessed on 02.09.2024), and 2482 human proteins have been predicted as putative actin-associating proteins (MEENAKSHI S ET AL., 2023). Based on their functions, ABPs are grouped into seven families: monomer-binding, severing, nucleating, filament polymerases, capping, crosslinking, and filament binding (POLLARD, 2016). These proteins can either promote or impair nucleation, elongation, or both and induce specific filament structural changes (**FIGURE 3**, POLLARD, 2016). ABPs work altogether *in vivo* to build dynamic actin networks of different architectures, turnover, and mechano-properties. This dynamic regulation enables the cell to rapidly respond to internal and external cues and undergo physiological processes (POLLARD, 2016).

Formins and Filopodium

Formins are a family of proteins that play a crucial role in actin filament assembly. Formins are mostly known to catalyze filament elongation as well as promote nucleation, although some isoforms have been shown to depolymerize, sever, or bundle filaments (PALMER ET AL., 2024). Formins are dimers composed of two conserved Formin-Homology domains (FH1 and FH2). Their FH2 domains form a ring-like structure that attaches to the barbed end of an actin filament. The FH1 domains of formin are more flexible and form “tentacle-like” structures. The precise mechanism behind Formin-mediated elongation is under debate. A current model by Palmer and colleagues proposes that FH1 domains bind profilin-associated G-Actin to bring it close to the filament for polymerization (PALMER ET AL., 2024). Upon addition of the subunit, formin would move toward the filament’s new barbed end to repeat this cycle (**FIGURE 4**).

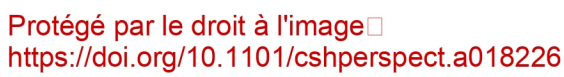

Figure 4: Formin-dependent elongation mechanism.

Certain formins can reliably add tens of subunits per second onto the filament, quickly resulting in linear actin polymers (PALMER ET AL., 2024).

Formin-dependent linear filaments are notably found in filopodia. Filopodia are polar, tubular, “finger-like” protrusions primarily present at the migratory cell's leading edge that deform the plasma membrane due to their elongation toward the cell’s “exterior” (**FIGURE 5**, BLANCHOIN ET AL., 2014). Filopodia can vary in length, depending on the cell type and organism, ranging from a few micrometers to tens of micrometers (MATTILA AND LAPPALAINEN, 2008). They are notably known to be able to interact with the cell’s environment, helping directed cell migration or neurite growth (**FIGURE 5A & 5C**, BLANCHOIN ET AL., 2014; MATTILA AND LAPPALAINEN, 2008) and are also implicated in cell-cell adhesion (**FIGURE 5B**, MATTILA AND LAPPALAINEN, 2008). Actin filaments inside filopodia are maintained tightly together by actin-bundling proteins such as fascin. This bundling is essential for forming and maintaining filopodia as well as providing the mechanical resistance needed to face the extracellular environment.



Figure 5: Roles of filopodia.

The Arp2/3 complex and lamellipodium

Contrary to polymerizing linear filaments, the Arp2/3 complex (abbreviated as 'Arp2/3') mediates actin branching. The Arp2/3 complex comprises seven subunits; five serve as scaffolds to bind to the mother filament, and two (Arp2 and Arp3) closely resemble G-Actin (POLLARD, 2016). In its resting state, Arp2/3 is physiologically inactive. The complex needs to be activated by Nucleation Promoting Factors (NPFs) such as the Wiskott-Aldrich syndrome (WASP) or the WASP-family verprolin-homologous (WAVE) family of proteins (TAKENAWA AND SUETSUGU, 2007). Indeed, NPFs allow the complex to undergo a conformational change, bringing Arp2 and Arp3 closer (**FIGURE 6**). Then, NPFs deliver the first actin monomers to the complex. Finally, NPFs promote the complex's binding to a pre-existing filament, which mimics a seed to form a new filament (**FIGURE 6**, GAUTREAU ET AL., 2022). Branches can then be stabilized by a specialized protein called cortactin (GAUTREAU ET AL., 2022) and can be disassembled by regulatory proteins, such as the Glial Maturation Factor (FREGOSO ET AL., 2023).

Protégé par le droit à l'image
DOI: 10.1016/j.tcb.2021.10.006

Figure 6: Arp2/3-dependent actin polymerization.

The successive formation of branches by Arp2/3 allows the formation of an expansive, dendritic network, which is key for quickly generating lamellipodia (**FIGURE 7A**). Lamellipodia are dynamic, relatively long, and flat structures (0.1-0.3µm in height, 1-5µm in length) that push the plasma membrane at the leading edge of a migrating cell (INNOCENTI, 2018). Lamellipodia are formed by waves of activation of the membrane-bound Rho GTPase called Rac that, in turn, activates WAVE, promoting Arp2/3-mediated actin polymerization (**FIGURE 7B**, INNOCENTI, 2018). Thus, lamellipodia mainly comprise branched actin filaments, although linear filaments are also present (INNOCENTI, 2018). Localized filament disassembly occurs at the rear of the lamellipodium, thus inducing a constant turnover of the actin network in a process called treadmilling. If the assembly of filaments outspeeds its depolymerization, treadmilling allows the actin network to continuously push the plasma membrane, enabling the formation of new cell adhesion to the extracellular space. This process, associated with the retractation of the cell's trailing edge, drives lamellipodia-based cell migration (**FIGURE 7C**, BLANCHOIN ET AL., 2014). Therefore, migration speed is, in part, regulated by the elongation rate of filaments and the availability of G-Actin (KRAUSE AND GAUTREAU, 2014).

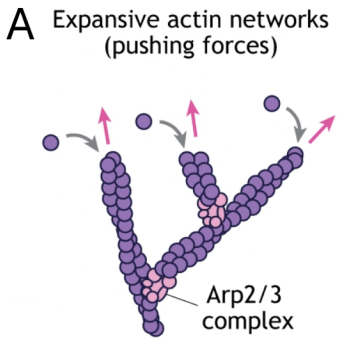

Protégé par le droit à l'image
https://doi.org/10.1038/nrm2406

Figure 7: Actin in lamellipodia. (A) An example of an expansive branched actin network.

Figure and legend adapted from Velle et al., 2024

Myosin and the actin cortex

A particular set of ABP is the myosin superfamily, composed of 12 subfamilies with diverse crucial roles in cellular processes (MASTERS ET AL., 2017). Myosins are molecular motors; they consume energy to produce movement. This movement comes from the myosin heavy chain composed of a head, lever arm, and tail. Energy comes from the hydrolyzation of ATP in the myosin's head, which also binds actin (MASTERS ET AL., 2017). The head is connected to the lever arm, which amplifies small conformational changes in the head domain to generate larger movements. The heavy chain tail domain is highly variable depending on the myosin subfamily. Specialized tail domains enable myosin to polymerize, bind to vesicles, organelles, or other proteins, allowing their transport (MASTERS ET AL., 2017; SYAMALADEVI ET AL., 2012). Accordingly, myosin subfamilies are present in different cell types and sub-cellular structures. Each myosin heavy chain is associated with two 'light chains' (regulatory and essential): essential proteins for myosin regulation and structural integrity (HEISSLER AND SELLERS, 2015). Two of these complexes bind to form a hexameric myosin 'monomer'. Depending on the myosin subfamily, monomers can polymerize to form myosin minifilaments (DULYANINOVA AND BRESNICK, 2013). However, some myosins, such as myosins I, function as monomers (MASTERS ET AL., 2017).

Myosin minifilaments, particularly from the ubiquitous class II, are best known for their role in inducing contractility within the actin cytoskeleton, notably during cell division and muscle contraction. This contraction occurs from the successive association and dissociation of myosin polymers' heads to different actin filaments through an ATP-dependent cycle, sliding filaments and creating tension (**FIGURE 8**, MASTERS ET AL., 2017). Importantly, myosin contraction is also associated with filament disassembly (BLANCHOIN ET AL., 2014).

Protégé par le droit à l'image
https://doi.org/10.1007/164_2016_29

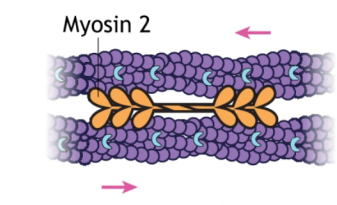

Figure 8: Myosin movement in relation to actin filaments.

(B) Example of a contractile actin network. Actin filaments are depicted in purple. Figure and legend adapted from Velle et al., 2024

The functions of myosins are tightly regulated. For example, non-muscle myosin II is directly regulated by phosphorylation. Unphosphorylated, the monomeric non-muscle myosin II is folded into an inactive state. Phosphorylation of the regulatory light chains changes myosin monomer conformation, enabling its polymerization into minifilaments (**FIGURE 9A**, MASTERS ET AL., 2017; BETAPUDI, 2014; DULYANINOVA AND BRESNICK, 2013). On the contrary, phosphorylation of monomers' heavy chains blocks their polymerization into minifilaments (DULYANINOVA AND BRESNICK, 2013). Additionally, myosins can be indirectly regulated. For example, during muscle contraction, a specialized family of ABPs called tropomyosin is associated with troponin, which together mask myosin's binding site on actin filaments until Ca^{2+} binding onto troponin (**FIGURE 9B**, LEHMAN ET AL., 1994). Interestingly, tropomyosins are also present in non-muscle cells, where they regulate the binding of other ABPs to actin filaments (RAJAN ET AL., 2023).

Altogether, myosin-mediated actin contraction leads to continuous cytoskeleton remodeling, which is crucial for numerous cellular functions.

A

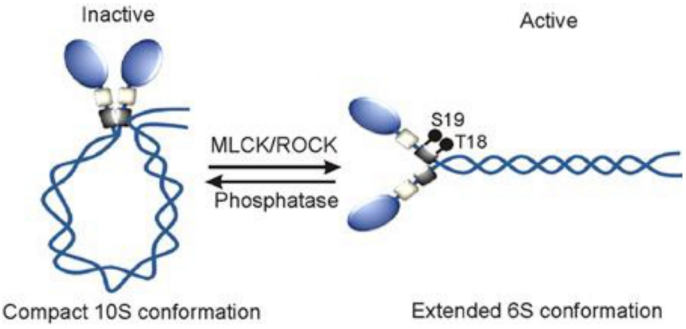

Protégé par le droit à l'image
https://musclesofthebody.weebly.com/tropomyosin-and-troponin.html

Figure 9: Myosin regulation. (A) Conformational change of Non-Muscle Myosin II by phosphorylation.

Figure and legend extracted from Betapudi, 2014

This is notably the case in the cell cortex (abbreviated as 'cortex', **FIGURE 10,** CHALUT AND PALUCH, 2016). The cortex is defined as a thin layer of contractile actomyosin filaments attached to the plasma membrane, enveloping almost every cell. Myosin embedded in entangled filaments in the cortex exerts forces that determine the cell's cortical tension (CHUGH AND PALUCH, 2018; HEER AND MARTIN, 2017). Because of the cortex's attachment to the plasma membrane by different specialized ABPs, such as the ezrin-radixin-moesin proteins (BLANCHOIN ET AL., 2014), cortical tension dictates the cell's shape. The cortex's architecture is fine-tuned by various ABPs such as formins, Arp2/3, and myosins, and is variable depending on the cell's type, subcellular structure, and phase in the cell cycle (**FIGURE 10**, SVITKINA, 2020). Therefore, the cortex is not homogenous and can locally contract, change its density of actin filaments (KELKAR ET AL., 2020), or its membrane-to-cortex distance (LEMBO ET AL., 2023 BIORXIV), leading to local deformations and reorganization of the cortex (KELKAR ET AL., 2020; LEMBO ET AL., 2023 BIORXIV) and, thus, of the cell.

Many actin networks are closely embedded within the cortex, such as the previously introduced filopodia and lamellipodia; some even emerge from it. The most apparent cortical reorganization is the formation of a contractile ring, which is necessary for cell division (BLANCHOIN ET AL., 2014). Cytokinesis rings are formed by local RhoA activation, an upstream activator of actin polymerization and myosin activity (**FIGURE 11A**). This results in local formin-mediated actin polymerization and non-muscle myosin 2 recruitment along these filaments (SCHWAYER ET AL., 2016). Additionally, pre-existing actin filaments neighboring the nascent ring are aligned and incorporated in it by cortical flows (**FIGURE 11A**, REYMANN ET AL., 2016; HSU ET AL., 2023). The contractile ring is attached to the membrane by aniline and maintained by septins (BRIDGES AND GLADFELTER, 2015).

Protégé par le droit à l'image
DOI: 10.1016/j.devcel.2016.09.011

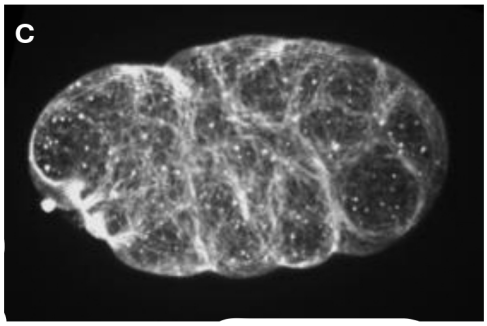

Figure 10: The actin cortex.

(C) Actin cortex of a one-cell stage C. elegans embryo observed with LifeAct::mKate2 (Grey). Figure from Anne-Cécile Reymann (C).

The newly formed ring then constricts. This process is mediated by filaments sliding thanks to myosin activity. The depolymerization of – end crosslinked filaments also seems to play a crucial role. Indeed, the depolymerization of a filament changes its – end location, which can be reattached by a crosslinker that slides back the filament (**FIGURE 11B**, SCHWAYER ET AL., 2016; ZUMDIECK ET AL., 2007; MENDES PINTO ET AL., 2012). Mitosis ends by abscission, physically separating the two daughter cells. Interestingly, actin rearrangement is required to complete the abscission. Indeed, a pool of branched actin regulated by cofilin serves as a mechanical barrier to precisely position the abscission machinery to the daughter cells' bridge in HeLa cells (ADVEDISSIAN ET AL., 2024). Additionally, capping proteins play an important role in abscission, as their depletion result in cytokinesis failure (GIBIEŽA AND PETRIKAITĖ, 2021; TERRY ET AL., 2018). Abscission failure leads to cytokinetic ring regression and binucleated cells.

In summary, actin dynamics are finely orchestrated by numerous ABPs to ensure the robustness of cytokinesis at every step, from ring assembly to abscission. Accordingly, any change in the biochemical composition of the contractile ring leads to altered dynamics, observable by a change in the speed of ring assembly or contraction, up to complete failure of cytokinesis apparent by ring regression or non-assembly of the contractile ring.

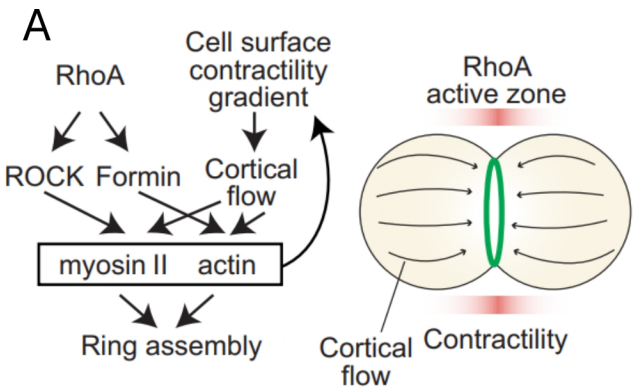

Protégé par le droit à l'image
DOI: 10.1016/j.devcel.2012.04.015

Figure 11: The contractile ring. (A) RhoA activation at the equatorial cell cortex stimulates downstream myosin activity and actin polymerization. A gradient in cell surface contractility induces cortical flow toward the ring, leading to myosin II enrichment and actin alignment.

Adapted from Rou Hsu et al., 2023

Additionally, the detachment of the cortex from the plasma membrane or the local rupture of the cortex can produce cell blebs. These are transient spherical membrane protrusions devoid of a cortex, growing rapidly due to the cell's hydrostatic pressure: the pressure exerted by the cytoplasm to the plasma membrane (**FIGURE 12**). A cortex is eventually rebuilt in the bleb, leading to its retractation. These protrusions often serve for cellular migration, both in physiological and pathological circumstances, although these structures are also observed during cell division and apoptosis (PACQUELET ET AL., 2019; PALUCH AND RAZ, 2013). Bleb formation can arise because of high internal cell pressure, high contractility, too few linker proteins, or a combination of those parameters.

Therefore, the location, size, and kinetics of bleb retractation can give us valuable insights into cortical tension, hydrostatic pressure, and actin dynamics (SAKAMOTO AND MURRELL, 2024). In that way, blebs can act as sensors of cortical and membrane mechanical properties.

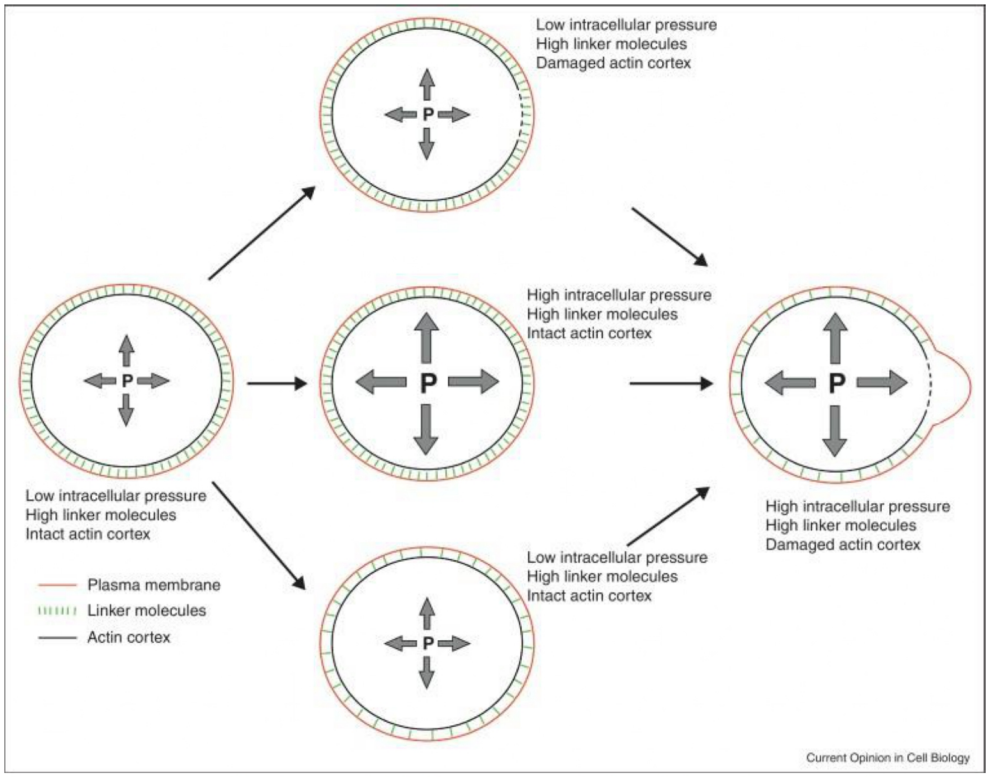

Figure 12: Parameters contributing to bleb formation. Cells with an intact actin cortex, high level of cortex–membrane linker proteins, and low intracellular pressure do not form blebs (left cell). Affecting each of the three parameters alone is typically insufficient for the generation of blebs (cells in middle). Blebbing cells are characterized by high myosin-dependent contractility that increases the intracellular pressure, reduced level of linker proteins and/or breaks in the actin cortex at the region where the bleb forms (right cell). Figure and legend adapted from Paluch & Raz 2013.

The G-/F-actin homeostasis, a finely tuned cellular challenge

From a pure biochemistry perspective, the elongation rate of actin filaments depends on the association and dissociation rates of actin subunits and the concentration of available actin monomers. *In vivo*, we have seen that filament elongation is also catalyzed by numerous ABPs, which are essential to dynamically form various actin networks. Thus, tight regulation is required to maintain a monomeric actin pool within the cell to ensure the fast remodeling of actin networks in response to mechano- or chemo-sensory triggers, (HUANG ET AL., 2022; POLLARD, 2016). The cell employs multiple strategies to achieve this balance, which I will review in the following paragraphs: disassemble existing filaments, prevent excessive elongation and nucleation, and sequester actin monomers.

Filament disassembly is catalyzed by severing proteins that first promote filament fragmentation, facilitating further disassembly. For example, cofilin is a severing protein that changes F-actin conformation upon binding. This leads to F-actin twisting, creating torsional stresses supporting their fragmentation and disassembly (WIOLAND ET AL., 2019). The disassembled subunits are then recycled into ATP-bound monomers and reenter the actin polymerization cycle, increasing the concentration of cytoplasmic G-Actin.

Excessive elongation is prevented by capping proteins that bind to the filament's + end, competing with formin-based filament elongation and thus increasing the G-actin pool (POLLARD, 2016).

To prevent an excessive formation of new actin seeds, which would reduce the pool of polymerizable G-actin, monomers can be sequestrated by specialized ABPs such as thymosin β4 and profilin. Thymosin β4 preferentially binds ATP-bound actin monomers, which prevents their incorporation into filaments and increases the cytoplasmic G-actin pool (POLLARD, 2016). Profilin also binds ATP-bound monomers and thus competes with thymosin β4. However, profilin has a lower dissociation constant than thymosin β4 for ADP-bound G-actin. Therefore, profilin is better associated with disassembled actin subunits than thymosin β4. When associated with ADP-bound G-actins, profilin catalyzes ATP recycling of the monomers to increase the concentration of polymerizable actin subunits, a process impossible for thymosin β4. Additionally, profilin can bind proline-rich sequences, such as formins' FH1 domains, which promote filament elongation ("FORMIN AND FILOPODIUM"; POLLARD, 2016).

Actin is not solely present in the cytoplasm. Indeed, a G-actin/cofilin complex can bind to Importin 9, which enables G-actin transport to the nucleus (**FIGURE 13**). This contributes to the precise regulation of the cytoplasmic G-actin pool by 'storing' G-Actin away from cytoplasmic filaments (KELPSCH AND TOOTLE, 2018). However, when needed, nuclear G-Actin can be translocated back into the cytoplasm by forming a complex with profilin and Exportin 6 (**FIGURE 13**, KELPSCH AND TOOTLE, 2018).

Actin transported into the nucleus is not just stored. Instead, it can polymerize and interact with numerous ABPs, some common with the cytoplasm, such as Arp2/3 (KELPSCH AND TOOTLE, 2018; MOKIN ET AL., 2024). Notably, nuclear actin is involved in DNA movement and reorganization. Indeed, actin helps to translocate damaged DNA to specific nuclear domains for reparation and to reorganize DNA from hetero- to euchromatin by ensuring the optimal activity of chromatin remodeling factors (KELPSCH AND TOOTLE, 2018; KLOC ET AL., 2021). Additionally, nuclear actin is known to regulate transcription. The precise mechanisms of this regulation have not yet been uncovered. Still, studies have shown the interaction of actin monomers with all three RNA polymerases, which seems essential for transcription (KLOC ET AL., 2021).

Nuclear actin polymerization also helps nuclear envelope breakdown. Indeed, Arp2/3-mediated nucleation of branches close to the nuclear envelope has been observed in echinoderms' oocytes. Branches penetrate the nuclear envelope, which is hypothesized to fragilize and facilitate its subsequent breakdown (KLOC ET AL., 2021). Other studies have linked nuclear actin with the maintenance of nuclear shape, apoptosis, and viral infections (KLOC ET AL., 2021).

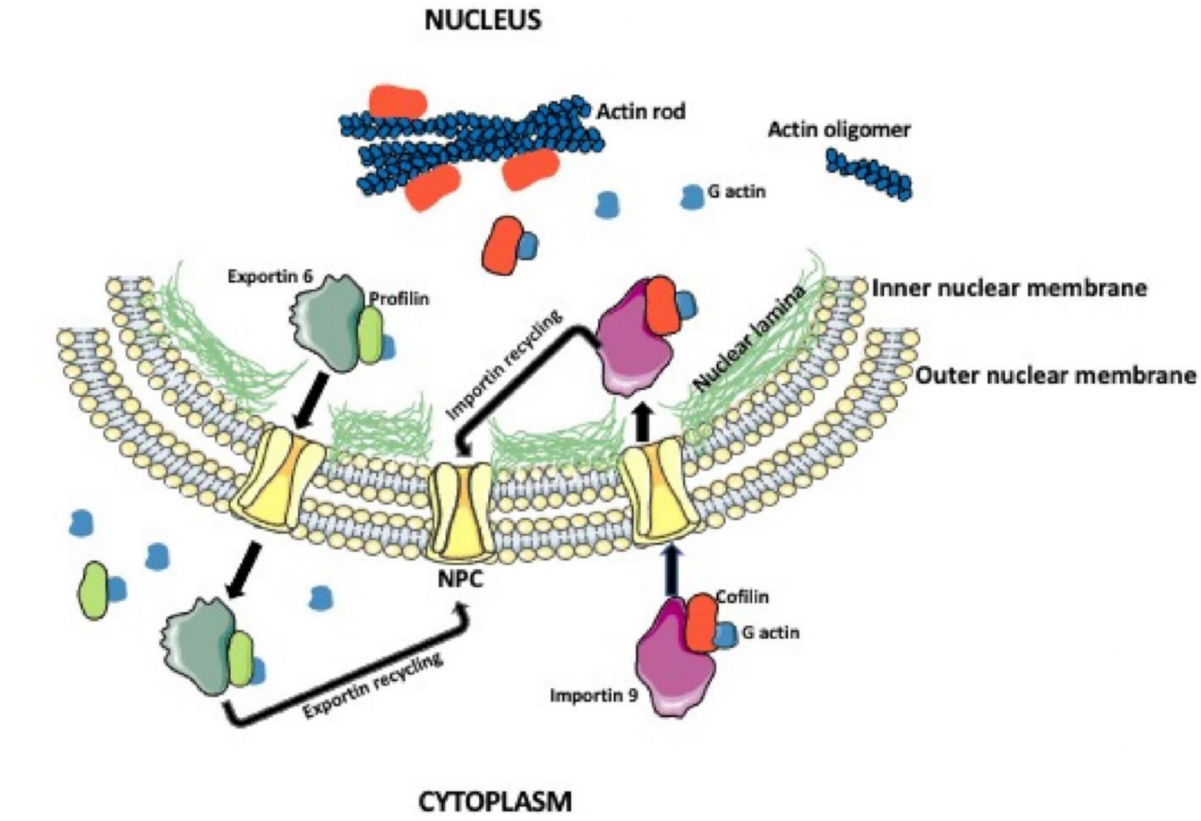

Figure 13: Nuclear actin transport. Actin monomers in the cytoplasm form a complex with cofilin and importin 9. The complex is imported into the nucleus, where actin is released, and the importin is cycled back to the cytoplasm. The export of the actin from the nucleus is facilitated by the profilin and exportin 6. While in the cytoplasm, exportin is recycled back into the nucleus. Figure and legend adapted from Kloc et al., 2021.

Interlude on human actin isotypes

The previous section introduced some known ABPs and their associated actin networks. However, in most eukaryotes, actin is not produced by a single gene. In humans, six genes code for actin, thus creating six isotypes (PARKER ET AL., 2020). This adds another layer of complexity to actin regulation. Indeed, although sharing highly similar structures and amino acid sequences (**FIGURE 14**), actin isotypes are not present at the same level in different cell types (KASHINA, 2020) and undergo specific functions (DUGINA ET AL., 2009; HEISSLER AND CHINTHALAPUDI, 2024). Indeed, four human actin are called "muscular", as they are expressed almost exclusively to specific types of muscles. Among them, *ACTC1* is mainly expressed in cardiac muscles, *ACTA1* in skeletal muscles, and *ACTA2* as well as *ACTG2* in smooth muscles. The two remaining human actin coding genes, *ACTB* and *ACTG1*, are termed cytoplasmic or non-muscular, as they are widely expressed in almost all cells (Parker et al., 2020).

My thesis work focused on the understanding of human cytoplasmic actin variants. Therefore, I will now introduce the current knowledge of the physiological functions of cytoplasmic actin.

Protégé par le droit à l'image
https://doi.org/10.1016/j.semcdb.2019.12.003

Figure 14: The six mammalian actin isotypes are highly conserved at the amino acid level.

The Cytoplasmic actins

Lookalikes from different parents

Human cytoplasmic actin proteins ACTB (β-actin) and ACTG1 (ɣ-actin) are structural lookalikes, differing by only four residues in their N-terminal domain (**Figure 14**). Those have similar physicochemical properties but result in a slight local change in their isoelectric point. Accordingly, both proteins have highly similar 3D structures with slightly different N-terminal parts (**Figure 15**, Arora et al., 2023). Despite their near-identical structures and ability to hetero-polymerize into filaments (Bergeron et al., 2010; Müller et al., 2013), these two proteins have different functions (Dugina et al., 2009) and form actin networks of various properties *in vitro* (Nietmann et al., 2023).

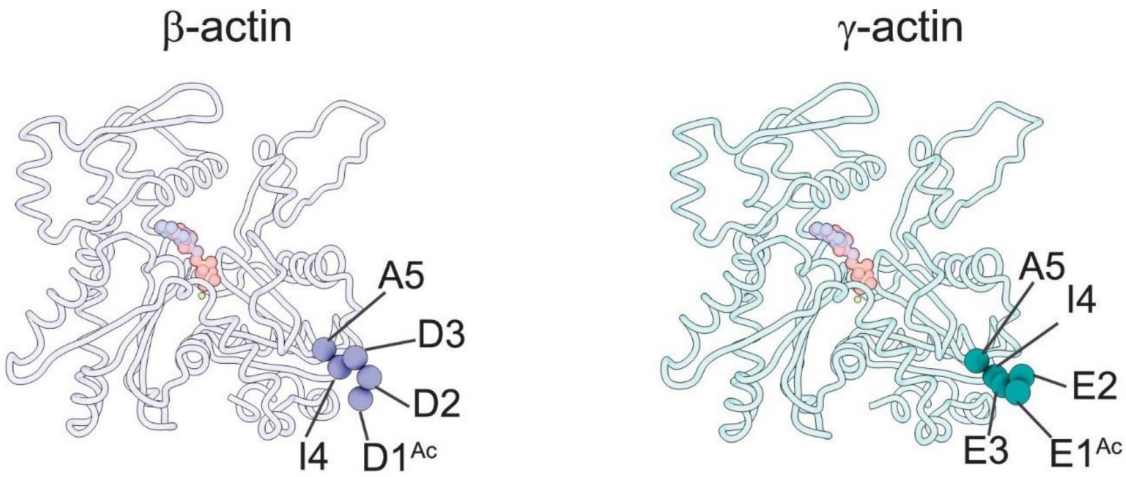

Figure 15: β and γ actin structures. Sequence variations at the N-terminus located in SD1 of actin isoforms. The protein backbone is shown in licorice representation, and the substituted amino acids are shown in spheres representation. Figure and legend adapted from Arora et al., 2023.

In vivo, *ACTB* and *ACTG1* are expressed at different levels in various tissues (Kashina, 2020; Vandekerckhove and Weber, 1981), cells (Kashina, 2020) and are differently enriched in some subcellular structures (Brockmann et al., 2011; Dugina et al., 2009; Migocka-Patrzalek et al., 2015). For example, β-actin is enriched in the contractile ring and stress fibers, while ɣ-actin is more present in the cell cortex and lamellipodia (**Figure 16**, Dugina et al., 2009). In polarized epithelial cells, adhesion junctions are composed of β-actin, while tight junctions are enriched in ɣ-actin (Baranwal et al., 2012). In the nucleus, β-actin seems enriched compared to ɣ-actin (Migocka-Patrzałek et al., 2015). However, some studies present contradictory results, notably in the case of cell migration. For example, Dugina and colleagues (2009) showed ɣ-actin enrichment in lamellipodia for one human and one rat fibroblast cell line (HSCF, REF-52) as well as one rat kangaroo kidney cell line (PtK2), while Bunnell et al. (2011) state that β-actin is specifically

needed for cell migration in mouse embryonic fibroblasts (BUNNELL ET AL., 2011; DUGINA ET AL., 2009). This may be due to changes in cell types, fixation methods, and the revelation of these specific isotypes. Indeed, these observations were done on fixed samples using antibodies, as live observation of specific actin isotypes is difficult; N- or C-Terminal fusion of a tag or a reporter leads to impaired actin dynamics and interactions with partners (BRAULT ET AL., 1999; VAN ZWAM ET AL., 2024). These antibodies target actin's N-terminus, a region highly post-translationally modified, which may alter the antibody binding and, thus, the revelation of the protein (VAN ZWAM ET AL., 2024).

Protégé par le droit à l'image
https://doi.org/10.1242/jcs.041970

Figure 16: Differential localization of ACTB and ACTG1.

Importantly, the ratio between β- and ɣ-actin is tightly regulated within cells. Indeed, previous studies observed that changing this ratio by overexpression of one type of actin could rearrange cellular actin networks (SIMICZYJEW ET AL., 2014). Accordingly, it has been observed that some ABPs have higher affinities for specific cytoplasmic actin isotypes (KASHINA, 2020; NIETMANN ET AL., 2023). Dysregulation of the β-/ɣ-actin ratio has been observed in cancer cells (SHAGIEVA ET AL., 2012) and during aging (LAI AND WONG, 2020), highlighting the importance of this regulation.

Still, numerous studies highlight the functional redundancy between β- and ɣ-actin. When one gene is knocked out, the other can often compensate, a process known as transcriptional adaptation or, in the case of actin, "isoactin switching" (VANSLEMBROUCK ET AL., 2020). Isoactin switching has been observed in gene knockouts of *Actb* (BUNNELL ET AL., 2011; TONDELEIR ET AL., 2012) as well as *Actg1* (BELYANTSEVA ET AL., 2009; BUNNELL AND ERVASTI, 2010). Actb loss increased the expression of Actg1 and Acta2, whereas Actg1 loss increased Acta2, Actb, Acta1, and Actc1 actin expression.

In summary, despite the high similarity between the ubiquitous actin proteins ACTB and ACTG1, they show specific localization, level of expression and partially overlapping function *in vivo*.

What controls these differences?

Since their discovery, the differences in location and roles between ACTB and ACTG1 have been an open question. Numerous teams have highlighted differences between β and ɣ-actin that could regulate their proteic individuality.

First, at the gene level, *ACTB* and *ACTG1* nucleotide sequences are more different than ACTB and ACTG1 amino acid sequences. Elegant work from Vedula et al. (2017) showed that cytoplasmic actin's nucleotide sequence is more critical than its amino acid sequence (VEDULA ET AL., 2017). Indeed, authors engineered mice in which the endogenous *Actb* locus was mutated to produce the Actg1 protein (*Actb*$^{c\text{-}g}$ for *Actb* coding gamma). Strikingly, edited animals were viable and showed no detectable phenotype compared to control, showing that the loss of production of Actb does not impair the animal's development. However, 100% of *Actb* homozygous null mice in which the nucleotide sequences have been altered (either by the deletion of exon 2 and 3 in BUNNELL ET AL., 2011 or by the insertion of a reporter in SHMERLING ET AL., 2005 AND SHAWLOT ET AL., 1998) die during embryonic development. This highlights that only the alteration of the proper nucleotide sequence and not the loss of the protein *per se* is detrimental to embryonic development. Interestingly, heterozygous *Actb* null mice (exons 2 and 3 deletions) do not die during embryonic development, although ~30% of animals die at an early age (5-18 weeks) (BUNNELL ET AL., 2011).

On the contrary, homozygous (*Actg1*$^{-/-}$) or heterozygous (*Actg1*$^{+/-}$) deletion of exons 2 and 3 of *Actg1* does not impair embryonic development in mice. However, *Actg1*$^{-/-}$ animals showed developmental delay and perinatal lethality, as 60% of animals die in their first ten months (BELYANTSEVA ET AL., 2009). This phenotype is absent in *Actg1*$^{+/-}$ mice (BELYANTSEVA ET AL., 2009). A recent study by the Ervasti group states that the lethality observed in *Actg1*$^{-/-}$ mice could be due to the loss of the nucleotide sequence rather than the loss of protein production (SUNDBY ET AL., 2022), as observed for *Actb*$^{-/-}$ mice (VEDULA ET AL., 2017).

In line with these phenotypic observations, authors found that Mouse Embryonic Fibroblasts (MEF) were similarly impacted. Indeed, *Actg1*$^{-/-}$ MEFs have mildly impaired proliferation, *Actb*$^{-/-}$ MEFs have largely impaired proliferation, and *Actb*$^{c\text{-}g}$ behaves as *Actb*$^{+/+}$ MEFs. Recent studies pushed the analysis further and demonstrated that the transcriptome, proteome, and phosphoproteome of *Actb*$^{-/-}$ MEFs were drastically affected compared to both *Actb*$^{+/+}$ and *Actb*$^{c\text{-}g}$ MEFs, which were virtually indistinguishable from one another (SUNDBY ET AL., 2024). This

evidence strongly supports the idea that the specific nucleotide sequence of *Actb*, rather than the loss of β-actin protein, is critical for proper cell function.

At the RNA level, ACTB mRNA specifically contains a 54-bp "zipcode" in its 3' UTR, enabling its transport to the cell periphery via the ZBP1 protein (CONDEELIS AND SINGER, 2005; KISLAUSKIS ET AL., 1993; RODRIGUEZ AND KASHINA, 2018). This mechanism ensures localized translation of β-actin, which is essential for development. Indeed, impaired transport of β-actin mRNA reduces the formation of dendritic and synaptic filopodia (EOM ET AL., 2003), as well as decreasing fibroblast motility and impairing Xenopus forebrain development (YANIV ET AL., 2003). Additionally, cytoplasmic actin mRNAs have different transcription dynamics. Indeed, ribosome profiling data show that the first 150 codons of ACTB mRNA are enriched in ribosomes a thousand-fold compared to those of ACTG1 mRNA (VEDULA AND KASHINA, 2018). It is hypothesized that the ACTB mRNA is poised and can be translated quickly in a "burst" manner, contrary to ACTG1.

At the protein level, the regulation of actin dynamics can be controlled by multiple factors. First, by post-translational modifications (PTM), i.e., *"covalent processing events that change the properties of a protein by proteolytic cleavage and adding a modifying group"* (RAMAZI AND ZAHIRI, 2021). These can be located in multiple loci throughout the actin monomer (TERMAN AND KASHINA, 2013), with 45% of residues known to be able to be post-translationally modified (VARLAND ET AL., 2019). Still, one PTM called arginylation (i.e., the addition of an arginine) is specific to the N-terminal part of β-actin and is essential for forming a cell's leading-edge lamellipodium (VARLAND ET AL., 2019).

Still at the protein level, Bergeron et al. (2010) observed that β- and ɣ-actin monomers have a different nucleotide exchange rate half time for ATP, with β-actin being faster than ɣ-actin. Additionally, the authors found that filament polymerization and Pi release are much slower for ɣ-actin than β-actin (BERGERON ET AL., 2010). Nonetheless, ɣ-actin filaments are more stable (1/2 depolymerization time are respectively 127±2 and 202±20 seconds). Importantly, these differences between monomers' properties were only valid for Ca^{2+} bound monomers and not for Mg^{2+} bound monomers, the latter being the main form of actin *in vivo* and may thus not be relevant (BERGERON ET AL., 2010).

Chapter conclusion

In this chapter, I presented the ubiquitous and essential actin protein that can build dynamic, complex, and specialized networks crucial for cell homeostasis. I like to compare actin and its complexity to an iceberg. If we look above the surface, we only see the iceberg's tip, which, in the case of actin, would be the actin networks within the cell. However, below the surface, a main part of the iceberg is submerged, which would be the numerous depths of complexity needed to build the actin networks from a common pool of actin monomers.

The first depth of complexity comes from the fact that actin networks do not form from one actin coding gene but from multiple that are differentially expressed within the cell. Indeed, actin isotypes have been shown to be expressed at different levels depending on cell types and to form different networks *in vitro*. Additionally, despite their very similar amino acid sequences, ACTB and ACTG1 were observed in specific subcellular structures.

Actin isotypes are post-translationally regulated to build different actin networks, adding another depth of complexity. Indeed, various actin-binding proteins exist that help increase the diversity of actin network organization. However, actin-binding proteins do not bind each actin isotype with the same efficiency and can compete with each other. Additionally, actin monomers have post-translational modifications that can be isotype-specific and required for specific functions, leading to multiple 'versions' of actin monomers within a cell.

The last depth of complexity comes pre-translationally. Indeed, *ACTB* and *ACTG1* nucleotide sequences differ by numerous silent variations, which have been shown to be more important than amino acid sequence differences. Moreover, *ACTB* and *ACTG1* have different translation dynamics as well as a specific binding domain required for *ACTB* mRNA localization. Furthermore, although not characterized, we could imagine that these genes have different epigenetic profiles.

I hope that this dive into the depths of actin intricacy highlights this protein complexity in physiological conditions. This complexity further shines in the case of actin variants, which I will introduce in the following chapter.

Chapter 2:
Non-Muscle Actinopathies

Chapter Introduction – The mutated cytoskeleton.

Due to the pleiotropy and ubiquity of all cytoskeletal components, mutations in actin, microtubules, or intermediate filaments coding genes can cause a wide range of diseases with varying symptoms and severities (Eriksson et al., 2009; Parker et al., 2020; Sferra et al., 2020). Depending on the altered cytoskeletal component, mutations can affect specific tissues and cellular functions. For example, mutated muscular actins mainly cause myopathies associated with their expression pattern: *ACTC1* mutations cause heart diseases, while *ACTG2* variants can cause visceral myopathies (Parker et al., 2020). However, the human cytoplasmic actin ACTB and ACTG1 are ubiquitous and, despite their apparent similarities, show many specificities, as introduced in Chapter 1. Therefore, cytoplasmic actin mutations can lead to many different symptoms that affect various tissues. Nonetheless, individual variants can affect some tissues more specifically than others.

In this second chapter, we will explore the implications of cytoskeletal mutations in the context of Non-Muscle Actinopathies. I will go through their discovery, symptoms, and variability. Then, I will highlight the current hypotheses to explain actin variants' pathophysiological mechanisms.

Non-Muscle Actinopathies – Discovery and genetic causes

Non-Muscle Actinopathies (NMA) are a set of rare human diseases associated with heterozygous mutations in the cytoplasmic actin coding genes *ACTB* and *ACTG1*. NMAs were first described by Baraitser and Winter in 1988 (BARAITSER AND WINTER, 1988). The authors described the clinical features of three patients suffering from iris coloboma (incomplete closure of iris during development (O'KEEFE, 2017), ptosis (dropping of the upper eyelid (FINSTERER, 2003), telecanthus (increased distance between the inner eye corners (SHARMA, 2014), eye hypertelorism (increased distance between the eyes (SHARMA, 2014), short stature, and mental retardation. The combination of these symptoms had not been documented yet. Therefore, the authors described it as a new syndrome called Baraitser-Winter cerebrofrontofacial syndrome (BWCFF) (BARAITSER AND WINTER, 1988). Since, other patients suffering from BWCFF were reported (RIVIÈRE ET AL., 2012; VERLOES ET AL., 2015), which led to an updated definition of BWCFF: *"BWCFF is a multiple congenital anomaly syndrome characterized by typical craniofacial features and intellectual disability. Many (but not all) affected individuals have pachygyria* (a cortical malformation characterized by broad convolution (KATTUOA AND DAS, 2024) *that is predominantly frontal, wasting of the shoulder girdle muscles, and sensory impairment due to iris or retinal coloboma and/or sensorineural deafness. Intellectual disability, which is common but variable, is related to the severity of the brain malformations. Seizures, congenital heart defects, renal malformations, and gastrointestinal dysfunction are also common"* (VERLOES ET AL., 1993, UPDATED 2022). BWCFF is the most frequent NMA. Still, as of 2022, fewer than 100 patients had been reported globally, qualifying it as an ultra-rare disorder (HARARI AND HUMBERT, 2020). Recent work from our human geneticist collaborator, Nataliya Di Donato, has increased the total known number of patients suffering from BWCFF to 120 (DI DONATO ET AL., 2024, MEDRXIV).

While BWCFF is the most common NMA, mutations in *ACTB* and *ACTG1* are also associated with other diseases (**FIGURE 17**). Indeed, mutations in *ACTB* can cause Dystonia-Deafness (CONBOY ET AL., 2017; EGGINK ET AL., 2017; FREITAS ET AL., 2020; GEARING ET AL., 2002; PROCACCIO ET AL., 2006; SKOGSEID ET AL., 2018; ZECH ET AL., 2017) a syndrome characterized by the patient's inability to hear, combined with involuntary muscle contractions. Mutations in *ACTG1* can cause mosaic Becker-Nevus syndrome (CAI ET AL., 2017), i.e., the formation of a hyperpigmented macule and muscle hypoplasia. Mutations in either gene can provoke the loss of function of

the associated gene, hearing loss, or other unrelated syndromes (CUVERTINO ET AL., 2017; DI DONATO ET AL., 2024 MEDRXIV). Altogether, 290 patients are known to suffer from NMA (**FIGURE 17**, DI DONATO ET AL., 2024 MEDRXIV).

Protégé par le droit à l'image
https://doi.org/10.1101/2024.08.21.24310320

Figure 17: Distribution of ACTB and ACTG1 pathogenic variants within Non-Muscle Actinopathies.

Phenotypic variability

NMAs are mainly caused by single-point substitution mutations resulting in missense *ACTB* or *ACTG1* variants, although short insertion-deletions (INDELs) were also reported (**Figure 17**, Cuvertino et al., 2017; Latham et al., 2018). Variants span the entirety of cytoplasmic actins' coding sequences, and most of them (54%, 157/290) are unique (**Figure 17**, Di Donato et al., 2024 medRxiv). Still, some loci are mutational hotspots associated almost exclusively with specific symptoms. For example, the variant R183W in *ACTB* was identified in 13 patients, all suffering from dystonia deafness (Conboy et al., 2017; Eggink et al., 2017; Freitas et al., 2020; Gearing et al., 2002; Procaccio et al., 2006; Skogseid et al., 2018; Zech et al., 2017); this symptom is exclusively found for this variant. Another example is the R196 locus, which is the most frequently mutated in NMA, affecting 6.55% of patients (19/290, Di Donato et al., 2024 medRxiv). Out of these 19 patients, one presents an R196S substitution, seven an R196C substitution, and eleven an R196H substitution. However, patients show various symptoms; 1/7 *ACTB* R196C patients (~14%) have coloboma, while 4/11 (~36%) *ACTB* R196H patients have this symptom (**Table 1**). Inversely, 4/7 *ACTB* R196C (~57%) patients have skin and integument disorders, while 2/11 ACTB R196H (~18%) have this type of disorder (**Table 1**, Di Donato et al., 2024 medRxiv). Thus, not only the mutation's locus but also the substitution affects the patient's symptoms. Although symptoms are generally similar within one variation, the severity of these symptoms can differ. It is especially clear looking at the intellectual disability (ID) level of patients having the same variation. For example, all seven *ACTB* R196C patients suffer from ID: 4 severely, two moderately, and one mildly (**Table 1**, Di Donato et al., 2024 medRxiv). This may be due to genomic or epigenomic differences from patient to patient.

Due to the high number of variants underlying high clinical variability, understanding the genotype-to-phenotype correlations of NMA is a complex and challenging task.

	Dystonia Deafness	*Coloboma*	*Skin and integument*	*Intellectual disability level*
R183W ACTB	13/13	0/13	1/13	None-Moderate
R196C ACTB	0/7	1/7	4/7	Mild-Severe
R196H ACTB	0/11	4/11	2/11	Mild-Severe
R196S ACTB	0/1	0/1	1/1	Severe

Table 1: Summary of mentioned symptoms for ACTB variants R183W, R196C, R196H and R196S. Based on data from Di Donato et al., 2024, Medrχiv.

Hypothesis on actin variant pathogenicity

Pathogenic actin variants have been studied for fifty years (Boxer et al., 1974), and four mechanisms by which actin variants can affect the cytoskeleton have been identified (Johannes N Greve et al., 2024).

The first and most common mechanism is that an actin variation can impact the affinity of the protein to different Actin Binding Proteins (ABP, introduced in Chapter 1) by directly affecting its binding site (**Figure 18**). This was first demonstrated by Drummond and colleagues in 1992 (Drummond et al., 1992). In this study, the authors engineered 25 actin variants in *Drosophila melanogaster* muscular actin Act88F. They identified that some variations could increase, decrease, or unalter profilin binding *in vitro*. Shortly after, a similar finding was realized in a human β-actin pathogenic single-point variant (Nunoi et al., 1999). Numerous other actin variants exhibiting altered binding to profilin were described (Greve et al., 2022; Tsujimoto et al., 2024, Biorxiv). Additionally, certain actin variants were also observed to have impaired interaction with myosin (Greve et al., 2022; Johannes N. Greve et al., 2024; Müller et al., 2012), tropomyosin (Müller et al., 2012), cofilin (Greve et al., 2022) and the Arp2/3 complex (Greve and Manstein, 2024, Biorxiv). Studies of these binding affinities are essential to understanding the pathophysiological mechanisms of actin variants, as actin regulations by ABP are critical for cell homeostasis. However, based on these data, it may be difficult to predict the pathogenicity of an actin variant. Indeed, because of the high number of ABPs and their various binding sites, it is plausible that one mutation can affect the binding affinities of numerous proteins, and one can be easily missed. This complicates the estimation of the resulting phenotypes.

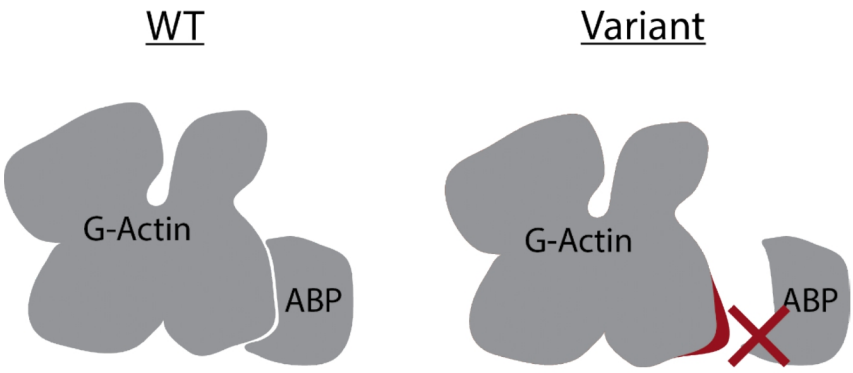

Figure 18: Scheme depicting how an actin variant could impact the association of an actin monomer with an actin-binding protein (ABP). Here, an actin variant causes a structural change (in red) which prevents the ABP to bind. WT=Wild-type.

Secondly, an actin variant can lead to haploinsufficiency. This is because the mutated actin may be degraded or unable to polymerize, reducing the availability of polymerizable G-Actin (**FIGURE 19**). This was observed *in vitro* for five actin variants identified in patients with cardiomyopathies (Glu99Lys, Pro164Ala, Met305Leu, Arg312His, and Glu361Gly) (VANG ET AL., 2005). Those led to probable haploinsufficiency as protein variants were misfolded and unable to polymerize (VANG ET AL., 2005). Interestingly, actin haploinsufficiency phenotypes might differ depending on the mutation type. For example, an actin mRNA containing a premature STOP codon will be degraded by nonsense-mediated mRNA decay (BROGNA AND WEN, 2009) and induce isoactin switching (WELKER ET AL., 2023). This process increases the production of another actin isotype to compensate, at least partially, for the loss of production of the actin variant (VANSLEMBROUCK ET AL., 2020). However, mRNA containing a missense variant will not be degraded. Therefore, isoactin switching will not activate, and compensation will not occur.

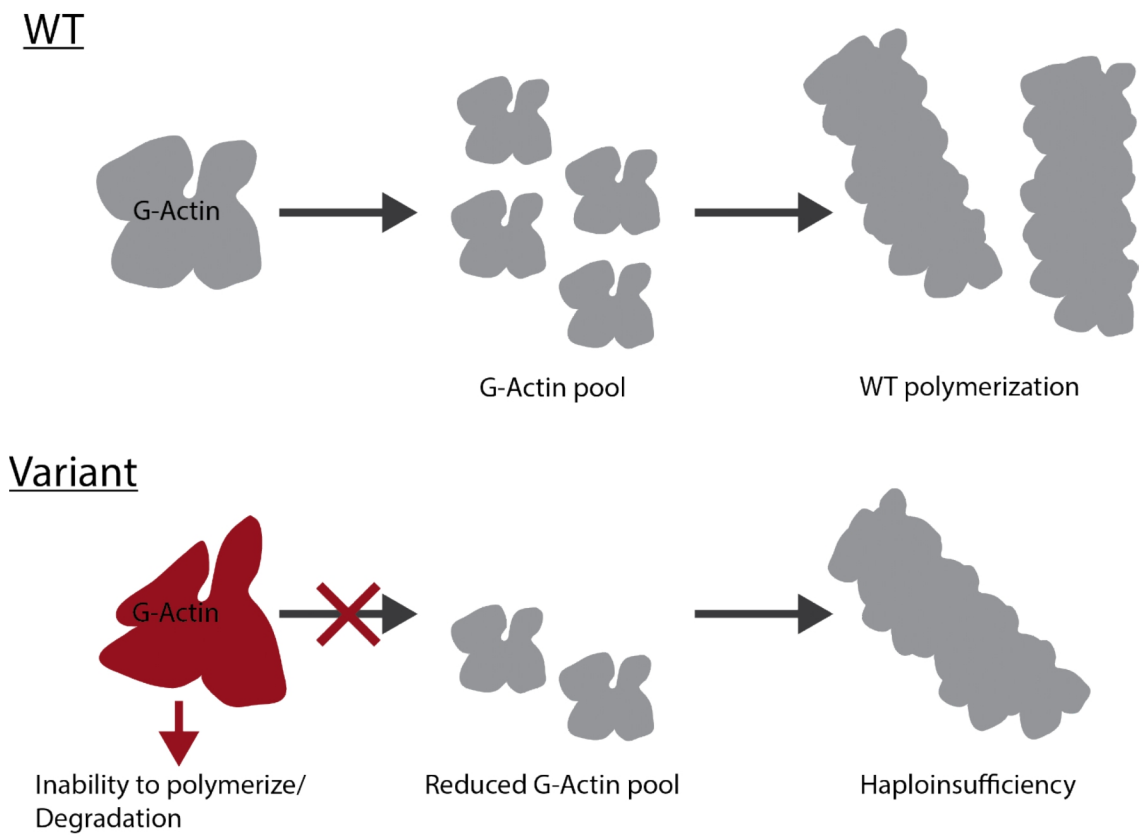

Figure 19: Scheme depicting how an actin variant could induce haploinsufficiency. The inability to polymerize or the degradation of a misfolded actin monomer (red) leads to a reduced actin pool and haploinsufficiency. WT=Wild-type.

Thirdly, studies show that some actin variants can change actin dynamics regardless of available ABP (**FIGURE 20**). For example, *in vitro* studies identified that the ACTB R183W variation leads to a slower polymerization rate than WT actin. The authors determined that an unusual interaction between W183 and Tyr69 altered the actin monomer's conformation, leading to slower polymerization and faster depolymerization of R183W actin filaments (HUNDT ET AL., 2014). This was also observed for the R196H variant (GREVE AND MANSTEIN, 2024), which additionally exhibited impaired filament stability. Moreover, some actin variants showed impaired association with WT actin (COSTA ET AL., 2004).

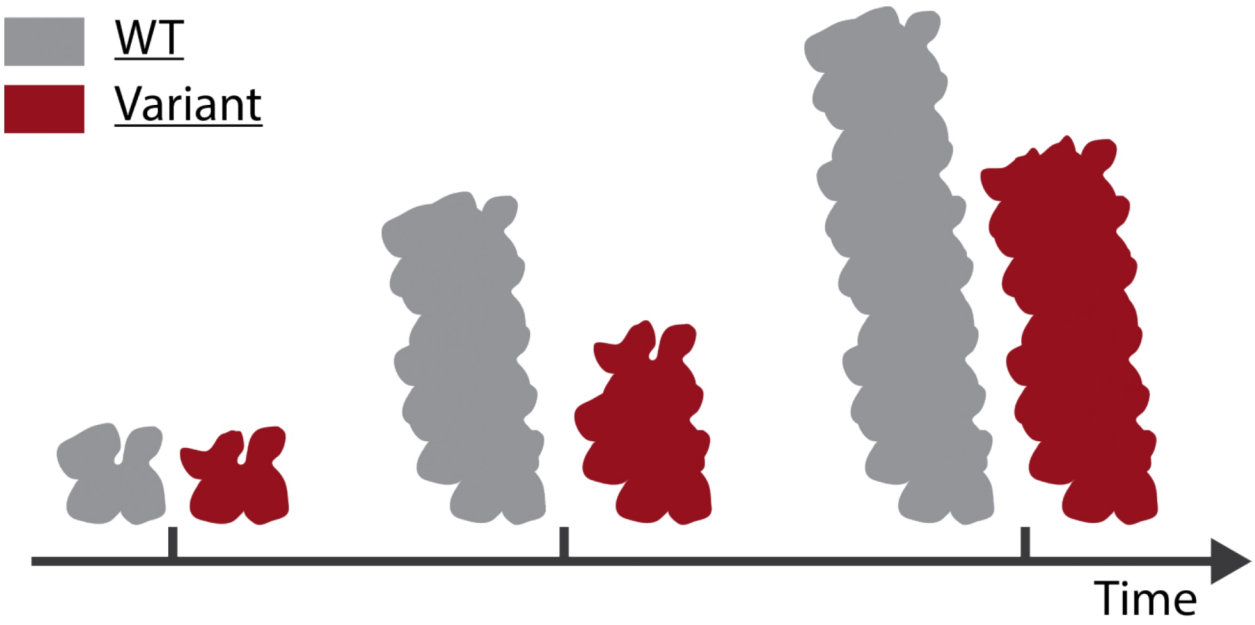

Figure 20: Scheme depicting impaired actin polymerization dynamics. Here, an actin variant (red) polymerizes slower than its wild-type (WT, grey) counterpart. This may be due to increased dissociation dynamics or decreased association dynamics.

Finally, an actin variant can form abnormal polymers proposed to deteriorate cytoskeletal functions (**FIGURE 21**). That is notably the case for muscular actin variants ACTA1, which have been associated with the formation of cytoplasmic and nuclear rods (COSTA ET AL., 2004; ILKOVSKI ET AL., 2004; SCHRÖDER ET AL., 2004). These variants have been proposed to act as dominant negative effect mutations, but their pathophysiological mechanisms are unknown.

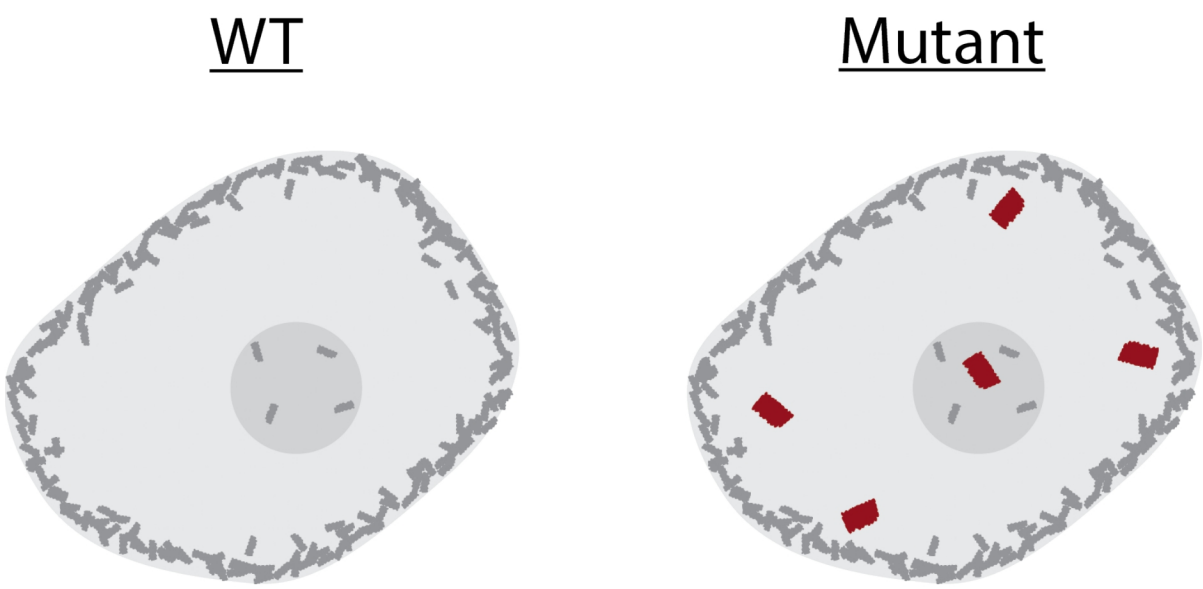

Figure 21: Actin variant forming actin rods. Scheme depicting a cell (Cytoplasm light grey, nucleus grey) with wild-type actin (WT, dark grey) and a cell with an actin variant (red) forming actin rods.

Chapter conclusion

In summary, we learned that Non-Muscle Actinopathies (NMA) are rare human diseases caused by cytoplasmic actin variations. We saw that NMAs are characterized by high clinical variability between each actin variant, leading to numerous symptoms of variable severities.

Past studies used cell cultures, *in vitro* biochemical studies on purified proteins, biophysical analysis, and *in silico* modeling to decipher the pathophysiological mechanisms of actin variants. This led to the proposal of four functional mechanisms to explain the pathogenicity of actin variants: interaction defects with actin-binding proteins, haploinsufficiency, altered dynamics, or formation of toxic aggregates.

While the value of *in vitro* studies is undisputable, they may not fully capture the more complex processes that occur in an organism. The controlled environments of *in vitro* studies often overlook the variety of actin-binding proteins, focusing on a few to assess their specific interaction affinities. Additionally, these environments are often homogenous in time and space, which does not replicate the dynamic molecular changes occurring upon internal or external mechano- or chemosensory cues. Moreover, cell types have different concentrations of actin isotypes, which could lead to variability in functional compensation between them. Therefore, there is a need for *in vivo* studies as a complement to *in vitro* and *in silico* works to fully grasp the impacts of actin variants.

Chapter 3: *Caenorhabditis elegans*

Chapter introduction

The previous chapter highlighted studies in which NMA-associated variants were studied mostly *in vitro*, *in silico*, or both. These studies are of great importance. However, they do not allow the study of the variants' impacts in a full organism (COSTA ET AL., 2004). Animal models allowing the study of actin variants are rare and are, to my knowledge, restricted to two categories. The first one comprises actin knock-outs that can be used to study Loss of Function (LoF) variations, as introduced in Chapter 1 (BELYANTSEVA ET AL., 2009; VEDULA ET AL., 2017). The second category includes studies in which known variations have been introduced in an animal. This category currently includes, to my knowledge, one study in which Tsujimoto and colleagues used *Xenopus leavis* to study the S348L variant (TSUJIMOTO ET AL., 2024 BIORXIV) as well as the mention of an unviable mice model recapitulating the T120I variant (DI DONATO ET AL., 2024 MEDRXIV).

The need for studies in the second category is evident. We can assign this gap to the expensive, time-consuming, and sometimes difficult process of generating viable animals in which an actin coding gene is mutated. To fill this gap, the Reymann lab used *Caenorhabditis elegans* (*C. elegans*) to reproduce nine actin variants in one of its actin coding genes (*act-2*) and study their effect on the animal's development.

In this chapter, I will introduce the nematode *C. elegans*. Firstly, its development as a model organism and a general introduction to its development and organs. Secondly, I will introduce *C. elegans*' actin coding genes and their involvement during the animal's development. Overall, I would like to convince readers that this animal is a suitable, if not ideal, model for studying NMA.

A brief history of *C. elegans*

Nematodes were already used in scientific research in the late XIXth century because of their transparency and invariant cell numbers (NIGON AND FÉLIX, 2017). At that time, animals from the *Ascaris* genus were popular among researchers. However, these organisms lacked reproducibility, and cultures were delicate due to the animals' parasitic nature. Thus, efforts were made to use free-living nematodes that are much easier to maintain. This led to the description of *Rhabditis elegans* by Emile Maupas, who described the development of this species and its reproduction mechanisms (MAUPAS, 1899; MAUPAS, 1900). Later, *Rhabditis elegans* will be renamed to *Caenorhabditis elegans* (*C. elegans,* **FIGURE 22**).



Figure 22: *Caenorhabditis elegans* anatomy.

Thanks to Sydney Brenner, *C. elegans* undoubtedly gained popularity in the second part of the 20th century. Sydney Brenner sought an animal model to study the nervous system. He wanted the animal to be "*small in size*", to have "*a rapid life cycle*" and "*a simple reproductive cycle and genome*" (ANKENY, 2001). Starting in 1966, after trying different model organisms, Sydney Brenner focused his studies on *C. elegans*. Indeed, this animal matched all of Brenner's criteria. Firstly, it is a small animal, as the adult measures around 1mm. Secondly,

C. elegans has a fast life cycle. Indeed, it takes around three days at 20°C to develop from a zygote to a fertile animal that can produce around 300 progenies. Thirdly, *C. elegans*' reproductive cycle and genome were already characterized by Maupas, Honda, and Nigon, who found that this animal possesses six pairs of chromosomes. The authors found that *C. elegans* are mostly self-fertile hermaphrodite animals, although meiosis defects produce a small percentage of males able to mate with hermaphrodites (MAUPAS, 1900; HONDA, 1925; NIGON, 1943).

Sydney Brenner and colleagues published the famous "*The Mind of a Worm*", where the whole architecture and connections of the nervous system were reconstructed (WHITE ET AL., 1986), as well as "*The Genetics of Caenorhabditis elegans*", in which Sydney Brenner discovered that certain gene mutations could affect specific organ development (BRENNER, 1974). For this work, Sydney Brenner was awarded the Nobel Prize in Physiology or Medicine in 2002, shared with H. Robert Horvitz and John E. Sulston "*for their discoveries concerning genetic regulation of organ development and programmed cell death*" (NOBEL PRIZE, 2002). Indeed, taking advantage of the animal's transparency, John E. Sulston could observe and describe every cell division in the invariant cell lineage of the animal, during which he observed programmed cell death for the first time (SULSTON ET AL., 1983). Then, H. Robert Horvitz was the first to describe the genetic regulation of this process (ELLIS AND HORVITZ, 1986; HORVITZ, 1999). Other non-exhaustive, key studies involving *C. elegans* include the first whole genome sequencing of a multicellular organism (*C. ELEGANS* SEQUENCING CONSORTIUM, 1998), the discovery of RNA interference (FIRE ET AL., 1998; NOBEL PRIZE, 2006), the introduction of Green Fluorescent Protein (GFP) to track protein localization (CHALFIE ET AL., 1994; NOBEL PRIZE, 2008), and the discovery of miRNA (LEE ET AL., 1993; WIGHTMAN ET AL., 1993 ; NOBEL PRIZE, 2024). Nowadays, *C. elegans* is a widely accepted animal model, and Sydney Brenner's legacy is easily traceable (**FIGURE 23**).

Protégé par le droit à l'image

Figure 23: Sydney Brenner's lineage.

Actin in *C. elegans*, state-of-the-art

In Chapter 1, I introduced the fact that different actin-coding genes are differentially expressed to maintain cell homeostasis. The same holds true for *C. elegans* and its five actin-coding genes: *act-1*, *act-2*, *act-3*, *act-4*, and *act-5*. Although these actin isotypes' specificities are less known than those of human actin isotypes, I will review the current state-of-the-art.

Genetic structure and expression

act-1, *act-2,* and *act-3* (*act-123*) are located in a ~10kb cluster on chromosome V (**FIGURE 24**). Within this cluster, from 5' to 3', is first located *act-3*, then *act-2*, and then *act-1*. *act-2* and *act-3* are in reverse orientation, while *act-1* is in forward orientation. Genetically, these three genes are highly similar.

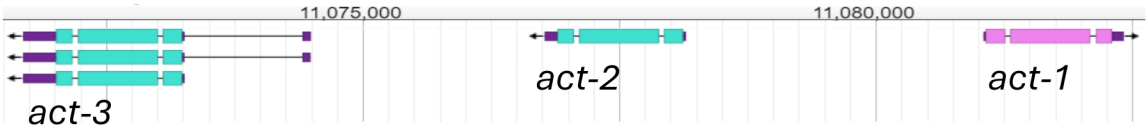

Figure 24: The *act-123* locus. *act-2* and *act-3* are in reverse orientation (turquoise), while *act-1* is in forward orientation (pink). *act-3* possesses three predicted transcripts. Upper numbers indicate the genetic position of the locus. Extracted from Wormbase's JBrowse, position V:11069053..11084366 (15.31 Kb). Accessed on 25/09/2024 (Sternberg et al., 2024).

At the nucleotide level, *act-1* and *act-3* share an identical coding sequence (**FIGURE 25**), producing the exact same protein (**FIGURE 26**). However, they have completely different 3' UTR (UnTranslated Region) as well as one variation in their 5' UTR and two variations in the second intron. On the other hand, *act-2* has more pronounced differences at the nucleotide level than *act-1* and *act-3* (**FIGURE 22**). Still, most of these variations are silent, and the ACT-1/ACT-3 proteins only have three amino acid substitutions of similar physico-chemical properties in contrast with ACT-2 (**FIGURE 23**). Compared to human actin proteins, ACT-2 is the most similar to ACTB and ACTG1, sharing 98 and 97% of amino acids. Accordingly, purified *C. elegans* actin can polymerize with rabbit muscular actin, highlighting the evolutionary conservation between nematode and mammalian actin proteins (ONO, 1999).

At the mRNA level, *act-3* has three predicted transcripts with different 5' UTR, while *act-1* and *act-2* have only one predicted transcript (**FIGURE 21**; STERNBERG ET AL., 2024). Although currently unknown, the implications of ACT-3 isoforms could potentially underlie important differences with ACT-1. *act-123* seem ubiquitously expressed and have functional redundancy

in the early embryo (WILLIS ET AL., 2006). We thus propose that these three genes constitute *C. elegans*' cytoplasmic actin.

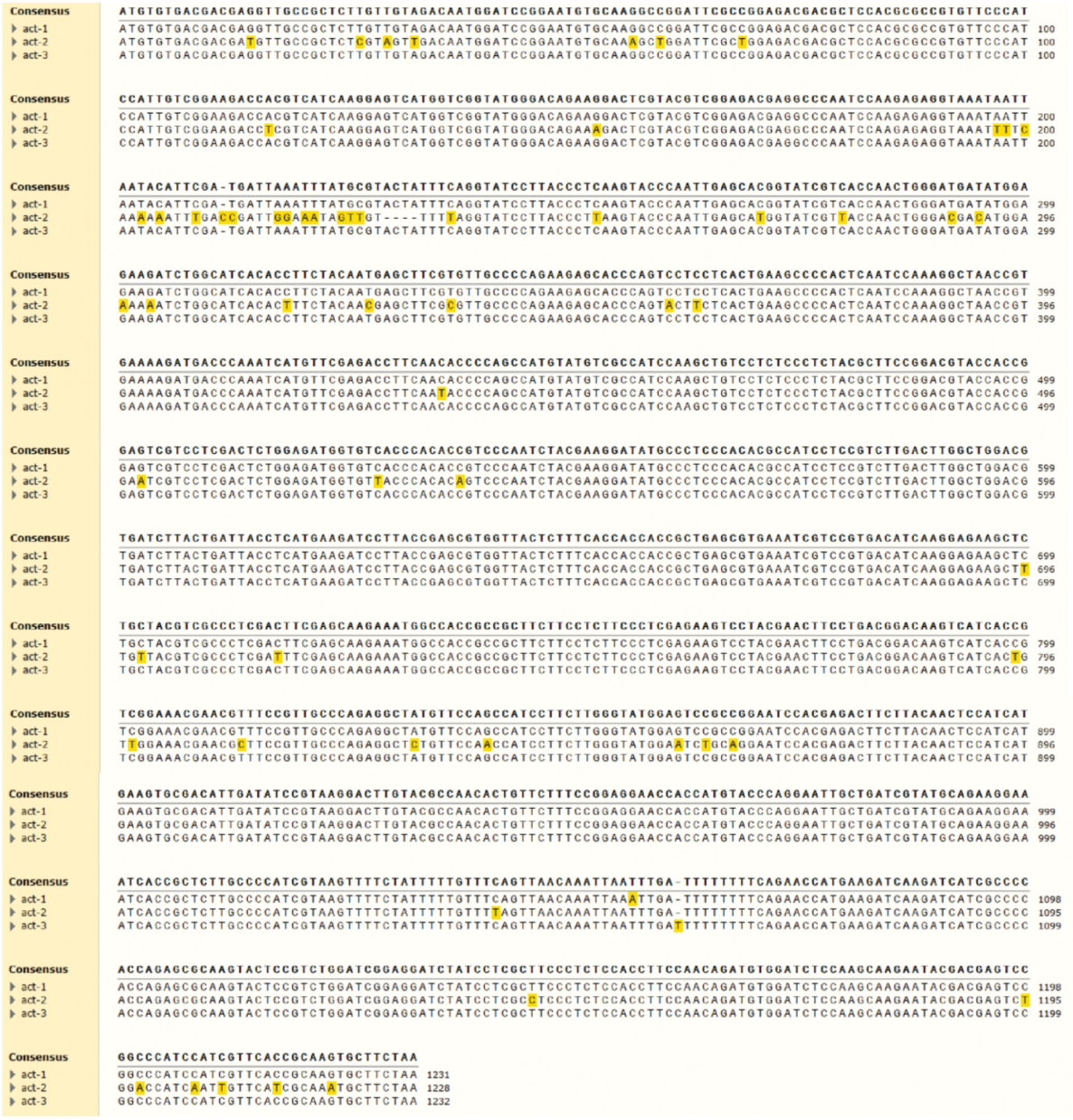

Figure 25: Nucleotide sequences alignment of *C. elegans*' actin genes *act-1*, *act-2*, and *act-3*. Yellow residues highlight differences between two or more sequences.

act-4 is located on the X chromosome and was historically hypothesized to be "*the main gene for cytoplasmic actin*" (WOOD, THE NEMATODE CAENORHABDITIS ELEGANS, 1988). Nevertheless, ACT-4 is enriched in the body wall and vulval muscles as well as in the pharynx (STONE AND SHAW, 1993), which is thus closer to a muscular actin pattern of expression. ACT-4 amino acid sequence is very similar to ACT-1/ACT-3 and ACT-2 (**FIGURE 26**), although many silent variations exist in their nucleotide sequences.



Figure 26: Amino acid sequences alignment of *C. elegans*' actin proteins. Yellow residues highlight differences between two or more sequences.

act-4 has two validated transcripts (A and B), leading to two protein isoforms. Transcript B differs from transcript A by excluding *act-4*'s first exon and UTRs. They also have different expression values, as transcript B is clearly less abundant than transcript A (STERNBERG ET AL., 2024; HTTPS://WORMBASE.ORG/DB/GET?NAME=M03F4.2A.1#061--10;CLASS=TRANSCRIPT; HTTPS://WORMBASE.ORG/DB/GET?NAME=M03F4.2B.1#061--10;CLASS=TRANSCRIPT). Transcriptomics analysis by Hammarlund and colleagues revealed that *act-4* mRNA is enriched in neurons compared with the other *C. elegans*' actin isotypes (HAMMARLUND ET AL., 2018). However, the authors did not look at the differential expression of transcripts A and B (HAMMARLUND ET AL., 2018). The potential specific functions of these transcripts are unknown.

Finally, *act-5* is present on chromosome III and has a single transcript. ACT-5 shows the most differences compared to the other *C. elegans*' actin coding genes (**FIGURE 22B**). Indeed, ACT-5 has 28 amino acid differences compared to ACT-2 and ACT-4, as well as 29 amino acid variations compared to ACT-1 and ACT-3. ACT-5 shows specific, localized expression in the intestinal and excretory cells where ACT-5 is essential for microvilli formation (MACQUEEN ET AL., 2005).

Null variants

C. elegans strains with endogenous null alleles of the different actin coding genes have been generated, often leading to harsh phenotypes. Three *act-5* null alleles (*ok1397*, *dt2017,* and *dt2019*) cannot be maintained when homozygous (ESTES ET AL., 2011; MACQUEEN ET AL., 2005). The same homozygous lethal phenotype is observed in an *act-4* null allele (*gk5951,* AU ET AL., 2019). However, an *act-2* knockout (*ok1229*) showed no obvious phenotypes except for a slight increase in embryonic lethality at 26°C (WILLIS ET AL., 2006). Although knockouts of either *act-1* or *act-3* were not published, the Reymann team obtained two *act-1* knockout alleles that show no obvious phenotypes (*bab725,* SEGiCel; *syb5801*, SunyBiotech). Nonetheless, a large deletion that is not mapped precisely but spans the *act-123* locus leads to the generation of homozygous sterile animals (*stDf4,* IWASAKI ET AL., 1996; https://cgc.umn.edu/strain/RW3455). Part of my PhD work was dedicated to further characterizing *act-2* null alleles.

Isoactin switching

As in humans, isoactin switching exists in *C. elegans*. Indeed, the laboratory of Didier Stainier recently published studies describing a transcriptional adaptation mechanism in actin mutant animals (JIANG ET AL., 2022; SEROBYAN ET AL., 2020; WELKER ET AL., 2023). These studies notably found that the presence of an endogenous *act-5* allele containing a premature STOP codon (*dt2019*) led to an increase in *act-3* mRNA synthesis (SEROBYAN ET AL., 2020). This *act-5* null allele also led to ACT-3 expression (extrachromosomal promotor reporter) in the intestine, where ACT-5 should be expressed in physiological conditions (SEROBYAN ET AL., 2020). Remarkably, this adaptation only requires a 25bp sequence of *act-5*(*dt2019*) (WELKER ET AL., 2023). ACT-3 expression pattern change is independent of the copy number of the *act-5* null allele *dt2019*. Indeed, isoactin switching was maintained in 100% of the F1 progeny of heterozygous *dt2019* animals, demonstrating transgenerational inheritance of transcriptional adaptation, even in wild-type animals (JIANG ET AL., 2022). Isoactin switching was also proposed to explain the mild phenotypes observed by the lab of Bruce Bowerman in the case of an *act-2* KO allele (*ok1229*, WILLIS ET AL., 2006).

C. elegans embryonic development

After this introduction of *C. elegans* and our current knowledge concerning its actin-coding genes, I will introduce some aspects of the animal's exceptionally reproducible and robust embryonic development (**FIGURE 27**; HALL ET AL., 2017), focusing on the involvement of actin throughout these processes.

Protégé par le droit à l'image
doi:10.3908/wormatlas.4.1

Figure 27: Embryonic development of *C. elegans* at 22°C.

Egg activation, symmetry breaking, and first-cell division

Every 20 minutes, ovulation occurs by gonadal sheath cell contraction that pushes an oocyte into the spermatheca. The spermatheca is filled with numerous amoeboid spermatozoa containing 'male' DNA. Quickly, one spermatid fertilizes the oocyte, leading to a series of processes collectively coined as egg activation. This includes forming an eggshell, completing meiosis, and reorganizing the oocyte cytoskeleton (SINGSON, 2010).

Eggshell formation

Sperm DNA entry triggers the formation of an eggshell: a rigid, impermeable, multi-layered protection (**FIGURE 28**, STEIN, 2018). This structure is formed in a matter of minutes. It helps to prevent polyspermy, meiosis failure, and is required for the proper establishment of polarity in the embryo (JOHNSTON ET AL., 2010, 2006). Accordingly, the eggshell is essential at the early stages of development (SCHIERENBERG AND JUNKERSDORF, 1992). However, some layers are dispensable, as removing the chitinous coat of the eggshell does not impair embryo development despite rendering it very fragile (SCHIERENBERG AND JUNKERSDORF, 1992).

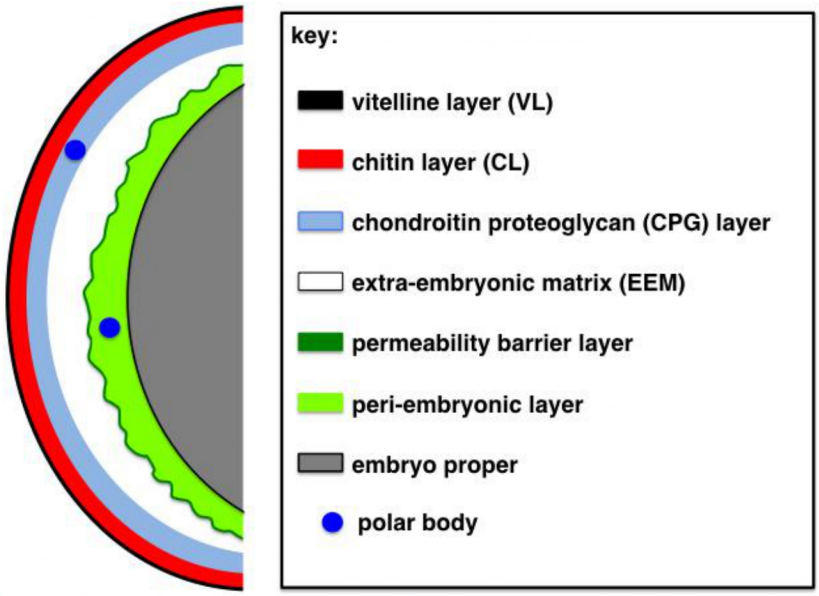

Figure 28: Schematic of the layers of the *C. elegans* eggshell. Shown is the trilaminar eggshell consisting of an outermost vitelline layer (VL; black), a middle chitin layer (CL; red), and an innermost chondroitin proteoglycan layer (CPG; blue). Separating the trilaminar outer eggshell from the inner permeability barrier (dark green) is the extra-embryonic matrix (EEM; white). Under the permeability barrier layer is an amorphous peri-embryonic layer (light green), which coats the embryo proper (gray). The plasma membrane of the embryo is shown as a black line. The polar bodies are shown in dark blue; the first polar body is immobilized in the CPG layer of the trilaminar outer eggshell, while the second polar body is mobile in the peri-embryonic layer. Figure and legend extracted from Stein, 2018.

Completion of meiosis

Concomitantly to eggshell formation, the female pronucleus completes meiosis. Meiosis is defined as a reduction of ploidy by a specialized cell division to generate haploid gametes apt for sexual reproduction (HILLERS, 2017; HURLOCK ET AL., 2020). In a *C. elegans*' oocyte, as in most multicellular organisms, two rounds of meiotic division are needed to create haploid maternal DNA. These cell divisions are asymmetric, forming the gamete and polar bodies, small cells containing half of the mother's cell genetic material. As mitosis, meiosis is highly dependent on actin and requires the formation of a contractile ring. However, contractile ring constriction is slightly different in meiosis compared to mitosis. Indeed, instead of ingressing circumferentially directly toward the midpoint of segregating chromosomes, the meiotic contractile ring ingresses laterally along one end of the spindle pole before closing (**FIGURE 29**, FABRITIUS ET AL., 2011). During this process, the male pronucleus is maintained at the opposite side of the embryo, presumably by a transient F-actin structure that cages it (MARUYAMA ET AL., 2007; PANZICA ET AL., 2017). Numerous studies observed meiosis defects linked to actin or actin-binding protein mutations, in the case of an RNAi of a scaffolding ABP called anillin (*ani-1*; DORN ET AL., 2010), or in *act-2* variant alleles (*or295* and *or621*; WILLIS ET AL., 2006). These lead to the presence of a supernumerary nucleus visible in the zygote, presumably from failure in polar body extrusion.

Protégé par le droit à l'image
https://doi.org/10.1016/j.ydbio.2011.08.013

Figure 29: Global contraction model for polar body formation. There is an actomyosin ring on the surface of the embryo with a more flexible actomyosin-free center through which the spindle is pushed. Force is generated by global actomyosin contractility. *In utero*, it appears that the contractile ring is moving inward along the spindle (arrowheads). Gray-eggshell, black-membrane/cortex, red — microtubules, green — myosin, blue — chromosomes. Figure and legend adapted from Fabritius et al., 2011.

Symmetry breaking and polarity establishment

Close to the completion of female meiosis, the paternal DNA migrates toward the actin cortex and marks the future posterior pole of the embryo (Samandar Eweis and Plastino, 2020).

Prior to male DNA migration, the zygotic cell cortex is homogeneously contractile (**FIGURE 30A**). However, the centrosome brought by the sperm releases a kinase called AIR-1 that locally inactivates actomyosin contractions at the embryo's posterior side by displacing the RhoGEF ECT-2 toward the anterior (**FIGURE 30B**, SAMANDAR EWEIS AND PLASTINO, 2020). ECT-2 is an activator of the RhoA RHO-1 that, in turn, leads to formin-mediated actin polymerization and myosin activation. This results in actomyosin foci movement and enrichment to the anterior, which creates asymmetrical cortical contractions. This asymmetry initiates a cortical flow toward the anterior side of the embryo and an opposite cytoplasmic flow (SAMANDAR EWEIS AND PLASTINO, 2020).

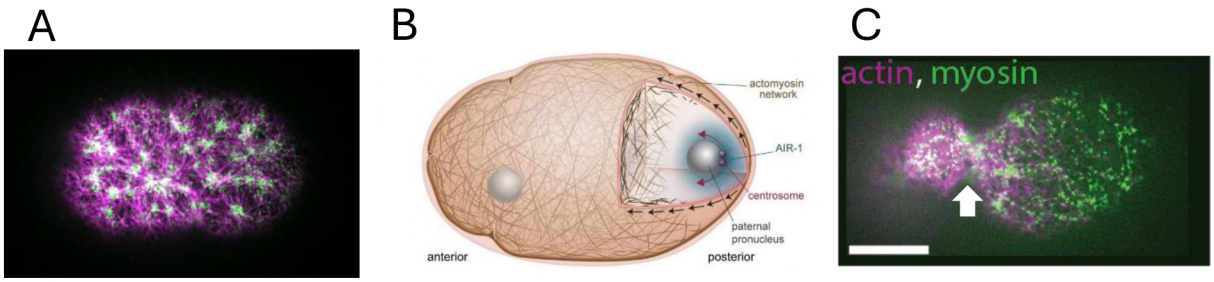

Figure 30: Symmetry breaking of the C. elegans' zygote. (A) Spinning disk acquisition of the cortex of a one cell stage embryo before symmetry breaking. (B) Symmetry breaking in the one-cell embryo. AIR-1 (blue cloud) is the cue that initiates polarization of the embryo. AIR-1 diffuses from the centrosome (red spheres) and downregulates actomyosin at the adjacent cortex. This causes a local weakening, and produces cortical flows (black arrows) directed away from this point. Figure and legend extracted from Eweis & Plastino, 2020. (C) Spinning disk acquisition of the cortex of a one cell stage embryo after symmetry breaking. The pseudocleavage is visible (white arrow). Scale bar = 10µm. Actin (LifeAct::mKate2) is purple and myosin (NMY-2::GFP) is green. Anterior is on the left, posterior on the right.

These flows are essential to break the zygote's symmetry (**FIGURE 30C**). Indeed, cortical flows contribute to the asymmetrical distribution of PAR proteins (abnormal embryonic PARtitioning of cytoplasm), although the opposite is also true (LANG AND MUNRO, 2017). PAR proteins allow the anteroposterior segregation of cell fate determinants through a complex inter-regulatory network (LANG AND MUNRO, 2017). Therefore, PAR polarity establishment coupled with actomyosin-driven flows are essential for the robustness in the success of

embryonic development (LANG AND MUNRO, 2017). Accordingly, disrupting the cell cortex dynamics by knocking down the CYK-1 formin or the non-muscle myosin NMY-2 impairs cortical flux and polarity establishment (PACQUELET, 2017; NAGANATHAN ET AL., 2018).

At the end of polarity establishment, cortical actin filaments align circumferentially to form the "pseudocleavage", a structure similar to the mitotic contractile ring that does not ingress completely (**FIGURE 30C**, SAMANDAR EWEIS AND PLASTINO, 2020). Then, pronuclei start to migrate toward each other (**FIGURE 31**). The posterior male pronucleus migrates anteriorly around 15% of the length of the embryo in a process partially mediated by the Arp2/3 complex (XIONG ET AL., 2011). At the same time, the female pronucleus migrates posteriorly through a dynein-mediated process (MEADERS AND BURGESS, 2020) while the pseudocleavage relaxes. The female pronucleus contacts the male pronucleus at the posterior side of the embryo and forms a complex with the male pronucleus upon their meeting. The newly formed complex migrates anteriorly to the middle of the embryo in a microtubule-dependent event called "centration" (**FIGURE 31**, DE SIMONE ET AL., 2018; NAZOCKDAST ET AL., 2017). Then, the pronuclear complex rotates 90°, and its pronuclear envelope breaks for pronuclei fusion (NAZOCKDAST ET AL., 2017).

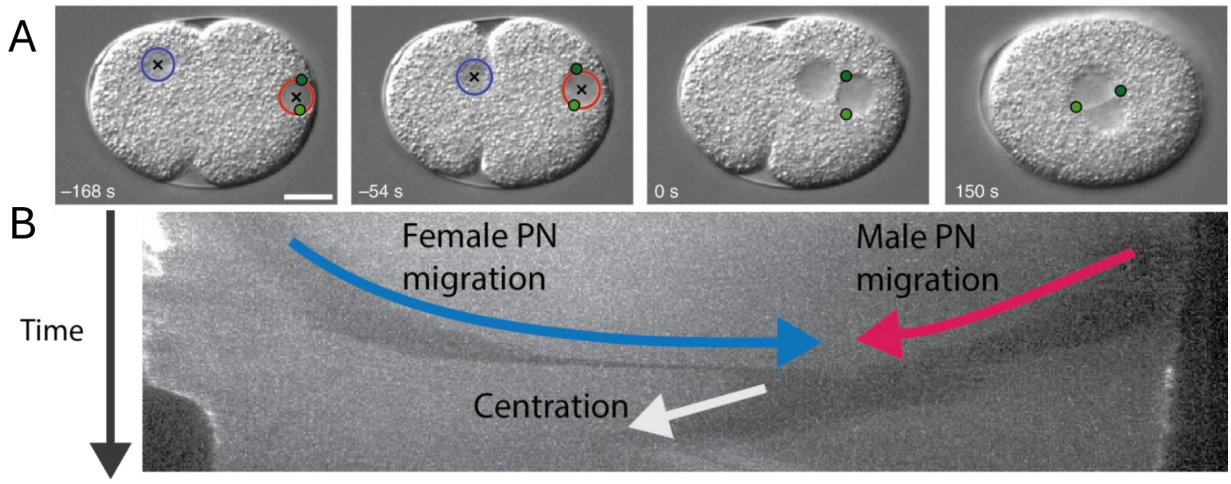

Figure 31: *C. elegans'* pronuclei migration. (A) Nomarski microscopy; centrosomes (green dots), the female pronucleus (blue circle), and the male pronucleus (red circle) are represented; black crosses: pronuclei centers—z-projections. 0 s: pronuclear meeting; scale bars: 10 µm. Figure and legend adapted from De Simone et al., 2018. (B) Kymograph of a one cell stage embryo where pronuclei migrations are visible (Maternal blue, Paternal red). Contact of pronuclei occurs at the embryo's posterior side, where they form a complex. White arrow depicts centration of the pronucleus complex. Anterior is on the left, posterior on the right.

In summary, the zygote's polarity establishment leads to an anteroposteriorly defined cell with a cortical anterior enrichment of actomyosin (**FIGURE 32**). Interestingly, the anterior side is enriched in filopodia and endocytic foci during this process (HIRANI ET AL., 2019). Although filopodia roles are currently unknown, we cannot exclude their implication in polarity establishment.

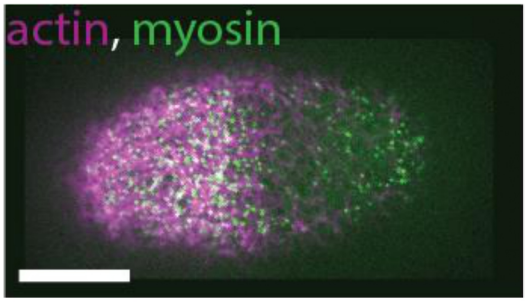

Figure 32: A *C. elegans* zygote with established anteroposterior polarity. Spinning disk acquisition of the cortex of a one cell stage embryo after polarity establishment. Scale bar = 10µm. Actin (LifeAct::mKate2) is purple and myosin (NMY-2::GFP) is green. Anterior is on the left, posterior on the right

Maintenance and the first cell division

Mitosis follows rapidly after pronuclei fusion. As mammalian cell division (introduced In CHAPTER 1), *C. elegans*, cytokinesis requires the formation of a contractile ring that will constrict to eventually enable the mother cell to divide into two daughter cells upon abscission.

C. elegans has proven to be a powerful system for understanding the molecular requirements of cell division, conserved between the nematode and mammals. Its transparency enables an easy observation of cell division in the context of altered gene function or expression. Indeed, this animal allows the use of drugs and precise regulation of gene knockdown levels by RNAi, thermosensitive, or null alleles to decipher the requirement in time and place of cell division molecular actors (CARVALHO ET AL., 2011; DAVIES ET AL., 2014; GÖNCZY ET AL., 2000; SÖNNICHSEN ET AL., 2005).

Contractile ring forms by local Rho1 (RhoA) activation and filament alignment (GLOTZER, 2005). RhoA activates the 'CYtoKinesis defect' (CYK-1) formin-mediated actin polymerization and recruitment of NMY-2 (non-muscle myosin 2) (PIEKNY AND MAINS, 2002). Accordingly, both genes are essential for cytokinesis, and actin depletion by latrunculin A leads to cytokinesis failure (CARVALHO ET AL., 2011). However, milder depletion of actin by RNAi only shows a defect in polarity establishment but not cytokinesis (VELARDE ET AL., 2007).

NMY-2 is essential at all steps of cytokinesis, as observed using a thermosensitive conditional loss of function allele of NMY-2 (DAVIES ET AL., 2014). However, using a similar

method, Davies and colleagues observed that CYK-1 is only essential until mid-constriction of the ring (DAVIES ET AL., 2014). This is reminiscent of capping protein requirement in the late steps of cytokinesis (GIBIEŽA AND PETRIKAITĖ, 2021). Partial knockdown of CYK-1 still allows the formation of a ring, although more fragile, while total depletion leads to cytokinesis defects. In contrast, branched filament formation is not required for cytokinesis in *C. elegans*, as knocking down a member of the Arp2/3 complex does not lead to cytokinesis failure (CHAN ET AL., 2019). Remarkably, Chan and colleagues discovered that impairing Arp2/3-mediated nucleation leads to increased actin formation within the contractile ring and delayed ring formation and constriction by competing with formin-mediated nucleation during cell division (CHAN ET AL., 2019).

Interestingly, anillin is not needed for cytokinesis in physiological conditions (MADDOX ET AL., 2005). However, anillin is needed for a cell division compensatory mechanism when CYK-1 and septin are simultaneously depleted in *C. elegans* (LEBEDEV ET AL., 2023).

The first cell division is highly reproducible and robust and results in a size asymmetry of the two daughter cells, AB and P1 (**FIGURE 33**, GREEN ET AL., 2008), based on the spindle displacement by microtubule-associated mechanisms (SAMANDAR EWEIS AND PLASTINO, 2020). In the case of cytokinetic furrow mispositioning, cortical blebbing can form at the furrow bases to reposition it and prevent DNA segregation errors (PACQUELET ET AL., 2019).

Protégé par le droit à l'image
https://doi.org/10.1016/S0091-679X(08)85009-1

Figure 33: Timeline of events in the *C. elegans* early embryo

Gastrulation

From the 2-cell stage embryo, cells continue to divide following precise time and space regulation, essential for proper cell-to-cell signaling and fate specification in a process partially mediated by the eggshell constraining the embryo (Bao et al., 2008; Yamamoto and Kimura, 2017). This leads to the formation of the dorsoventral and the left-right axis at the 4- and 6-cell stage embryo. After a series of controlled rounds of cell divisions, the embryo comprises 26 cells and is expelled from the mother's uterus (Nance et al., 2005). At this stage, gastrulation starts, concomitantly to cell division. This event lasts around 3 hours at 20°C and ends around the embryonic 300th cell stage (Nance et al., 2005). Gastrulation is a conserved, essential process during which the three germ layers (ectoderm, mesoderm, and endoderm) are established and concomitantly undergo stereotyped morphogenetic movements in the embryo (Hunter and Fernandez-Gonzalez, 2013). *C. elegans'* gastrulation is marked by the internalization of 66 cells, starting with the endodermal cells Ea and Ep (Goldstein and Nance, 2020). The internalizations of these cells are the most studied, as the subsequent cell divisions make the next internalizing cells smaller and harder to observe *in vivo*.

Ea and Ep constrict apically to internalize in a non-muscle myosin-based process (**Figure 34**, Lee and Goldstein, 2003; Nance and Priess, 2002). The mechanical mechanism of this apical constriction has recently been characterized by Zhang and colleagues (2023). The authors found that actomyosin networks in the apical cortex of Ea and Ep were randomly oriented (Zhang et al., 2023). The authors hypothesized that this distribution associated with myosin contraction and severing of 'buckled' actin filaments could drive apical constriction (Zhang et al., 2023).

Studies observed that RNAi of two Arp2/3 subunits slowed down Ea and Ep internalization but only led to partially penetrant arrest at gastrulation (Roh-Johnson and Goldstein, 2009; Severson et al., 2002). Rho Johnson and Goldstein hypothesize that Ea and Ep internalization is not a fully cell-autonomous process. Indeed, they observed that three neighboring cells of Ea and Ep form dynamic Arp2/3-mediated cell protrusions during gastrulation (Roh-Johnson and Goldstein, 2009). However, it is unclear if such structures are required, as specific depletion has not yet been successfully performed (Roh-Johnson and Goldstein, 2009).

Although less studied, the following cells seem to also internalize by apical constriction (GOLDSTEIN AND NANCE, 2020), except the germline precursors that seem to be pulled by adhering to internalizing endodermal cells (CHIHARA AND NANCE, 2012).

Once cells have internalized, the final step of gastrulation, called ventral cleft closure, occurs. Ventral cleft closure is a process during which neuroblasts migrate to fill the "scar" left by the internalization of cells during gastrulation (**FIGURE 35**; CHISHOLM AND HARDIN, 2005). This step involves actin-based motility as the loss of an Arp2/3 complex activator (*wve-1*) leads to ventral cleft closure defects (WITHEE ET AL., 2004), which impairs the next step of embryonic development called ventral enclosure (VUONG-BRENDER ET AL., 2016).

Protégé par le droit à l'image
DOI: 10.1242/dev.102228

Protégé par le droit à l'image
https://doi.org/10.1534/genetics.119.300240

Figure 34: *C. elegans*' gastrulation.

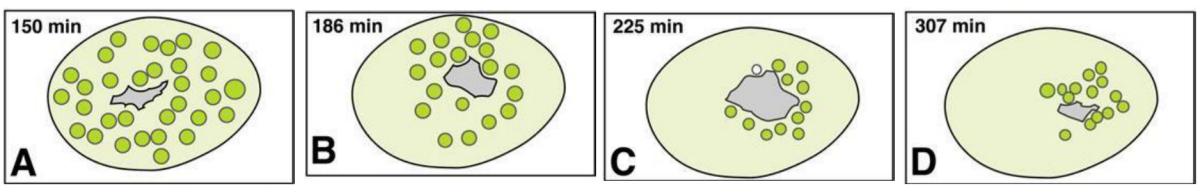

Figure 35: *C. elegans*' ventral cleft closure. Ventral view schematics of ventral neuroblast positions (green circles) during closure of the ventral cleft (grey zone). Figure and legend adapted from Chisholm, & Hardin, 2005.

Ventral enclosure

Soon after the end of gastrulation by ventral cleft closure, ventral enclosure takes place. Ventral enclosure leads to the engulfment of the embryo in epidermal cells that will form the animal's skin. This process begins with lamellipodia-based migration of the two anterior-most epidermal cell pairs from the embryo's dorsal until contact at the ventral side (**FIGURE 36**, VUONG-BRENDER ET AL., 2016). As expected for lamellipodia-based migration, branched actin polymerization is essential. Indeed, genetic or drug-based inhibition of the Arp2/3 complex leads to failure in completing ventral enclosure and the subsequent death of the embryo (VUONG-BRENDER ET AL., 2016). The leading cells are followed by eight pairs of posterior epidermal cells called pocket cells. Unlike leading cells, pocket cells do not migrate until contact (VUONG-BRENDER ET AL., 2016). Instead, they stop, leaving a "ventral pocket". Pocket cells then form an apical *"actin-rich border"*, which allows the pocket cells to undergo a purse-string contraction, closing the ventral pocket (**FIGURE 36**, MARTIN AND SUZANNE, 2022). Shortly after, the ventral enclosure ends with the head engulfment by anterior epidermal cells (CHISHOLM AND HSIAO, 2012).

Despite a modest requirement of branched-based networks in early embryogenesis, they are essential to ensure the success of the early steps of morphogenesis, which can thus serve as a proxy to probe Arp2/3 functionality.

Protégé par le droit à l'image
https://doi.org/10.1016/bs.ctdb.2015.11.012

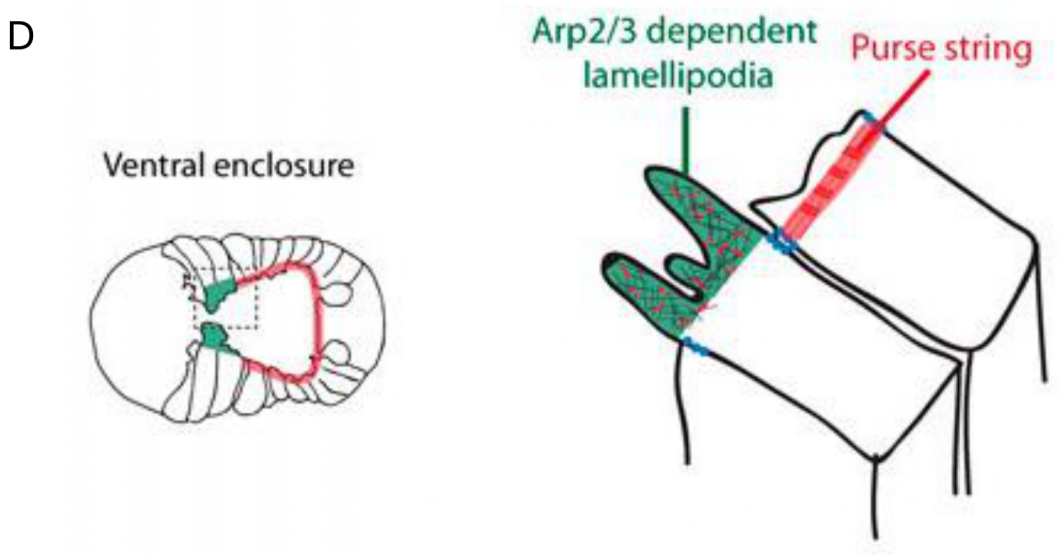

Figure 36: *C. elegans*' ventral enclosure.

(D) Epithelial sealing mechanisms during ventral enclosure in *C. elegans*. Figure and legend extracted from Martin & Suzanne, 2022.

Elongation

After ventral enclosure, the embryo starts elongating. During this process, the bean-shaped embryo lengthens into a worm-like shape without cell division. Elongation is a relatively long process, lasting around 4 hours at 20°C and requiring again the cytoskeleton (Priess and Hirsh, 1986). Elongation is divided into two phases based on their lengthening mechanisms. First, the "bean to 1.8-fold" stage is a short phase where elongation depends exclusively on the epidermis. Secondly, the "1.8- to 4-fold stage" depends on the interplay between the epidermis and the muscle cells, whose contractions are essential for morphogenesis to occur (**FIGURE 37**, DAI AND BEN AMAR, 2024).

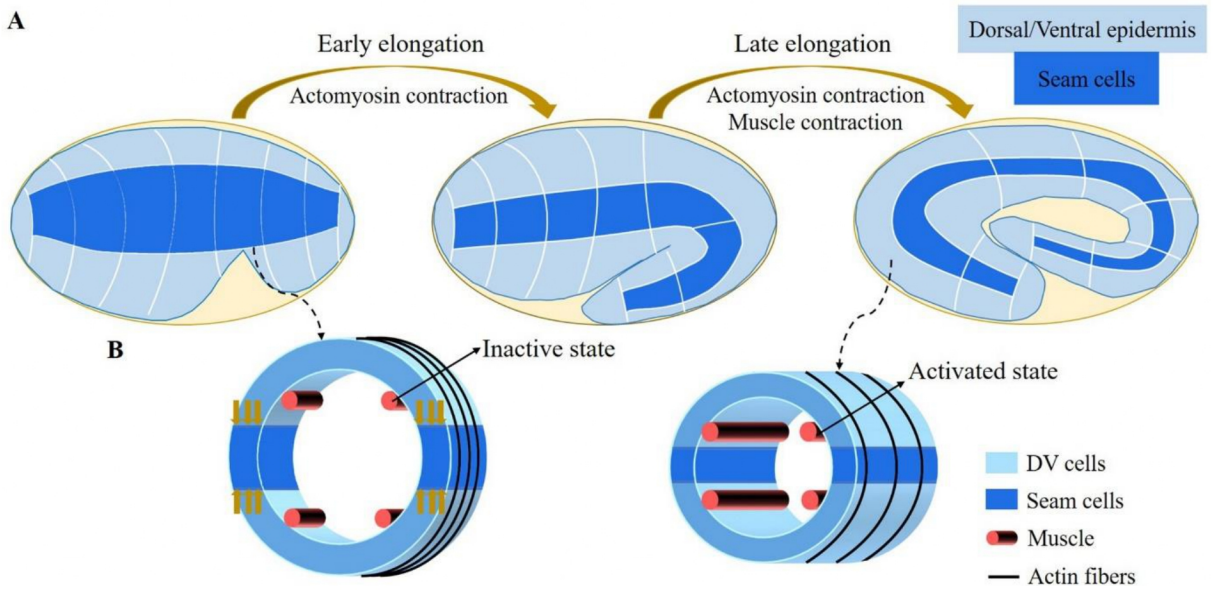

Figure 37: *C. elegans* elongation. (A) Overview of *C. elegans* embryonic development. Three epidermal cell types are found around the circumference: dorsal, ventral, and seam cells. (B) Schemes showing a *C. elegans* cross-section of the embryo. Small yellow arrows in the left image indicate the contraction force that occurred in the seam cell. Four muscle bands under the epidermis and actin bundles surround the outer epidermis. Figure and legend extracted from Dai & Amar, 2024

Bean to 1.8-fold stage

The “bean to 1.8-fold” elongation step refers to the start and end shape of the embryo. The 1.8-fold stage means that the length of the embryo is 1.8 times the length of the eggshell. At these stages, the embryo can be simplified as a tube with dorsal and ventral epidermal cells (DV) separated by “central” epidermal seam cells that encapsulate inactive muscle cells (**Figure 37**, Dai and Ben Amar, 2024). These cells have different actomyosin structures. In the DV cells, actin filaments are organized in parallel circumferential bundles, whereas the seam cells' actin filaments are less organized (**Figure 38**, Vuong-Brender et al., 2016). Additionally, seam cells are enriched in myosin (Gally et al., 2009). These differential actin structures are important for the bean to 1.8-fold transition. Indeed, the actomyosin organization of seam cells allows their contraction, while the actin bundles in the neighboring DV cells maintain the embryo’s integrity and allow a directed circumferential contraction (Vuong-Brender et al., 2017). The resulting biophysical forces drive the first step of embryonic elongation. This step is thus dependent on actomyosin forces in non-muscle cells. During this process, actin filaments in the seam cells rearrange to be more organized, eventually leading to the formation of a circumferential pattern, as in DV cells, at the end of this first elongation stage (**Figure 38**, Gillard et al., 2019).

Protégé par le droit à l'image □
DOI: 10.1016/j.cub.2019.02.059

Figure 38: Actin during the first stage of *C. elegans*’ elongation.

1.8 to 4-fold

The second elongation stage starts concomitantly with the activation of muscle cells beneath the epidermis (VUONG-BRENDER ET AL., 2016). This muscle activation is essential for morphogenesis, as mutants that fail to contract muscles fail to elongate past the 1.8-fold stage (called Pat for paralyzed at two-fold), and is clearly visible as the embryo "twitches" within its eggshell.

During late elongation, muscles from the left and right sides of the embryo do not contract simultaneously (VUONG-BRENDER ET AL., 2016). Because the muscle cells are connected to the epidermis by hemidesmosomes, these contractions induce epidermal cell shape changes by mechanotransduction (Zhang et al., 2011). Indeed, the asynchronous contraction of muscle leads to a cycle between the compression of epidermal cells, when muscles are contracted, followed by stretching when the opposite muscles are contracted (VUONG-BRENDER ET AL., 2016). Contraction forces are sufficient to drive an architectural change in the epidermal cells' actin filaments. Indeed, a recent study demonstrated that epidermal cell contraction transiently bends the circumferential actin filaments at an angle superior to 54° (**FIGURE 39**, LARDENNOIS ET AL., 2019). This angle is critical and has been associated *in vitro* with an increase in actin severing by ABP (LARDENNOIS ET AL., 2019). In the embryo, the actin microfilaments are quickly re-stabilized after breakage but slightly shorter (**FIGURE 39**). That is how, little by little, cycle by cycle, the embryo elongates until it reaches a length four times the length of the eggshell (YANG ET AL., 2024, BIORXIV; DAI AND BEN AMAR, 2024; LARDENNOIS ET AL., 2019).

Protégé par le droit à l'image
https://doi.org/10.1038/s41586-019-1509-4

Figure 39: Actin during the second stage of *C. elegans*' elongation.

Therefore, proper actin dynamics and stability is required to properly drive elongation. Indeed, defects in the re-stabilization of actin microfilaments lead to a characteristic phenotype of retractation, where the embryo retracts to its length before elongation (LARDENNOIS ET AL., 2019). Contractility also needs to be tightly regulated as hypocontractility leads to impaired elongation and small embryos, whereas hypercontractility can lead to the burst of the embryo (VUONG-BRENDER ET AL., 2016).

Ready to hatch?

Approximately 3 hours (at 20°C) are needed between the end of elongation and hatching. The embryo moves a lot in its eggshell at this stage, rendering its observation difficult. Nonetheless, studies have shown that the animal's first cuticle is generated during this period (CHISHOLM AND HARDIN, 2005). Additionally, pharyngeal pumping starts 50 minutes before hatching., which is hypothesized to weaken the eggshell by chitinase secretion (HALL ET AL., 2017; CHISHOLM AND HARDIN, 2005).

Conclusion on the embryonic development of *C. elegans*:

In this section, we learned that actin is essential during multiple steps of the exceptionally reproducible embryonic development of *C. elegans* to form an animal ready to face the environment outside of its eggshell. To complete embryonic development, actin must be spatiotemporally organized into structures highly regulated by different ABPs, such as a contractile ring during cell division or lamellipodia during ventral enclosure. Failures in these processes have been reported by various groups when working with RNAi, drugs, or mutant strains and are thus highly documented. Therefore, observing failure in specific developmental processes could hint at the molecular aspects and pathways implicated in a mutant background, bridging the gap between the cellular and the molecular scale. I introduced only some highly anatomically recognizable events during embryonic development, omitting other, non-less important processes such as dorsal intercalation (WALCK-SHANNON AND HARDIN, 2016), the formation of the digestive system (DIMOV AND MADURO, 2019), the formation of the nerve ring (ALTUN, 2017), or the essential involvements of other cytoskeletal components (Hurd, 2018; Zuela and Gruenbaum, 2016).

Post-embryonic development

After hatching, the animal is at the L1 stage. Contact with food starts its post-embryonic development, where the animal will go through 4 larval stages (L2, L3, L4, and adult), separated by four molting events (**FIGURE 40**, ALTUN AND HALL, 2009). Under extreme conditions, *C. elegans* can go into an arrested stage called 'Dauer' after its first molting event, during which the larva can survive without food for up to 4 months or until conditions ameliorate (**FIGURE 40**). This state will not be thoroughly introduced in this manuscript on purpose. I redirect interested readers to HU, 2018. In this section, I will introduce some aspects of the post-embryonic neurodevelopment and gonadogenesis of *C. elegans*, highlighting actin involvement during these processes and how they can serve as models for specific actin-related processes.

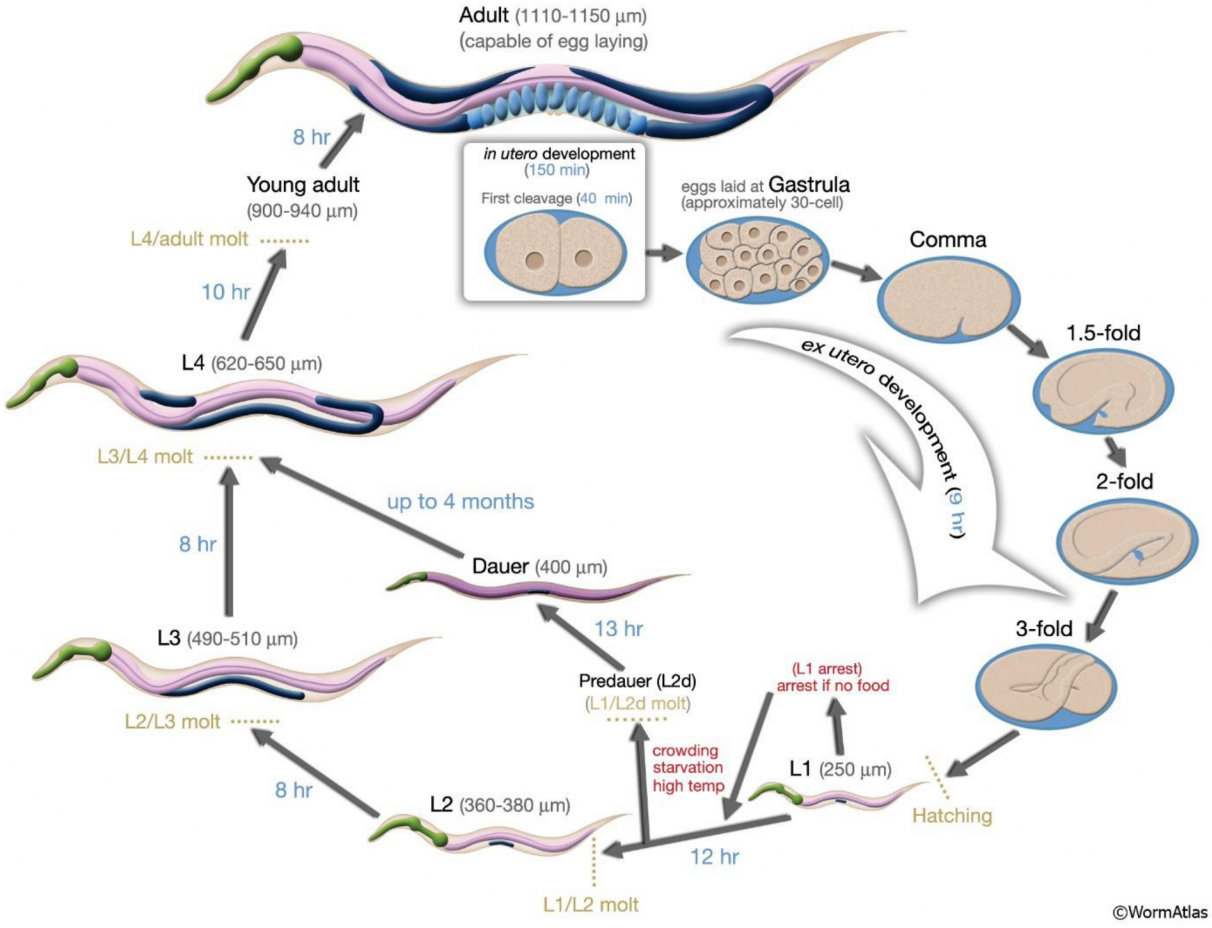

Figure 40: Life cycle of *C. elegans* at 22°C. 0 min is fertilization. Numbers in blue along the arrows indicate the length of time the animal spends at a certain stage. First cleavage occurs at about 40 minutes post-fertilization. Eggs are laid outside at about 150 minutes post-fertilization and during the gastrula stage. The length of the animal at each stage is marked next to the stage name in micrometers (µm). Figure and legend extracted from Altun and Hall, 2009.

Nervous system

General information on C. elegans' nervous system

The nervous system is a complex network of interconnecting neuronal and glial cells. They communicate together and with other organs through electrical and chemical transmitters with specialized processes called synapses, which allow the organism to respond to mechanical and sensory inputs. The hermaphrodite *C. elegans* nervous system comprises 302 neurons, subdivided into 118 classes (HOBERT, 2010). These classes were initially based on anatomical features (WHITE ET AL., 1986) but were confirmed recently using transcriptomic data (TAYLOR ET AL., 2021). Neuronal structure and function are supported by 56 glial cells (SHAHAM, 2015).

The animal's head contains most neurons, mainly organized into the "nerve ring", often described as the animal's brain (ALTUN, 2017). The rest of the neurons are present across the animal's body, organized into multiple ganglia (**FIGURE 41A**, HOBERT, 2010). As in Humans, *C. elegans* possess interneurons, motor neurons, and sensory neurons (**FIGURE 41B**, HOBERT, 2010). Neurons are often present as left and right pairs in the animal (-L and -R suffixes) that seem to have similar functions. However, more and more studies show that some neuronal pairs have slightly different transcriptomic profiles that might have roles in fine-tuning behavioral phenotypes (BERTRAND ET AL., 2011; CHAREST ET AL., 2020; DAVIS ET AL., 2021; QUINTIN AND CHARVIN, 2022).

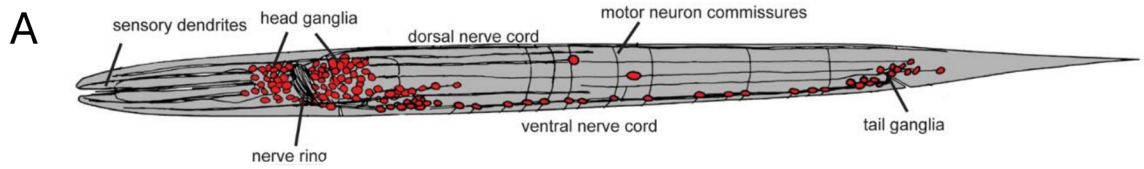

Protégé par le droit à l'image
https://doi.org/10.1093/genetics/iyae116

Figure 41: The *C. elegans* nervous system. (A) Overall organization of the *C. elegans* nervous system (Hobert, 2010).

Neurogenesis

C. elegans' neurodevelopment and neuronal connectivity are exceptionally reproducible and invariant (WHITE ET AL., 1986). Neurons are mostly born through a series of anteroposterior asymmetric divisions (SULSTON ET AL., 1983), generally regulated by the Wnt/β-catenin pathway. Briefly, the increase in posterior localization of Wnt drives the accumulation of β-catenin (SYS-1) in the newly born posterior daughter cell, thereby inducing the expression of target genes via the POP-1 transcription factor (**FIGURE 42**, BERTRAND, 2016). These, along with previously inherited transcription factors (BERTRAND, 2016), drive the expression of neuronal gene batteries unique to each neuronal class (POOLE ET AL., 2024). This unique combination is maintained by the terminal selector genes and determines neuronal function and identity (POOLE ET AL., 2024).

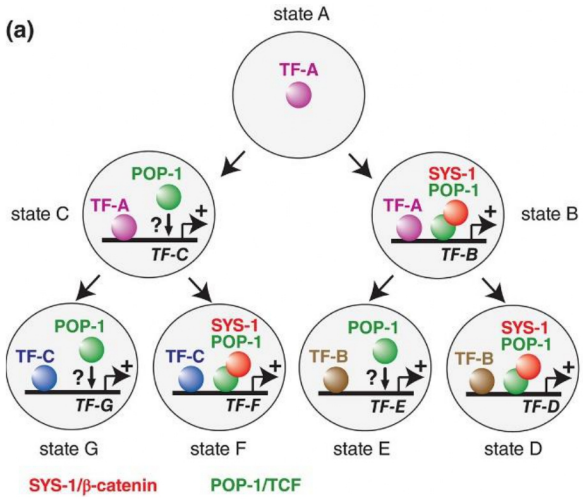

Figure 42: Examples of asymmetric divisions during neurogenesis. Model for the integration of β-catenin asymmetries into the gene regulatory network of *C. elegans* during two rounds of division. Figure and legend extracted from Bertrand, 2016.

Neurogenesis ends post-embryonically, with the birth and positioning of 80 neuronal cells (SULSTON ET AL., 1983). Interestingly, some post-embryonic neurons are born through transdifferentiation, the change of identity from one cell type to another (Jarriault et al., 2008; Lambert et al., 2021). Several transdifferentiation events occur in the animal, involving or not cell division. In the following sections, I will introduce the post-embryonic development of specific neurons that can serve as models to study actin-driven, distinct processes, i.e., cell migration, asymmetric division, and dendritic development, that could be impaired in non-muscle actinopathies.

Neuronal models of cell migration and asymmetric division - The Q neuroblasts

The Q.r/l neuroblasts are located approximately at two-thirds of the animal's body length after hatching (Purple cells in **FIGURE 43,** RELLA ET AL., 2016). During the L1 stage, these cells divide multiple times to give rise to three neuronal pairs: the SDQL/R, AQR/PQR, and the AVM/PVM neurons. Concomitantly to cell division, the neuronal progenitors migrate toward the animal's extremities (**FIGURE 43**). In more detail, the Q.r neuroblast divides into Q.ra and Q.rp. These cells migrate anteriorly before dividing again. Q.ra divides into a small cell called Q.raa and a larger cell called Q.rap. The latter will differentiate into AQR, which will migrate anteriorly, while Q.raa will die by apoptosis (RELLA ET AL., 2016). Q.rp also divides asymmetrically: Q.rpp dies while Q.rpa migrates anteriorly before another round of division, leading to the formation of SDQR and AVM. A similar process happens concomitantly for the Q.l neuroblast, with progenitors migrating posteriorly and forming the PQR, SDQL, and PVM neurons (**FIGURE 43,** RELLA ET AL., 2016).

Protégé par le droit à l'image
https://doi.org/10.1002/dvg.22931

Figure 43: Q progenitors' development.

These processes are tightly regulated and serve as models for neuronal migration and asymmetric cell divisions (RELLA ET AL., 2016). Interestingly, Q.a and Q.p asymmetric cell divisions are set up by different mechanisms. Indeed, the Q.p cells divide asymmetrically by the displacement of their spindle toward the posterior. In addition, the daughter cells' size asymmetry is increased by Arp2/3-mediated actin polymerization at the anterior pole of the dividing cell (**FIGURE 44A**, CHAI ET AL., 2022). These mechanisms are not observed during Q.a division. Instead, Q.a asymmetric division seems to be regulated by an asymmetrical distribution of NMY-2 regulated by the HAM-1 transcription factor (**FIGURE 44B**, FENG ET AL., 2013). The asymmetrical distribution of myosin was thought to be sufficient for the size asymmetry of Q.a progenitors and to induce the apoptosis of Q.aa (OU ET AL., 2010). However, recent studies did not observe a reduction of cell size asymmetry for Q.a progenitors when a thermosensitive allele of NMY-2 was inactivated (ROBINSON ET AL., 2024). On the contrary, Q.p progenitors had a reduction in cell size asymmetry in these conditions (ROBINSON ET AL., 2024), which was not observed in previous studies (OU ET AL., 2010).

Protégé par le droit à l'image □
DOI: 10.1126/science.1196112

Figure 44: Mechanisms of Q.p and Q.a asymmetrical division.

Even if recent studies do not show the same results, it is clear that actomyosin networks play a key role in the Q neuroblast's progenitors' asymmetric divisions. The failure to set up the asymmetry of either of these two cell divisions leads to a distinct phenotype: the formation of supernumerary neuron-like cells derived from the normally apoptotic cells (OU ET AL., 2010; ROBINSON ET AL., 2024). Thus, the observation of a supernumerary neuron could hint at the molecular processes impaired in an animal.

Neuronal models of dendritic process – The PVD neurons

PVDL/R are a pair of sensory neurons symmetrically located in the animal's midbody. During larval development, these neurons grow a massive, non-overlapping dendritic network, fully developed at the end of the L3 stage (**FIGURE 45**, SMITH ET AL., 2010). Indeed, from a primary dendrite spanning the length of the animal (excluding its head), perpendicular dendrites will form that will, in turn, be the seed for new perpendicular dendrites that will branch a final time to form the particular structure of PVD dendrites called the "menorah" (**FIGURE 45**).

The formation of the menorah is actin driven. Recently, Shi and colleagues (2021) found that the growth of new dendrites occurred through a series of stereotypical events (SHI ET AL., 2021). First, localized swellings of branched actin filaments form. From these swellings, linear actin filaments form filopodia-like structures that rise and form the base of a new branch. Accordingly, inhibition of actin-regulating pathways in *C. elegans*, such as the Arp2/3 complex activator *wve-1,* leads to easily observable structural defects of PVD dendrites (**FIGURE 45**, SHI ET AL., 2021). The large size and stereotypical structure make the menorah an ideal model for studying dendritic development in *C. elegans* post-embryonically.

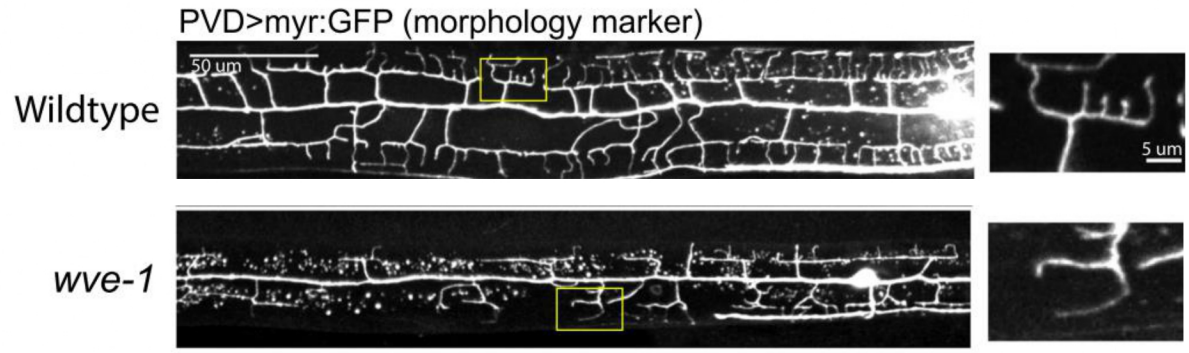

Figure 45: The PVD menorah. Representative images of PVD dendrite morphology in wild-type and *wve-1* null animals at the L4 stage. Yellow rectangles indicate locations of magnified views on the right. Figure and legend extracted from Shi et al., 2021.

Hermaphrodite Gonadogenesis

The gonad is a tissue essential for sexual reproduction developed post-embryonically. Adult hermaphrodite *C. elegans* animals possess two symmetrical U-shaped gonads with a characteristic proximo-distal arrangement (**FIGURE 46A**). Adult gonads comprise a distal syncytium where germ "cells" are lined up circumferentially. Each cell has an apical opening called the "rachis bridge" facing the shared syncytial cytoplasm called the rachis that together form a characteristic hexagonal pattern (**FIGURE 46B, C**, GERHOLD ET AL., 2022). Germ cells will undergo meiosis and mitosis along the proximal side, where a small proportion of germ cells grow to form oocytes. In this section, I will describe the gonadal development and maintenance, highlighting actin involvement in this process.

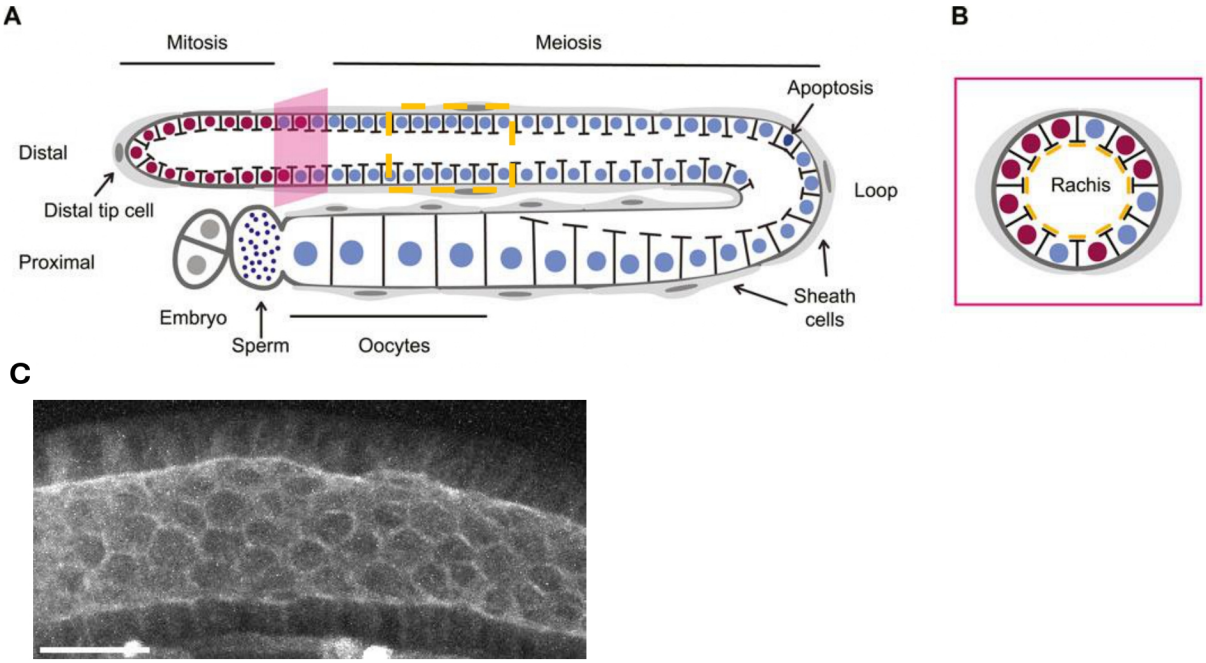

Figure 46: The *C. elegans* hermaphrodite gonad. Rachis bridges in the *C. elegans* hermaphrodite gonad. (A) The *C. elegans* hermaphrodite gonad is composed of two U-shaped tubes. Mitotic germ cells at the distal tip of each arm enter meiosis as they move proximally, and maturing oocytes are found at the proximal tip, adjacent to the spermatheca. (B) Germ cells are arranged in a rough monolayer around a common core of cytoplasm called the rachis. Each germ cell maintains a stable rachis bridge connecting it to the rachis. Figure and legend extracted from Gerhold et al., 2022. (C) 3D projection of a region located in the boxed region in (A) of a gonad from a wild-type animal expressing LifeAct::mKate2 (grey) to show the hexagonal pattern formed by the rachis bridges. Scale bar =50µm.

Gonadogenesis starts at the L1 stage and ends at the adult stage (**FIGURE 47**, GERHOLD ET AL., 2022). Four cells are born embryonically and are essential for gonadogenesis: Z1, Z2, Z3, and Z4. Z1 and Z4 will give rise to the somatic gonad, while Z2 and Z3 are interconnected and will form the germline. At the beginning of the L1 stage, these four cells are present medially at the animal's ventral side. At the end of the L1 stage, somatic gonad precursors have divided into 12 cells, including the DTC cells that terminate each gonad arm (**FIGURE 47**, LINTS & HALL, 2009). Z2 and Z3 also divide, but incompletely. Indeed, a cytokinetic ring forms and starts to ingress but stops before complete cytokinetic closure and abscission. This process is hypothesized to form the gonad's proto-rachis and the subsequent rachis bridges by cytokinetic ring stabilization and connection (**FIGURE 48**, BAUER ET AL., 2021). Accordingly, these structures are enriched in the same proteins as the cytokinetic ring, such as aniline, formin, capping, and myosin (MADDOX ET AL., 2005; PRITI ET AL., 2018; RAY ET AL., 2023).

Protégé par le droit à l'image
doi:10.3908/wormatlas.1.23

Figure 47: The *C. elegans* hermaphrodite gonad development.

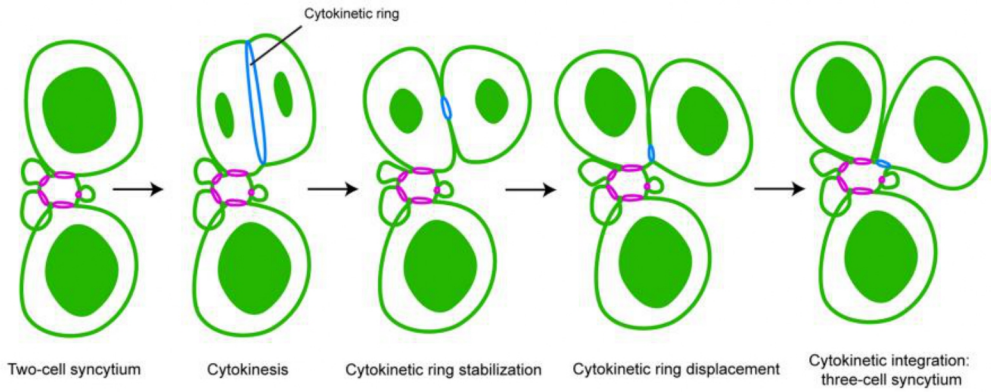

Figure 48: Proposed model for the initial expansion of primordial *C. elegans* germ line by incomplete progenitor germline cell cytokinesis. The model depicts plasma membrane and chromatin in green, stable intercellular bridges in magenta and the cytokinetic ring in blue at various mitotic stages. Figure and legend extracted from Bauer et al., 2021.

During the L2 stage, gonadal arms extend each toward one extremity of the animal (**FIGURE 47**). Until recently, the gonads' elongation was thought to be driven by cell-autonomous DTC migration, leading the following germ cells. Instead, the Zaidel-Bar lab found that the dividing germ cells push DTC during their proliferation (AGARWAL ET AL., 2022). Indeed, the germ cells are confined in a basement membrane, and their proliferation exerts enough pressure to push DTC, which subsequently relieves this pressure by local metalloprotease secretion, degrading the extracellular matrix and allowing for migration to proceed.

At the L3 stage, each gonad arm turns completely in the opposite direction to form the characteristic U shape of the gonads (**FIGURE 47**). This turn is directed by the DTC, which changes its previous homogenous cell-matrix adhesions to a dorsally enriched adhesion. This leads to a turn, as a rolling skateboarder would grab a pole. During this process, the DTC is under stress, and actomyosin networks, with other actors, seem to play a role in maintaining the cell's integrity by controlling its contractility (AGARWAL ET AL., 2024). After the turn, gonad elongation continues and is complete at the late L4 stage (**FIGURE 47**). Sperm is produced at the L4 larval stage and stored in the spermatheca.

At the adult stage, there is a switch in gametogenesis: oogenesis occurs, and the animal becomes fertile. Oocyte growth is mediated by cytoplasmic distaloproximal flows from the rachis that bring cytoplasmic material (KIM ET AL., 2013). Flows depend on actomyosin contractility but not on the germline architecture (PRITI ET AL., 2018).

Still, the gonad architecture needs to be maintained for proper oocyte generation. Germ cell shape is precisely controlled by actomyosin contractility (PRITI ET AL., 2018), and an increased or decreased contractility leads to gross germline defects, as observed when the expression of a capping protein is modified (RAY ET AL., 2023). Other genes were associated with defects in the gonad architecture and function by a large RNAi screen that uncovered 102 phenotypic classes (GREEN ET AL., 2011). The authors found that genes of similar functions cause comparable phenotypic defects. Among them, multiple ABPs (CAP-1, ANI-2, POD-1) and actin isotypes (ACT-4, ACT-5) were tested, and their knock-down resulted in different phenotypic classes (GREEN ET AL., 2011). Thus, the gonad architecture is a great model for studying the functions impaired by different actin variants, which could provide hints on their molecular consequences.

Chapter conclusion

In this chapter, we have explored the significance of *Caenorhabditis elegans* as a powerful model organism for studying the effects of actin variants, especially in the context of Non-Muscle Actinopathies. We learned how this animal entered the scientific stage in the XIXth century, which allowed key discoveries. We learned the current state-of-the-art of *C. elegans*' actin coding genes and how they compare with human cytoplasmic actins. Because of the organism's reproducibility and robustness, *C. elegans* represents an excellent model for studying actin mutations and their impact on cellular and developmental processes. As described, actin is crucial for numerous steps of the embryonic and post-embryonic development of *C. elegans* by forming specific, specialized networks. Thus, observing the phenotypical outcomes of specific variations can hint at how they specifically affect actin dynamics and provide valuable insights into the pathophysiological mechanisms of these variants.

I would like to end this introduction with a quote from John Sulston, which I find related to my PhD thesis: "*If we understand the worm, we understand life. Which of course we're nowhere near.*" (BROWN, 2002, JOHN SULSTON INTERVIEW: ONE MAN AND HIS WORM).

Chapter 4: Thesis project and scientific questions

As introduced in Chapter 2, single-point substitutions or loss of function mutations in the human cytoplasmic actin coding genes *ACTB* or *ACTG1* lead to diseases called "Non-Muscle Actinopathies" (NMA). NMAs are rare, with only 290 patients reported comprising 157 unique variants (DI DONATO ET AL., 2024 MEDRXIV). Due to the pleiotropic role of actin, syndromes associated with these diseases are diverse and include, non-exhaustively, neurodevelopmental delay, intellectual disability, and craniofacial dysmorphism, all ranging from mild to severe. However, the high number of variants and the massive clinical variability of NMAs present a significant challenge in understanding the genotype-to-phenotype correlations of associated actin variants, making medical prognostics of novel variants complex.

Tremendous efforts were made to reveal the pathophysiological mechanisms of specific variants using *in vitro* assays, as detailed in Chapter 2. However, very few studies have been published using animal models recapitulating NMA-causing actin variants. To bridge this gap, the Reymann team proposed to use the nematode *C. elegans.* Indeed, as we have seen in Chapter 3, *C. elegans* allows easy access to all biologically relevant scales: from general animal fitness to stereotypical organization within the body and embryo development, up to cell-scale events and single molecular dynamics *in vivo*. This project was performed in collaboration with a European consortium, "EJP RD PredACTINg" combining the expertise of five groups led by the human geneticist Dr. Med. Di Donato; Prof. Dr. Manstein, Prof. Dr. Kellermayer, Dr. Bianco, and Dr. Reymann. This combination of teams allowed us to study the impact of actin variants at different scales, from molecular properties to phenotypic outcome, using *in silico* modeling*, in vitro* purified proteins or patient-derived cell cultures, and *C. elegans* models.

Within this consortium, the Reymann team decided to insert endogenously ten actin variants identified in the human *ACTB* and *ACTG1* genes into *C. elegans'* cytoplasmic actin coding gene *act-2*. To span the range of severities observed in humans, we chose to study variants associated with different NMA. Seven cause Baraitser-Winter Cerebrofrontofacial syndrome of various severities (ACTB p.L65V, ACTB p.G74S, ACTB p.G74V, ACTB or ACTG1 p.T120I, ACTB p.R196C, ACTB p.R196H, and ACTG1 p.T203M), one cause mosaic Becker-Nevus syndrome (ACTB p.R147S) that is likely lethal in a non-mosaic context, one suspected to cause haploinsufficiency (ACTB p.G302A) and one associated with dystonia-deafness (ACTB or

ACTG1 p.R183W). Before starting my PhD, two lab technicians, Nadine Arbogast and Delphine Suhner, successfully created, using CRISPR/Cas9 genome engineering, six actin variant strains which I further used in my research. Three additional strains were outsourced to a private company called Suny Biotech (https://www.sunybiotech.com), and one variant has not been recapitulated yet (ACTB p.G302A) and will therefore not be further discussed.

The main objective of my PhD project was to characterize each of these variants. Specifically, we wondered whether these *C. elegans* models recapitulate some aspects of human NMA. Ultimately, our goal was to determine whether *C. elegans* could contribute to the future medical prognosis of NMA.

To this aim, I initiated a comprehensive quantitative multiscale characterization of nematode fitness and specific organ function. I observed a diversity of variant-specific perturbations. These included actin cytoskeleton network defects, cell-scale abnormalities, morphogenesis failure, behavioral phenotypes, and neurogenesis defects. Because of the invariability and robustness of *C. elegans* development, defects of these kinds are rare and can give us valuable insights into the molecular consequences of a variation. These results are detailed in Chapter 5 in the form of a manuscript currently under review at iScience. The following chapter will focus on my preliminary findings concerning the pattern of expression of neuronal genes in mutant animals. In the 7th chapter, I will discuss questions brought up by our results and how these data can hint at the pathophysiological mechanisms of the studied variants. I will discuss if *act-2* was a good choice to recapitulate both ACTB and ACTG1 actin variants in Chapter 8, and conclude the discussion in the final 9th Chapter.

Results

Chapter 5: Multiscale characterization of *C. elegans act-2* variants

Manuscript Click here to view linked References

Multiscale characterization of *Caenorhabditis elegans* mutants to probe functional mechanisms of human actin pathological variants

Théo Hecquet[1,2, 3, 4], Nadine Arbogast[1,2, 3, 4], Delphine Suhner[1,2, 3, 4], Anaïs Goetz[1,2, 3, 4], Grégory Amann[1,2, 3, 4], Selin Yürekli[1,2, 3, 4], Fiona Marangoni[1,2, 3, 4], Johannes N. Greve[5], Nataliya Di Donato [6], Anne-Cécile Reymann[1,2, 3, 4]

1. Université de Strasbourg, *IGBMC UMR 7104- UMR-S 1258, F-67400 Illkirch, France*
2. CNRS*, UMR 7104, F-67400 Illkirch, France*
3. Inserm, *UMR-S 1258, F-67400 Illkirch, France*
4. *IGBMC, Institut de Génétique et de Biologie Moléculaire et Cellulaire, F-67400 Illkirch, France*
5. Institute for Biophysical Chemistry, Hannover Medical School, Fritz–Hartmann–Centre for Medical Research, 30625 Hannover, Germany
6. Department of Human Genetics, Hannover Medical School, 30§625 Hannover, Germany

Abstract

Actin plays a crucial role in diverse physiological processes via the formation of dynamic networks that determine cellular shape and mechanical properties. *De novo* variants in cytoskeletal β- and γ-actin, encoded by human *ACTB* and *ACTG1* genes, lead to a wide range of rare diseases, termed Non-Muscle Actinopathies (NMA). Variants range from missense, frameshift, truncating variants up to whole gene deletions and can induce diverse symptoms. So far, the high clinical variability and genotype-phenotype correlations in NMA remain largely unresolved. To address this question, we used CRISPR to insert in the *C. elegans* homologue *act-2* gene nine of the mutations identified in patients. Using these animal models, we performed a quantitative multiscale characterization. We uncovered a variety of perturbations: actin network defects at the micro scale, cell scale abnormalities, morphogenesis failure, as well as weaker behavioural phenotypes. Importantly, the range of developmental defects observed correlates with the severity of patients' symptoms. Thus, we provide evidence that a *C. elegans*-based approach represents a new way to investigate the mechanisms underlying NMA physiopathology or ultimately screen for therapeutic strategies.

Keywords

C. elegans, cytoplasmic actin, Non-Muscle Actinopathy, Baraitser-Winter Cerebrofrontofacial Syndrome

Introduction

The ability to dynamically assemble the actin cytoskeleton in response to internal and external triggers is a hallmark of a healthy and functional cell. Finely tuned actin architectures coordinated to fulfil specific cellular needs and constant reorganization for adapting to external cues, drive a multitude of cellular processes including motility, adhesion, morphogenesis, mechanotransduction, internal organisation and trafficking (Blanchoin et al. 2014; Murrell et al. 2015). Altered cytoskeletal integrity is implicated in many disorders ranging from hearing loss to cancer to rare developmental diseases (Parker, Baboolal, and Peckham 2020; Lai and Wong 2020). The human genome encodes six highly conserved actin isoforms, which are produced in a time- and tissue-specific manner and every actin isoform has been associated with human pathologies (Parker, Baboolal, and Peckham 2020). *De novo* missense variants, frameshift or truncating variants as well as gene deletions in the *ACTB* and *ACTG1* genes, which encode the ubiquitously expressed cytoplasmic β- and γ-actin, cause substantial cellular dysfunction and lead to a range of rare disorders, termed Non-Muscle Actinopathies (NMA) (Cuvertino et al. 2017; Latham et al. 2018; Polubothu et al. 2020; Rivière et al. 2012; Verloes et al. 2015; 1993). One particularity of this category of diseases is the broad spectrum of symptoms found in patients. NMA can range from very mild to severe neurological impairment and cortical malformations as well as reduced life expectancy of the affected patients. So far, 287 patients and 157 unique mutations have been reported to cause NMA. The most frequently associated NMA disease, named Baraitser-Winter cerebrofrontofacial syndrome (BWCFF), is associated with characteristic facial malformations, intellectual disability, cortical malformations, epilepsy, hearing loss and a variety of congenital anomalies (Rivière et al. 2012; Verloes et al. 2015). Even within the BWCFF subclass of NMA, a large range of symptom severity is observed.

To date, a definitive genotype-phenotype correlation within the NMA field has yet to emerge, and the functional mechanisms causing symptoms in patients remain largely elusive. It is likely that the complexity originates from both the multifaceted roles of actin and its numerous molecular partners (Actin Binding Proteins; ABP). Furthermore, the existence of compensatory mechanisms between isoforms constitute a challenge in the study of actin *in vivo* (Dugina et al. 2009; Vedula et al. 2017; Boiero Sanders et al. 2022; Michelot and Drubin 2011). Actin variants have been proposed to affect the cytoskeleton by four mechanisms: haploinsufficiency leading to insufficient availability of actin monomers, alteration of the actin filament assembly or disassembly kinetics, alteration of actin interactions with binding partners and assembly of toxic actin oligomers detrimental for proper cytoskeletal function (Greve et al. 2023). At the structural level, *in silico*

models correlate some NMA mutations with nucleotide-binding, monomer-monomer interaction and canonical G-actin-ABP interaction surfaces (Latham et al. 2018). In addition, the use of purified recombinant human actin proteins allows us to quantitatively assess defects in terms of folding, thermal stability, nucleotide-binding, G- to F-actin transition and interaction with ABPs for some variants (Greve et al. 2023; 2022), validating some of these hypotheses. *In vivo*, the effects of *Actb* and *Actg1* deletions have been studied in mouse embryonic fibroblasts and in the whole animal (Patrinostro et al. 2018; Bunnell and Ervasti 2010; Bunnell et al. 2011). Notably, *Actb* deletion leads to proliferation defects in mouse embryonic fibroblasts as well as mice embryonic lethality, whereas *Actg1* null mutant mice are viable (Vanslembrouck, Ampe, and Van Hengel 2020). Currently, however, a comprehensive system capable of bridging these different scales and validating the suggested molecular to functional relationship is still missing.

To fill this gap, we chose to use the free-living nematode *Caenorhabditis elegans* (*C. elegans*) as a model to study NMA, as it provides easy access to all biologically relevant scales: from general animal fitness to stereotypical organization and development, up to cell-scale events and single molecular dynamics *in vivo*. *C. elegans* has already been used as a model for numerous diseases, notably for the study of neurodegenerative and neuromuscular disorders (Markaki and Tavernarakis 2010), thus demonstrating its capabilities in assessing the molecular to functional link in human diseases. The ease of genetic manipulation and the ability to obtain a stable, isogenic strains within a matter of weeks streamlines the process of strain characterization and enables us to investigate the consequences of multiple NMA variants in a reasonable amount of time.

As is true for humans, *C. elegans* relies on different cytoplasmic actin paralogs to sustain cellular cytoskeleton integrity in all cell types. Three ubiquitously expressed actin genes (*act-1, act-2* and *act-3*) are present in a cluster and operate in a partially redundant manner, notably during early embryogenesis (Hayashi, Ono, and Ono 2019; Willis et al. 2006; S. Ono and Pruyne 2012). These three cytoplasmic *C. elegans* actin are also required for proper muscle function (S. Ono 2014). Indeed, some mutations in the *act-2* gene exhibit uncoordinated adult movement or pharyngeal pumping defects (Krause et al. 1989; Landel et al. 1984; Avery 1993; Willis et al. 2006). A fourth actin-coding gene named *act-4* is expressed in different tissues, notably in neurons and in muscle cells. However, *act-4* is not as abundant or ubiquitously expressed in the early embryo as the essential cytoplasmic actin- as *act-1, act-2, act-3* (Serobyan et al. 2020). By contrast, *act-5* shows a strong tissue-specific expression in the gut and excretory cell (MacQueen

et al. 2005). Among the *C. elegans* proteins, ACT-2 has the highest similarity to human cytoplasmic actin proteins, sharing 98% of amino acids with β-actin and 97% with γ-actin.

In this study, we assess the consequences of actin variants associated with BWCFF or other NMA in a model organism, and present a quantitative multiscale characterization of *C. elegans* mutants. As cytoplasmic actin is required pleiotropically, we performed a global survey of mutants using well-established methods to assay both nematode fitness and specific organ function. We propose a classification of selected NMA variants with respect to the observed phenotypes in *C. elegans* and compare this classification to the severity of the patient's symptoms. This initial study of actin variants showed a strong correlation in the degree of pathological severities between *C. elegans* and human, thus validating the use of *C. elegans* as a tool to study NMA. Importantly, this work paves the way towards the prediction of clinical severity in patients carrying novel actin variants from the outset of diagnosis.

Results

Generation of *C. elegans* models recapitulating human non-muscle actinopathies

With respects to the three *C. elegans* cytoplasmic actin genes: while *act-1* and *act-3* share identical coding sequences, they differ from *act-2* by three non-synonymous and many silent variations as well as distinct intronic regions. This allows a slightly facilitated CRISPR/Cas9 genome editing for *act-2* than for the others (Paix et al. 2015) Therefore, we decided to insert a series of genetic modifications identified in the human *ACTB* and *ACTG1* genes into the *C. elegans act-2* locus. In order to span the range of severities observed in human, we chose to study an initial set of nine mutations which included mutations associated with BWCFF (*ACTB* p.L65V, *ACTB* p.G74S, *ACTB* p.G74V, *ACTB* or *ACTG1* p.T120I, *ACTB* p.R196C, *ACTB* p.R196H and *ACTG1* p.T203M) (Verloes et al. 2015; Chacon-Camacho et al. 2020; Vontell et al. 2019); as well as non-BWCFF NMA diseases (*ACTB* p.R147S and *ACTB* or *ACTG1* p.R183W) (Figure 1). Among them, p.R196 is a hot-spot identified in over 19 patients, presenting clinical variability with a high degree of brain malformation (83%, Figure 1A) (Verloes et al. 2015; Cianci et al. 2017). *ACTB* p.R147S represents a hotspot postzygotic disruption causing the mosaic skin disorders known as Becker nevus syndrome (Cai et al. 2017). This variant is likely lethal in a homozygous context (Happle 2017). *ACTB* p.R183W is associated with dystonia deafness

(Eggink et al. 2017; Conboy et al. 2017; Gearing et al. 2002; Procaccio et al. 2006; Zech et al. 2017; Skogseid et al. 2018; Freitas et al. 2019).

We mapped these mutated residues on a structural model of the *C. elegans* ACT-2 monomer (G-actin) and filament to assess possible localisation of the variants in different regions of the molecule identified with specific functions (Figure 1B). The variants are distributed across all four subdomains (SD) of the actin monomer. Two examined residues (G74, R183) are located within the nucleotide-binding cleft and, although not directly involved in nucleotide coordination or hydrolysis, contribute significantly to the release of inorganic phosphate following ATP hydrolysis (Oosterheert et al. 2023). The R147 residue is part of the target-binding cleft of the actin monomer, located between SD1 and SD3, which is lined with predominantly hydrophobic residues and represents a main interaction interface for G-actin binding proteins (Bunnell and Ervasti 2010; Dominguez and Holmes 2011). Residue T120 is part of the so-called pathogenic helix of actin (K113-T126), which constitutes a hotspot for mutations in several human actin isoforms leading to BWCFF (cytoskeletal β- and γ-actin), non-syndromic hearing loss (cytoskeletal γ-actin), thoracic aortic aneurysm (smooth muscle α-actin) and nemaline myopathy (skeletal muscle α-actin) (as reviewed in (Rubenstein and Wen 2014)). Residues R196 and T203 are both located in SD4 and are part of regions of the actin monomer that are heavily involved in the formation of monomer-monomer contacts within the actin filament due to formation of a salt bridge by the neighbouring residue E195. T203 is part of a threonine-rich loop that contributes to lateral and longitudinal contacts in the filament (Dominguez and Holmes 2011; Reynolds et al. 2022). The L65 residue is located in SD2 in close proximity to the DNase-loop that contributes to lateral and longitudinal interfaces and undergoes structural rearrangement upon nucleotide hydrolysis, directly affecting filament stability (Oosterheert et al. 2023; Reynolds et al. 2022).

Using these selected variants associated with various human symptoms, we generated strains harbouring each a NMA mutation in the *act-2* gene using CRISPR/Cas9 gene editing (Figure 1C). We verified that no additional mutations were present in the other four actin genes and backcrossed the strains several times before analysis. Additionally, we generated two new prospective null alleles for *act-2* (*rey016* and *rey021*) (Figure 1C), each resulting in a premature STOP codon within exon 2 (see methods section for more details). For comparison, we assayed a previously characterized *act-2* knock-out (KO) strain (allele *ok1229*) obtained via an EMS screen, which harbours a larger deletion extending beyond the 3' UTR (Willis *et al.* 2006).

ACT-2 missense variants affect the general viability of *C. elegans* to different degrees

We first compared the general viability of the different mutant *act-2* strains obtained at 20°C. We found that some mutant animals for p.R147S or p.T203M developed into homozygous adults but their very few progenies were 100% lethal during embryogenesis, suggesting a strong maternal effect lethal phenotype. We thus maintained these variants as heterozygous animals using the nT1 balancer (Ferguson and Horvitz 1985). Interestingly, one mutation (p.G74V) caused lethality in both homozygous and heterozygous state, suggesting a gain of function. Indeed, for this variant we obtained very few edited surviving F1 animals after injections, with some embryo production. Sequencing of several of these F1 animals confirmed the presence of a heterozygous G74V variant in the *act-2* gene (Figure S1B). These p.G74V mutant embryos, however, displayed complete lethality. Because we were unable to maintain a stable line expressing this variant, we did not pursue its characterization. Nonetheless, another variant of the same residue (p.G74S) could be maintained as homozygous. All other variants (p.L65V, p.T120I, p.R183W, p.R196C, p.R196H) as well as the KO *rey016, rey021* and *ok1229* were viable at a homozygous state and were thus maintained as such, although some of them had very few progeny. In conclusion, out of the nine single point mutation variants generated, six could be maintained as homozygous, two as heterozygous and one was inadequately viable (Figure 1D). This initial finding emphasizes the importance of these loci for development and health, and highlights the remarkable conservation of actin across species.

act-2 gene knock-out affects reproduction and embryo viability

In order to assess how individual point variants compare with gene KO, we performed a detailed analysis of phenotypes in absence of ACT-2 protein expression. We assessed both the newly CRISPR generated *act-2* KO strains (*rey016 and rey021* allele) as well as the EMS generated strain, *ok1229* (Willis et al. 2006). We first verified if transcriptional adaptation of another actin coding gene could compensate for the loss of *act-2*, as proposed by Willis *et al*. (Willis et al. 2006). Such a transcriptional adaptation has been reported in an *act-5* variant (Serobyan et al. 2020; Welker et al. 2023). Therefore, we measured the expression of mRNA of all actin coding genes using single animal RT-qPCR in L4 animals devoid of embryos, to avoid developmental differences in the experimental read-out (Figure 2A) (Ly, Reid, and Snell 2015). We found that both *ok1229* and *rey021* strains show a clear absence of *act-2* mRNA. By contrast, *act-1* and *act-3* expressions were increased compared to wild-type (N2) animals (*act-1* fold

change: *ok1229* = 2.5, *rey021* = 6.7; *act-3* fold change: *ok1229* = 4, *rey021* = 3.6), unlike *act-4* and *act-5* which only had minor fluctuations of expression (Figure 2A). We conclude that there is transcriptional adaptation for actin in *C. elegans*: *act-1* and *act-3* compensating for *act-2* loss.

With respects to fertility and embryonic lethality, the *ok1229* allele was described as thermosensitive, showing embryonic lethality at 26°C but not at 15°C (Willis et al. 2006). Therefore, we monitored the brood sizes and percentage of unhatched eggs of *rey021* at different temperatures, as well as for WT and *ok1229* animals. We observed a reduction in the number of eggs produced by the *ok1229* and *rey021* strains compared to the WT strain both at low and high temperatures (Figure 2B). However, we did not detect a significant decrease in embryonic development success unlike previously reported for the *ok1229* strain (Figure 2B') (Willis et al. 2006). The *rey021* KO allele exhibited a higher percentage of unhatched eggs - above 50% - for both temperatures (Figure 2B'). Thus, these results established a difference in the developmental success of the different *act-2* KO alleles , the *ok1229* allele showing a milder phenotype. As brood sizes and embryonic lethality were similar for the *rey021* strain at both temperatures, we do not see evidence of thermosensitivity for this allele. Thus, all further experiments were performed at the standard 20°C temperature.

In order to determine if the KO allele effect was dominant or recessive, we quantified brood size and embryonic lethality from heterozygotes hermaphrodites for our two CRISPR generated strains. Generally, *act-2* KO animals were reduced compared to WT but *rey021*/+ animals showed an increase in the number of progeny compared to *rey021*/*rey021* (Figure 2C). The progeny of heterozygous *rey021*/+ and *rey016*/+ hermaphrodites showed an embryonic viability similar to that of the WT (Figure 2C'). Taken together, the *act-2* KO is severely impaired but this phenotype can be partially suppressed in the heterozygous condition, as expected for an actin maternal loss of function.

Reproductive capacity is a quantitative readout to classify actin mutants

Assessing general animal fecundity and embryonic fitness in *C. elegans* allows for the quantitative detection of potential defects in oocyte production, embryogenesis or vulva function (Schafer 2005), three actin-dependent processes. Thus, we measured the number of eggs laid and hatched by single homozygous animals expressing an *act-2* variant at 20°C. A reduction in egg laying was observed for all *act-2* variants, except for the p.G74S and p.R183W variant strains, which appeared unaffected (Figure 3A). The most severe reductions in fecundity were observed

for the p.R147S and p.T203M missense variants (mean number of eggs laid: p.R147S = 2.3, p.T203M = 31.0, WT = 270.1), surpassing the reduction seen in the *act-2* KO condition (*rey021*=78) and partially rescued in the heterozygous condition (Figure S3A). All other missense variants showed a fecundity reduction less pronounced than the KO animals.

The number of unhatched eggs also varied significantly among actin variants with a trend consistent with that of fecundity (Figure 3B). The p.R147S and p.T203M variants exhibited 100% embryonic lethality if homozygous (Figure 3B) and respectively 72.7% and 58.3% if heterozygous, thus stronger than the homozygous and heterozygous *act-2* gene KO (respectively 39.75 and 16%, Figure S3B). This indicates that a high percentage of heterozygote p.R147S and p.T203M embryos die before hatching. The p.L65V missense variant also showed significant embryonic lethality (33.2%) although with an increased variability**.** The p.R196H variant was affected to a significant level unlike the p.R196C variant, as showed by none overlapping 95% credibility intervals of the posterior distributions of the embryonic lethality rates calculated with Bayesian methods (Figure 3B). No other missense variants displayed a significant impairment of embryo survival. Taken together, our data suggest that p.R147S and p.T203M are dominant negative; p.G74S and p.R183W are not impaired in their reproductive capacity; while the other studied variants behave as partial loss-of-function alleles, with embryo viability comparable to WT.

Gonad internal architecture is impaired in selected mutants

As we observed an impairment in the reproductive capacity of the actin mutant strains, we investigated whether these defects were associated with abnormal organization in the *C. elegans* reproductive system. We performed a detailed analysis of gonad morphology by spinning-disk confocal microscopy using strains expressing both an actin filament probe (mex5p::Lifeact::mKate2), and endogenously labelled non-muscle myosin molecular motors (NMY-2::GFP). *C. elegans* adult hermaphrodites possess two syncytial mirror gonads shaped by highly organized actin structures. These structures include a connected cytoplasm-filled core, called the rachis, surrounded by germ cells with openings facing the rachis and shaped by stable actomyosin rings (Figure 3C). These rings are originating from incomplete cytokinesis of primordial germ cells forming the typical specific honeycomb architecture in the functional adult gonad (Bauer et al. 2021). We first characterized the gonad morphology by measuring germ cell and rachis sizes (Figure 3D). In this analysis, the p.L65V variant presented strikingly lower values, whereas the p.T203M showed a more moderate reduction. Interestingly, the variant p.G74S presented higher rachis/gonad ratio than the control even though this is not correlated with a

perturbation of fertility. Other variants had values more similar to the WT strain but exhibited greater variances. Second, we quantified defects using established criteria (Green et al. 2011) (Figure 3E). In correlation with the strong decrease of rachis size, the most pronounced phenotypes are found in the p.L65V animals, notably illustrated by the presence of 80% of degenerated gonads devoid of oocytes or early embryos. This suggests severe impairment in gonad morphogenesis and/or maintenance in these animals. Still, the penetrance was not 100% as 1 of 5 p.L65V animals harboured a normal looking gonad, which explains the viability of the strain. Other noticeable phenotypes present in animals expressing different point mutation were: the presence of 20% multinucleated oocytes in p.T203M animals as well as a 11% penetrance in p.T120I, multinucleated germ cells in p.T203M (100%), p.T120I (33%) and p.G74V (25%). To conclude, two main phenomena can explain a reduction in brood size in actin variant genetic backgrounds: abnormal gonad internal organization; and oocyte defects likely due to DNA segregation errors, emphasizing the importance of ACT-2 in meiosis.

ACT-2 variants affect the success rate in different embryogenesis stages

We next sought to determine causes of the observed embryonic lethality. To this end, we quantified the precise stage at which embryonic lethality occurs in the actin-mutant strains (Marston and Goldstein 2006; T.K. Vuong-Brender, Yang, and Labouesse 2016) as well as the eggshells' shapes by measuring their aspect ratios and 2D areas (Figure S3C, D). To do so, we monitored the entire duration of embryogenesis using time-lapse transmitted light video-microscopy (Figure 3F). In line with the previous embryonic lethality counts, we detected a variable proportion of *act-2* mutant embryos unable to hatch (Figure 3F). Embryonic defects were categorized into various classes. First, at the zygotic stage due to a failure to complete cell division (orange in Figure 3F). Second, developmental arrest during gastrulation (yellow in Figure 3F), a key event involving cell shape changes and migration, highly dependent on Arp2/3 actin networks (Nance 2005; Zhang, Medwig-Kinney, and Goldstein 2023). Third, in the vast majority, developmental arrest occurred at later steps of development. Indeed we observed embryonic arrest during ventral enclosure (light purple in Figure 3F), a process also known to rely on both protrusive and contractile actin-related events (Bernadskaya et al. 2012). Additionally, we observed two types of arrests during elongation with Pat embryos (paralyzed at two-fold, purple in Figure 3F), suggesting muscular defective conditions and/or defective hemidesmosomes; and rupturing embryos, an obvious sign of tissue mechanics impairment (dark purple in Figure 3F) (T.K. Vuong-Brender et al. 2017). Interestingly, the total percentage of defects and their

frequencies varied among the different strains but the KO condition showed a high proportion of lethality in each category (Figure 3F). In contrast, homozygous p.R147S embryos suffered severely from early embryonic death (cytokinesis and gastrulation defects) while in heterozygous p.R147S embryos, early death was reduced, and they tended to die more frequently during ventral enclosure or in later stages of elongation. As elongation requires efficient muscle contractions, this result corroborated the p.R147S impaired muscular capacity measured in the motility assay. The few embryos expressing the p.T203M allele, arrested at different stages of morphogenesis between gastrulation and elongation with different ratios depending on the genetic condition. These findings suggest that the p.R147S and p.T203M variants are more detrimental or toxic for early embryogenesis than the complete absence of ACT-2 protein (*rey021* condition), supporting a dominant negative effect. To conclude, this analysis revealed variant-specific differences in the mechanisms leading to actin-related lethality, likely associated to a fine-tuning of specific actin organization, dynamics or mechanoproperties at these key stages of morphogenesis.

Altered cell mechanics but surprisingly mild cortical actin disorganization in early embryos

We then asked whether defects emanate from abnormal cytoskeletal organization or impaired force production, such as abnormal cytoskeletal contractility linked to actin-myosin interaction. These possibilities are not mutually exclusive and could be linked, as architectural defects can impair contractility (Ennomani et al. 2016). We thus increased the time and scale resolution by performing spinning-disk confocal microscopy on strains carrying the LifeAct probe to follow actin filaments organization as well as an endogenously labelled non-muscle myosin (NMY-2::GFP) to assess contractility during the first cell divisions of *C. elegans (Reymann et al. 2016)*.

With respect to cortical architecture and dynamics, we were surprised by the outstandingly normal general organization of the actin networks observed in some *act-2* variants (Figure 4A), even though reduced polymerization capacities have been quantified biochemically using purified proteins (Greve and Manstein 2024). Visual inspection did not reveal major signs of impaired actin density or general organization in most embryos. Similarly, we did not detect signs of impairment in the reproducible sequence of events taking place in zygotes for most embryos. These events, which highly depend on proper cortical organization and contractility, include polarity establishment associated with cortical flows, pseudo cleavage formation, and the maintenance

phase where polarity is stably maintained (Rose and Gönczy 2014). This was evidenced by the unchanged size of the daughter cell AB in variant conditions (Figure S4). It is possible that many NMA actin variants can copolymerize with WT actin, resulting in mild phenotypes of disorganization that are still compatible with life in both human and *C. elegans.*

Although most cells maintain seemingly normal actin cortical networks, we observed some cell-scale defects, revealing impaired cytoskeletal properties in some embryos (Figure 4B, C, D, E, F). As expected from previous analyses, we identified cell-division defects where ingression progresses smoothly but subsequently retracts (Figure 4B). This suggests that cytokinesis-ring assembly and contractility might not be impaired, but rather than failure happens at the last steps of cytokinesis completion during abscission. We also observed meiosis defects, identified by the presence of an additional nucleus present either in the AB cell or in the P0 zygote, likely due to incomplete polar body extrusion (Figure 4C). As meiosis and cytokinesis completion share common mechanical principles linked to actin, such as the formation of a contractile actin ring required to bring together closing membrane domains (Dorn et al. 2010; Flynn and McNally 2017), these failures may share a similar origin. In addition, we noticed the presence of blebs in some embryos (Figure 4D, E). Blebs are transient cell protrusions that can be triggered by two main events: the detachment of the cortex from the plasma membrane or the formation of a crack in the cortex. Blebs then grow due to the internal hydrostatic pressure imposed by cortical contractility (Charras and Paluch 2008). Blebs were mostly observed at the 2-cell stage, at the interface between the AB and P1 cells before cell rounding prior to division. We observed larger blebs, mostly in p.L65V, p.T120I and p.T203M variants, emanating from AB, sometimes dragging the nucleus into the bleb, before a fast retraction period. Retraction coincided with the increase of myosin at the cortex at cytokinesis onset. Embryos presenting the blebbing phenotype also had transiently abnormal cell shapes, an overall less round, more wavy cortical surface (Figure 4D) and seemingly diminished cell-cell contacts, particularly between P1 and ABp cells at the 4-cell stage. This phenotype resembles cortical blebs that were proposed to reposition the cytokinesis ring of the zygote in *ani-1(RNAi);pig-1(gm344)* embryos in the presence of excessive myosin accumulation at the anterior cortex (Pacquelet et al. 2015). While we do not observe mispositioning of the furrow or abnormal nuclei migration, the similar phenotype suggest a shared site of cortical instability.

Motility is mildly impaired for a few *act-2* variants

Like its actin cytoplasmic paralogues, ACT-2 protein is also required in muscle cells (Willis et al. 2006), evidenced by dominant mutations in *act-2* impacting *C. elegans* motility, with uncoordinated phenotypes on 2D surfaces (Krause et al. 1989). As no such strong phenotype was observed in our studied *act-2* mutants, we quantified the animals' capacity to migrate inside a pluronic gel towards a chemoattractant (food source) in a 3D burrowing assay (Lesanpezeshki et al. 2019). We observed that 82.4% of WT animals and 50.2% of mobility-deficient control animals (*unc-2*(*gk366*)) reached the food after 2 hours (Figure 5A). We detected altered 3D migration for the KO *rey021* and for the variants p.T120I, p.R183W, p.R196C, p.R196H and p.T203M, while other variants showed unaffected migration (p.L65V, p.G74S, p.R147S). We verified that these effects were not due to impaired chemosensation (Figure S5). Note that in this assay we observed an increased number of immobile animals for variants *rey021* and p.T203M only. In conclusion, six out of nine assessed *act-2* variants have impaired 3D motility while two variants have a substantial population of animals defective both for 2D and 3D movement.

Low penetrance of neurogenesis defects

In human, neurodevelopmental defects are the most frequent symptoms across the NMA spectrum. We thus studied neurons in *C. elegans* L4 animals. To this aim, we took advantage of a multicolour neuronal labelling transgene present in the NeuroPAL strain (Yemini et al. 2021). The NeuroPAL transgene encodes for the expression of a combination of 41 neuron specific reporters for gene expression and neuronal activity, associated with four different fluorophores. This labelling allows each neuron in the animal to be identified by a unique set of fluorophores, distinguishing them from neighbouring neurons. After introducing the NeuroPAL transgene in the actin variant strains, we mapped all neurons present in the animal's midbody and tail, which include every type of neuron. For every observed animal, we did not detect altered neuronal positions. However, we did observe rare events, for each allele except p.R196H, wherein we detected the presence of an extra numerary neuron (adjacent to SDQR or in the lumbar ganglion) or a missing neuron (such as DVB or PDA, Figure 5C). These altered numbers suggest that NMA neurodevelopment defects may be reproduced in our mutant models.

Data integration to build a comparative tool

Taking advantage of the multiscale characterization performed on each mutant, our final goal was to classify the different missense variants in terms of severity. We used each of the

quantitative results as variables to create a Principal Component Analysis (PCA) graphical representation (Figure 6, variables available in Figure S6). This dimension reduction allowed us to group phenotypes into different classes and allowed us to identify the few most promising variables to be used for classification purposes (Figure S6). In the PCA plot, the WT strain is located in the top left quadrant close to the mildly affected variants, defining class I (p.L65V, p.G74S, p.T120I, p.R183W, p.R196C, p.R196H). One can note the singular position of the p.L65V, isolated in the class I group, underlying that the in-depth analysis points towards more severe consequences for this variant. This result correlates with human data, where an *ACTB* p.L65V patient presented severe symptoms and early death. The KO *rey021* strain is also isolated in a more central position. Stronger phenotypes such as in p.R147S or p.T203M variants are positioned in the right half, defining the class II. Interestingly, heterozygous variants (*rey021*/+, p.R147S/nT1 and p.T203M/nT1*)* are placed closer to the WT point than their homozygous counterpart. Using quantitative multiscale analysis of a panel of actin variants, we have provided access to a valuable comparative tool enabling the positioning of newly identified variants on a graded map of survival potential if those would be similarly be reproduced in the *C. elegans* model and assessed.

Discussion

Patients affected by the rare disorders from the Non-Muscle Actinopathies (NMA) spectrum and its subclass BWCFF, exhibit a large range of symptoms and diverse survival potential, leading to complicated medical prognostics. Given the ubiquitous nature of actin, involved in numerous cellular events at all stages of development and throughout the animal lifespan, there is an importance to analysing multiple parameters in animal models. Parameters which should span diverse length scales: from macroscopic actin organisation to cell behaviours and phenotypes at the organism scale, in order to effectively distinguish the impact of each actin variant. In this study, we used the fast-growing and simple model organism *C. elegans* to study *in vivo* the quantitative impact of some of the associated single cytoplasmic actin variants. Using CRISPR/Cas9 genome editing, we successfully generated new *C. elegans* models expressing endogenously either *de novo* actin variants identified in human patients or premature STOP mutations to reproduce loss-of-function conditions. For each variant, we quantified general fitness, reproductive capacities, muscle-based motility, embryonic development, and neuronal differentiation. The final step using

an integrated PCA analysis enabled us to summarize the phenotypic classification providing a valuable tool to position newly identified variants of unknown significance on an existing map. We believe that these data support the use of *C. elegans act-2* mutation as a pertinent and promising model for the investigation of NMA.

In the functional characterization of *act-2*, a key finding is the significant phenotypic difference between our newly generated CRISPR *act-2* knock-out strains and the only previously reported KO strain that had a temperature-sensitive viability phenotype. Our work clearly indicates that the CRISPR-induced *act-2* KO mutation impacts embryonic development considerably at all temperatures. We can only hypothesize the reason for the difference. Similarly to human loss of a cytoplasmic actin allele that induces a compensatory transcriptional adaptation (Cuvertino et al. 2017), *C. elegans* showed transcriptional adaptation to compensate *act-2* loss, as the closely related actin paralogue genes *act-1* and *act-3* were found to be upregulated. One hypothesis might that different gene compensation efficiencies are at work in the embryo but not in the L4 animals in these two genetic contexts.

Another significant finding was that three actin variants exhibited stronger phenotypes than the *rey021 act-2* KO, namely p.G74V, p.T203M and p.R147S. The p.G74V variant lead to an animal producing 100% lethal embryo even as heterozygote, while embryos from variants p.T203M and p.R147S are 100% lethal only when the mother is homozygote. The latter mutations behaved as semi-dominant since these phenotypes were only partially improved in heterozygotes. This suggests that the presence of these mutated actin proteins disrupts proper function, either through essential perturbations of actin filament assembly or by interactions with actin-binding proteins. This insight into allele behaviour, distinguishing dominant negative from loss-of-function variants provides valuable information that would not have been obtained if not using *in vivo* animal models.

Using these models, we observed an unexpected striking difference between two substitutions at the same locus. Animals expressing the p.G74S variant show only mild effects on embryogenesis viability whereas the p.G74V animals are significantly more affected, as mentioned above. This position is of particular interest because of the neighbouring His73 which is known to undergo irreversible methylation, regulating actin's interdomain flexibility in multiple species and known to affect smooth muscle contraction in mice for example (Wilkinson et al. 2019). Additionally, due to its location within the nucleotide-binding cleft, this variant might impact the phosphate release following actin monomer incorporation into the filament. Consequently, the binding of ADF/cofilin would be perturbed, leading to impaired disassembly kinetics. Of note, *C.*

elegans' ADF/cofilin homologue UNC-60 induces lethality when knocked down (K. Ono 2003). Biochemical analysis and *in vitro* studies using purified actin variants could examine these hypotheses and compare biochemically how the presence of the hydrophobic Valine is more detrimental than Serine.

Additionally and from a more fundamental perspective, characterizing actin variants is also powerful to reveal new actin-networks properties. The observed abnormal gonad internal organization, is highlighting the importance of ACT-2 for proper cytoskeleton architecture establishment in this tissue. Oocyte defects are likely due to DNA segregation errors, emphasizing the importance of ACT-2 in meiosis. Blebs, on the other hand, are intrinsically linked to cortical contractility and to cortex-to-membrane attachment, thus reinforcing the possibility that membrane-to-cortex attachment might be impaired, as suggested also by late cytokinesis defects. We use this rationale to suggest that variant p.L65V to be detrimental to gonad cytoskeleton organisation and meiosis; p.R147S possibly impairing mostly branched actin networks essential at different morphogenesis stages; and p.T203M, p.T120I, and p.R196C/H impacting contractility as indicated by blebbing, paralysed arrest and impaired motility. As we have demonstrated that developmental arrest at critical embryonic stages occurs at varying frequencies depending on the nature of the variant or copy number - in the case of p.R147S - we propose that these key developmental stages act as specific “barriers” to developmental success. Barriers of different difficulty linked to the precise site of mutation, that must be successively overcome during embryogenesis. As developmental timings were not drastically affected (Hall, D.H., Herndon, L.A., and Altun, Z. 2017), we suspect that these barriers might have a biomechanical origin (Figure S3C).

Observed defects commonly display incomplete penetrance and the general organization of actin at a macroscopic scale is often remarkably unaffected. This suggests an adaptation of cytoskeletal actin to perturbations, possibly originating from the cell's ability to maintain the adequate large-scale physical properties of the cortex, also known as “morphogenetic degeneracies in the actomyosin cortex” (Naganathan et al. 2018). Compensation mechanisms may ensure the robustness of embryo development by maintaining proper cytoskeleton mechanical properties. Note that a similar robustness to cytoskeleton perturbation, in that case a resistance to microtubule disassembly, was observed in the context of *C. elegans* embryonic elongation (Priess and Hirsh 1986; Quintin et al. 2018). In our context, this could also be explained by a functional compensation by other actin isotypes expressed in early embryogenesis, notably ACT-1 or ACT-3 (Willis et al. 2006), which might compensate for polymerization defects. *In vitro*

experiments with purified proteins using mixtures of WT and mutant such as for p.R196H, also show a partial rescue of polymerization defects (Greve and Manstein 2024). Thus, biological variations such as gene expression fluctuation, gene compensation, ABP concentrations, mechanochemical feedback or fluctuation of properties impacting cell or tissue mechanics, determine the embryogenesis success of each individual. Consequently, each embryo may respond differently to these compensation mechanisms and might arrest at a different developmental stage.

Finally, the initial investigation of the consequences of actin perturbation on neurogenesis revealed a weakness in acquiring the correct number of neurons, albeit not penetrant. SDQ neurons are born from an asymmetric division followed by the death of their sister cell while DVB and PDA are born from the transdifferentiation of a rectal epithelial cell (Riva et al. 2022). Even at low penetrance, these numbers are indicate an important defect due to the extreme robustness of *C. elegans* lineage, 100% success in wild type conditions (Chai et al. 2022; Riva et al. 2022). These findings suggest a potential weakness in the process of neuronal asymmetric division or fate acquisition, which might be amplified in the context of human cortical development where neuron numbers are far greater and asymmetric divisions have been reported in the striatum. The asymmetric divisions required for neuronal fate acquisition can depend on the asymmetry of Arp2/3 nucleated cortical actin polymerisation (Chai et al. 2022). As both actin polymerisation and Arp2/3 nucleation were already described to be impaired for some variants studied *in vitro* (Greve and Manstein 2024), this result is not surprising and will require further investigation in *C. elegans*. It may lead to essential findings in the path to identify the molecular to functional mechanisms at the origin of NMA neuronal pathophysiology. Importantly, the NeuroPAL data using nuclei as proxy of neuronal cell positioning, did not reveal other gross defects in terms of cell migration. This might come from the redundancy at work during development that is ensuring the robustness of final neuronal positioning in *C. elegans*. Assessing migration dynamics and axonal networks may uncover additional abnormalities not visible in the current analysis.

Altogether, this work provides a new animal-model library for the study of actin variants associated with NMA. We show that different non-synonymous mutations in nematodes lead to a broad range of phenotypes as in human, and that the severity of *C. elegans* phenotypes correlates with patients' survival potential. Several *ACTB* p.R147 patients were identified only as post-zygotic mutations, thus expressed as mosaics in a subset of epithelial cells suggesting a lethality issue in human if expressed in all cells. Several patients with variant p.T203M in *ACTG1* suffer from severe BWCFF symptoms including microcephaly, profound intellectual disability and non-

ambulance. This locus is in fact a hot spot for *ACTG1* but no patient for *ACTB* has been identified so far, raising the question of lethality for *ACTB* in humans. Similarly, the *C. elegans* variant p.G74V showed 100% lethality -for which no other quantitative data can be retrieved, thus manually positioned further away on the right axis in a class III. In agreement, patients with p.G74V variant in *ACTG1* are severely affected, while no *ACTB* p.G74V variant has been discovered so far. To conclude, the severity of this initial set of *C. elegans* mutants correlates with that reported in human patients.

With commercial gene editing services in *C. elegans* offering quick delivery times and automated analysis of various criteria, it is plausible that *C. elegans* NMA models be used in the future as indicators to aid clinical prognosis for humans. All the tools generated here could be used to investigate the mechanisms underlying NMA pathophysiology and to screen for therapeutic strategies in the future.

Methods

C. elegans handling :

Animals were cultured on Nematode Growth Medium plates seeded with OP50 at 20°C unless otherwise stated (Brenner 1974). Bristol strain (N2) was used as a reference. We thank the Caenorhabditis Genetics Center for providing the strains N2, DW101 and EU1383. Complete list of strains used and their genotype are available in Table 3. All novel actin variants models were generated in the Reymann lab except two, which were outsourced to Suny Biotech® (recognisable by the allele prefix syb).

C. elegans generation :

We performed *dpy-10* co-CRISPR edition using purified homemade Cas9 protein, synthetic tracrRNA and ssODN from IDT, as described in Paix *et al* (Paix et al. 2015). Table of crRNA and repair template used are listed in Table 1. Additional silent mutations were introduced either to add or remove a restriction enzyme recognition site for genotyping strategies as well as mutate PAM or nucleotides within the sg guides. All generated strains were then outcrossed 4 times with N2 and all actin coding genes were sequenced to verify that only *act-2* was mutated (primers list Table 2). Sequencing was performed by Eurofins®. Results are analysed using

SnapGene®. The *rey016* allele consists of an insertion-deletion in exon 2 (33bp insertion + 816bp deletion) resulting in a frameshift and a premature STOP codon at the amino acid 70. The *rey021* allele presents a 35bp insertion causing a frameshift and a premature STOP codon at the amino acid 120. The *ok1229* harbours a large deletion starting at the 213th amino acid and extending beyond the 3' UTR

Note that *C. elegans'* actin including *act-2* possess an additional cysteine after the initial methionine in N-terminus compared to Human ACTB and ACTG1 (*ACTB* being MDDDIAA and *act-2* M**C**DDDVAA, Figure Sup 1A). For simplicity and easier reference to patient's variation, in order to be in frame with human numbering, we will hereafter refer to the mutations' loci by omitting this additional cysteine. For example, human variation ACTB p.L65V will be referred to as act-2 p.L65V instead of *act-2* p.L66V.

Table 1: List of guides and repair template sequences

Mutation and allele name	crRNA	Repair	Enzyme used for Genotyping
p.L65V, *rey012*	CAAUUGGGUACUUAAGGGUA	Ggtaaattttcaaaaaatt g acc gat tgg aaa tag ttg ttt tta ggt A**TC** **GT**C ACT CTT AAA TAC CCA ATT GAG CAT GGT ATC G	BfuI
p.G74S, *rey022*	CGUUACCAACUGGGACGACA	CTT ACC CTT AAG TAC CCA ATT GAG CAT AGT ATC GTG ACA AAT TGG GAT GAC A**TG** **G**AA AAA ATC TGG CAT CAC	BsmF1
p.G74V	AGCAUGGUAUCGUUACCAAC	g ttt tta gGT ATC CTT ACC CTT AAG TAC CCA ATT GAA CAT GTT ATT GTC ACT AAC **TGG** GAC GAC ATG GAA AAA ATC TGG C	PciI
p.T120I, *rey014*	AUACAUGGCUGGGGUAUUGA	CT AAC CGT GAA AAG ATG ATC CAA ATC ATG TTC GAG **ACA** TTC AAT ACA CCA GCA ATG TAC GTC GCC ATC CAA GCT G	BsaBI

p.R147S, *syb3920*	NA.	CAA GCT GTC CTC TCC CTC TAC GCT TCC GGG TCG ACC ACG GGA ATC GTC CTC GAC TCT GGA GAT	AccI
p.R183W, *syb5567*	NA.	ACG CAC ACA GTC CCA ATC TAC GAA GGA TAT GCC CTC CCA CAC GCC ATC CTC CGT CTT GAC TTG GCC GGA TGG GAT CTT ACT GAT TAC CTC ATG AAG ATC CTT ACC GAG CGT GGT TAC TCT TTC ACC ACC ACC GCT GAG CGT GAA ATC GTC CGT GAC ATC AAG GAG AAG CTT TGT TAC GTC GCG	HaeIII
p.R196C, *syb3909*	NA.	GGA ATC GTC CTC GAC TCT GGA GAT GGT GTT ACG CAC ACA GTC CCA ATC TAC GAA GGA TAT GCC CTC CCA CAC GCC ATC CTC CGT CTT GAC TTG GCT GGA CGT GAT CTT ACT GAT TAC CTC ATG AAG ATC TTG ACC GAA TGC GGT TAC TCT TTC ACC ACC ACC GCT GAG CGT GAA ATC GTC CGT GAC ATC AAG GAG AAG CTT TGT TAC GTC GCG CTC GAT TTC GAG CAA GAA ATG GCC ACC GCC	BglII
p.R196H, *rey020*	AUGAAGAUCCUUACCGAGCG	CTT ACT GAT TAC CTC ATG AAA ATT CTT ACC GAG CAT **GG**T TAC TCT TTC ACC ACC ACC GCT GAG CGT GAA ATC	AlWI

p.T203M, *rey023*	GACGAUUUCACGCUCAGCGG	G AAG ATC CTT ACC GAG CGT GGT TAC TCT TTC ACC **ACT** ATG GCA GAG CGA GAA ATT GTG CGT GAC ATC AAG GAG	MspAII
KO, *rey021*	AGCAUGGUAUCGUUACCAAC	NA.	
KO, *rey016*	AUACAUGGCUGGGGUAUUGA	NA.	

Legend : Lower case (non-coding), upper case (coding), red (silent mutation), blue (non-synonymous mutation of interest), bold (PAM sequence), underlined (crRNA sequence)

Table 2: List of PCR primers used

Gene	Forward primer	Reverse primer	Hybridization temperature	Amplicon length
act-1	oAC064 ttccccacgtgttctgtg	oAC056 GTTTGTGCAAGTTGACGAAG	54°C	1323 pb
act-2	oAC070 CTCGTAGTTGACAATGGATC	oAC069 CCAACAGTGATGACTTGTCCG	56°C	776pb
act-2	oAC043 gctggtttaattggaaagct	oAC052 gtcagccagttcaccacgaa	55°C	2544 pb
act-3	oAC065 ccttcccacacccacttg	oAC066 gggaccataacgatttggtg	60°C	1495 pb
act-4	oAC067 ctcgaccgaattctcgcc	oAC068 ggttgcgggataatacgaac	50°C	1379 pb
act-5	oAC061 CGTTTTCTATAAACTCGACTTC	oAC062 GAAATGGAAGGCACATGT	51°C	1500 pb

Table 3: List of strain used for this study

Name	Genotype	From
ACR061	*act-2* (*rey012* [Leu65Val]) V	This study
ACR096	*nmy-2*(*cp7*[*nmy-2*::gfp + LoxP *unc-119*(+) LoxP]) I; *geIs001* ([*mex-5*p::Lifeact::mKate::*nmy-2*UTR, *unc-119* (+)]) ; *unc119*(*ed3*) III; *act-2* (*rey012* [Leu65Val]) V	This study
ACR153	*otIs696* ; *act-2* (*rey012* [Leu65Val]) V	This study
ACR108	*act-2* (*rey022* [Gly74Ser]) V	This study

ACR224	*nmy-2*(*cp7*[*nmy-2*::gfp + LoxP *unc-119*(+) LoxP]) I; *geIs001* ([*mex-5*p::Lifeact::mKate::*nmy-2*UTR, *unc-119* (+)]) ; *unc119*(*ed3*) III; *act-2* (*rey022* [Gly74Ser]) V	This study
ACR165	*otIs696* ; *act-2* (*rey022* [Gly74Ser]) V	This study
ACR070	*act-2* (*rey014* [Thr120Ile]) V	This study
ACR139	*nmy-2*(*cp7*[*nmy-2*::gfp + LoxP *unc-119*(+) LoxP]) I; *geIs001* ([*mex-5*p::Lifeact::mKate::*nmy-2*UTR, *unc-119* (+)]) ; *unc119*(*ed3*) III; *act-2* (rey014 [Thr120Ile]) V	This study
ACR137	*otIs696* ; *act-2* (*rey014* [Thr120Ile]) V	This study
ACR168	*act-2*(*syb3920*[Arg147Ser]/nT1[*qIs51*]) V	This study
ACR216	*otIs696* ; *act-2*(*syb3920*[Arg147Ser]/nT1[*qIs51*]) V	This study
PHX5567	*act-2* (*syb5567* [Arg183Thr]) V	This study
ACR125	*act-2* (*syb3909*[Arg196Cys]) V	This study
ACR135	*nmy-2*(*cp7*[*nmy-2*::gfp + LoxP *unc-119*(+) LoxP]) I; *geIs001* ([*mex-5*p::Lifeact::mKate::*nmy-2*UTR, *unc-119* (+)]) ; *unc119*(*ed3*) III; *act-2* (*syb3909*[Arg196Cys]) V	This study
ACR166	*otIs696* ; *act-2* (*syb3909*[Arg196Cys]) V	This study
ACR085	*act-2* (*rey020* [Arg196His]) V	This study
ACR107	*nmy-2*(*cp7*[*nmy-2*::gfp + LoxP *unc-119*(+) LoxP]) I; *geIs001* ([*mex-5*p::Lifeact::mKate::*nmy-2*UTR, *unc-119* (+)]) ; *unc119*(*ed3*) III; *act-2* (*rey020* [Arg196His]) V	This study
ACR136	*otIs696* ; *act-2*(*rey020*[Arg196His]) V	This study
ACR099	*act-2*(*rey023*[Thr203Met]) / DnT1[*qIs50*] (IV;V)	This study
ACR122	*geIs001* ([*mex-5*p::Lifeact::mKate::*nmy-2*UTR, *unc-119* (+)]) ; *unc119*(*ed3*) III; *act-2*(*rey023* [Thr203Met]) / DnT1[*qIs50*] (IV;V)	This study

ACR219	*otIs696* ; *act-2*(*rey023*[Thr203Met]) / DnT1[*qIs50*] (IV;V)	This study
EU1383/ACR162	*act-2*(*ok1229*) V	Willis et al., 2006
ACR161	*act-2* (*rey016*(KO)) V	This study
ACR149	*act-2* (*rey021*(KO)) V	This study
ACR173	*otIs696* ; *act-2*(*rey021*[KO]) V	This study
DW101	*atl-1*(*tm853*) V/ DnT1[*qIs50*] (IV;V)	S. Mitani
VC854	*unc-2*(*gk366*) X	The C. elegans Deletion Mutant Consortium, 2012
SWG007	*nmy-2*(*cp7*[*nmy-2*::gfp + LoxP *unc-119*(+) LoxP]) I; *geaIs001* ([*mex-5*p::Lifeact::mKate::*nmy-2*UTR, *unc-119* (+)]) ; *unc119*(*ed3*) III	Reymann et al., 2016
OH15495	*otIs696*	Yemini et al., 2021
N2	Wild-type	Brenner, 1974

Phenotypic characterization:

Egg-laying assay

Total brood size of single hermaphrodites was quantified, by transferring single L4 animals from well to well every day on 6 well plates. Eggs from the previous day are counted. 36-48 hours after, the number of larvae is counted to determine the hatching percentage. Plates were maintained at the desired temperature (15°C or 20°C or 25°C) and checked for any contamination or lethality of the P0 hermaphrodite, in which case the animal was discarded from analysis. Note that heterozygotes *act-2* KO *rey016*/+ and *rey021*/+ (Figure 2C) were assessed in non-balanced nT1 background. We verified the animals' genotype by sequencing their progeny after experiment completion.

Motility burrowing assay

We followed Lesanpezeshki et al. protocol (Lesanpezeshki et al. 2019) and Ana Carvalho optimisation (personal communication). Liquid Pluronic gel (F-127 Pluronic from Sigma, dilution at 4 degrees of 13g in 37mL water) and all consumables were maintained at 10 degrees prior use. Height of gel was 0.6µm. Concentrated (100mg/mL) OP50 was use as chemoattractant. The negative control, *unc-2*(gk366) is a KO of the ortholog of human CACNA1B (calcium voltage-gated channel subunit alpha1 B), thus predicted to enable high voltage-gated calcium channel activity expressed in whole body wall muscle and required for proper animal motility. We used standard chemosensation assay where staged young adults were washed 4 times and placed at the center of an empty plate. Concentrated (100mg/mL) OP50 and Ultra Pure H_20 were placed on opposite extremities of the plate. After one hour, the number of animals on each side of the plates were counted as well as the animals that did not move from their original positions ("Immobile animals" in Figure S2C). Chemotaxis index was calculated using $I = \frac{n_{OP50} - n_{H_2O}}{n_{Total} - n_{immobile\ animals}}$.

RT-qPCR :

Single animal RT-qPCR was performed with minimal changes from Ly, Reid and Snell (Ly, Reid, and Snell 2015). Briefly, a single animal was transferred to a 0.2mL Eppendorf tube without the help of bacteria into 2µL of lysis buffer (5 mM Tris-HCl pH 8.0, 0.5% Triton X-100, 0.5%, Tween 20, 0.25 mM EDTA and 1 mg/mL proteinase K). The tube was incubated at 65°C for 10 min, then at 85°C for 1min in a T100™ Thermal Cycler. After lysis completion, we used the Maxima H Minus cDNA synthesis kit. Genomic DNA was removed by adding one microliter of a master mix containing 1µL of dsDNAse buffer, 1µL of DsDNAse and 8µL of nuclease free water to one microliter of lysis product. The solution was incubated at 37°C for 2 minutes and immediately chilled on ice. cDNA synthesis was performed by placing one microliter of cDNA synthesis mix to the lysate. We then generated cDNA by adding one µL of a mix containing 0.5µL oligo dT primer, 0.5µL 10mM dNTP, 6.5µL nuclease free water, 2µL RT buffer and 0.5µL Maxima H Minus enzyme mix. We centrifuged our tubes and incubated it at 25°C for 10 minutes, then at 55°C for 30 minutes then 5 minutes at 85°C. We diluted the cDNA to 25 µL with nuclease free water and used it immediately. We used a LightCycler® for qPCR. We used the Lightcycler® 480 SYBR Green | Master mix and followed its protocol thoroughly. Primers used for amplification are (all in 5' -> 3' ; hybridization temperature = 54°C) *act-1* (Forward : GCCCCATCAACCATGAAG, Reverse : gtttgtgcaagttgacgaag), *act-2* (Forward : CTCGTAGTTGACAATGGATC, Reverse : CCTCTCTTGGATTGGGCC), *act-3* (Forward : GCCCCATCAACCATGAAG, Reverse : ggtaaggcgaagagcTTAGA), *act-4* (Forward : ATCGATTGTCCACCGCAAG, Reverse :

ggttgcgggataatacgaac), *act-5* (Forward : GCTCCAAGCACAATGAAG, Reverse : gaaatggaaggcacatgt), *iscu-1* (Forward : GAAGGTTATCGATCACTACGAG, Reverse : CGTTATCGTCGACTCGAATC). *iscu-1* was used as a reference gene (Hoogewijs et al. 2008; Ly, Reid, and Snell 2015). Primer pairs efficiencies were measured using standard curve (Figure S2A).

Microscopy :

Embryonic development time-lapse imaging

L4 animals were put on a plate at 20°C 24h before acquisition. To obtain embryos, dissections were realised on a slide covered with an Idylle® 9 well Stencell (Pasturel, Strale, and Studer 2020) with 5µL of M9 and 4 animals of the desired genotype in each well (Pasturel, Strale, and Studer 2020). Then, corpses were removed from each well using a mouth micropipette. The slide containing the dissected animals was then sticked to a #1.5 coverslip (Marienfeld Superior) and placed on a Zeiss Axio-Observer 7. DIC images were then acquired using a Hamamatsu orca flash 4.0 LT camera, every 10 second for 40 minutes and then every 10 minutes for at least 14 hours with a 20x/0.8 PLAN-Apochromat objective.

Early embryogenesis

L4 animals were put on a plate at 20°C 24 hours before acquisition. Dissection of 5 animals was realised in 5µL of M9. The slide containing the dissected animals was then placed on a 2% agarose pad and placed on an inverted microscope Nikon EclipseTi-2 equipped with YOKOGAWA CSU X1 spinning disk head. Pictures were then acquired using a Photometrics Prime 95B camera each 2 or 10 second for 15 minutes with a plan apo 100x/1.45 Nikon objective.

Gonad imaging

L4 animals were placed in 10uL of 1mM Levamisole and placed on a 2% agarose pad. Acquisition of gonads were done one a LEICA DMI8 inverted microscope equipped with Yokogawa CSU W1 Spinning disk. Z-stacks were acquired using a Hamamatsu Orca Flash 4.0 camera with a 40X HCX PL APO oil immersion objective with a 0.2µm Z-step. Gonads widths were measured using FIJI by drawing a line with a 120-pixel width across the gonads germs cells and rachis in front of the +1 oocyte. Classification of phenotypes was done visually as represented in Green et al., 2011(Green et al. 2011). Heatmap was built using the heatmap.2 function from R package gplots. The mean number of observed phenotypes for each variable were scaled in the row direction.

NeuroPal

L4 animals were placed in 7µL of 125mM sodium azide and placed on a 2% agarose pad. Acquisitions were done accordingly to https://www.hobertlab.org/wp-content/uploads/2019/09/Configuring-Your-Microscope-for-NeuroPAL-v2.pdf on a Confocal Inverted Leica TCS SP8X equipped with DMI6000 microscope White Light Laser using an 40x/1.3 HC PL APO CS oil immersion objective with a distance of 0.9µm between each Z. Mapping and comparison of the expected expression pattern is performed using the published tools and reference atlas map.

In silico analysis

The primary sequence of ACT-2 from *C. elegans* was obtained from the UniProt database (ID: P10984). We used Alphafold2 (Jumper et al. 2021) to predict the structure of ACT-2 G-actin. Calculations were performed on the Halime HPC cluster at the Institute for Biophysical Chemistry at Hannover Medical School. We visualized ATP in the nucleotide binding cleft of ACT-2 G-actin by aligning the predicted ACT-2 structure with the structure of bovine ATP-bound G-actin (PDB-ID: 2BTF, (Schutt et al. 1993)). The homology model of the ACT-2 filament was generated using the SWISS-MODEL server (Waterhouse et al. 2018) with the ADP-bound human cytoskeletal β-actin filament (PDB-ID: 8DNH, (Arora et al. 2023) as a template. ChimeraX (Pettersen et al. 2021) was used for visualization of the structures and assessment of the potential implications of the variants for actin structure.

Data analysis, visualisation and statistics

We used R 4.4.1 through R-Studio 2023.12.1 and JAGS for all data analysis with all the required additional packages in their latest version available. Codes are available on our lab github. The statistical analysis were performed in the frame of Bayesian methods. The experimental data was enriched within the Bayesian framework by inference based on posterior distribution description. For embryonic lethality: Poisson distribution was used to estimate the embryonic lethality rates using an offset to account for the dependency with the number of eggs laid per animal (brood size) and specific parameters values for each genotype. Parameters were either given informative Normal priors: considering a very small lethality rate for WT N(0.01, 0.1), more probable lethality for all mutants N(0.1, 0.1) except the KO homozygotes for which we estimated a possible lethality of half the embryos N(0.5, 0.1). The analysis was also computed using low informative priors for all genotypes N(0,0.01) and gave similar results within a thousandth. Note that the observed 100% embryonic lethal genotypes were not included in the

model. The posterior distribution was computed using the Markov chain Monte Carlo method (McMC). A burn-in of 2000 iterations, followed by 50000 iterations was used for each of the 3 McMC chains, yielding a final 28800 iterations-sample for retrieving posterior distribution characteristics. Convergence of the McMC sample chains was checked graphically. Convergence was observed in each case. For each analysis on the main outcome, we computed the 95% credible interval of the embryonic failure rates for each genotype.

For the 3D motility assay, we compared the observed success rate to reach the chemoattractant after 2h by calculating their respective posterior distributions using two binomial distributions. We used the following priors: for WT mean = 0.9, sd=0.1 thus a probability modelled as p~dbeta(7.2, 0.8) and for all mutants a mean=0.5, sd=0.2 thus a probability modelled as p~dbeta(2.65, 2.65). A burn-in of 5000 iterations, followed by 105000 iterations was used for the McMC chain, in order to retrieve the posterior distributions. The odds ratio (OR), an estimation of the multiplication of the risk to fail reaching the target compared to WT, as well as the probability (p) that the difference between the two mean posterior probabilities is superior to 0.2 are indicated.

Acknowledgments

We would like to particularly thank the Imaging Center of IGBMC (ici.igbmc.fr) with the assistance of Elvire Guiot, Erwan Grandgirard, Yves Lutz and Bertrand Vernay. We warmly thank Dietmar Manstein (D.J.M) for his significant contributions to the project design and throughout grant application procedures. We also thank Juliette Godin, Sophie Quintin, Michel Labouesse and Patrick Reilly for critical reading of the manuscript. Thanks to Robert W. Fernandez post doc from Oliver Hobert's lab for training us to NeuroPAL as well as to our junior visitor scientists Fanny Bouvier, Emil Zessin and Johann Marois for their help.

Funding

This work was funded by European Joint Program for Rare Diseases through the European Union's Horizon 2020 research and innovation program under the EJP RD COFUND–EJP N° 825575. N.D.D. and D.J.M./J.N.G. with support from the German Federal Ministry of Education and Research under Grant Agreements 01GM1922A and 01GM1922B, respectively. A-C.R. under the project ANR-19-RAR4-0001-03. A-C.R. was also supported by the French Fondation Maladies Rares under the project SAM-2022-121409. This work of the Interdisciplinary Thematic Institute IMCBio+, as part of the ITI 2021-2028 program of the University of Strasbourg, CNRS

and Inserm, was supported by IdEx Unistra (ANR-10-IDEX-0002), and by SFRI-STRAT'US project (ANR-20-SFRI-0012) and EUR IMCBio (ANR-17-EURE-0023) under the framework of the France 2030 Program. N.D.D received grant support from Deutsche Forschungsgemeischaft (DFG) (DI 2170/3-1 and DI 2170/5-1), Else-Kröner-Fresenius Stiftung (2020_EKES.04) and German Federal Ministry of Education and Research under Grant Agreements 01GM1922A. We acknowledge the Imaging Center of IGBMC, member of the national infrastructure France-BioImaging supported by the French National Research Agency (ANR-10-INBS-04). A-C.R. is a CNRS investigator. N.A. is an Unistra technician personnel. J.N.G. is supported by the HiLF I grant for early career researchers from Hannover Medical School. Some strains were also provided by the CGC, which is funded by NIH Office of Research Infrastructure Programs (P40 OD010440).

Authors contribution

Conceptualisation A-C.R., N.D.D., T.H.; Methodology A-C.R., T.H.; Investigation, A-C.R., T.H., N.A., A.G. S.Y., F.M., J.G.; Writing -Original Draft, A-C.R., T.H.; Writing -Review & Editing, A-C.R., T.H., J.G., N.D.D.; Funding Acquisition, A-C.R., N.D.D, D.J.M, J.G.; Resources, A-C.R.; Supervision, A-C.R..

"The authors declare no competing interest."

References

Arora, Amandeep S, Hsiang-Ling Huang, Ramanpreet Singh, Yoshie Narui, Andrejus Suchenko, Tomoyuki Hatano, Sarah M Heissler, Mohan K Balasubramanian, and Krishna Chinthalapudi. 2023. "Structural Insights into Actin Isoforms." Edited by Pekka Lappalainen, Anna Akhmanova, and Vitold Galkin. *eLife* 12 (February):e82015. https://doi.org/10.7554/eLife.82015.

Avery, L. 1993. "The Genetics of Feeding in Caenorhabditis Elegans." *Genetics* 133 (4): 897–917. https://doi.org/10.1093/genetics/133.4.897.

Bauer, Jack, Vincent Poupart, Eugénie Goupil, Ken C. Q. Nguyen, David H. Hall, and Jean-Claude Labbé. 2021. "The Initial Expansion of the C. Elegans Syncytial Germ Line Is Coupled to Incomplete Primordial Germ Cell Cytokinesis." *Development (Cambridge, England)* 148 (18): dev199633. https://doi.org/10.1242/dev.199633.

Bernadskaya, Yelena Y, Andre Wallace, Jillian Nguyen, William A Mohler, and Martha C Soto. 2012. "UNC-40/DCC, SAX-3/Robo, and VAB-1/Eph Polarize F-Actin during Embryonic Morphogenesis by Regulating the WAVE/SCAR Actin Nucleation Complex." Edited by Andrew D Chisholm. *PLoS Genetics* 8 (8): e1002863. https://doi.org/10.1371/journal.pgen.1002863.s003.

Blanchoin, Laurent, Rajaa Boujemaa-Paterski, Cécile Sykes, and Julie Plastino. 2014. "Actin Dynamics, Architecture, and Mechanics in Cell Motility." *Physiological Reviews* 94 (1): 235–63. https://doi.org/10.1152/physrev.00018.2013.

Boiero Sanders, Micaela, Christopher P Toret, Audrey Guillotin, Adrien Antkowiak, Thomas Vannier, Robert C Robinson, and Alphée Michelot. 2022. "Specialization of Actin Isoforms Derived from

the Loss of Key Interactions with Regulatory Factors." *The EMBO Journal* 41 (5): e107982. https://doi.org/10.15252/embj.2021107982.

Brenner, S. 1974. "The Genetics of Caenorhabditis Elegans." *Genetics* 77 (1): 71–94.

Bunnell, Tina M., Brandon J. Burbach, Yoji Shimizu, and James M. Ervasti. 2011. "β-Actin Specifically Controls Cell Growth, Migration, and the G-Actin Pool." *Molecular Biology of the Cell* 22 (21): 4047–58. https://doi.org/10.1091/mbc.e11-06-0582.

Bunnell, Tina M., and James M. Ervasti. 2010. "Delayed Embryonic Development and Impaired Cell Growth and Survival in *Actg1* Null Mice." *Cytoskeleton* 67 (9): 564–72. https://doi.org/10.1002/cm.20467.

Cai, Emily D., Bryan K. Sun, Audris Chiang, Anna Rogers, Laura Bernet, Binbin Cheng, Joyce Teng, Kerri E. Rieger, and Kavita Y. Sarin. 2017. "Postzygotic Mutations in Beta-Actin Are Associated with Becker's Nevus and Becker's Nevus Syndrome." *The Journal of Investigative Dermatology* 137 (8): 1795–98. https://doi.org/10.1016/j.jid.2017.03.017.

Chacon-Camacho, Oscar F., Tania Barragán-Arévalo, Camilo E. Villarroel, Mónica Almanza-Monterrubio, and Juan Carlos Zenteno. 2020. "Previously Undescribed Phenotypic Findings and Novel *ACTG1* Gene Pathogenic Variants in Baraitser-Winter Cerebrofrontofacial Syndrome." *European Journal of Medical Genetics* 63 (5): 103877. https://doi.org/10.1016/j.ejmg.2020.103877.

Chai, Yongping, Dong Tian, Zhiwen Zhu, Yuxiang Jiang, Shanjin Huang, Dou Wu, Guangshuo Ou, and Wei Li. 2022. "Wnt Signaling Polarizes Cortical Actin Polymerization to Increase Daughter Cell Asymmetry." *Cell Discovery* 8 (1): 22. https://doi.org/10.1038/s41421-022-00376-4.

Charras, Guillaume, and Ewa Paluch. 2008. "Blebs Lead the Way: How to Migrate without Lamellipodia." *Nature Reviews. Molecular Cell Biology* 9 (9): 730–36. https://doi.org/10.1038/nrm2453.

Cianci, Paola, Grazia Fazio, Sara Casagranda, Marco Spinelli, Carmelo Rizzari, Gianni Cazzaniga, and Angelo Selicorni. 2017. "Acute Myeloid Leukemia in Baraitser–Winter Cerebrofrontofacial Syndrome." *American Journal of Medical Genetics Part A* 173 (2): 546–49. https://doi.org/10.1002/ajmg.a.38057.

Conboy, Erin, Filippo Vairo, Darrel Waggoner, Carole Ober, Soma Das, Radhika Dhamija, Eric W. Klee, and Pavel Pichurin. 2017. "Pathogenic Variant in ACTB, p.Arg183Trp, Causes Juvenile-Onset Dystonia, Hearing Loss, and Developmental Delay without Midline Malformation." *Case Reports in Genetics* 2017:9184265. https://doi.org/10.1155/2017/9184265.

Cuvertino, Sara, Helen M Stuart, Kate E Chandler, Neil A Roberts, Ruth Armstrong, Laura Bernardini, Sanjeev Bhaskar, et al. 2017. "ACTB Loss-of-Function Mutations Result in a Pleiotropic Developmental Disorder." *The American Journal of Human Genetics* 101 (6): 1021–33.

Dominguez, Roberto, and Kenneth C. Holmes. 2011. "Actin Structure and Function." *Annual Review of Biophysics* 40 (Volume 40, 2011): 169–86. https://doi.org/10.1146/annurev-biophys-042910-155359.

Dorn, Jonas F, Li Zhang, Véronique Paradis, Daniel Edoh-Bedi, Sylvester Jusu, Paul S Maddox, and Amy Shaub Maddox. 2010. "Actomyosin Tube Formation in Polar Body Cytokinesis Requires Anillin in C. Elegans." *Current Biology* 20 (22): 2046–51.

Dugina, Vera, Ingrid Zwaenepoel, Giulio Gabbiani, Sophie Clément, and Christine Chaponnier. 2009. "β- and γ-Cytoplasmic Actins Display Distinct Distribution and Functional Diversity." *Journal of Cell Science* 122 (16): 2980–88. https://doi.org/10.1242/jcs.041970.

Eggink, Hendriekje, Martje E. van Egmond, Corien C. Verschuuren-Bemelmans, Marleen C. Schönherr, Tom J. de Koning, D.L. Marinus Oterdoom, J. Marc C. van Dijk, and Marina A.J. Tijssen. 2017. "Dystonia-Deafness Syndrome Caused by a β-Actin Gene Mutation and Response to Deep Brain Stimulation." *Movement Disorders* 32 (1): 162–65. https://doi.org/10.1002/mds.26842.

Ennomani, Hajer, Gaëlle Letort, Christophe Guérin, Jean-Louis Martiel, Wenxiang Cao, François Nédélec, Enrique M De La Cruz, Manuel Théry, and Laurent Blanchoin. 2016. “Architecture and Connectivity Govern Actin Network Contractility.” *Current Biology*, February, 1–12.

Ferguson, E. L., and H. R. Horvitz. 1985. “Identification and Characterization of 22 Genes That Affect the Vulval Cell Lineages of the Nematode Caenorhabditis Elegans.” *Genetics* 110 (1): 17–72. https://doi.org/10.1093/genetics/110.1.17.

Flynn, Jonathan R., and Francis J. McNally. 2017. “A Casein Kinase 1 Prevents Expulsion of the Oocyte Meiotic Spindle into a Polar Body by Regulating Cortical Contractility.” *Molecular Biology of the Cell* 28 (18): 2410–19. https://doi.org/10.1091/mbc.e17-01-0056.

Freitas, Julian Letícia, Thiago Cardoso Vale, Orlando G.P. Barsottini, and José Luiz Pedroso. 2019. “Expanding the Phenotype of Dystonia-Deafness Syndrome Caused by ACTB Gene Mutation.” *Movement Disorders Clinical Practice* 7 (1): 86–87. https://doi.org/10.1002/mdc3.12854.

Gearing, Marla, Jorge L. Juncos, Vincent Procaccio, Claire-Anne Gutekunst, Elaine M. Marino-Rodriguez, Kymberly A. Gyure, Shoichiro Ono, et al. 2002. “Aggregation of Actin and Cofilin in Identical Twins with Juvenile-Onset Dystonia.” *Annals of Neurology* 52 (4): 465–76. https://doi.org/10.1002/ana.10319.

Green, Rebecca A., Huey-Ling Kao, Anjon Audhya, Swathi Arur, Jonathan R. Mayers, Heidi N. Fridolfsson, Monty Schulman, et al. 2011. “A High-Resolution C. Elegans Essential Gene Network Based on Phenotypic Profiling of a Complex Tissue.” *Cell* 145 (3): 470–82. https://doi.org/10.1016/j.cell.2011.03.037.

Greve, Johannes N., and Dietmar J. Manstein. 2024. “Baraitser–Winter Syndrome Hotspot Mutation R196H in Cytoskeletal β–Actin Reduces F–Actin Stability and Perturbs Interaction with the Arp2/3 Complex.” https://doi.org/10.1101/2024.03.20.585892.

Greve, Johannes N., Anja Marquardt, Robin Heiringhoff, Theresia Reindl, Claudia Thiel, Nataliya Di Donato, Manuel H. Taft, and Dietmar J. Manstein. 2023. “The Non–Muscle Actinopathy–Associated Mutation E334Q in Cytoskeletal γ–Actin Perturbs Interaction of Actin Filaments with Myosin and ADF/Cofilin Family Proteins.” Preprint. https://doi.org/10.7554/eLife.93013.1.

Greve, Johannes N., Frederic V. Schwäbe, Thomas Pokrant, Jan Faix, Nataliya Di Donato, Manuel H. Taft, and Dietmar J. Manstein. 2022. “Frameshift Mutation S368fs in the Gene Encoding Cytoskeletal β-Actin Leads to ACTB-Associated Syndromic Thrombocytopenia by Impairing Actin Dynamics.” *European Journal of Cell Biology* 101 (2): 151216. https://doi.org/10.1016/j.ejcb.2022.151216.

Hall, D.H., Herndon, L.A., and Altun, Z. 2017. “Introduction to C. Elegans Embryo Anatomy.” *WormAtlas*. https://doi.org/doi:10.3908/wormatlas.4.1.

Happle, Rudolf. 2017. “Becker’s Nevus and Lethal Beta-Actin Mutations.” *Journal of Investigative Dermatology* 137 (8): 1619–21. https://doi.org/10.1016/j.jid.2017.04.003.

Hayashi, Yuriko, Kanako Ono, and Shoichiro Ono. 2019. “Mutations in Caenorhabditis Elegans Actin, Which Are Equivalent to Human Cardiomyopathy Mutations, Cause Abnormal Actin Aggregation in Nematode Striated Muscle.” *F1000Research* 8 (March):279. https://doi.org/10.12688/f1000research.18476.1.

Hoogewijs, David, Koen Houthoofd, Filip Matthijssens, Jo Vandesompele, and Jacques R Vanfleteren. 2008. “Selection and Validation of a Set of Reliable Reference Genes for Quantitative Sod Gene Expression Analysis in C. Elegans.” *BMC Molecular Biology* 9 (1): 9. https://doi.org/10.1186/1471-2199-9-9.

Jumper, John, Richard Evans, Alexander Pritzel, Tim Green, Michael Figurnov, Olaf Ronneberger, Kathryn Tunyasuvunakool, et al. 2021. “Highly Accurate Protein Structure Prediction with AlphaFold.” *Nature* 596 (7873): 583–89. https://doi.org/10.1038/s41586-021-03819-2.

Krause, Michael, Martha Wild, Brad Rosenzweig, and David Hirsh. 1989. “Wild-Type and Mutant Actin Genes in Caenorhabditis Elegans.” *Journal of Molecular Biology* 208 (3): 381–92. https://doi.org/10.1016/0022-2836(89)90503-2.

Lai, Wing-Fu, and Wing-Tak Wong. 2020. “Roles of the Actin Cytoskeleton in Aging and Age-Associated Diseases.” *Ageing Research Reviews* 58 (March):101021. https://doi.org/10.1016/j.arr.2020.101021.

Landel, C. P., M. Krause, R. H. Waterston, and D. Hirsh. 1984. “DNA Rearrangements of the Actin Gene Cluster in Caenorhabditis Elegans Accompany Reversion of Three Muscle Mutants.” *Journal of Molecular Biology* 180 (3): 497–513. https://doi.org/10.1016/0022-2836(84)90024-x.

Latham, Sharissa L., Nadja Ehmke, Patrick Y. A. Reinke, Manuel H. Taft, Dorothee Eicke, Theresia Reindl, Werner Stenzel, et al. 2018. “Variants in Exons 5 and 6 of ACTB Cause Syndromic Thrombocytopenia.” *Nature Communications* 9 (1): 4250. https://doi.org/10.1038/s41467-018-06713-0.

Lesanpezeshki, Leila, Jennifer E. Hewitt, Ricardo Laranjeiro, Adam Antebi, Monica Driscoll, Nathaniel J. Szewczyk, Jerzy Blawzdziewicz, Carla M. R. Lacerda, and Siva A. Vanapalli. 2019. “Pluronic Gel-Based Burrowing Assay for Rapid Assessment of Neuromuscular Health in C. Elegans.” *Scientific Reports* 9 (1): 15246. https://doi.org/10.1038/s41598-019-51608-9.

Ly, Kien, Suzanne J. Reid, and Russell G. Snell. 2015. “Rapid RNA Analysis of Individual Caenorhabditis Elegans.” *MethodsX* 2:59–63. https://doi.org/10.1016/j.mex.2015.02.002.

MacQueen, A. J., J. J. Baggett, N. Perumov, R. A. Bauer, T. Januszewski, L. Schriefer, and J. A. Waddle. 2005. “ACT-5 Is an Essential Caenorhabditis Elegans Actin Required for Intestinal Microvilli Formation.” *Molecular Biology of the Cell* 16 (7): 3247–59. https://doi.org/10.1091/mbc.e04-12-1061.

Markaki, Maria, and Nektarios Tavernarakis. 2010. “Modeling Human Diseases in *Caenorhabditis Elegans*.” *Biotechnology Journal* 5 (12): 1261–76. https://doi.org/10.1002/biot.201000183.

Marston, Daniel J, and Bob Goldstein. 2006. “Actin-Based Forces Driving Embryonic Morphogenesis in Caenorhabditis Elegans.” *Current Opinion in Genetics & Development* 16 (4): 392–98.

Michelot, Alphée, and David G Drubin. 2011. “Building Distinct Actin Filament Networks Review in a Common Cytoplasm.” *Current Biology* 21 (14): R560–69.

Murrell, Michael, Patrick W Oakes, Martin Lenz, and Margaret L Gardel. 2015. “Forcing Cells into Shape: The Mechanics of Actomyosin Contractility.” *Nature Publishing Group* 16 (8): 486–98.

Naganathan, Sundar Ram, Sebastian Fürthauer, Josana Rodriguez, Bruno Thomas Fievet, Frank Jülicher, Julie Ahringer, Carlo Vittorio Cannistraci, and Stephan W. Grill. 2018. “Morphogenetic Degeneracies in the Actomyosin Cortex.” *eLife* 7 (October):e37677. https://doi.org/10.7554/eLife.37677.

Nance, Jeremy. 2005. “Gastrulation in C. Elegans.” *WormBook*.

Ono, K. 2003. “Specific Requirement for Two ADF/Cofilin Isoforms in Distinct Actin-Dependent Processes in Caenorhabditis Elegans.” *Journal of Cell Science* 116 (10): 2073–85.

Ono, Shoichiro. 2014. “Regulation of Structure and Function of Sarcomeric Actin Filaments in Striated Muscle of the Nematode *Caenorhabditis Elegans*.” *The Anatomical Record* 297 (9): 1548–59. https://doi.org/10.1002/ar.22965.

Ono, Shoichiro, and David Pruyne. 2012. “Biochemical and Cell Biological Analysis of Actin in the Nematode Caenorhabditis Elegans.” *METHODS* 56 (1): 11–17.

Oosterheert, Wout, Florian E. C. Blanc, Ankit Roy, Alexander Belyy, Micaela Boiero Sanders, Oliver Hofnagel, Gerhard Hummer, Peter Bieling, and Stefan Raunser. 2023. “Molecular Mechanisms of Inorganic-Phosphate Release from the Core and Barbed End of Actin Filaments.” *Nature Structural & Molecular Biology* 30 (11): 1774–85. https://doi.org/10.1038/s41594-023-01101-9.

Pacquelet, Anne, Perrine Uhart, Jean-Pierre Tassan, and Grégoire Michaux. 2015. “PAR-4 and Anillin Regulate Myosin to Coordinate Spindle and Furrow Position during Asymmetric Division.” *Journal of Cell Biology* 210 (7): 1085–99. https://doi.org/10.1083/jcb.201503006.

Paix, A, A Folkmann, D Rasoloson, and G Seydoux. 2015. “High Efficiency, Homology-Directed Genome Editing in Caenorhabditis Elegans Using CRISPR-Cas9 Ribonucleoprotein Complexes.” *Genetics* 201 (1): 47–54.

Parker, Francine, Thomas G. Baboolal, and Michelle Peckham. 2020. “Actin Mutations and Their Role in Disease.” *International Journal of Molecular Sciences* 21 (9): 3371. https://doi.org/10.3390/ijms21093371.

Pasturel, Aurélien, Pierre-Olivier Strale, and Vincent Studer. 2020. “Tailoring Common Hydrogels into 3D Cell Culture Templates.” *Advanced Healthcare Materials* 9 (18): 2000519. https://doi.org/10.1002/adhm.202000519.

Patrinostro, Xiaobai, Pallabi Roy, Angus Lindsay, Christopher M. Chamberlain, Lauren J. Sundby, Colby G. Starker, Daniel F. Voytas, James M. Ervasti, and Benjamin J. Perrin. 2018. “Essential Nucleotide- and Protein-Dependent Functions of *Actb* /β-Actin.” *Proceedings of the National Academy of Sciences* 115 (31): 7973–78. https://doi.org/10.1073/pnas.1807895115.

Pettersen, Eric F., Thomas D. Goddard, Conrad C. Huang, Elaine C. Meng, Gregory S. Couch, Tristan I. Croll, John H. Morris, and Thomas E. Ferrin. 2021. “UCSF ChimeraX: Structure Visualization for Researchers, Educators, and Developers.” *Protein Science: A Publication of the Protein Society* 30 (1): 70–82. https://doi.org/10.1002/pro.3943.

Polubothu, S., D. Abdin, M. Barysch, A. Thomas, N. Bulstrode, R. Evans, L. Solman, et al. 2020. “Dermatological Signs Lead to Discovery of Mosaic ACTB Variants in Segmental Odontomaxillary Dysplasia.” *The British Journal of Dermatology* 183 (6): 1128–30. https://doi.org/10.1111/bjd.19339.

Priess, J. R., and D. I. Hirsh. 1986. “Caenorhabditis Elegans Morphogenesis: The Role of the Cytoskeleton in Elongation of the Embryo.” *Developmental Biology* 117 (1): 156–73. https://doi.org/10.1016/0012-1606(86)90358-1.

Procaccio, Vincent, Gloria Salazar, Shoichiro Ono, Melanie L. Styers, Marla Gearing, Antonio Davila, Richard Jimenez, et al. 2006. “A Mutation of Beta -Actin That Alters Depolymerization Dynamics Is Associated with Autosomal Dominant Developmental Malformations, Deafness, and Dystonia.” *American Journal of Human Genetics* 78 (6): 947–60. https://doi.org/10.1086/504271.

Quintin, Sophie, Shaohe Wang, Julien Pontabry, Ambre Bender, François Robin, Vincent Hyenne, Frédéric Landmann, Christelle Gally, Karen Oegema, and Michel Labouesse. 2018. “Correction: Non-Centrosomal Epidermal Microtubules Act in Parallel to LET-502/ROCK to Promote *C. Elegans* Elongation (Doi:10.1242/Dev.126615).” *Development* 145 (10): dev167262. https://doi.org/10.1242/dev.167262.

Reymann, Anne-Cecile, Fabio Staniscia, Anna Erzberger, Guillaume Salbreux, and Stephan W Grill. 2016. “Cortical Flow Aligns Actin Filaments to Form a Furrow.” *eLife* 5 (October):e17807.

Reynolds, Matthew J., Carla Hachicho, Ayala G. Carl, Rui Gong, and Gregory M. Alushin. 2022. “Bending Forces and Nucleotide State Jointly Regulate F-Actin Structure.” *Nature* 611 (7935): 380–86. https://doi.org/10.1038/s41586-022-05366-w.

Riva, Claudia, Martina Hajduskova, Christelle Gally, Shashi Kumar Suman, Arnaud Ahier, and Sophie Jarriault. 2022. “A Natural Transdifferentiation Event Involving Mitosis Is Empowered by Integrating Signaling Inputs with Conserved Plasticity Factors.” *Cell Reports* 40 (12): 111365. https://doi.org/10.1016/j.celrep.2022.111365.

Rivière, Jean-Baptiste, Bregje W M Van Bon, Alexander Hoischen, Stanislav S Kholmanskikh, Brian J O’Roak, Christian Gilissen, Sabine Gijsen, et al. 2012. “De Novo Mutations in the Actin Genes

ACTB and ACTG1 Cause Baraitser-Winter Syndrome." *Nature Genetics* 44 (4): 440–44. https://doi.org/10.1038/ng.1091.

Rose, Lesilee, and Pierre Gönczy. 2014. "Polarity Establishment, Asymmetric Division and Segregation of Fate Determinants in Early C. Elegans Embryos." *WormBook*, 1–43.

Rubenstein, Peter A., and Kuo-Kuang Wen. 2014. "Insights into the Effects of Disease-causing Mutations in Human Actins." *Cytoskeleton* 71 (4): 211–29. https://doi.org/10.1002/cm.21169.

Schafer, William. 2005. "Egg-Laying." *WormBook*.

Schutt, Clarence E., James C. Myslik, Michael D. Rozycki, Nalin C. W. Goonesekere, and Uno Lindberg. 1993. "The Structure of Crystalline Profilin–β-Actin." *Nature* 365 (6449): 810–16. https://doi.org/10.1038/365810a0.

Serobyan, Vahan, Zacharias Kontarakis, Mohamed A El-Brolosy, Jordan M Welker, Oleg Tolstenkov, Amr M Saadeldein, Nicholas Retzer, Alexander Gottschalk, Ann M Wehman, and Didier Yr Stainier. 2020. "Transcriptional Adaptation in Caenorhabditis Elegans." *eLife* 9 (January):e50014. https://doi.org/10.7554/eLife.50014.

Skogseid, Inger Marie, Oddveig Røsby, Ane Konglund, James P. Connelly, Bård Nedregaard, Greg Eigner Jablonski, Nadja Kvernmo, Asbjørg Stray-Pedersen, and Joel C. Glover. 2018. "Dystonia-Deafness Syndrome Caused by ACTB p.Arg183Trp Heterozygosity Shows Striatal Dopaminergic Dysfunction and Response to Pallidal Stimulation." *Journal of Neurodevelopmental Disorders* 10 (1): 17. https://doi.org/10.1186/s11689-018-9235-z.

Vanslembrouck, Bieke, Christophe Ampe, and Jolanda Van Hengel. 2020. "Time for Rethinking the Different B-actin Transgenic Mouse Models?" *Cytoskeleton* 77 (12): 527–43. https://doi.org/10.1002/cm.21647.

Vedula, Pavan, Satoshi Kurosaka, Nicolae Adrian Leu, Yuri I Wolf, Svetlana A Shabalina, Junling Wang, Stephanie Sterling, Dawei W Dong, and Anna Kashina. 2017. "Diverse Functions of Homologous Actin Isoforms Are Defined by Their Nucleotide, Rather than Their Amino Acid Sequence." *eLife* 6 (December):e31661. https://doi.org/10.7554/eLife.31661.

Verloes, Alain, Nataliya Di Donato, Julien Masliah-Planchon, Marjolijn Jongmans, Omar A. Abdul-Raman, Beate Albrecht, Judith Allanson, et al. 2015. "Baraitser–Winter Cerebrofrontofacial Syndrome: Delineation of the Spectrum in 42 Cases." *European Journal of Human Genetics* 23 (3): 292–301. https://doi.org/10.1038/ejhg.2014.95.

Verloes, Alain, Séverine Drunat, Daniela Pilz, and Nataliya Di Donato. 1993. "Baraitser-Winter Cerebrofrontofacial Syndrome." In *GeneReviews®*, edited by Margaret P. Adam, Jerry Feldman, Ghayda M. Mirzaa, Roberta A. Pagon, Stephanie E. Wallace, Lora JH Bean, Karen W. Gripp, and Anne Amemiya. Seattle (WA): University of Washington, Seattle. http://www.ncbi.nlm.nih.gov/books/NBK327153/.

Vontell, Regina, Veena G. Supramaniam, Alice Davidson, Claire Thornton, Andreas Marnerides, Muriel Holder-Espinasse, Suzanne Lillis, et al. 2019. "Post-Mortem Characterisation of a Case With an ACTG1 Variant, Agenesis of the Corpus Callosum and Neuronal Heterotopia." *Frontiers in Physiology* 10. https://www.frontiersin.org/journals/physiology/articles/10.3389/fphys.2019.00623.

Vuong-Brender, Thanh Thi Kim, Martine Ben Amar, Julien Pontabry, and Michel Labouesse. 2017. "The Interplay of Stiffness and Force Anisotropies Drives Embryo Elongation." *eLife* 6 (February):e23866. https://doi.org/10.7554/eLife.23866.

Vuong-Brender, Thanh T.K., Xinyi Yang, and Michel Labouesse. 2016. "C. Elegans Embryonic Morphogenesis." In *Current Topics in Developmental Biology*, 116:597–616. Elsevier. https://doi.org/10.1016/bs.ctdb.2015.11.012.

Waterhouse, Andrew, Martino Bertoni, Stefan Bienert, Gabriel Studer, Gerardo Tauriello, Rafal Gumienny, Florian T Heer, et al. 2018. "SWISS-MODEL: Homology Modelling of Protein

Structures and Complexes." *Nucleic Acids Research* 46 (W1): W296–303. https://doi.org/10.1093/nar/gky427.

Welker, Jordan M., Vahan Serobyan, Elhamalsadat Zaker Esfahani, and Didier Y. R. Stainier. 2023. "Partial Sequence Identity in a 25-Nucleotide Long Element Is Sufficient for Transcriptional Adaptation in the Caenorhabditis Elegans Act-5/Act-3 Model." *PLoS Genetics* 19 (6): e1010806. https://doi.org/10.1371/journal.pgen.1010806.

Wilkinson, Alex W., Jonathan Diep, Shaobo Dai, Shuo Liu, Yaw Shin Ooi, Dan Song, Tie-Mei Li, et al. 2019. "SETD3 Is an Actin Histidine Methyltransferase That Prevents Primary Dystocia." *Nature* 565 (7739): 372–76. https://doi.org/10.1038/s41586-018-0821-8.

Willis, John H., Edwin Munro, Rebecca Lyczak, and Bruce Bowerman. 2006. "Conditional Dominant Mutations in the Caenorhabditis Elegans Gene Act-2 Identify Cytoplasmic and Muscle Roles for a Redundant Actin Isoform." *Molecular Biology of the Cell* 17 (3): 1051–64. https://doi.org/10.1091/mbc.e05-09-0886.

Yemini, Eviatar, Albert Lin, Amin Nejatbakhsh, Erdem Varol, Ruoxi Sun, Gonzalo E. Mena, Aravinthan D.T. Samuel, Liam Paninski, Vivek Venkatachalam, and Oliver Hobert. 2021. "NeuroPAL: A Multicolor Atlas for Whole-Brain Neuronal Identification in C. Elegans." *Cell* 184 (1): 272-288.e11. https://doi.org/10.1016/j.cell.2020.12.012.

Zech, Michael, Robert Jech, Matias Wagner, Tobias Mantel, Sylvia Boesch, Michael Nocker, Angela Jochim, et al. 2017. "Molecular Diversity of Combined and Complex Dystonia: Insights from Diagnostic Exome Sequencing." *Neurogenetics* 18 (4): 195–205. https://doi.org/10.1007/s10048-017-0521-9.

Zhang, Pu, Taylor N. Medwig-Kinney, and Bob Goldstein. 2023. "Architecture of the Cortical Actomyosin Network Driving Apical Constriction in *C. Elegans*." *Journal of Cell Biology* 222 (9): e202302102. https://doi.org/10.1083/jcb.202302102.

Figure legends

Figure 1 : Insertion of Non-Muscle Actinopathies variants in the *C. elegans act-2*

(A) Dot heatmap of patients' symptoms. Intellectual disability (ID) level letter code : n=none, m=mild, mo=moderate, s=severe, p=profound. MRI = Magnetic Resonance Imaging. BWCFF = Baraitser-Winter Cerebro Fronto Facial syndrome. (B) Structural model of ACT-2 G-actin generated by Alphafold2. Subdomains of ACT-2 are colored in grey (SD1), light grey (SD2), blue (SD3) and light blue (SD4). Homology model of the ACT-2 filament (based on PDB-ID: 8DNH). ACT-2 protomers are colored in different shades of blue. The mutated residues investigated in this study are shown in red. The ATP bound to the individual protomers is shown as a stick-model. The zoom-in shows the location and structural environment of the individual mutated residues in more detail. (C) Schematic *act-2* representation highlighting the loci of single point variants obtained via CRISPR edition (Adapted from http://wormweb.org/exonintron). Three *act-2* gene knockouts are also depicted: *rey016*, *rey021* and *ok1229* (Willis et al., 2006). Note that the amino acid numbering is here in frame with human ACTB/ACTG1, consider -1 AA in the frame of *C. elegans* due to an additional cysteine in second N-ter position, the base pair are however kept in the *C. elegans act-2* frame. (D) Table summarizing the overall viability of *C. elegans act-2* variants at 20°C.

Figure S1 :

(A) Amino acid alignment of *C. elegans'* ACT-2, human ACTB and ACTG1 showing high conservation of amino acid as well as amino acid physico-chemical properties (Snapgene). Loci of interest are framed with black boxes. (B) Alignment of sequences obtained from the sequencing of F1 animals from the CRISPR/Cas9 *act-2* p.G74V generation show the presence of the Gly to Ser variant (Snapgene, black box). Top rows show the reference *act-2* sequence and its translation. Bottom rows show the obtained sequence, peaks and predicted translation.

Figure 2 : *act-2* gene knock-outs affects fertility despite compensation mechanisms

(A) Single animal RT-qPCR showing the normalized amount of mRNA for each *C. elegans* actin coding genes in the *act-2* homozygous *ok1229* and *rey021*. Normalization was done with the amount of mRNA quantified for the housekeeping gene *iscu-1* and with the WT values set to 1. Different colors show different replicates. Small dot is the value for one animal while bigger dots correspond to the experiment's mean. Diamonds show the mean of all replicates. (B) Progeny number of homozygous *act-2* KO (*ok1229* and *rey021*) at the mentioned temperatures were counted during 48h. The sum of eggs laid for one animal is shown as a dot or a triangle. (B') Percentage of eggs that failed to hatch. The mean number of eggs that did not hatch for one animal is shown as a dot or a triangle. Mean value is represented by a diamond. (C) Progeny number at 20°C were counted for 72h for homozygous (*rey016*/*rey016*) (*rey021*/*rey021*) or heterozygous (*rey016*/+) (*rey021*/+) *act-2* KO animals. The sum of eggs laid for one animal is shown as a dot. (C') Percentage of eggs that failed to hatch. The mean number of eggs that did not hatch for one animal is shown as a dot. Mean value is represented by a diamond.

Figure S2 :

(A) Standard curve analysis to determine the efficiency of amplification of the 6 primer pairs used for RT-qPCR. Efficiency is calculated using $E = 10^{\frac{1}{slope}}$.

Figure 3 : *act-2* variants affect egg-laying capacities and embryogenesis success

(A) Progeny number at 20°C were counted for 72h for homozygous *act-2* variants. The sum of eggs laid for one animal is shown as a dot. Mean is represented as a diamond. (B) Percentage of eggs that failed to hatch. The percent of dead eggs for one animal is shown as a dot. Mean is represented as a diamond. The rightmost plot presents the 95% credibility intervals of the posterior distributions of the embryonic lethality rates considering the priors described in the methods section and our observed data set. These are calculated with a Bayesian model based on Poisson laws with an offset to account for the progeny numbers. Experimental values are represented by red diamonds (mean) and blue circles (median). (C) Actin organization in a WT gonad observed using an actin probe (LifeAct::mKate2). Green and purple arrows represent the space measured to calculate the rachis/gonad ratio measured in front of the -1 oocyte. (D) Boxplot presenting the ratio between the rachis and the gonad‘s width of homozygote animals. Mean is represented as a diamond. (E) Heatmap of observed phenotypes, in percent. (F) Stacked histogram of the end status of embryogenesis for different *act-2* variants in percent. Schemes on the right represent the different defects observed. * embryos coming from heterozygous balanced animals. (See Movies 1, 2, 3, 4 and 5).

Figure S3 :

(A) Progeny number at 20°C were counted for 72h for heterozygous *act-2* variant animals. The sum of eggs laid for one animal is shown as a dot. Mean is represented as a diamond. B. Percentage of eggs that failed to hatch. The mean number of eggs that did not hatch for one animal is shown as a dot. Mean is represented as a diamond. (C, D) Red boxes show the area where no WT eggshells are present. Red points show embryos that will subsequently die while blue triangles mean that the embryo will survive. Embryo schemes above are at the right scale. * embryos coming from heterozygous balanced animals. (C) Aspect ratio measurement of embryos' eggshell. Aspect ratio is defined as the ratio between the major and minor axis. (D) 2D Area measurement of embryos' eggshell. E. Timeline of recognizable morphogenesis stages during *C. elegans'* embryogenesis. Time counted after fertilization, from (Hall, D.H., Herndon, L.A., and Altun, Z. 2017). Leftmost plot presents the timing in minutes between the bean stage and the comma stage. Rightmost plot presents the timing in minutes between the comma stage and hatching. * embryos coming from heterozygous balanced animals.

Figure 4 : Actin mutation effects on cortical organization in early embryos

(A) Cortical plane of embryos at different stages, LifeAct::mKate2 shown in magenta and NMY-2::GFP shown in green, to reveal actin filaments and myosin distribution. p.T203M animals only have LifeAct::mKate2. (PN = Pronuclei) Anterior is on the left. B, C, D. Equatorial plane image of embryos expressing LifeAct::mKate2 (magenta) and NMY-2::GFP (green). (B) Cytokinesis defect observed. The cytokinesis ring relaxes after completion of a first ingression (pink arrow), cytokinesis then proceeds to divide directly the zygote in four cells. See Movie 6. (C) Meiosis defects. An additional nucleus is visible (blue arrow). Nuclei are circled. See Movie 7. (D) Blebbing. Large protrusion called bleb extrude from the anterior cell (orange arrow). After actin and myosin reassembly the bleb retracts and division seems to occur normally. See Movie 8. (E) Abnormal membrane ruffling is observed in some embryos (white arrow). (F) Cortical plane of embryos presenting other phenotypes. Abnormal aspect ratio of the cortex implies a rounder

embryo (see also Figure S4). Abnormal division axis (red arrows) leads to abnormal cell-cell contacts. Breaks in cortex are highlighted by green arrows. Scale bar is 10µm.

Figure S4 :

Size of the anterior cell AB (Magenta arrow) divided by the embryo's size (Green arrow) in percent.

Figure 5 : Actin mutations can affect muscle function and/or neuronal cell number

(A) 3D animal migration assay. Percentage of animals reaching a chemoattractant after migration inside a pluronic gel, monitored every 15 minutes for 2 hours. Results for individual wells (N) for each variant are visible as transparent dots, n is the total number of animals assessed and bars show the standard deviation. The final proportion for each variant was compared to that of WT in the frame of Bayesian statistics, using two binomial distributions. The odds ratio (OR) as well as the probability (p) that the difference is superior to 0.2 are indicated. (B) Variation of the neuronal cell number are observed in *act-2* variant conditions. Reconstructed image of an animal expressing the NeuroPal transgene. Insets show representative images of identified defects compared to the WT *act-2* reference: presence of a micronucleus (Orange), an extra (Magenta) or a missing cell (Green). Scale bar is 50 µm. (C) Summary of neuronal phenotypes observed in the actin variants.

Figure S5 :

Chemotaxis assay. The chemotaxis index is calculated $I = \frac{n_{OP50} - n_{H_2O}}{n_{Total} - n_{immobile\ animals}}$ and show the proportion of animals chemoattracted to concentrated OP50 (100mg/mL) (in red). Blue bars show the percentage of animals that did not move from where they were placed for the assay.

Figure 6 : Data integration to build a comparative tool

Principal Component Analysis plot of analysed actin variant animals reveal clusters which can be associated to classes of phenotypes. Corresponding table with data is available in Figure S6A. p.G74V was added manually as no data could be retrieved for this strain. Arrows link homozygotes to their respective heterozygotes.

Figure S6 :

(A) Variables used for to build the Principal Component Analysis plot presented in Figure 6, as well as their quality of representation in each dimension (cos2). (B) Principal Component Analysis plot of analysed actin variant animals using variables quantified without introducing fluorescent reporters. p.G74V was added manually as no data can be retrieved for this strain. Arrows link homozygotes to their respective heterozygotes.

Figure 1

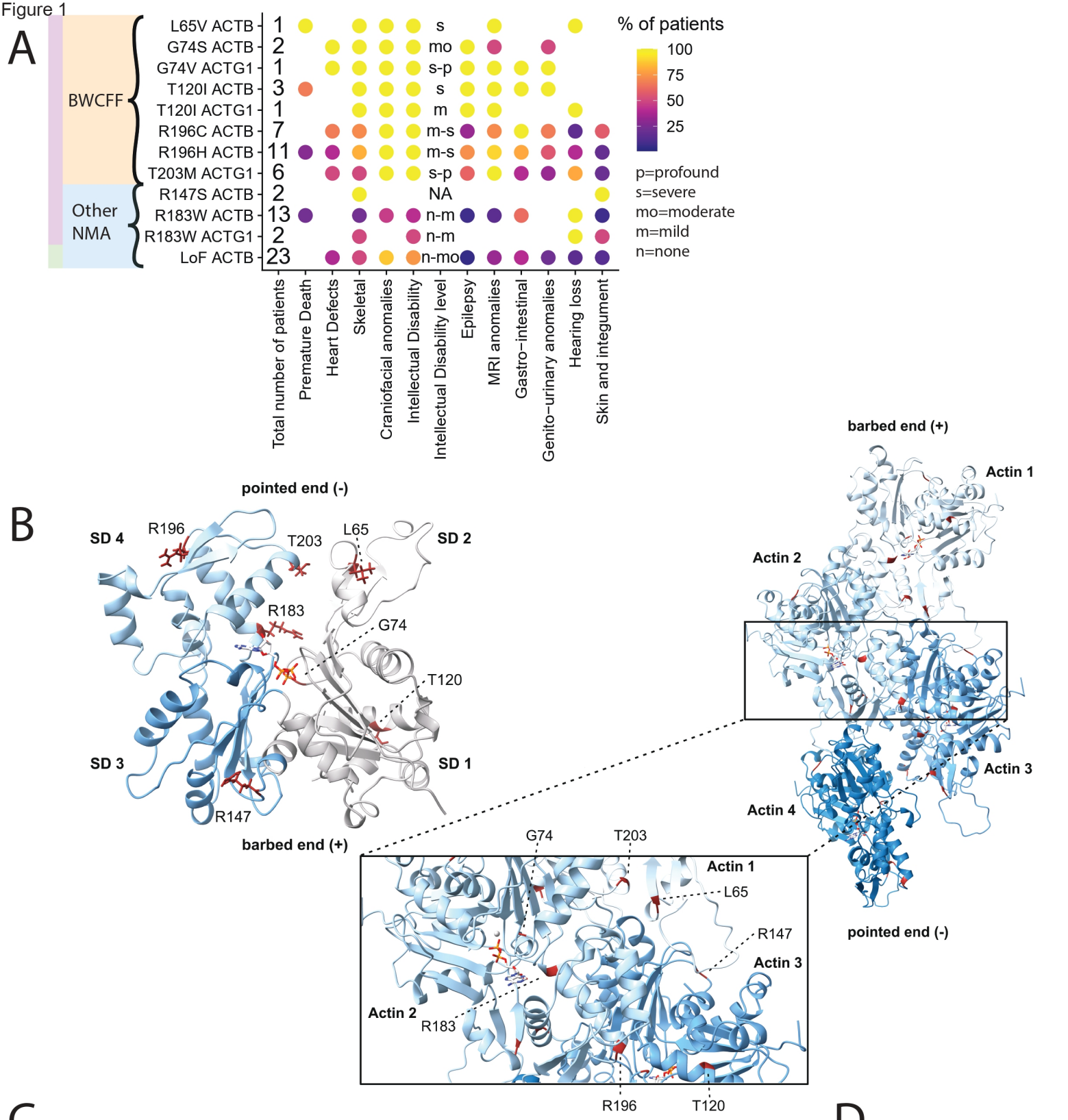

act-2 variant	*C. elegans* variant viability
p.L65V	Homozygote
p.G74S	Homozygote
p.G74V	Not viable
p.T120I	Homozygote
p.R196C	Homozygote
p.R196H	Homozygote
p.T203M	Heterozygote
KO *ok1229*	Homozygote
KO *rey016*	Homozygote
KO *rey021*	Homozygote
p.R147S	Heterozygote
p.R183W	Homozygote

Figure 1

Figure 2

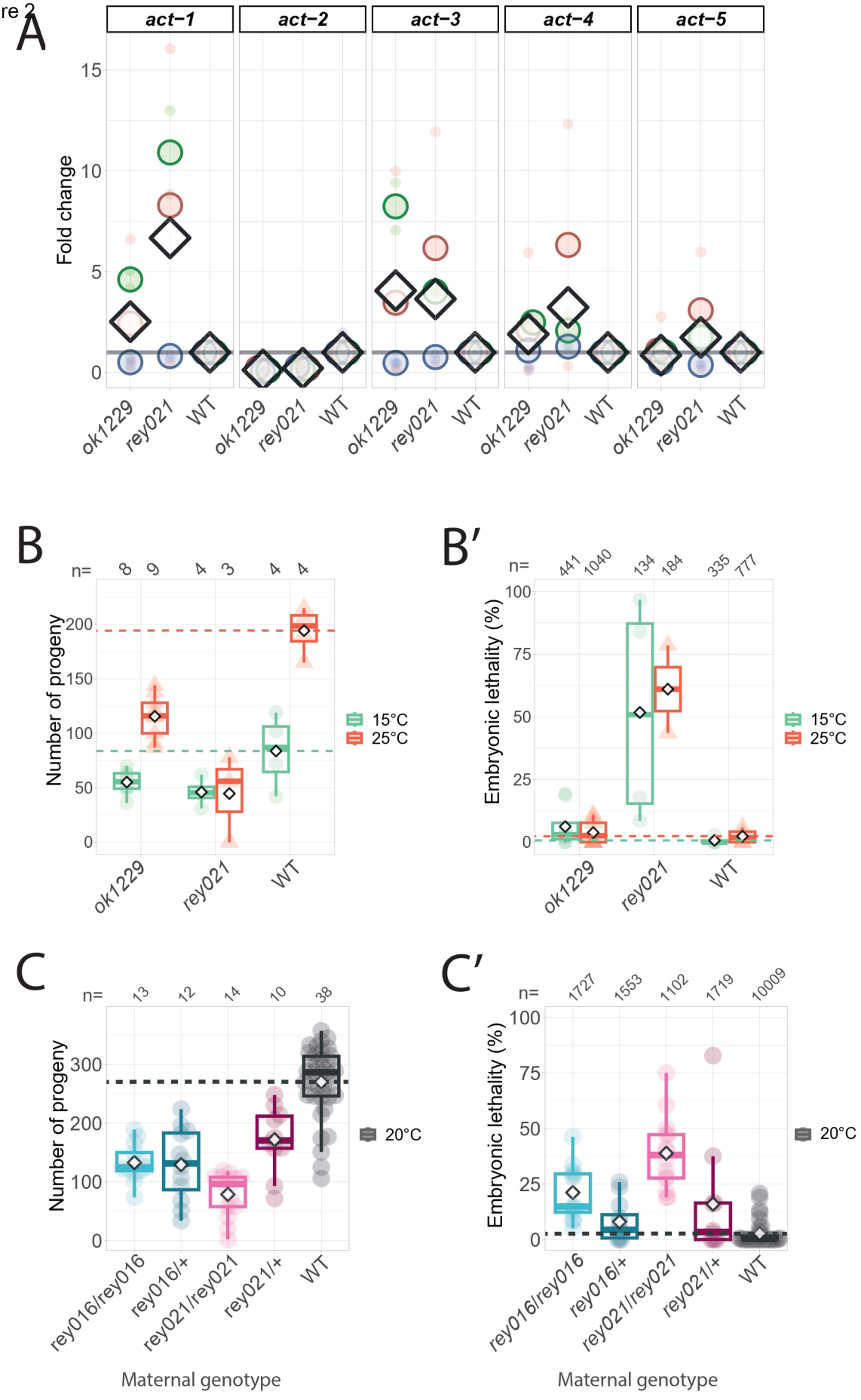

Figure 2

Figure 3

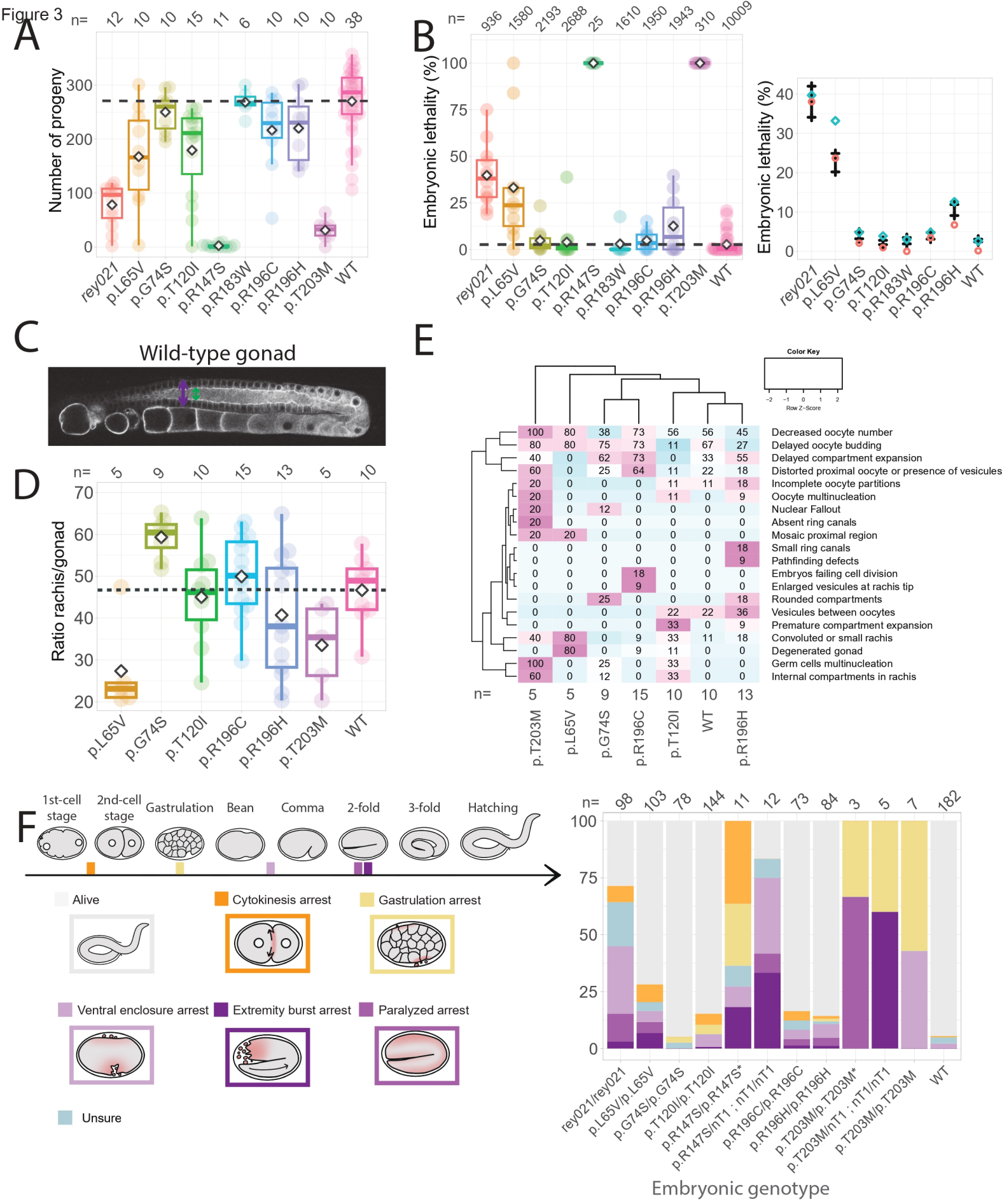

Figure 3

Figure 4

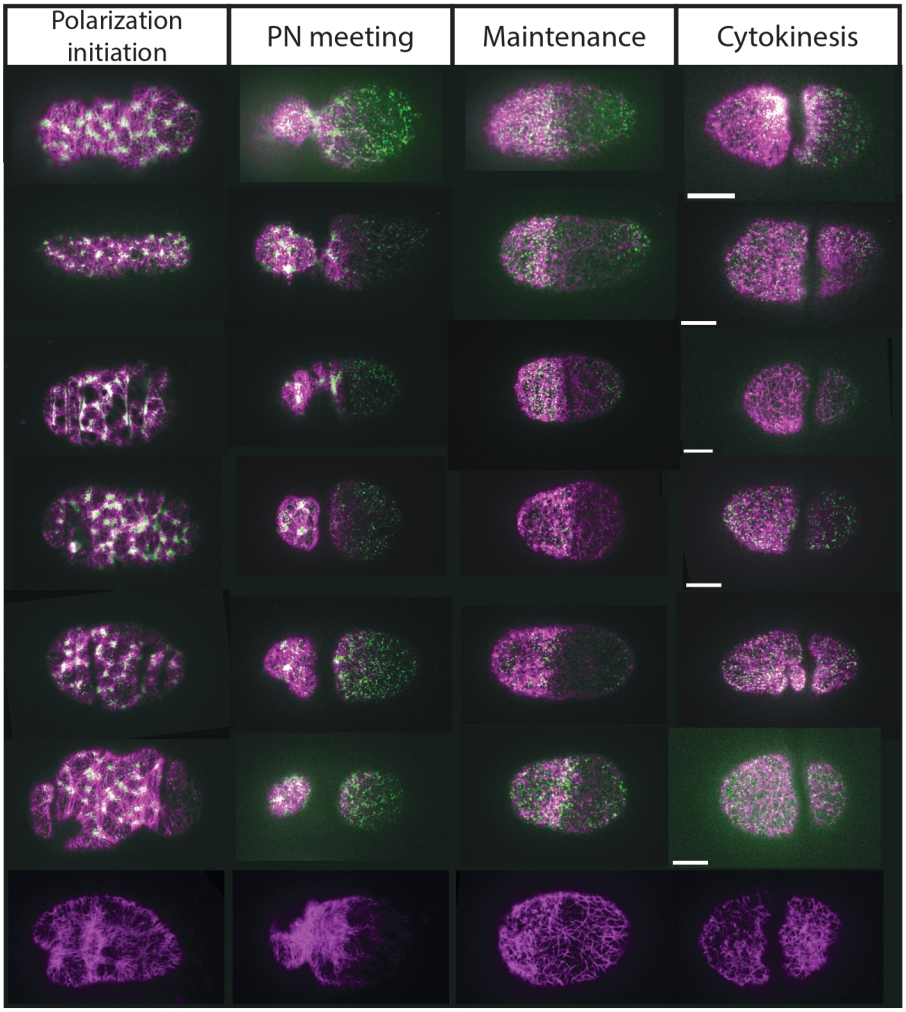

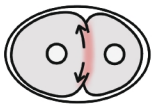

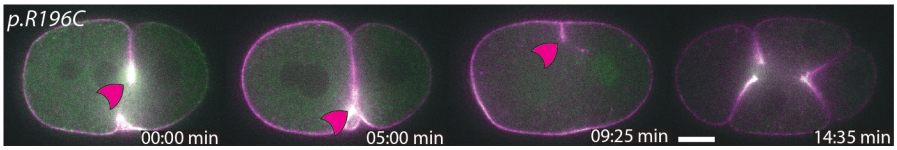

L65V	G74S	T120I	R196C	R196H	T203M*	WT
1/7	1/5	0/4	2/12	0/9	3/6	0/10



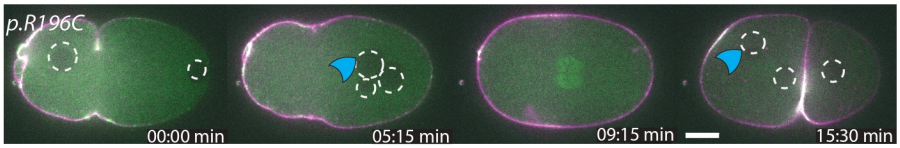

L65V	G74S	T120I	R196C	R196H	T203M*	WT
6/7	2/5	1/4	7/12	2/9	0/6	1/10



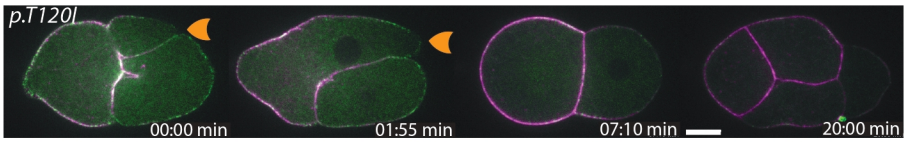

L65V	G74S	T120I	R196C	R196H	T203M*	WT
3/7	0/5	2/4	1/12	1/9	2/6	0/10



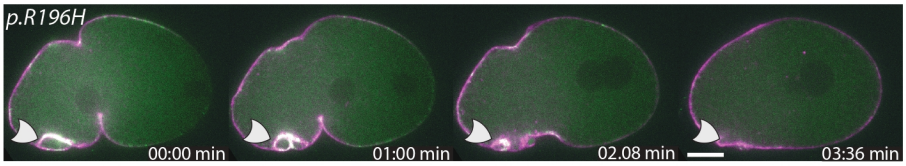

L65V	G74S	T120I	R196C	R196H	T203M*	WT
0/7	0/5	3/4	0/12	1/9	0/6	0/10

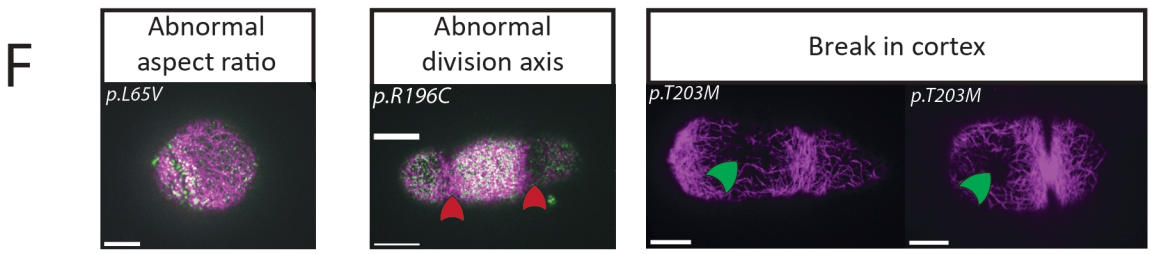

Figure 4

Figure 5

A

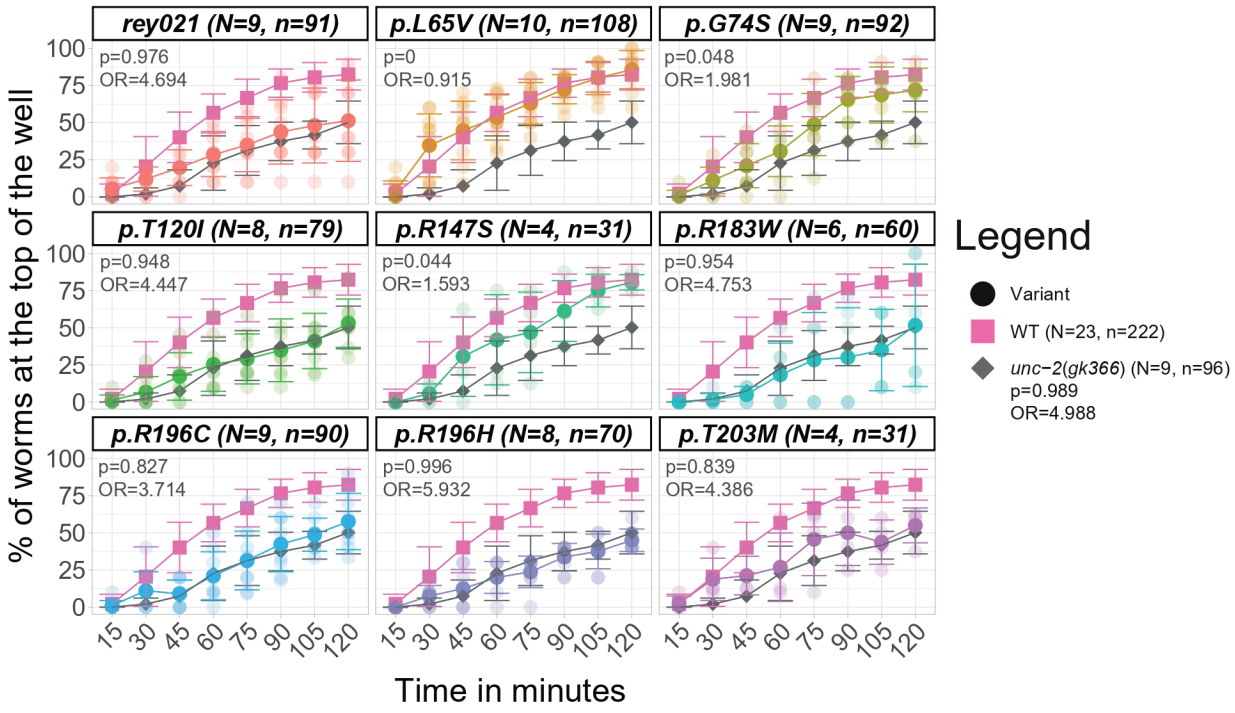

B

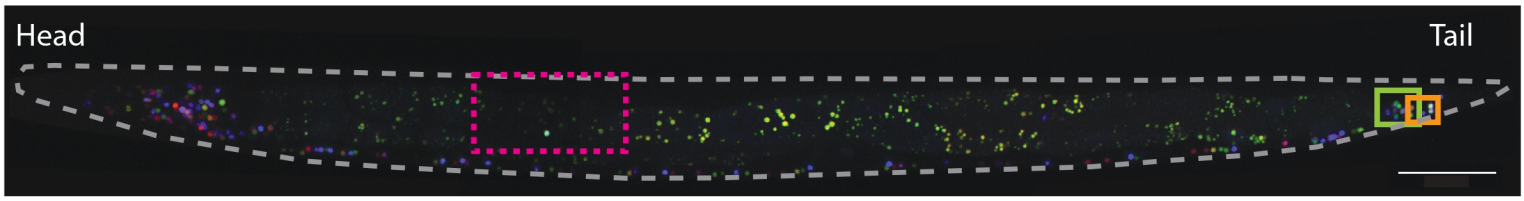

p.T120I



Additional neuronal cell (1/7)

p.R196C

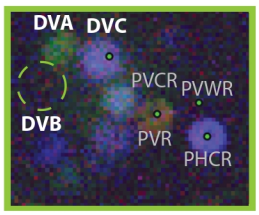

No DVB (1/15)

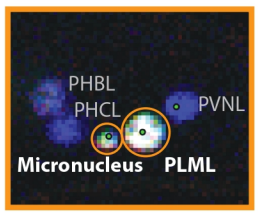

PLML micronucleus (1/15)

C

		L65V	G74S	T120I	R147S	R196C	R196H	T203M	*rey021*	WT
Additional Neuron	SDQR	0/8	0/7	1/7	0/8	1/6	0/3	0/2	1/6	0/5
	Other	1/14	1/14	0/16	0/14	0/15	0/15	1/4	1/15	0/14
Micronucleus		0/14	0/14	0/16	1/14	1/15	0/15	0/4	2/15	0/14
Missing Neuron	DVB	0/14	1/14	0/16	0/14	1/15	0/15	0/4	1/15	0/14
	PDA	0/14	1/14	0/16	0/14	0/15	0/15	0/4	0/15	0/14
	Other	0/14	1/14	3/16	1/14	0/15	0/15	1/4	2/15	0/14

Figure 5

Figure 6

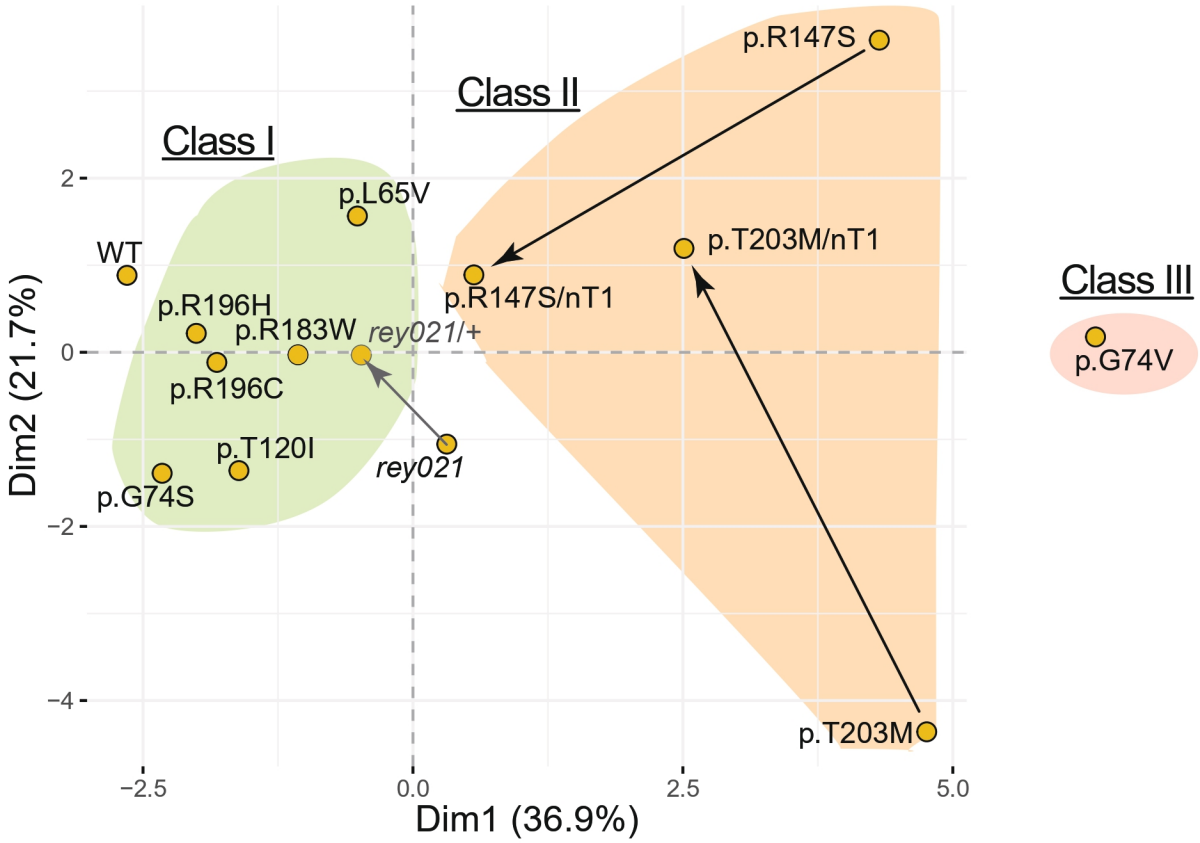

Figure 6

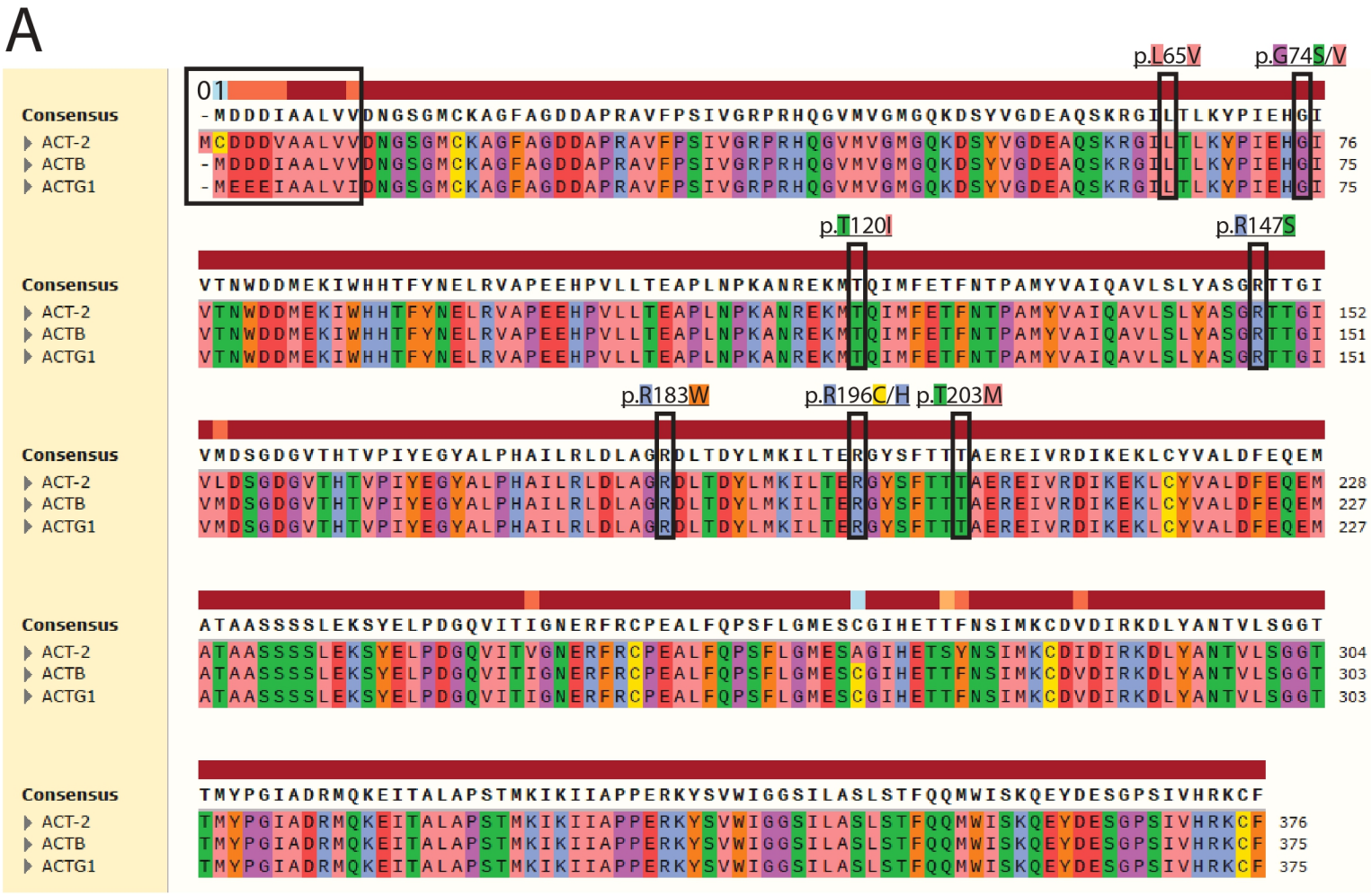
A
p.L65V
p.G74S/V
p.T120I
p.R147S
p.R183W
p.R196C/H
p.T203M
Consensus
ACT-2
ACTB
ACTG1
B
Wild-type
CCAATTGAGCATGGTATCGTTACCAACTGG
p.G74V
CCAATTGAACATGTTATTGTCACTAACTGG

Figure S1

$$E = 10^{\frac{1}{slope}}$$

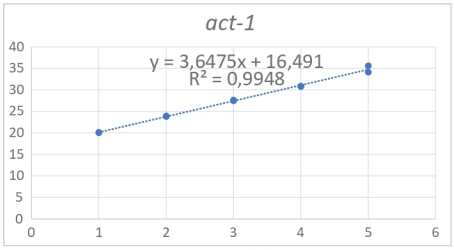

E = 1.88

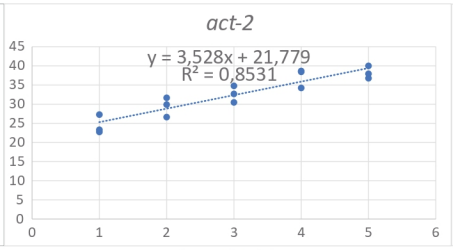

E = 1.92

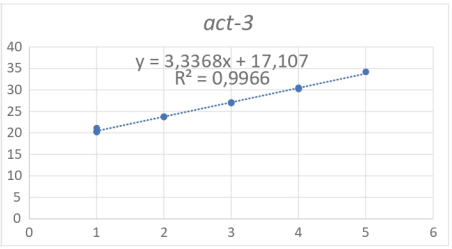

E = 1.99

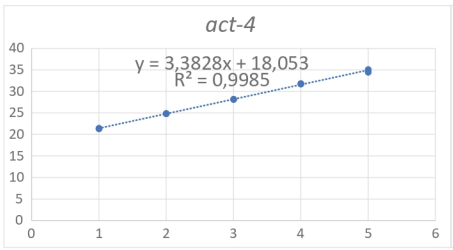

E = 1.97

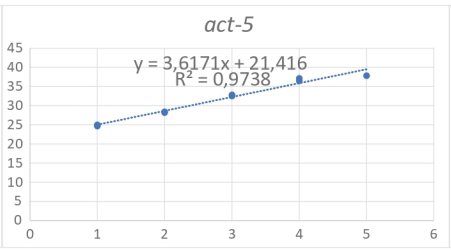

E = 1.89

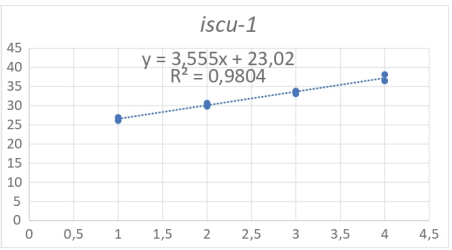

E = 1.91

Figure S2

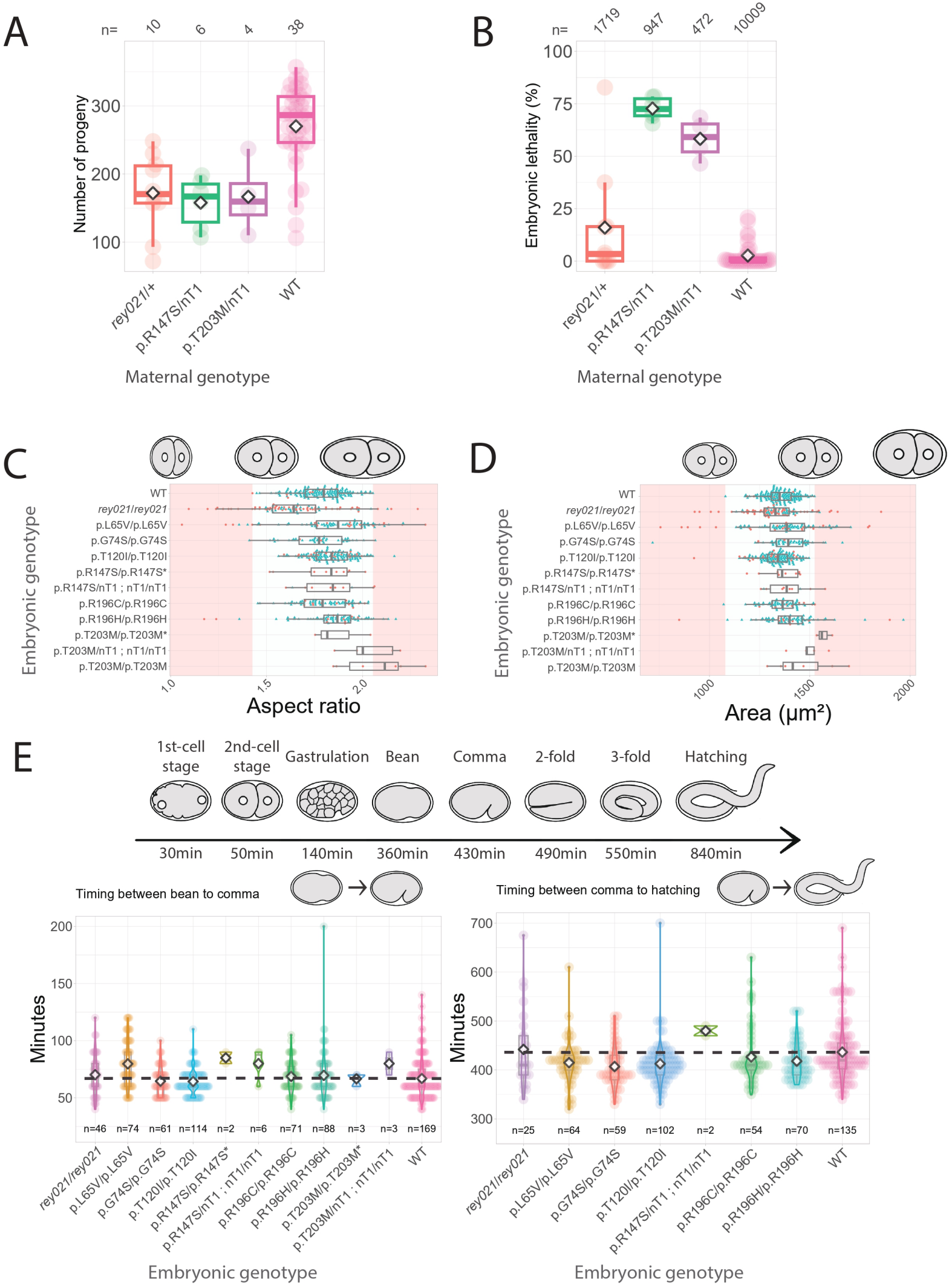
A
n= 10 6 4 38
Number of progeny
300
200
100
rey021/+
p.R147S/nT1
p.T203M/nT1
WT
Maternal genotype
B
n= 1719 947 472 10009
Embryonic lethality (%)
100
75
50
25
0
rey021/+
p.R147S/nT1
p.T203M/nT1
WT
Maternal genotype
C
Embryonic genotype
WT
rey021/rey021
p.L65V/p.L65V
p.G74S/p.G74S
p.T120I/p.T120I
p.R147S/p.R147S*
p.R147S/nT1 ; nT1/nT1
p.R196C/p.R196C
p.R196H/p.R196H
p.T203M/p.T203M*
p.T203M/nT1 ; nT1/nT1
p.T203M/p.T203M
1.0
1.5
2.0
Aspect ratio
D
Embryonic genotype
WT
rey021/rey021
p.L65V/p.L65V
p.G74S/p.G74S
p.T120I/p.T120I
p.R147S/p.R147S*
p.R147S/nT1 ; nT1/nT1
p.R196C/p.R196C
p.R196H/p.R196H
p.T203M/p.T203M*
p.T203M/nT1 ; nT1/nT1
p.T203M/p.T203M
1000
1500
2000
Area (µm²)
E
1st-cell stage
2nd-cell stage
Gastrulation
Bean
Comma
2-fold
3-fold
Hatching
30min
50min
140min
360min
430min
490min
550min
840min
Timing between bean to comma
Timing between comma to hatching
Minutes
200
150
100
50
n=46 n=74 n=61 n=114 n=2 n=6 n=71 n=88 n=3 n=3 n=169
rey021/rey021
p.L65V/p.L65V
p.G74S/p.G74S
p.T120I/p.T120I
p.R147S/p.R147S*
p.R147S/nT1 ; nT1/nT1
p.R196C/p.R196C
p.R196H/p.R196H
p.T203M/p.T203M*
p.T203M/nT1 ; nT1/nT1
WT
Embryonic genotype
Minutes
700
600
500
400
300
n=25 n=64 n=59 n=102 n=2 n=54 n=70 n=135
rey021/rey021
p.L65V/p.L65V
p.G74S/p.G74S
p.T120I/p.T120I
p.R147S/nT1 ; nT1/nT1
p.R196C/p.R196C
p.R196H/p.R196H
WT
Embryonic genotype

Figure S3

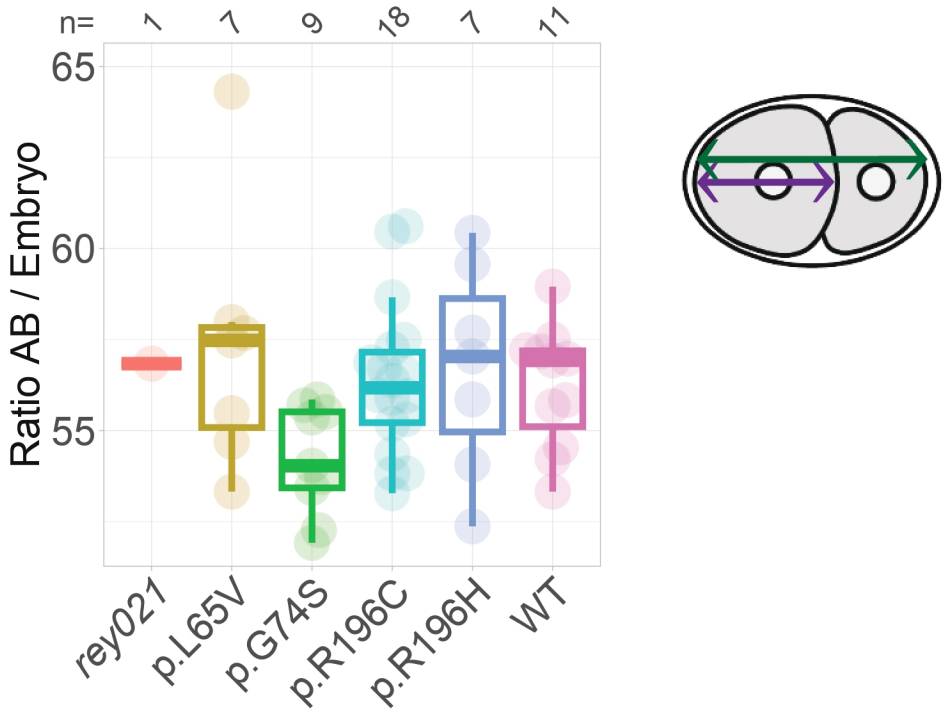
n=
1
7
9
18
7
11
65
60
55
Ratio AB / Embryo
rey021
p.L65V
p.G74S
p.R196C
p.R196H
WT

Figure S4

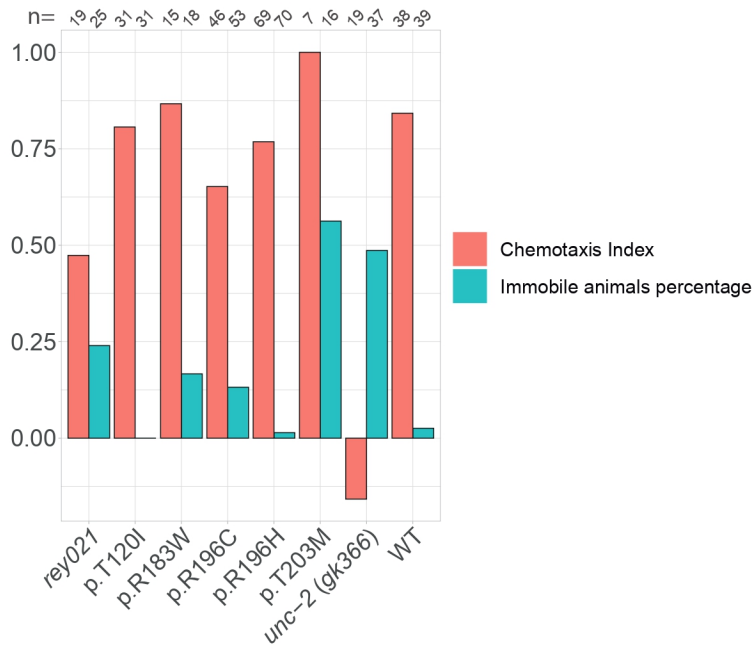
n=
19
25
31
31
15
18
46
53
69
70
7
16
19
37
38
39
1.00
0.75
0.50
0.25
0.00
rey021
p.T120I
p.R183W
p.R196C
p.R196H
p.T203M
unc-2 (gk366)
WT
Chemotaxis Index
Immobile animals percentage

Figure S5

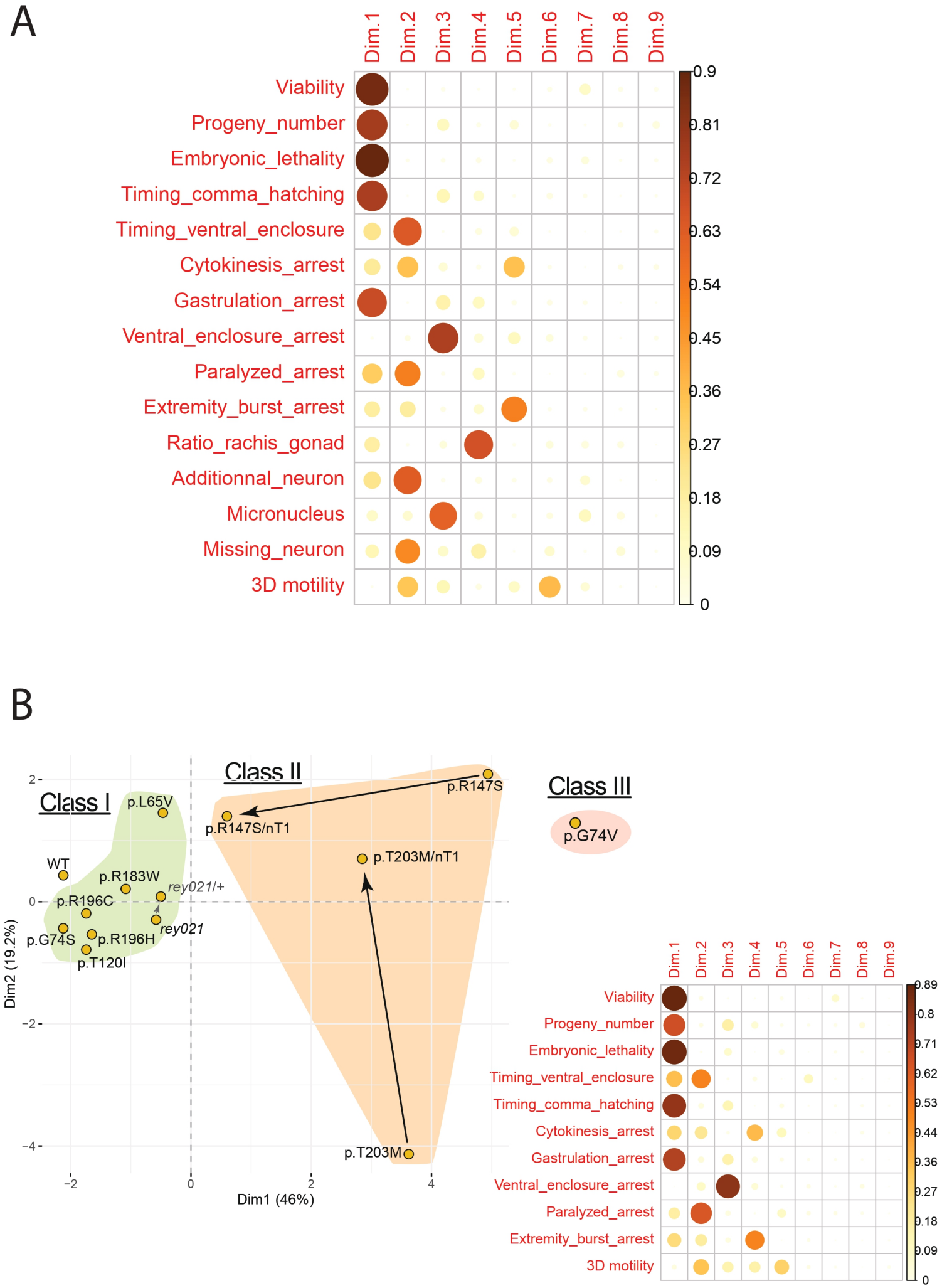
A
Dim.1
Dim.2
Dim.3
Dim.4
Dim.5
Dim.6
Dim.7
Dim.8
Dim.9
Viability
Progeny_number
Embryonic_lethality
Timing_comma_hatching
Timing_ventral_enclosure
Cytokinesis_arrest
Gastrulation_arrest
Ventral_enclosure_arrest
Paralyzed_arrest
Extremity_burst_arrest
Ratio_rachis_gonad
Additionnal_neuron
Micronucleus
Missing_neuron
3D motility
0.9
0.81
0.72
0.63
0.54
0.45
0.36
0.27
0.18
0.09
0
B
Class I
Class II
Class III
p.L65V
WT
p.R183W
rey021/+
p.R196C
rey021
p.G74S
p.R196H
p.T120I
p.R147S
p.R147S/nT1
p.T203M/nT1
p.T203M
p.G74V
Dim2 (19.2%)
Dim1 (46%)
2
0
−2
−4
−2
0
2
4
Dim.1
Dim.2
Dim.3
Dim.4
Dim.5
Dim.6
Dim.7
Dim.8
Dim.9
Viability
Progeny_number
Embryonic_lethality
Timing_ventral_enclosure
Timing_comma_hatching
Cytokinesis_arrest
Gastrulation_arrest
Ventral_enclosure_arrest
Paralyzed_arrest
Extremity_burst_arrest
3D motility
0.89
0.8
0.71
0.62
0.53
0.44
0.36
0.27
0.18
0.09
0

Figure S6

Legend of the Supplemental Figures

Movie 1 :

Cytokinesis arrest, p.R196C embryo. Scale bar = 10µm.

Movie 2:

Gastrulation arrest, p.G74S embryo. Scale bar = 10µm.

Movie 3:

Ventral enclosure arrest, *rey021* embryo. Scale bar = 10µm.

Movie 4:

Extremity burst arrest, p.L65V embryo. Scale bar = 10µm.

Movie 5:

Paralyzed arrest, *rey021* embryo. Scale bar = 10µm.

Movie 6:

Cytokinesis defects, p.R196C embryo. LifeAct::mKate2 (Magenta), NMY-2::GFP (Green). Scale bar = 10µm. Anterior on the left.

Movie 7:

Meiosis defects, p.R196C embryo. LifeAct::mKate2 (Magenta), NMY-2::GFP (Green). Scale bar = 10µm. Anterior on the left.

Movie 8:

Bleb defects, p.T120I embryo. LifeAct::mKate2 (Magenta), NMY-2::GFP (Green). Scale bar = 10µm. Anterior on the left.

Chapter 6: Neuronal gene expression pattern

Introduction and experimental procedure

Because Non-Muscle Actinopathies are largely associated with neurodevelopmental defects, we wondered whether actin variants could alter the normal gene expression of neurons, which could imply neurodevelopment defects. To investigate this possibility, I quantified the intensity values of the three 'colors' expressed in NeuroPAL (mTagBFP2 as 'Blue', CyOFP1 as 'Green', and mNeptune2.5 as 'Red'). Indeed, the NeuroPAL transgene comprises 41 neural reporters associated with three fluorophores, in addition to a panneuronal reporter. Thus, multiple genes express the same fluorophore (**FIGURE 49**, YEMINI ET AL., 2021). Nonetheless, the invariant neural class-specific combination of reporter expression allows the identification of almost every neuron in *C. elegans*.

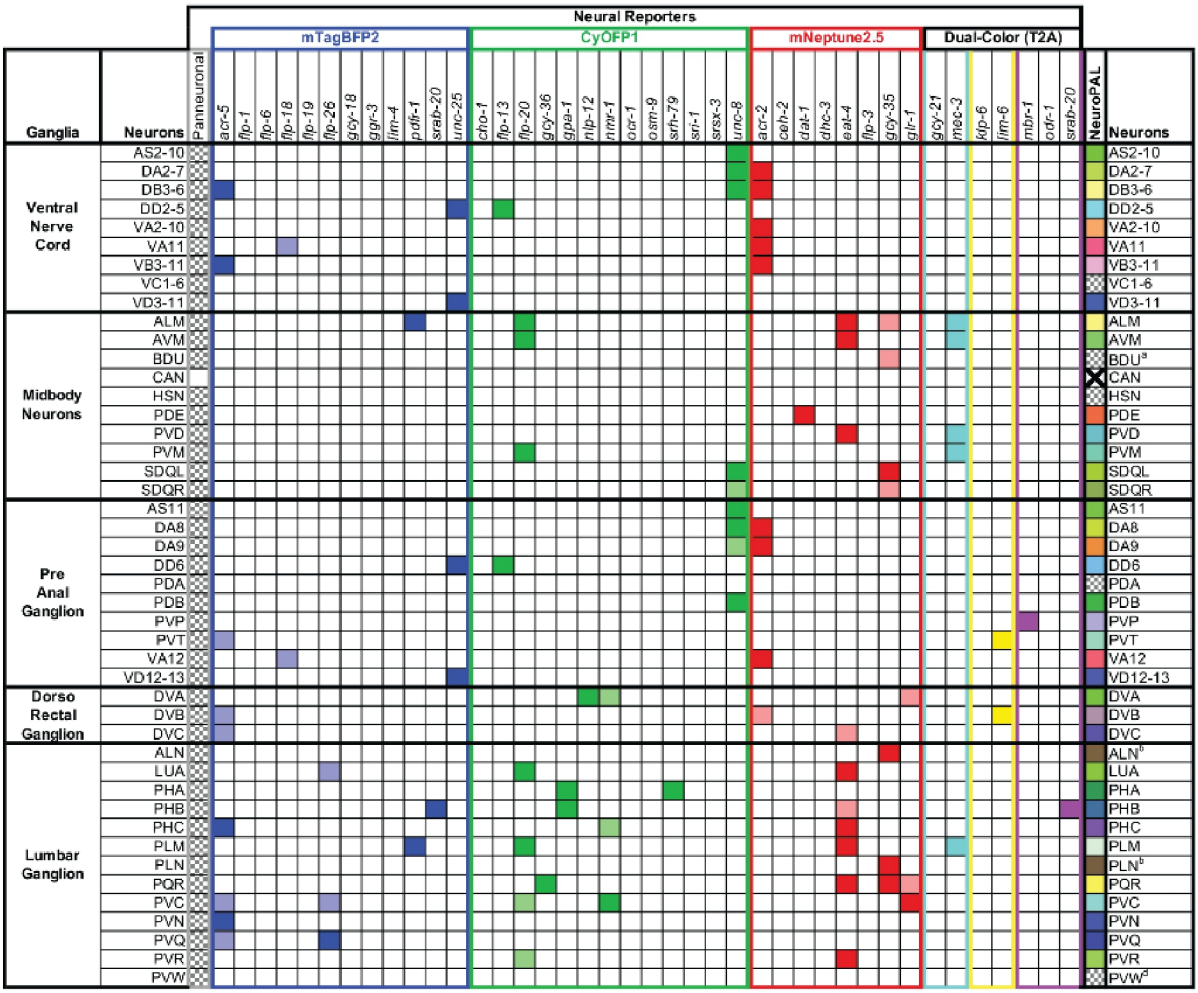

Figure 49: NeuroPAL neural reporters' table. Only assessed neurons are represented in this table. Adapted from Yemini et al., 2021

I used the published 'NeuroPAL_ID' software (Version 1, YEMINI ET AL., 2021) to identify 105 neurons in the animal's tail and midbody for actin variants L65V, G74S, T120I, R147S, R196C, R196H, and *rey021*. Using the 'Save-ID' button, I extracted the intensity values of each color for all labeled neurons. I imported the resulting Excel sheets into RStudio (2024.04.2 R version 4.1.2), where I used a custom function I developed (bigttest_FC_MeanMedian.R) for analysis.

The bigttest_FC_MeanMedian function sequentially compares the intensity values of a chosen color for all neurons sharing the same name between two datasets inputted (data_a and data_b). For example, writing "bigttest_FC_MeanMedian(data_OH15495, data_Variant, blue)" onto RStudio with the function loaded will compare the blue intensity values of each neuron sequentially between OH15495 and a variant strain (first ALML, then ALMR, and so on). To determine which frequentist statistical test to use for comparison, the function tests the normality of data distribution for each neuron using a Shapiro-Wilk test. If the intensity values of the same neuron label in data_a and data_b both follow a Gaussian distribution, a t-test is realized to compare their means. Otherwise, a Mood test is realized to compare their medians. Following statistical analysis, the $\log_2$ fold-change of intensity values is calculated. This analysis is repeated for each neuron, which leads to a large number of p-values, increasing immensely the probability of observing a false positive. Indeed, for a p-value threshold at 0,05 and 105 statistical tests, the probability of observing a false positive is 99.5% ($probability_{percent} = (1 - (1 - 0.05)^{105}) * 100$) (JAFARI AND ANSARI-POUR, 2019). Thus, calculated p-values are adjusted by the False Discovery Rate. This is done by sorting all p-values in an ascending order and multiplying them individually by $\frac{m}{k}$ where k is the position number of the sorted p-value, and m is the total number of independent tests realized (here 105) (BENJAMINI AND HOCHBERG, 1995; JAFARI AND ANSARI-POUR, 2019). Additionally, I checked if the intensity value for a color x was significantly lower in a variant strain compared with the wild-type strain. If so, the 'check_false_positive.R' function I developed verifies if this neuron should express a reporter gene in the control strain (**FIGURE 49**). If not, the p-value is deleted to avoid false positives. All codes are available on our team's Gitlab.

Results

This analysis revealed that the presence of ACT-2 variants L65V and R196C did not change the expression pattern of NeuroPAL's neural reporters compared to the reference strain OH15495 (recapitulated in **TABLE 2**, **FIGURE 50**). However, the variants G74S, R147S, and r*ey021* caused some cell-specific changes in the levels of neural reporters compared to the reference strain (**FIGURE 51**, **TABLE 2**).

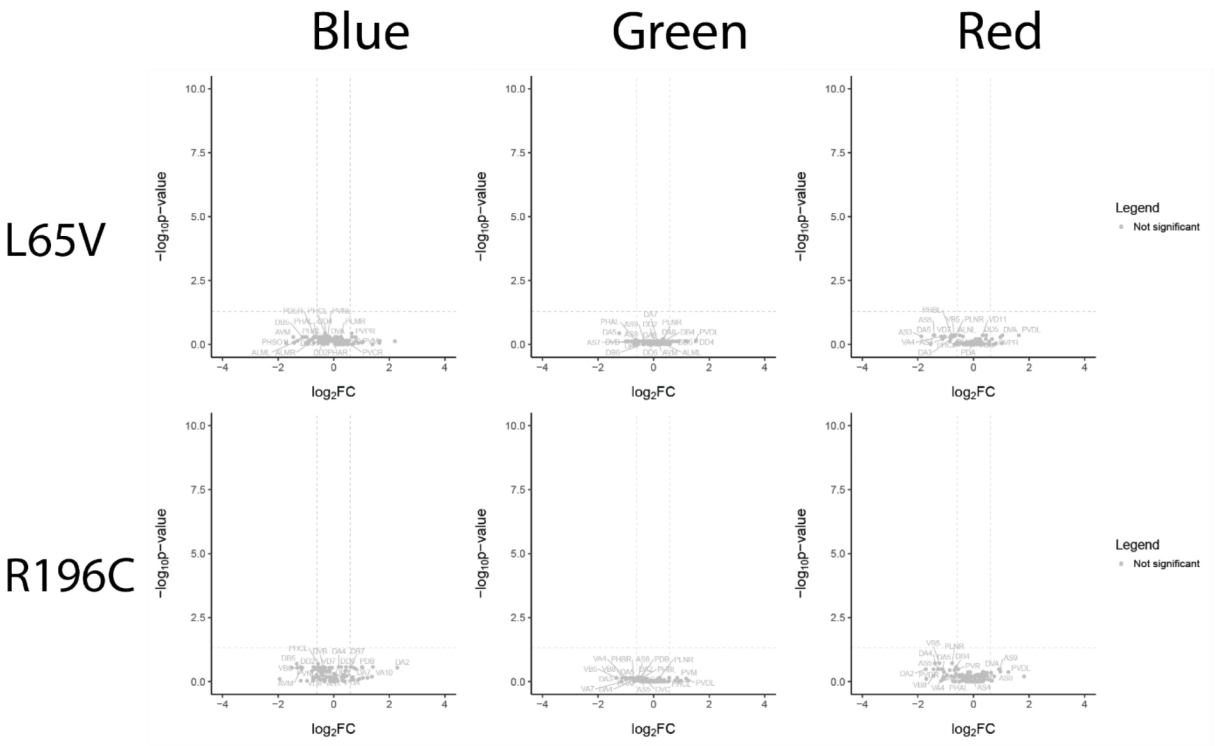

Figure 50: Neural reporter expression for variants L65V and R196C. Volcano plots showing no differences in neural reporter expression for variants L65V and R196C compared to the reference strain OH15495. Significance is shown on the Y-axis, with a threshold at p=0.05 (dotted horizontal line). Logarithmic fold-change is depicted on the X-axis, with a threshold set at 0.6 (equivalent to a ~1.5 fold-change of expression, dotted vertical line).

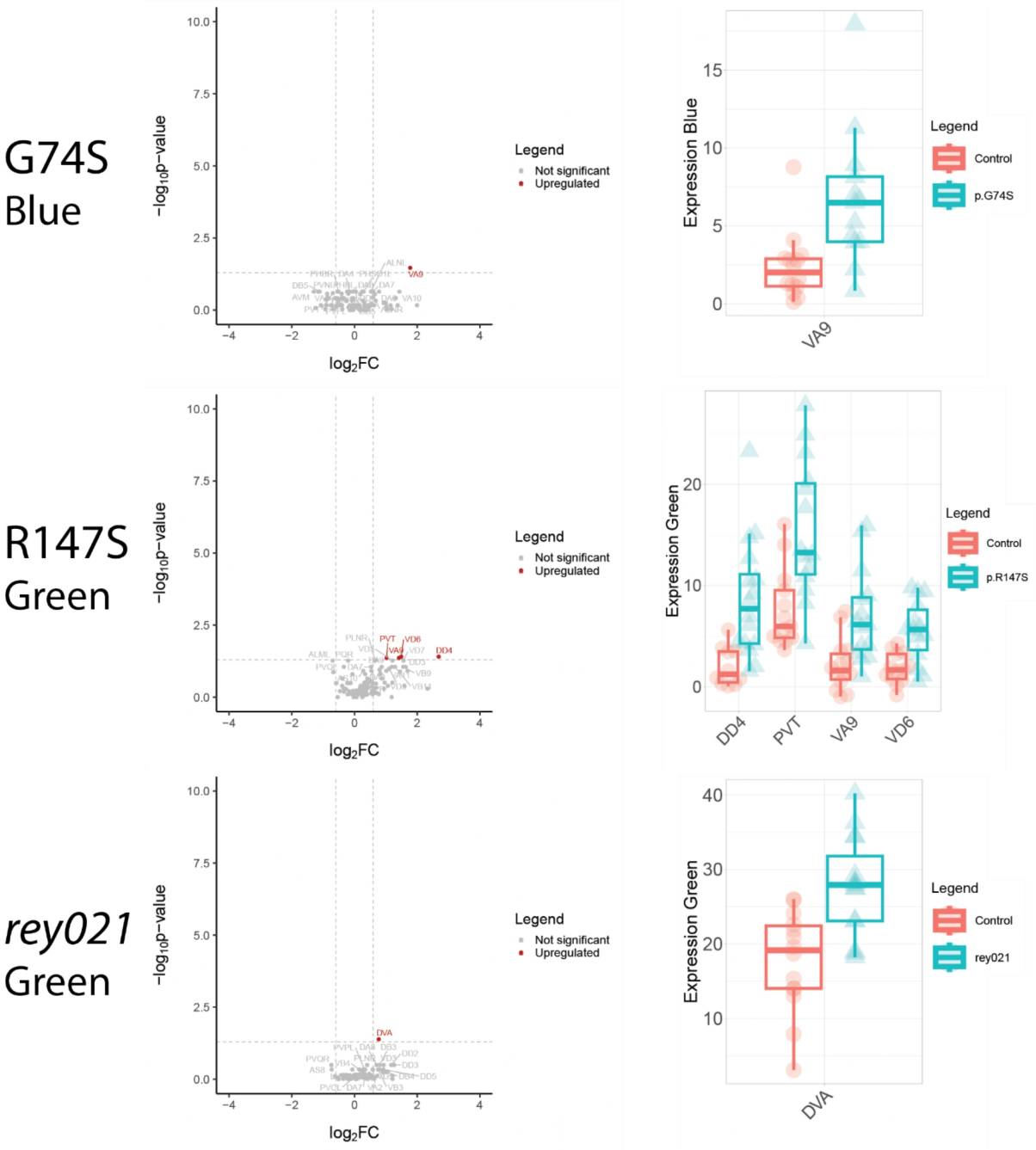

Figure 51: Neural reporter expression for variants G74S, R147S, and *rey021*. Left panels present volcano plots showing cell-specific differences in neural reporter expression for variants G74S, R147S, and *rey021* compared to the reference strain OH15495. Significance is shown on the Y-axis, with a threshold at p=0.05 (dotted horizontal line). Logarithmic fold-change is depicted on the X-axis, with a threshold set at 0.6 (equivalent to a ~1.5 fold-change of expression, dotted vertical line). Right panels show boxplots of individual color expression for neurons presented in the relative left panel.

The variants T120I and R196H were the most affected. Indeed, 17% (18/105) of neurons have an increase in 'green' intensity of expression for variant R196H and 22% (23/105) for variant T120I (**FIGURE 52**, **TABLE 2**). The latter additionally has one neuron (PVPR) overexpressing 'blue.' Most of these are motor neurons (italics in **TABLE 2**), mainly expressing the *unc-8* 'green' reporter (bold in **TABLE 2**, **FIGURE 49**). Neurons expressing the *unc-8* green reporter do not express another 'green' reporter in wild-type conditions (**FIGURE 46**). Still, we

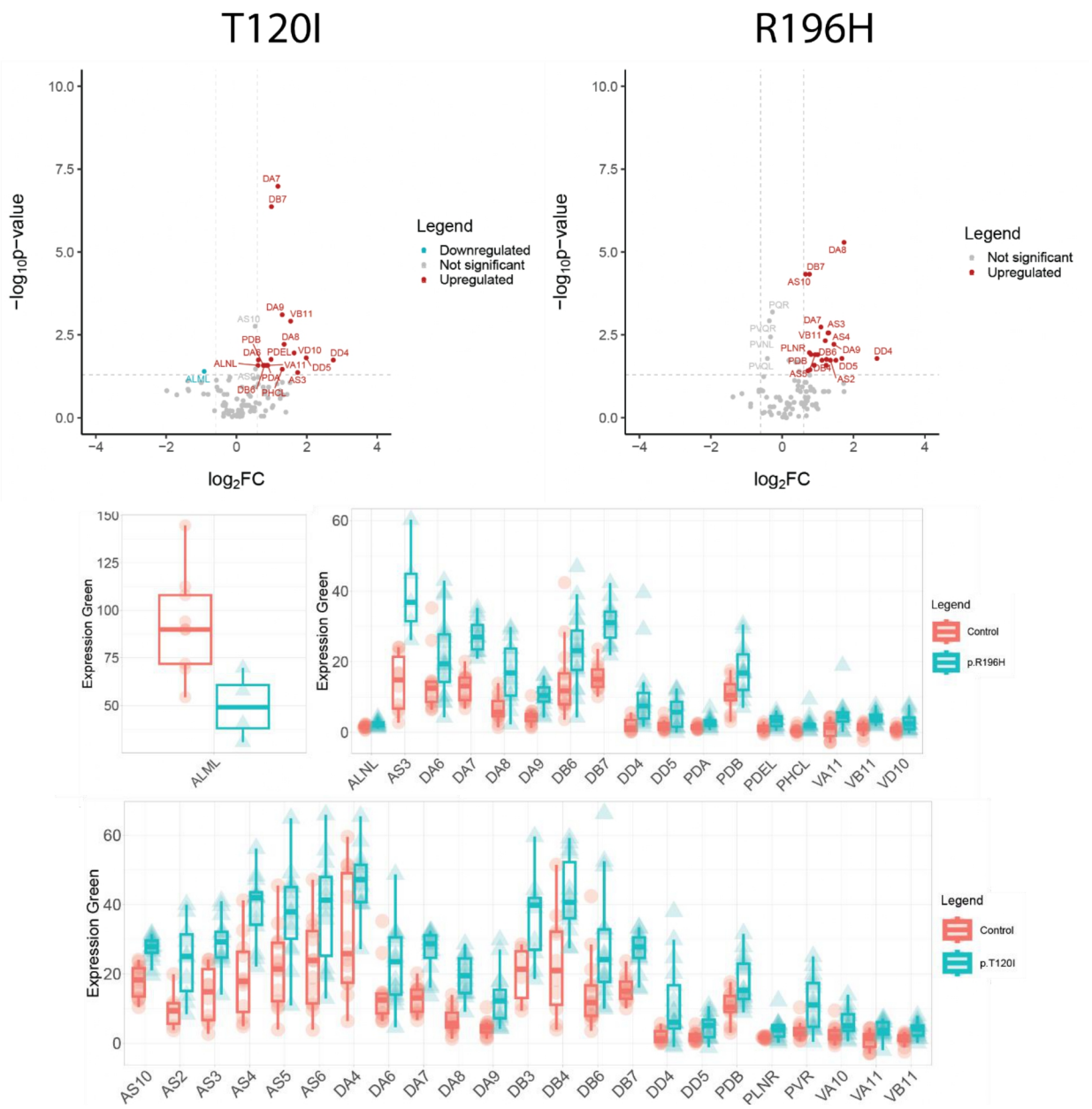

Figure 52: Neural reporter expression for variants T120I and R196H. Upper panels present volcano plots showing differences in neural reporter expression for variants T120I and R196H compared to the reference strain OH15495. Significance is shown on the Y-axis, with a threshold at p=0.05 (dotted horizontal line). Logarithmic fold-change is depicted on the X-axis, with a threshold set at 0.6 (equivalent to a ~1.5 fold-change of expression, dotted vertical line). Lower panels show boxplots of individual color expression for neurons presented in the upper panels.

cannot determine if this increase in 'green' expression is due to the overexpression of *unc-8* or to the abnormal expression of one (or multiple) of the other 13 'green' reporters comprised in the NeuroPAL transgene (**FIGURE 49**).

Interestingly, comparing the green expression values between R196H and T120I shows no significant changes, implying that these two variants change the neuronal expression pattern similarly (**FIGURE 53**).

To conclude, in addition to rare events of defective neurogenesis observed by the presence of a supernumerary neuronal cell, micronucleus, or the absence of a neuron (CHAPTER 5), actin variants also seem to induce changes in neural gene expression patterns. Notably, *act-2* T120I and R196H variants seem to alter, more specifically, the motoneurons gene expression pattern, which will need further characterization.

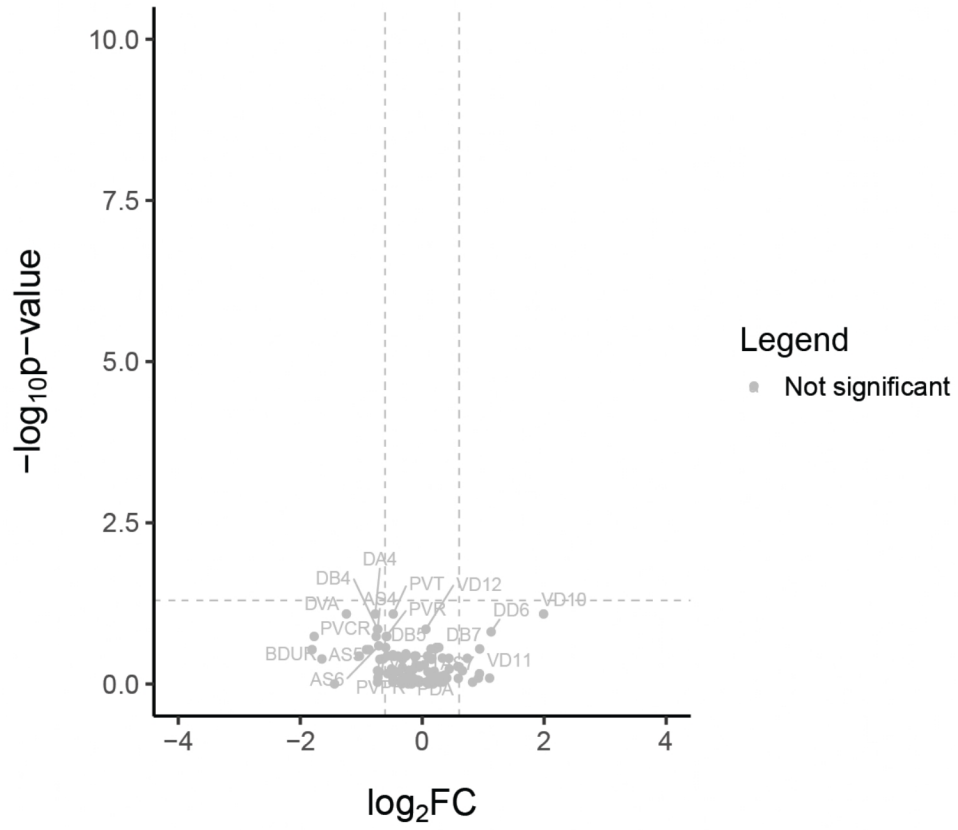

Figure 53: Neural reporter expression between variants T120I and R196H. Volcano plots showing no differences in neural reporter expression between variants T120I and R196H. Significance is shown on the Y-axis, with a threshold at p=0.05 (dotted horizontal line). Logarithmic fold-change is depicted on the X-axis, with a threshold set at 0.6 (equivalent to a ~1.5 fold-change of expression, dotted vertical line).

Variation	Color	Expression Change?	Upregulated	Downregulated
L65V	Blue	No		
	Green	No		
	Red	No		
G74S	Blue	Yes	***VA9***	
	Green	No		
	Red	No		
T120I	Blue	Yes	PVPR	
	Green	Yes	***AS2, AS3, AS4, AS5, AS6, AS10, DA4, DA6, DA7, DA8, DA9, DB3, DB4, DB6, DB7,*** *DD4, DD5*, ***PDB***, PLNR, PVR, *VA10, VA11, VB11*	
	Red	No		
R147S	Blue	No		
	Green	Yes	***DD4***, PVT, ***VA9, VD6***	
	Red	No		
R196C	Blue	No		
	Green	No		
	Red	No		
R196H	Blue	No		
	Green	Yes	ALML, ALNL, ***AS3, DA6, DA7, DA8, DA9, DB3, DB6,*** *DD4, DD5, PDA*, ***PDB***, PDEL, PHCL, *VA11, VB11, VD10*	ALML
	Red	No		
rey021	Blue	No		
	Green	Yes	DVA	
	Red	No		

Table 2: Summary of altered expression pattern for each analyzed actin variant. Italics indicate motor neurons. Bold indicates neurons expressing the *unc-8* GFP reporter.

Discussion and Perspective

Chapter 7: Open questions on phenotypic characterization

Chapter introduction

My PhD work focused on the multiscale characterization of actin variants, which eventually led to their classification using a Principal Component Analysis (HECQUET ET AL., 2024 BIORXIV). An intrinsic trait of Science is the fact that one answer leads to multiple questions. My work is no exception to this rule, and numerous questions have yet to be answered, some of which I will discuss:

First, we have observed that two null alleles of *act-2* led to drastically different outcomes on embryonic lethality: Why so? Which allele should one use to assess the true consequences of an *act-2* knockout?

Second, I observed that some *act-2* variants impact gene expression in specific neurons. But can we hypothesize on the cause and consequences of this change in gene expression?

Third, how can we explain the variance observed in my results?

Finally, we observed a good correlation between the severity observed in human actin variants and the same variant recapitulated in *C. elegans act-2*. Thus, we concluded that *C. elegans* is a promising model for studying non-muscle actinopathies-associated variants in an animal model. Can we go deeper and dissect the results we obtained in *C. elegans* to hypothesize on the pathophysiological mechanism and the molecular consequences of the studied actin variant?

Why do two null *act-2* alleles cause different phenotypes?

A puzzling part of my thesis concerned the differences observed between different *act-2* knock-outs, notably between *ok1229* (WILLIS ET AL., 2006) and *rey021* (HECQUET ET AL., 2024 BIORXIV). Knowing the consequences of an *act-2* knockout is of great importance to recapitulate human actin loss of function mutations and compare it to other *act-2* variants. *rey021* causes a high embryonic lethality, while *ok1229* does not (HECQUET ET AL., 2024 BIORXIV). According to single-worm RT-qPCR, both alleles are null (**FIGURE 2** in CHAPTER 5). So why are they so different? Here, I will objectively present the differences between both alleles so readers can make an advised decision on which they want to use in their studies.

Firstly, these alleles have been generated by different methods; *ok1229* has been generated by the *C. elegans* knockout consortium using Ethyl Methane Sulfonate (EMS) mutagenesis, while *rey021* has been generated by the Reymann lab using CRISPR-Cas9. *ok1229* is a large deletion removing a third of *act-2* and an additional 871bp past *act-2*'s coding sequence, while *rey021* is a 35bp insertion leading to a frameshift and a premature STOP codon at codon 120 (**FIGURE 54**). Both methods can result in undesired mutations, potentially underlying their phenotypic differences. To get rid of these potential off-target mutations, we outcrossed both strains to the WT reference strain (N2) and ensured that their other actin coding genes showed no other variation. Nonetheless, the *ok1229* deletion removes a non-coding RNA gene called T04C12.14, present close to *act-2* 3' UTR. The function of this non-coding RNA is unknown, as well as the potential implications of its loss. The only information available is that it is *"enriched in neurons and somatic gonad precursor"* according to RNA-seq studies (STERNBERG ET AL., 2024, https://wormbase.org/db/get?name=WBGene00195159;class=Gene). Moreover, outcrossing may not remove genetically linked mutations. Therefore, future studies could use whole-genome sequencing to look for potential off-target mutations that may underlie the phenotypic differences of both alleles.

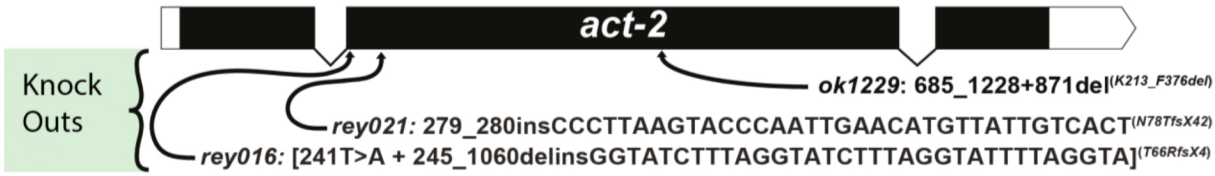

Figure 54: The *act-2* gene. Schematic *act-2* representation highlighting the loci of three *act-2* gene knockouts : *rey016*, *rey021* (Hecquet et al., 2024 biorχiv) and *ok1229* (Willis et al., 2006). Note that the amino acid numbering is here in frame with human ACTB/ACTG1, consider -1 AA in the frame of *C. elegans* due to an additional cysteine in second N-ter position, the base pair are however kept in the *C. elegans act-2* frame. Figure and legend adapted from Hecquet et al., 2024.

Secondly, I hypothesize that differences between the strains could come from variations in isoactin switching (VANSLEMBROUCK ET AL., 2020). As introduced, isoactin switching is achieved by the degradation of a defective mRNA (WELKER ET AL., 2023), creating small "probes" that change the expression of adapting genes. Notably, a recent study by Welker and colleagues identified that a 25bp sequence present in *act-5* could change the pattern and level of expression of *act-3* by binding to a locus in its promoter region, despite a sequence similarity of only 60% (WELKER ET AL., 2023). In our case, we found that the *ok1229* and *rey021* alleles increase the production of *act-1* and *act-3* mRNA (HECQUET ET AL., 2024 BIORXIV). However, the mRNA transcripts of both alleles end at different points. Indeed, the *ok1229* transcript contains 278 additional nucleotides than the *rey021* transcript. Therefore, the degradation of these nucleotides may produce a probe competent for isoactin switching that is not present in the *rey021* allele mRNA. Moreover, *rey021* differs from *ok1229* by comprising a 35 base pair (bp) insertion (**FIGURE 54**). We cannot rule out that this insertion induces transcriptional adaptation of other genes. Therefore, phenotypes induced by the *rey021* allele could reflect the effect of transcriptional adaptation that should not be present in the case of an *act-2* knockout without the *rey021* 35bp insertion.

In conclusion, with current data, deciding which allele reflects the true consequences of an *act-2* knockout is difficult. Nevertheless, we do observe a partial rescue of embryonic lethality when *rey021* is present as a heterozygote allele, which is also the case for mice Actb or Actg1 knockouts (HECQUET ET AL., 2024 BIORXIV; BELYANTSEVA ET AL., 2009; BUNNELL ET AL., 2011). Additionally, I have quantified the embryonic lethality of an additional *act-2* putative null allele (*rey016*, **FIGURE 54**) that showed similar results to *rey021* (HECQUET ET AL., 2024 BIORXIV). That is

why I personally believe that the *rey021* allele reflects the true consequences of an *act-2* knockout. However, *rey016* comprises a STOP codon upstream of *ok1229* deletion and *rey021* insertion. Therefore, *rey016* does not invalidate the hypothesis that the additional bp present in the *ok1229* mRNA transcript induces transcriptional adaptation.

Future experiments could try to rescue the phenotype observed in *rey021* and *rey016* with a plasmid driving the expression of a wild-type version of *act-2*. Moreover, one could try genetically distinguishing both alleles using Whole Genome Sequencing. Indeed, although we did not find undesired variations in other actin-coding genes, variations may be present in other genes that were not removed by outcrossing. Otherwise, we could generate and characterize a strain whose *act-2* coding sequence is completely deleted.

What could be the cause and consequences of neuronal change in gene expression?

As introduced, actin is not solely present in the cytoplasm but also in the nucleus, where it helps, among others, to regulate transcription. Accordingly, Sundby and colleagues observed that Actb$^{-/-}$ mouse embryonic fibroblasts have different transcriptome, proteome, and phosphoproteome than wild-type cells (SUNDBY ET AL., 2024).

Using the results from NeuroPAL analyses, I was able to observe significant changes in neuronal expression patterns, notably for motoneurons of *act-2* T120I and R196H animals (**FIGURE 52**, CHAPTER 6). Accordingly, these variants have impaired 3D motility unrelated to defects in chemotaxis, which could underlie the impaired function of motoneurons (**FIGURE 5A AND S5** in HECQUET ET AL., 2024 BIORXIV). However, from my data, it is impossible to decipher which gene(s) have a change of expression. Thus, additional experiments are needed to decipher which genes are over- or under-expressed in specific neurons. The cause of this gene expression change and its consequences on neuronal functions and composition are unknown yet. I would propose three hypotheses to explain how an actin variant could change gene expression.

Firstly, one could argue that a previous asymmetric division was impaired due to an *act-2* variant, leading to an abnormal distribution of cell fate determinants and a subsequent change in gene expression. Secondly, we could imagine that an *act-2* variant modifies the chromatin accessibility of these cells, changing gene expression. However, this hypothesis implies that *act-2* is present in the nucleus, which I personally believe could be true but was not addressed. In fact, to my knowledge, nuclear actin has never been studied nor observed in *C. elegans*. Thirdly, the change in gene expression may be a sign of the nervous system's robustness, compensating for other defects to function normally.

Because we observed that variants T120I and R196H affect gene expression similarly, and more specifically to a certain type of neuron, I would personally opt for the third hypothesis. Interestingly, most neurons with altered gene expression express an *unc-8* reporter. UNC-8 is an epithelial Na^+ channel. A recent study found that UNC-8 is involved in the synaptic remodeling of the DD motoneurons between the L1 and L2 larval stages, which transition from forming synapses with ventral muscles to dorsal muscles (CUENTAS-CONDORI ET AL., 2023).

The authors observed an enrichment of UNC-8 in the ventral side of DD neurons in the L1 animal. Active UNC-8 import Na^+ inside the cytoplasm, which enhances Ca^{2+} import by voltage gated calcium channels (CUENTAS-CONDORI ET AL., 2023). The Ca^{2+} level is further maintained by the Ca^{2+} activated phosphatase called calcineurin. Calcineurin dephosphorylates dynamin (*dyn-1*), which induces its association with syndapin (*sdpn-1*). Syndapin, in turn, recruits the WAVE regulatory complex, which promotes Arp2/3-mediated actin polymerization (**FIGURE 55**, CUENTAS-CONDORI ET AL., 2023). This calcineurin-mediated pathway is known to be important for activity-dependent bulk endocytosis: an essential process to recycle membrane in response to intense neuronal activity to enable the formation of new synaptic vesicles and ensure proper neuronal activity (**FIGURE 55**, CUENTAS-CONDORI ET AL., 2023). The authors observed that UNC-8-mediated activity-dependent bulk endocytosis is necessary to transport presynaptic components from the ventral to the dorsal side of DD neurons during synapse remodeling (CUENTAS-CONDORI ET AL., 2023).

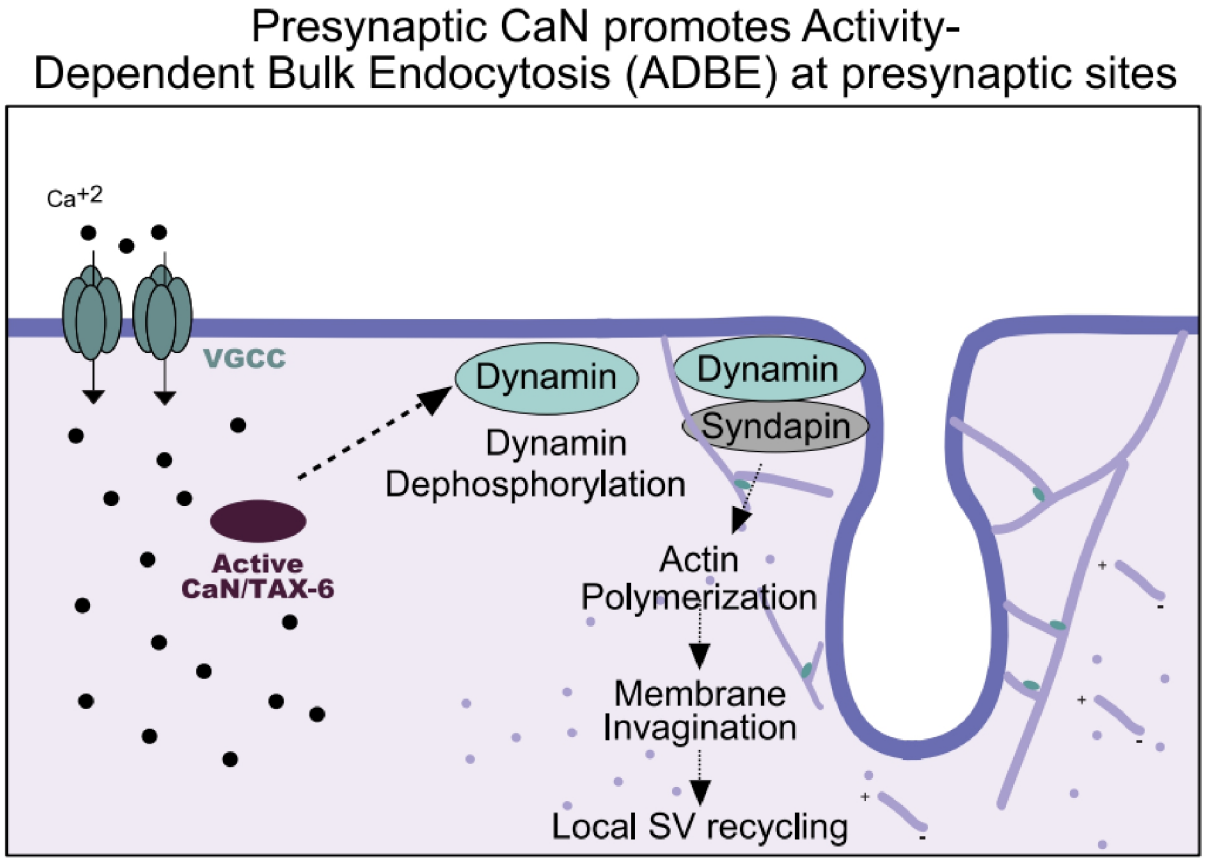

Figure 55: The Activity-dependent bulk endocytosis pathway. During activity-dependent bulk endocytosis, synaptic activity elevates intracellular Ca^{2+} to activate calcineurin (CaN/TAX-6). Dephosphorylation of dynamin by CaN promotes the formation of the dynamin-syndapin complex for membrane localization to drive branched-actin polymerization for bulk endosome formation and local synaptic vesicles (SV) recycling. Figure and legend extracted from Cuentas-Condori et al., 2023.

Interestingly, Cuentas-Condori and colleagues observed reduced actin dynamics and motile vesicles in *unc-8* mutants (CUENTAS-CONDORI ET AL., 2023). Additionally, *unc-8* overexpression in another class of motoneuron called VD induces presynaptic disassembly, which is rescued by RNAi of the Arp2/3 activator *wve-1* (CUENTAS-CONDORI ET AL., 2023). Therefore, *unc-8* is an upstream activator of activity-dependent bulk endocytosis in *C. elegans*.

Even if synaptic remodeling is specific to DD neurons, activity-dependent bulk endocytosis is a common and conserved process to ensure proper neuronal activity. Accordingly, impaired activity-dependent bulk endocytosis causes neurodevelopmental disorders (BONNYCASTLE ET AL., 2021; PENG ET AL., 2021).

We do not know whether the increased intensity of 'green' observed in *act-2* R196H and T120I animals comes from *unc-8* overexpression or from the expression of another gene with the same reporter. However, I personally hypothesize that this change in the 'green' expression comes from the overexpression of *unc-8*, which may be essential to compensate for a poor activity-dependent bulk endocytosis in act-2 T120I and R196H animals, potentially because of impaired branching dynamics. This could be verified by assessing the level expression of an endogenous reporter of *unc-8* and verifying the level of activity-dependent bulk endocytosis in remodeling DD neurons, as Cuentas-Condori and colleagues (CUENTAS-CONDORI ET AL., 2023).

Concerning Human actin variants, Nataliya Di Donato has used bulk RNA sequencing on 18 fibroblast cultures derived from different patients. Subsequent transcriptomic analysis found a few mRNAs differentially expressed compared to WT fibroblasts. However, those were hypothesized to come from genetic differences unrelated to patients' actin variant, and no further studies were done (UNPUBLISHED DATA, NATALIYA DI DONATO). Our results imply that bulk transcriptomics may have missed variations at the single-cell level or that fibroblasts do not have their gene expression patterns modified, but other cell types do.

Can we identify the pathophysiological mechanisms of studied actin variants?

Our work allowed the comparison of severities of different actin variants. We found that variants induce phenotypes at different frequencies, showing that specific variants impact some aspects of actin dynamics and/or regulation differently. My thesis work showed that the general severity of phenotypes found in *C. elegans* correlates well with severities of Human NMAs of the same actin variant (HECQUET ET AL., 2024 BIORXIV). However, it did not elaborate on the four mechanisms proposed to explain an actin variant pathogenicity: interaction defects with actin-binding proteins, haploinsufficiency, altered dynamics, or formation of toxic aggregates, which I will discuss now.

Actin aggregates

Foremost, we did not observe the formation of obvious macroscopic actin aggregates in the gonad and in the cortex and cytosol of early embryos for variants L65V, G74S, T120I, R196C, R196H, and T203M as assessed by LifeAct reporter analysis (HECQUET ET AL., 2024 BIORXIV). Importantly, we could not generate viable strains expressing a LifeAct probe under the ubiquitous *mex-5* promotor for variants R147S and *rey021*, which were thus not assessed. The LifeAct probe is known to stabilize actin filaments, and alter actin dynamics when expressed at high concentrations (Belyy et al., 2020; Melak et al., 2017). It is possible that in a WT strain, LifeAct does slightly affect actin dynamics but that this effect is amplified in the presence of the R147S or *rey021* actin variants, preventing the embryo from developing. Actin aggregates can be observed in the case of muscular actin variants (COSTA ET AL., 2004; ILKOVSKI ET AL., 2004; SCHRÖDER ET AL., 2004), and have been observed in muscles of a transgenic *C. elegans* cardiomyopathy model (HAYASHI ET AL., 2019). Using a LifeAct probe expressed by the muscle-specific promotor *myo-3*p, we did look at L65V and R196H actin organization in muscle cells but did not observe aggregates (**FIGURE 56**). Other variants have not been assessed yet.

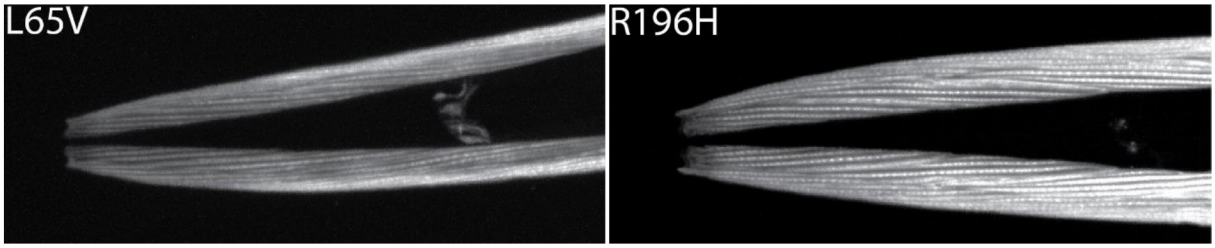

Figure 56: Muscles of animals with *act-2* variants L65V and R196H. Maximum intensity projection of muscles close to the animal's mouth observed by an actin probe (myo3p::LifeAct::mKate2). Anterior is on the left.

We did not look at actin organization in the R183W variant, as we obtained the strain recently. Nonetheless, a recent study highlights that this variant induces an abnormal localization of actin structures around the nucleus in HeLa cells (**FIGURE 57A**), as well as forming aggregates in HEK293 cell lines (**FIGURE 57B**, LACOSTE ET AL., 2024). Therefore, actin aggregates could explain the pathogenicity of this actin variant. The obtention of a LifeAct expressing *act-2* R183W variant or the use of another fluorescent actin probe, such as phalloidin, could reveal if this variant also induces aggregates in *C. elegans*.

Protégé par le droit à l'image
DOI: 10.1016/j.cell.2024.09.003

Figure 57: ACTB R183W variant in cultured cells.

Haploinsufficiency

Haploinsufficiency can be induced if the polymerizable actin pool is reduced by mRNA or protein degradation, or if the resulting protein cannot polymerize (**FIGURE 16**, CHAPTER 2 'HYPOTHESIS ON ACTIN VARIANT PATHOGENICITY'). A previous study has associated a drastic decrease in actin production (24% of total WT actin) with reduced viability in *Saccharomyces cerevisiae*. However, a smaller decrease in actin expression (~40% of total WT actin) does not impact the organism's viability (BOIERO SANDERS ET AL., 2022). We did not quantify the total amount of actin in our variant strains yet, which is planned using quantitative western blot. However, we did not detect a reduced amount of mRNA for variants L65V, R196C, and R196H using single-worm RT-qPCR (**FIGURE 58**).

Intriguingly, the Mannstein's group has observed a reduction of total actin protein amount in R196H fibroblasts derived from patients (36% of total WT actin). However, Di Donato's group could not replicate this result in fibroblast derived from another patient with the same R196H variation (UNPUBLISHED RESULT). This discrepancy might be due to genomic differences from one patient to another, or different experimental procedures.

Nevertheless, our collaborator Johannes N. Greve found that multiple cytoplasmic actin loss-of-function variations such as S338_I341del, A331Vfs*27, and S368Lfs*1326 lead to impaired protein expression and/or have reduced stability compared to WT actin, probably leading to haploinsufficiency (NATALIYA DI DONATO, 2024; UNPUBLISHED RESULTS). Thus, haploinsufficiency is a probable pathophysiological mechanism of the *act-2* null *rey021* variation.

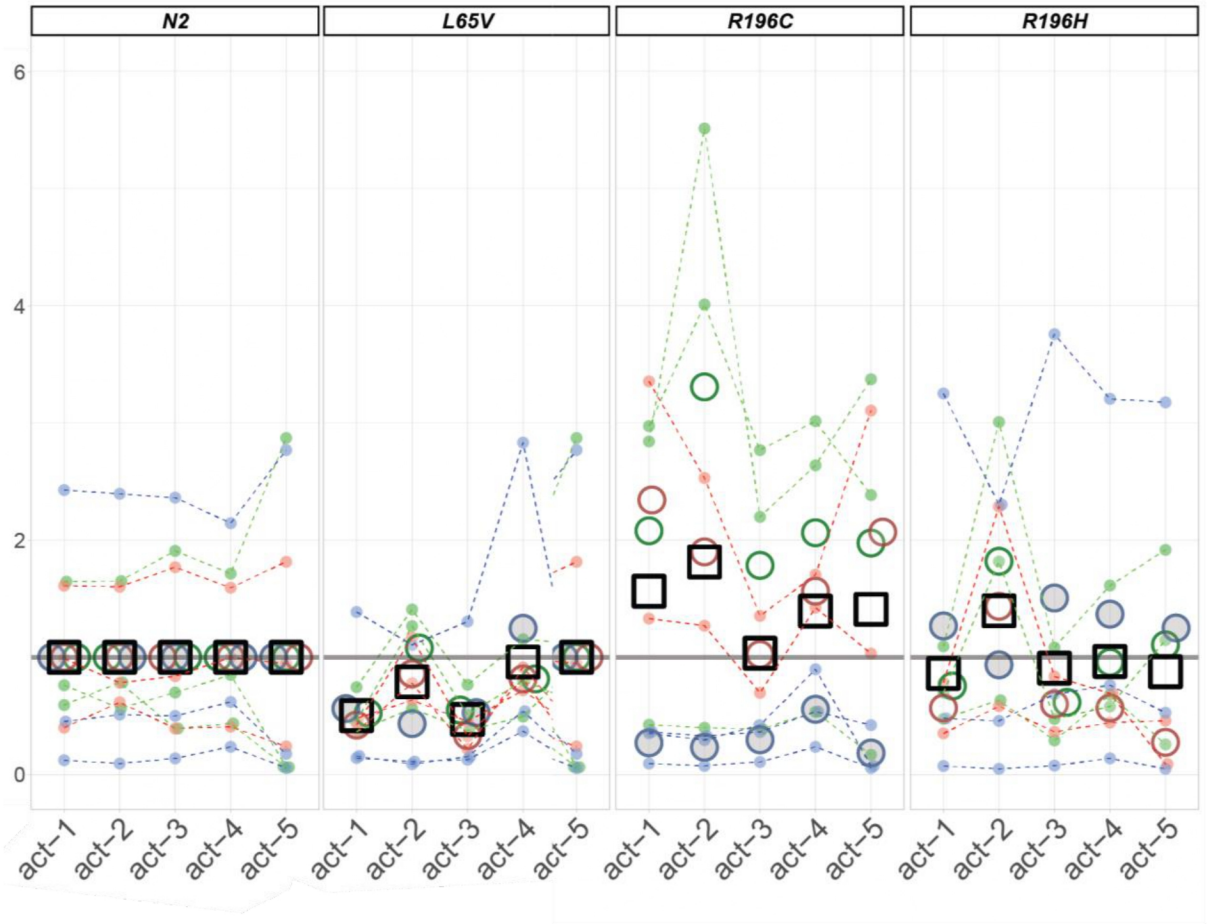

Figure 58: Single animal RT-qPCR of actin coding genes of variants L65V, R196C, and R196H. Graph shows the normalized amount of mRNA for each *C. elegans* actin coding genes in *act-2* homozygous L65V, R196C, and R196H animals. Normalization was done with the amount of mRNA quantified for the housekeeping gene *iscu-1* and with the WT values set to 1. Different colors show different replicates. The small dot is the value for one animal, while bigger dots correspond to the experiment's mean. Black squares show the mean of all replicates.

Impaired actin dynamics

The remaining mechanism proposed to explain pathophysiological mechanisms of actin variants is impaired actin dynamics, either due to impaired interactions with ABPs or with other actin subunits. *In vitro* data have shed light on altered actin mechanisms for some of the studied variants. In the following paragraphs, I will try to correlate some of these mechanisms with my data and propose new hypotheses needing further studies.

R196H and R196C

The R196H variant has recently been associated with impaired association with the Arp2/3 complex (XIONG ET AL., 2011; GREVE AND MANNSTEIN, 2024, BIORXIV). In *C. elegans*, embryonic arrest of R196H embryos occurs mainly during ventral enclosure, a process highly dependent on cell migration and, thus, of Arp2/3 mediated actin polymerization (Vuong-Brender et al., 2016). Moreover, I have observed reduced male pronuclear migration for variant R196H (**FIGURE 59**), which has been associated with Arp2/3 defects (XIONG ET AL., 2011). Furthermore, if my hypothesis on *unc-8* overexpression is confirmed in this variant, it may be to compensate for impaired Arp2/3-based actin polymerization involved in activity-dependent bulk endocytosis (See 'WHAT COULD BE THE CAUSE AND CONSEQUENCES OF NEURONAL CHANGE IN GENE EXPRESSION?', CUENTAS-CONDORI ET AL., 2023). Thus, our data *in vivo* seems to correlate with *in vitro* data.

In addition to phenotypes associated with Arp2/3 defects, we found that the R196H *act-2* variant induces rounded compartments in gonads, which is the only variant along with G74S that shows this phenotype (**FIGURE 60**). Interestingly, this phenotype was observed in animals with reduced expression of genes encoding for the chaperonin complex, which is essential for protein folding (GREEN ET AL., 2011; WAGNER ET AL., 2024). The chaperonin complex is crucial to folding newly synthesized actin monomers, among others (VALLIN AND GRANTHAM, 2019). Additionally, a study shows that the chaperonin complex can bind *in vitro* to a capping and severing ABP called gelsolin to inhibit its severing activity (SVANSTRÖM AND GRANTHAM, 2016). Therefore, this tissue disorganization can indicate a defect in the interaction between *act-2* and the *C. elegans* gelsolin homolog *gsnl-1* or members of the chaperonin complex. Importantly, *gsnl-1* is predicted to bind to *act-2* (LEE ET AL., 2008).

The other variant we recapitulated at this locus, R196C, has not been tested *in vitro*. *C. elegans* mutant animals do not have rounded compartments or defective male pronuclear migration, implying that the R196H and R196C variants affect differentially actin dynamics

(FIGURES 59 AND 60). Accordingly, R196C animals have gonads with enlarged vesicles at their rachis' tip; although at a low frequency, this phenotype is unique to this variant (FIGURE 60). Green and colleagues observed this phenotype in RNAi of genes with different functions. Therefore, it is difficult to hypothesize how R196C impairs actin dynamics.

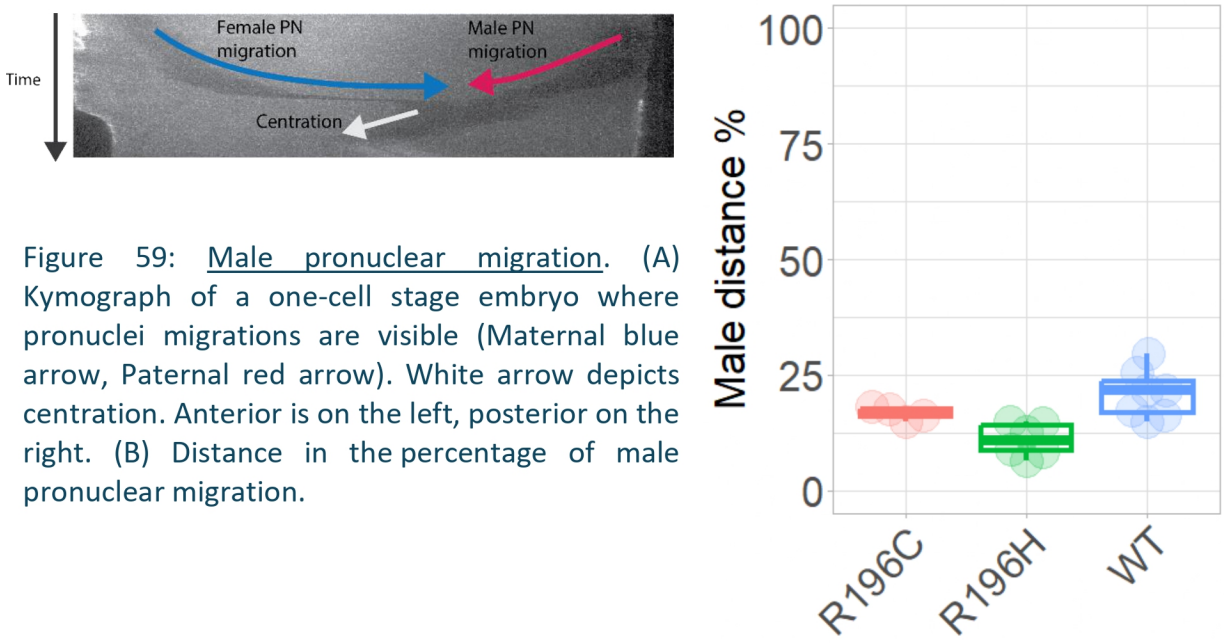

Figure 59: Male pronuclear migration. (A) Kymograph of a one-cell stage embryo where pronuclei migrations are visible (Maternal blue arrow, Paternal red arrow). White arrow depicts centration. Anterior is on the left, posterior on the right. (B) Distance in the percentage of male pronuclear migration.

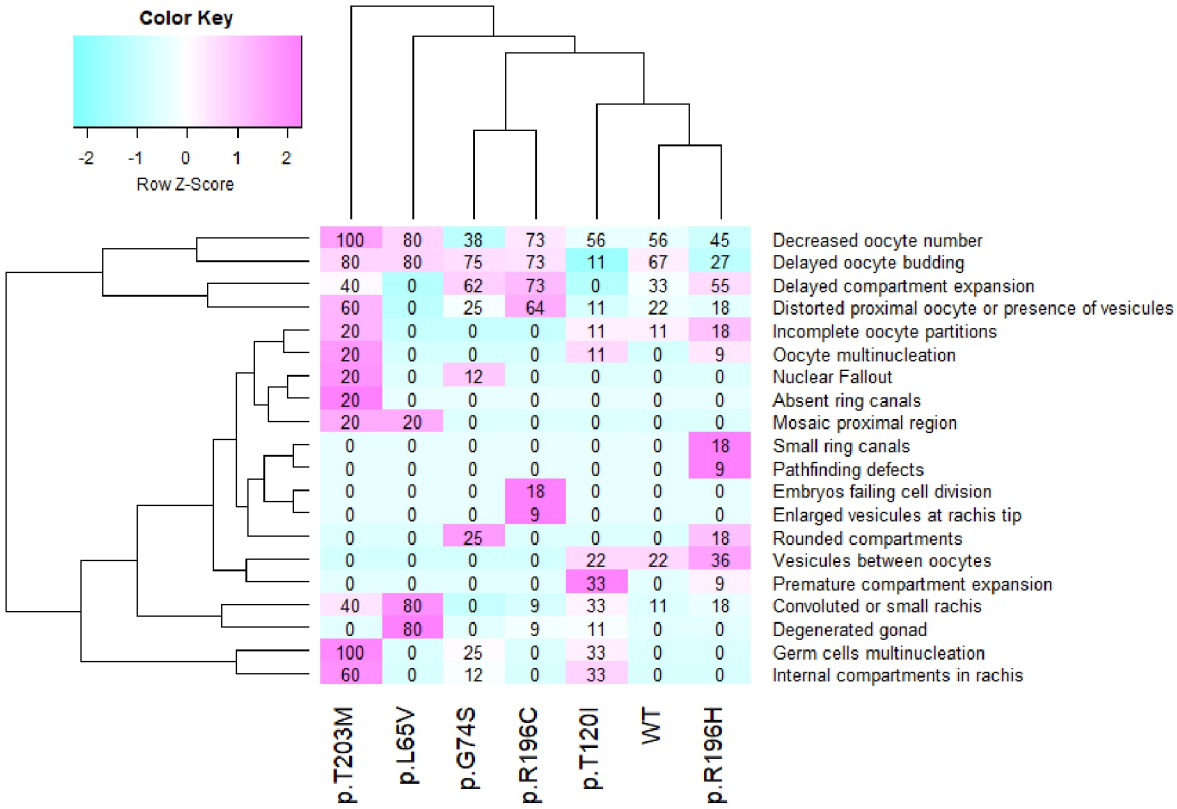

Figure 60: Gonadal defects. Heatmap of phenotypes observed in gonads of homozygotes *act-2* variants in percent. Figure and legend extracted from Hecquet et al., 2024 Biorχiv

R147S

The R147 actin residue is known to interact with tropomyosin in Humans (**FIGURE 61A,** HITCHCOCK-DEGREGORI AND BARUA, 2017; PARKER ET AL., 2020). *C. elegans* possesses an ortholog of tropomyosin called *lev-11* (ANYANFUL ET AL., 2001). Reduction of *lev-11* expression by RNAi leads to harsh phenotypic defects such as cytokinesis failure or arrest around the 300-cell stage (ANYANFUL ET AL., 2001; ONO AND ONO, 2004), which correlate with observed phenotypes for the R147S variant (HECQUET ET AL., 2024 BIORXIV). However, RNAi of *lev-11* is also associated with uncoordinated locomotion (ANYANFUL ET AL., 2001), which is not observed in our case. The R147 actin residue is also known to interact with the chaperonin complex (**FIGURE 61B**, KELLY ET AL., 2022). We have not assessed the gonad organization of this variant yet, so we cannot check if this variant leads to the formation of rounded compartments, a sign of a defective chaperonin complex (GREEN ET AL., 2011). Further studies are thus needed to determine whether the interaction between *act-2* R147S and *lev-11* or a member of the chaperonin complex is impacted.

Protégé par le droit à l'image
https://doi.org/10.1007/978-3-319-49674-0_9

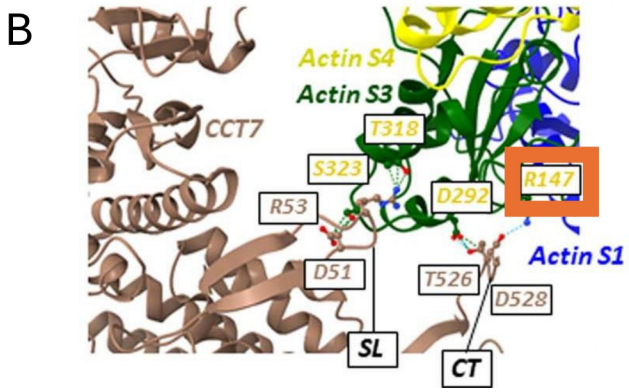

Figure 61: Actin binding proteins interacting with actin's R147 residue.

(B) β-actin subdomains are colored: subdomain 1 (S1, blue), subdomain 3 (S3, dark green), and subdomain 4 (S4, yellow); green dashes indicate van der Waals contacts; blue dashes indicate hydrogen bonds; TRiC structural features labelled are apical CCT7 uses the stem-loop and C-terminus to interact with actin subdomain 3. stem-loop (SL) and C-terminus (CT). Figure and legend extracted from Kelly et al., 2022. Orange boxes highlight the R147 residue.

T203M and T120I

Variants T120I and T203M induce similar phenotypes. Notably, they both have gonads with multinucleated germ cells and oocytes (**FIGURE 60**). Green and colleagues observed these phenotypes in RNAi of key molecular players of actomyosin contractility, such as *nmy-2*, *act-4*, or the upstream actomyosin activator *rho-1* (GREEN ET AL., 2011). Accordingly, these two variants produce cell blebs, signs of impaired cortical tension, or membrane-to-cortex attachment (**FIGURE 62**).

Interestingly, multinucleation is also present in an RNAi of the DYNamin related *dyn-1* (GREEN ET AL., 2011). As introduced above in "WHAT COULD BE THE CAUSE AND CONSEQUENCES OF NEURONAL CHANGE IN GENE EXPRESSION?", *dyn-1* is implicated in activity-dependent bulk endocytosis (**FIGURE 52**, CUENTAS-CONDORI ET AL., 2023) A*ct-2* T120I shows an increased 'green' expression in NeuroPAL acquisitions, which I proposed to come from the overexpression of an *unc-8* reporter. This reinforces my hypothesis that the *act-2* T120I variant could impair activity-dependent bulk endocytosis, which is rescued by overexpression of *unc-8* in some neurons for the nervous system to function robustly. The low number of NeuroPAL acquisitions I did for variant T203M prevented me from statistically comparing intensity values with the control strain, but this should be analyzed in more detail in the near future.

Variants T120I and T203M phenotypes do not match perfectly, implying that they impact actomyosin contractility differently (**FIGURE 60**). For example, *act-2* T120 animals can have germ cells that grow prematurely in oocytes ('premature compartment expansion', **FIGURE 60**). In contrast, *act-2* T203M animals have absent ring bridges and thus form closed germ cells ('absent ring canals' **FIGURE 60**). However, further analyses are needed to clarify the molecular pathways impaired in these variants.

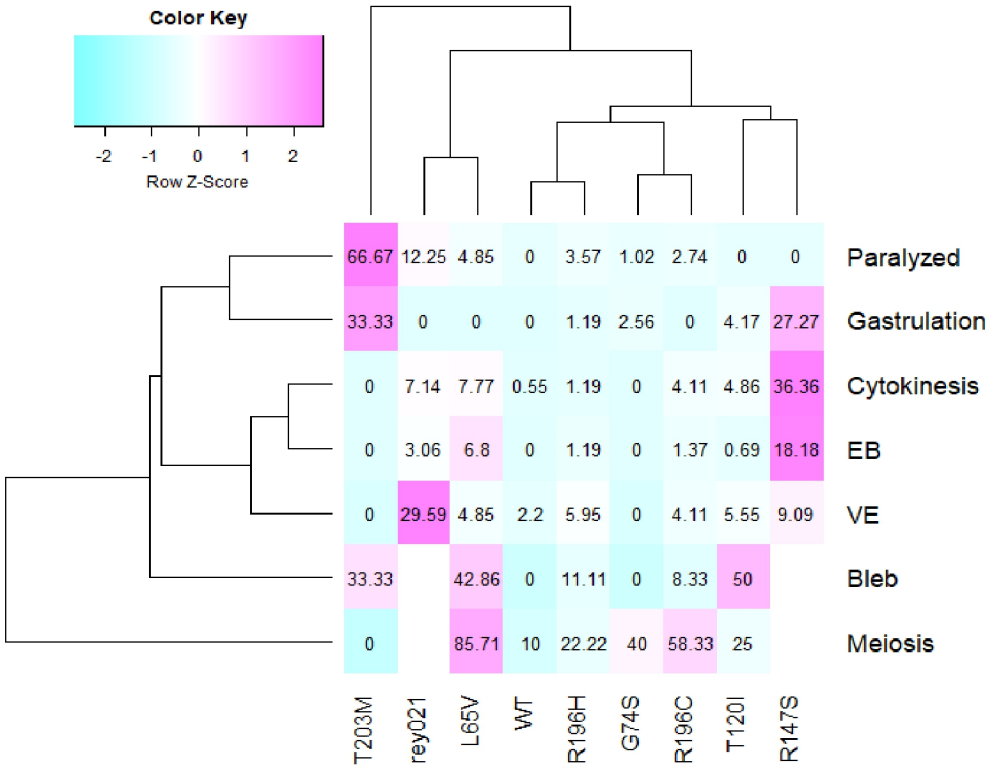

Figure 62: Embryogenesis defects. Heatmap of phenotypes observed in embryos of homozygotes *act-2* variants in percent.

L65V

The L65V Human cytoplasmic actin variant was not characterized *in vitro*. In *C. elegans*, the L65V *act-2* variant is associated with a high incidence of meiosis defects and degenerated gonad, more so than every other studied variant (**FIGURE 60 & 62**, HECQUET ET AL., 2024 BIORXIV). Degenerated gonads were observed in the RNAi of seven genes in the study of Green and colleagues (GREEN ET AL., 2011). One of these genes is *cmd-1*, coding for calmodulin (GREEN ET AL., 2011). Calmodulin is activated upon Ca^{2+} influx within the cell, which in turn regulates actin dynamics directly by activating the INF2 formin, the Cobl actin nucleator, and inactivating the myelin basic protein MBP, another actin nucleator (**FIGURE 63**, IZADI ET AL., 2018). Calmodulin is also affecting actin dynamics indirectly by being upstream of Rho GTPases (**FIGURE 63**, IZADI ET AL., 2018). Interestingly, RNAi of *cmd-1* was also associated with meiosis defects, such as meiotic spindle misplacement and the presence of a supernumerary pronucleus in the zygote, the latter being often observed in *act-2* L65V embryos (**FIGURE 62**, VAN DER VOET ET AL., 2009). Moreover, *act-2* is predicted to be an interactant of *cmd-1* (ZHONG AND STERNBERG, 2006). Therefore, I think the *act-2* L65V variant may impair the function of *cmd-1* through a feedback loop unknown to my knowledge, which will need further characterization. For example, we could use a biosensor for active Rho in the L65V background to see whether its activation is impaired, which could be a sign of a defective indirect activity of calmodulin.

Protégé par le droit à l'image
https://doi.org/10.1016/j.bbrc.2018.07.159

Figure 63: Calmodulin roles in actin regulation.

Why do we observe such variance in our results?

Looking at our results, it is clear that variant strains can lead to large variability. For example, variant L65V has an embryonic lethality ranging from 0% to 100% (HECQUET ET AL., 2024 BIORXIV). I hypothesize that some of this variation can come from embryos surviving meiosis defects. Indeed, *act-2* variants can lead to the presence of an extra nucleus in the zygote or in one of the early blastomeres, which was especially evident for variant L65V (6/7 animals expressing LifeAct::mKate2 and NMY-2::GFP, HECQUET ET AL., 2024 BIORXIV).

I isolated one of these embryos and found that it hatched and survived a few days, although the animal did not produce any progeny. Still, a few studies have been published working with tetraploid and triploid *C. elegans* animals as early as 1951 (NIGON, 1951; LOZANO ET AL., 2006; MADL AND HERMAN, 1979; MISARE ET AL., 2023). Tetra- and triploid animals were associated with numerous phenotypic defects such as reduced brood size, embryonic lethality, high induction of males, larval arrest (MADL AND HERMAN, 1979), increased adult body size (LOZANO ET AL., 2006), reduced longevity, larger embryos, and increased number of apoptotic cells in the gonad (MISARE ET AL., 2023). Although I have not assessed all these phenotypes, L65V animals do have reduced brood size, higher embryonic lethality, and larger embryos, which could be due to polyploidy (HECQUET ET AL., 2024 BIORXIV). Therefore, it is highly plausible that viable tri- or tetraploid animals originating from meiosis defects were included in experiments, increasing the results' variability.

Chapter conclusion

In summary, the cause of the different outcomes of *rey021* and *ok1229 act-2* null alleles remains unanswered. Nonetheless, I propose that undetected genetic differences or changes in isoactin switching may underlie this change.

Then, I proposed that the overexpression of 'green' I observed in my NeuroPAL acquisitions for variants T120I and R196H (CHAPTER 6) is not stochastic and is due to an overexpression of *unc-8*. I propose that this could increase or rescue branched actin-mediated activity-dependent bulk endocytosis in a dose-dependent manner to ensure proper neuronal function.

Afterward, I proposed that *act-2* variants' zygotes or early embryos having an extra nucleus could survive, producing polyploid animals. Polyploid "wild-type" animals are known to have developmental phenotypes that may be increased in an *act-2* variant context. These animals may constitute a different population in my experiments, increasing the results' variance.

Finally, based on data from *C. elegans* and *in vitro* studies, I hypothesized about the molecular consequences of a few actin variants I studied. Notably, I proposed that variant R196H could impair actin association with gelsolin or with the chaperonin complex, that T120I and T203M impact cell contractility in different ways, and that L65V may impact the calmodulin pathway. Understanding the molecular pathways impaired in actin-variant animals is the next key step in the understanding of non-muscle actinopathies. A current PhD student in the lab called Marjolaine Dufour-Nicodex focuses on this characterization at the single particle level, which will provide valuable insights into the association dynamics of actin with its partners *in vivo*. She will also characterize the biomechanical properties of the zygotic cortex *in vivo*, shedding light on the impaired cell contractility our data indicate for example.

Chapter 8: *act-2* as a Human cytoplasmic actin counterpart

Chapter Introduction

During my PhD, I was able to compare the effect of different actin variants in *C. elegans* (HECQUET ET AL., 2024 BIORXIV). When designing this project, the Reymann team had to choose in which *C. elegans*' actin coding gene to insert the selected variants. Among the five *C. elegans* actin coding genes, ACT-5 is known to have a distinct localization in the intestinal and excretory cells (MACQUEEN ET AL., 2005), and ACT-4 is enriched in muscles (STONE AND SHAW, 1993), making these two genes inadequate to model cytoplasmic actin variants. The remaining genes: *act-1*, *act-2*, and *act-3*, are more ubiquitously expressed. Among these three genes, *act-2* is slightly easier to target for genome engineering than *act-1* and *act-3*, as the latter have an identical coding sequence. Therefore, Anne-Cécile initially chose *act-2* as a target to replicate Human cytoplasmic actin variants causing Non-Muscle Actinopathies.

Non-Muscle Actinopathies are caused by variants in two different genes: ACTB and ACTG1. However, we recapitulated the chosen variants only in *act-2*, without distinction whether they were found in ACTB or ACTG1. This raises an important interrogation: Was *act-2* a good choice to model both *ACTB* and *ACTG1* human actin variants? I will try to answer this by dividing it into sub-questions. First, could *act-2* be an ortholog of *ACTB* or *ACTG1*? Second, are the phenotypes observed in *C. elegans* specific to act-2?

Could *act-2* be an ortholog of ACTB or ACTG1?

Protein localization

Despite very similar amino acid sequences, ACTB and ACTG1 vary in their localization (CHAPTER 1, 'LOOKALIKES FROM DIFFERENT PARENTS'). Determining the localization of specific actin isotypes in living organisms is difficult. C-terminal fusions of a fluorophore or a Tag lead to impaired prevent proper polymerization of the monomers. N-terminal fused actin can incorporate into filaments but lead to impaired actin dynamics, post-translational modifications, and interactions with partners, potentially altering the localization of the tagged protein (BRAULT ET AL., 1999; VAN ZWAM ET AL., 2024). Moreover, overexpression of actin, tagged or not, can impact actin dynamics (MELAK ET AL., 2017). In *C. elegans*, antibodies targeting specific actin isotypes do not exist. Because of the high amino acid sequence similarity between Human and *C. elegans* actin proteins, Human antibodies specific to ACTB or ACTG1 may work in *C. elegans*. However, they have not yet been tested for specificity. Nonetheless,

the teams of Geraldine Seydoux and Bruce Bowerman have both generated extrachromosomal arrays of an N-Terminal fused ACT-2 with GFP (respectively FBR001, UNPUBLISHED and EU1382, WILLIS ET AL., 2006). FBR001 drives the expression of GFP::ACT-2 through a ubiquitous promoter (*pie-1*), while EU1382 uses the endogenous *act-2* promoter. FBR001 is very slow-growing and shows multiple health defects. On the contrary, Willis and colleagues do not report gross defects for EU1382 (WILLIS ET AL., 2006). The authors observed GFP::ACT-2 in the cortex and cytoplasm of every cell in the embryo beginning at the 20th cell stage and in epidermal cells during elongation (**FIGURE 64**). The authors hypothesized that earlier expression of ACT-2 could be missed by the silencing of the extrachromosomal array (WILLIS ET AL., 2006). In adults, GFP::ACT-2 is present in body wall muscle cells and some neurons, although not specified (**FIGURE 64,** WILLIS ET AL., 2006). Even if these results are of great interest as they suggest a role of ACT-2 in animal elongation, motility, and maybe neurogenesis, they are insufficient to indicate a proximity of ACT-2 with ACTB or ACTG1.

Protégé par le droit à l'image
https://doi.org/10.1091/mbc.e05-09-0886

Figure 64: *act-2*p::GFP::ACT-2 expression.

To make a guess on *act-2* orthology, we ideally would like to observe endogenous ACT-2 expression during the early embryogenesis of *C. elegans*. Indeed, this would allow us to monitor meiosis and cell division where β- and ɣ-actin have easily noticeable differential patterns during these events (**FIGURE 16B**, BROCKMANN ET AL., 2011; DUGINA ET AL., 2009). Recently, Van Zwam and colleagues identified a locus in a conserved part of actin suitable for adding a

tag without disrupting the protein's dynamics (VAN ZWAM ET AL., 2024). This locus, located between T229 and A230, was called IntAct. Upon this discovery, the Reymann team promptly decided to introduce a tag in the IntAct locus in one of *C. elegans*' actin coding proteins. Sophie Quintin successfully generated a strain harboring a codon-optimized ALFA tag in the IntAct locus, specifically in the endogenous *act-2* gene (ACT-2$^{\alpha}$). This strain has a normal number of progeny and does not show embryonic lethality, suggesting that the tag does not disrupt *act-2* expression and dynamics (**FIGURE 65**). To reveal ACT-2$^{\alpha}$ localization, we can either fix animals and stain them with an antibody targeting ALFA or drive the *in vivo* expression of a nanobody fused to a fluorophore to observe ACT-2 dynamics in living cells. For the latter, Sophie Quintin generated a strain expressing both ACT-2$^{\alpha}$ and an anti-ALFA Nanobody fused to mKate2 driven by the ubiquitous *mex-5* promoter (ACT-2$^{\alpha}$; Nb::mKate2). This strain has a low brood size and a high embryonic lethality (**FIGURE 65**). This suggests that adding the fluorophore to the tagged ACT-2 is detrimental *in vivo*.

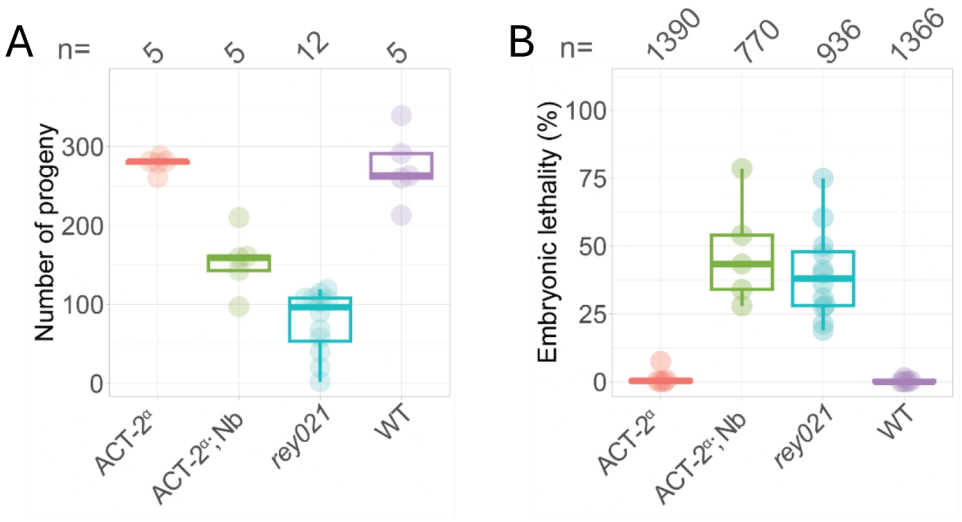

Figure 65: Progeny number and embryonic lethality of ACT-2α, ACT-2α; Nb::mKate2, *rey021*, and WT animals. (A) Progeny number at 20°C were counted for 72h for homozygous animals. The sum of eggs laid for one animal is shown as a dot. (B) Percentage of eggs that failed to hatch. The percent of dead eggs for one animal is shown as a dot. Nb=Nanobody. Data from Maria Izabella Saad. *rey021* values were extracted from Hecquet et al., 2024, Biorχiv.

Spinning disk acquisition of ACT-2$^{\alpha}$; Nb::mKate2 shows an embryonic and adult spatiotemporal distribution of ACT-2$^{\alpha}$. Sophie Quintin observed ACT-2$^{\alpha}$ expression at all embryonic stages (**FIGURE 66**). In the zygote, ACT-2$^{\alpha}$ is observed as small foci enriched in the cortex but is also visible in the cytosol. Intriguingly, no networks of filaments are visible in the cortex or in the cytokinesis ring (**FIGURE 66**), contrasting with the usual filamentous networks

visible in LifeAct embryos. In elongating embryos, ACT-2$^{\alpha}$ is present in the muscles, nerve ring, intestine, and gonad cell precursors. The same expression pattern is present in L1 animals (**FIGURE 66**). However, in L4 and adult animals, the nerve ring and intestinal expression are lost, and there is a clear enrichment of ACT-2$^{\alpha}$ in the gonads. Interestingly, the loss of expression of intestinal ACT-2 between the L1 and L4 stages correlates with the lethality observed in *dt2017 act-5* knockout animals during the first larval stage, implying that ACT-2 may be specifically required for early intestinal development but not for later development nor maintenance (MACQUEEN ET AL., 2005).

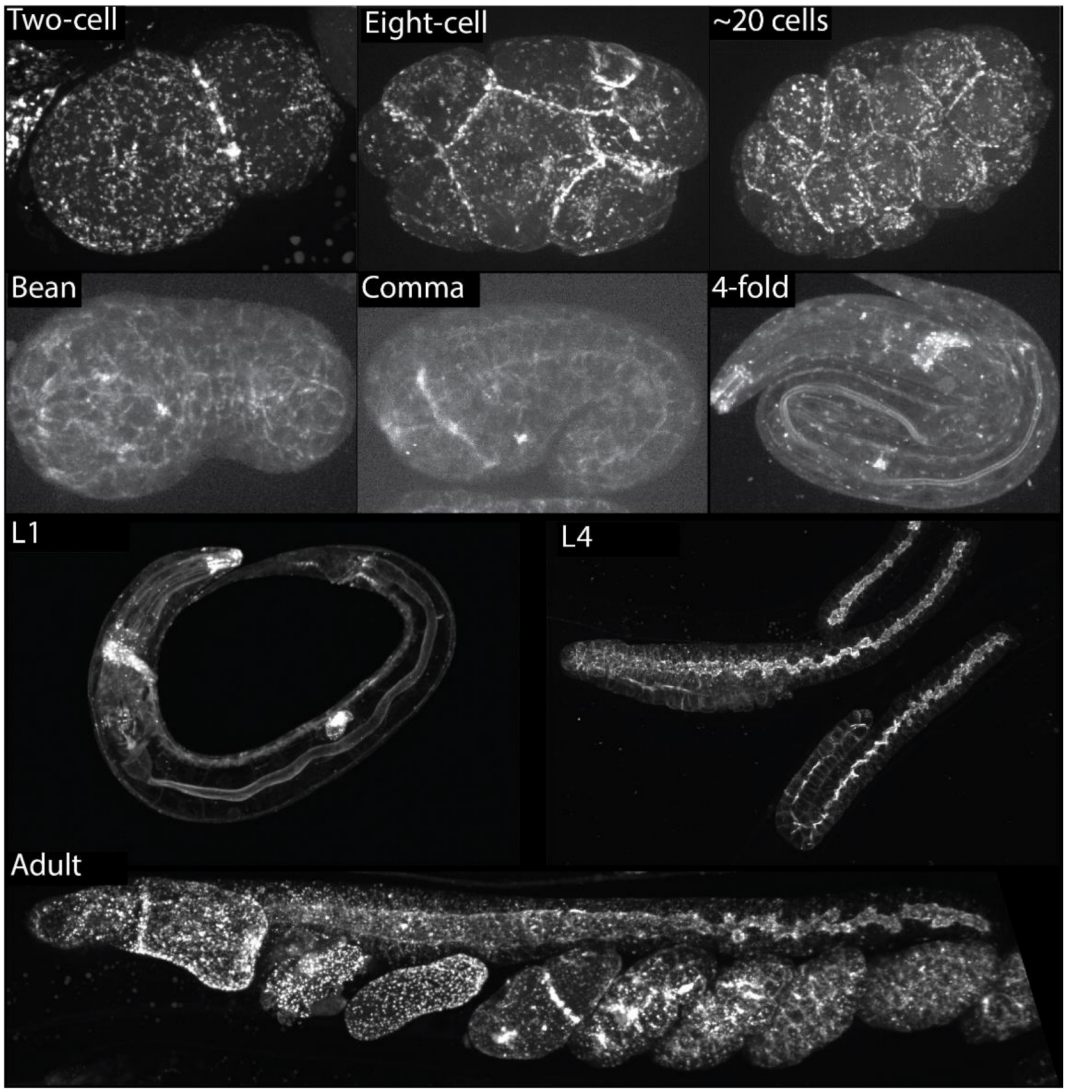

Figure 66: ACT-2α; Nb::mKate2 expression during *C. elegans*' development. *In vivo* ACT-2$^{\alpha}$ expression (grey) observed by the expression of a Nanobody fused to a mKate2 reporter. Max intensity Z projections. Data from Sophie Quintin.

To further confirm that no ACT-2$^{\alpha}$; Nb::mKate2 is visible in the zygotic mitotic contractile ring, we decided to look at the CYK-1 formin, which is enriched in this network. Therefore, the Reymann team added in the ACT-2$^{\alpha}$; Nb::mKate2 genetic background, the

endogenous CYK-1::GFP expression. CYK-1::GFP presence does not match that of ACT-2$^{\alpha}$; Nb::mKate2, except for a few puncta (**FIGURE 67A**). This implies that ACT-2$^{\alpha}$; Nb::mKate2 may not be polymerizable by the CYK-1 formin and may thus only show the localization of branched Arp2/3-mediated actin polymerization. This result in *C. elegans* embryos matches what was observed in yeast (van Zwam et al., 2024). Indeed, introducing a tagged nanobody targeting IntAct in yeast prevents actin from incorporating in formin-mediated networks (VAN ZWAM ET AL., 2024). Therefore, ACT-2$^{\alpha}$; Nb::mKate2 localization might be artefactual due to steric hindrance in formin-driven actin polymerization. Accordingly, the distribution of ACT-2$^{\alpha}$; Nb::mKate2 in the *C. elegans* cortical plane resembles the LifeAct distribution observed when a CYK-1 thermosensitive allele is inactivated (**FIGURE 67B**, DAVIES ET AL., 2014). Thus, embryonic lethality may be due to ACT-2$^{\alpha}$; Nb::mKate2's inability to polymerize linear filaments. Interestingly, the embryonic lethality value closely resembles the *rey021* ACT-2 knockout phenotype (**FIGURE 66**, HECQUET ET AL., 2024 BIORXIV). Thus, tagged nanobody binding may induce a Loss of Function of ACT-2.

A

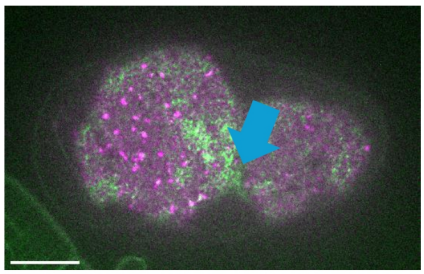

Protégé par le droit à l'image
DOI: 10.1016/j.devcel.2014.05.009

Figure 67: ACT-2α; Nb::mKate2 is absent from the zygotic contractile ring. (A) ACT-2α; Nb::mKate2 (Magenta); CYK-1::GFP (green) observed in the zygotic cortex during ring formation. The blue arrow point to the forming contractile ring. Scale bar = 10µm Anterior on the left. Data from Sophie Quintin and Anne-Cécile Reymann.

To conclude, even if such live observation based on a fluorescent nanobody targeted against ALFA gives valuable insights into the cell types in which ACT-2 is expressed, it is not ideal for observing its subcellular localization. For this, we should thus turn to fixed immunostaining experiments and reveal ACT-2$^{\alpha}$ using an antibody targeting the ALFA tag. Nonetheless, this tool will be very powerful to observe if an *act-2* variant changes the *act-2* physiological expression pattern, or to quantify specifically the amount of ACT-2 by western blot. For the moment, we cannot correlate ACT-2$^{\alpha}$ location with either ACTB or ACTG1.

mRNA

Another way to distinguish ACTB and ACTG1 is to look at their mRNA. Mammalian ACTB mRNA differs from ACTG1 by being enriched in ribosomes (VEDULA ET AL., 2017) and having a 54bp zipcode in its 3' UTR (VEDULA AND KASHINA, 2018). In Humans, the zipcode is recognized by the ZBP1 protein. However, ZPB1 does not have a recognized *C. elegans* orthologue. Similarly, BLASTN and BLASTP of the human *ZPB1* sequences or BLASTN of the Human ACTB zipcode onto the *C. elegans* genome do not retrieve any plausible results. Therefore, it is unlikely that a similar mechanism is at play in this animal.

Regarding ribosome density, I used the GWIPS-viz genome browser (https://gwips.ucc.ie/, MICHEL ET AL., 2014) to quantify ribosome profiling of the three *C. elegans'* cytoplasmic actins *act-1*, *act-2*, and *act-3*. Unfortunately, *act-1* and *act-3* have low coverage of mRNA -sequencing and, thus, of ribosome profiling measurements (**FIGURE 68**). These low coverages prevent us from comparing the three *C. elegans*' cytoplasmic actin counterparts and hypothesizing on their orthology with Human cytoplasmic actins.



Figure 68: Ribosome profiling of *act-1*, *act-2*, and *act-3*. Ribosome profiling of *act-1* (A), *act-2* (B), and *act-3* (C). Ribosome profiles of all studies are shown as red peaks and mRNA-seq coverage data as green peaks. https://gwips.ucc.ie/, Michel et al., 2014

DNA

Altering the ACTB nucleotide sequence to generate a gene knockout in mice induces embryonic lethality, while ACTG1 knockout mice are embryonically viable (Belyantseva et al., 2009; Vedula et al., 2017). ACT-2 knockouts have been a constant question during my thesis, with the discovery of the drastic phenotypic differences between the *rey021* knockout and the previously published *ok1229* knockout (discussed above, Hecquet et al., 2024 Biorxiv). Indeed, *rey021* induces high embryonic lethality, while *ok1229* does not (Hecquet et al., 2024 Biorxiv; Willis et al., 2006). Whether *rey021* or *ok1229* is chosen as a reference, ACT-2 seems more similar to ACTB or ACTG1.

Correlation with Human actin variants phenotypes

We recapitulated five variants specific to ACTB (L65V, G74S, R147S, R196C, and R196H), two variants specific to ACTG1 (G74V and T203M), and two variants found both in ACTB and ACTG1: T120I and R183W. The latter, having been obtained recently, was not fully characterized yet. However, patients possessing variants T120 and R183W on either ACTB or ACTG1 have relatively similar symptoms, which prevents us from hypothesizing on ACT-2 similarity with ACTB or ACTG1 (Di Donato et al., 2024 Medrxiv). The two variants specific to ACTG1 (G74V and T203M) are the most severe we recapitulated, as they can cause profound intellectual disabilities in patients. Accordingly, *C. elegans* models are very severe: *act-2* G74V animals are not viable, and T203M animals are only fertile as heterozygotes (Hecquet et al., 2024 Biorxiv). Therefore, it seems that our library of animals correlates well with both ACTB and ACTG1 Human variants.

Conclusion

In summary, it is still difficult to hypothesize on *act-2* orthology with human cytoplasmic actin. Nonetheless, *act-2* variants recapitulate both ACTB and ACTG1 Human variants well. Still, one can wonder if the phenotypes observed in *act-2* variant animals are specific to the actin variation or the actin gene it is recapitulated in. In other terms: Are the phenotypes observed in *C. elegans* specific to *act-2*?

Are the phenotypes observed in *C. elegans* specific to *act-2*?

Based on the differences between cytoplasmic actin in Humans, we can wonder if the phenotypes observed in *C. elegans* are specific to *act-2*. Previous studies show that *act-1*, *act-2*, and *act-3* are partially redundant, at least during early embryogenesis (WILLIS ET AL., 2006). Thus, we can expect some similarities between *act-2* and *act-1* or *act-3* variants. In the lab, two lab technicians, Nadine Arbogast and Grégory Amann, have started to introduce some variants I studied in *act-2* in its cytoplasmic actin counterparts. They recently generated one strain possessing the T120I variant both in *act-1* and *act-3* (*act-1; act-3*). This genotype could be better, as two actin-coding genes are mutated. Note that we cannot obtain, from this strain, a single variant by crossing out one of them because of the proximity between *act-1* and *act-3* (~6500bp). T120I *act-1; act-3* animals are viable at a homozygous state, and we did not face particular obstacles during its outcrosses. We decided to start characterizing this new strain by monitoring its number of progeny and embryonic lethality percentage (**FIGURE 69**). Intriguingly, the number of progeny and embryonic lethality of this strain does not match those of the *act-2* T120I variant but is similar to the WT strain. This implies that ACT-1, ACT-2, and ACT-3 have different functions and that the T120 locus is more important in ACT-2 than ACT-1 and ACT-3 for embryonic development. Further characterization of this strain, and of the newly generated *act-1* null alleles, will allow us to determine the extent of differences between *act-1; act-3* T120I with *act-2* T120I, as well as, more generally, the differences between *C. elegans*' actin isotypes.

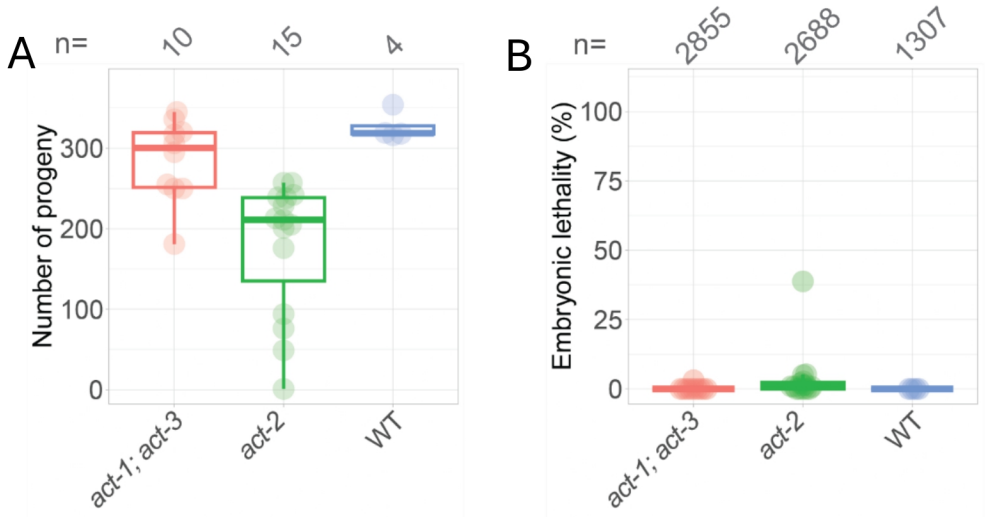

Figure 69: Progeny number and embryonic lethality of the T120I variant in different actin isotypes. (A) Progeny number at 20°C were counted for 72h for homozygous T120 actin variant animals. The sum of eggs laid for one animal is shown as a dot. (B) Percentage of eggs that failed to hatch. The percent of dead eggs for one animal is shown as a dot. T120I *act-2* values were extracted from Hecquet et al., 2024, Biorχiv.

Chapter conclusion

In summary, to the question: "Was *act-2* a good choice to model both ACTB and ACTG1 Human actin variants?" I think we can safely answer "yes". Even if we don't know whether *act-2* is more similar to one Human cytoplasmic actin coding gene, Human variants' severity from both ACTG1 and ACTB correlate well with that of *act-2* variants.

The current and future development of tools labelling specific actin isotypes, without disrupting actin expression and dynamics will provide important knowledge on their potential differential involvement and level of expression in different subcellular structures and steps of development.

Chapter 9: Conclusion

My PhD project focused on the characterization, in the model organism *Caenorhabditis elegans* (*C. elegans*), of nine Human actin variants causing Non-Muscle Actinopathies (NMA). NMA-associated variants have mostly been studied *in vitro*, and only two point mutations were recently recapitulated in animal models ((Xenopus S348L) Tsujimoto et al., 2024 Biorχiv; (Mice T120I) Di Donato et al., 2024, Medrχiv). This lack of *in vivo* studies creates a gap in knowledge regarding the molecular consequences of NMA-associated actin variants. Because *C. elegans* was already successfully used as a disease model (MARKAKI AND TAVERNARAKIS, 2020), and because actin is highly conserved between Humans and *C. elegans*, we hypothesized that this animal could be a good model for studying NMA-associated actin variants and bridge this gap.

During my PhD, I realized a comprehensive, quantitative, multiscale, phenotypic characterization of these new animal models. This showed a good correlation with the severity observed in Human variations (Hecquet et al., 2024). My PhD work thus provides the first *C. elegans* library for studying NMA-associated actin variants. Additionally, these strains can, more fundamentally, be used to probe the contribution of specific actin residues for embryogenesis and the properties of actin networks.

Nonetheless, numerous things must be kept in mind. First, we assessed animals having variations at a homozygote state, while NMAs are usually caused by heterozygote variations. We may observe different phenotypes in heterozygote animals due to compensation with the WT gene copy. We should look at this possibility in the near future. Second, the phenotypes observed in adult animals were relatively mild compared with embryonic phenotypes. We may explain this as adult animals bypassed the numerous barriers of development and, thus, form a population of “escapers” that may have milder phenotypes than expected. One could try to control the expression of actin variants in a time and space manner to probe for the full extent of phenotypes caused by an actin variant in adult animals. Third, I hypothesized on the molecular consequences of some variations in *C. elegans*. However, extensive work is needed to determine whether my hypotheses are true and if the same consequences are observed in Humans. The Reymann team, and notably Marjolaine Dufour-Nicodex, is currently working with collaborators from the PredACTINg consortium to link phenotypes we observed *in vivo* with *in vitro* data.

In the more distant future, we hope that the characterization of *C. elegans'* phenotypes could serve as a basis to use this animal to investigate the medical prognosis of Human actin variants of unknown significance.

References

Advedissian, T., Frémont, S., Echard, A., 2024. Cytokinetic abscission requires actin-dependent microtubule severing. Nat. Commun. 15, 1949. https://doi.org/10.1038/s41467-024-46062-9

Agarwal, P., Berger, S., Shemesh, T., Zaidel-Bar, R., 2024. Active nuclear positioning and actomyosin contractility maintain leader cell integrity during gonadogenesis. Curr. Biol. 34, 2373-2386.e5. https://doi.org/10.1016/j.cub.2024.03.049

Agarwal, P., Shemesh, T., Zaidel-Bar, R., 2022. Directed cell invasion and asymmetric adhesion drive tissue elongation and turning in C. elegans gonad morphogenesis. Dev. Cell 57, 2111-2126.e6. https://doi.org/10.1016/j.devcel.2022.08.003

Altun, Z.F. and Hall, D.H. 2009. Introduction. In WormAtlas. doi:10.3908/wormatlas.1.1

Altun, Z.F. 2017. Nervous system in the embryo, development of the nerve ring. In WormAtlas. doi:10.3908/wormatlas.4.2

Ankeny, R.A., 2001. The natural history of Caenorhabditis elegans research. Nat. Rev. Genet. 2, 474–479. https://doi.org/10.1038/35076538

Anyanful, A., Sakube, Y., Takuwa, K., Kagawa, H., 2001. The third and fourth tropomyosin isoforms of *Caenorhabditis elegans* are expressed in the pharynx and intestines and are essential for development and morphology1. J. Mol. Biol. 313, 525–537. https://doi.org/10.1006/jmbi.2001.5052

Arora, A.S., Huang, H.-L., Singh, R., Narui, Y., Suchenko, A., Hatano, T., Heissler, S.M., Balasubramanian, M.K., Chinthalapudi, K., 2023. Structural insights into actin isoforms. eLife 12, e82015. https://doi.org/10.7554/eLife.82015

Au, V., Li-Leger, E., Raymant, G., Flibotte, S., Chen, G., Martin, K., Fernando, L., Doell, C., Rosell, F.I., Wang, S., Edgley, M.L., Rougvie, A.E., Hutter, H., Moerman, D.G., 2019. CRISPR/Cas9 Methodology for the Generation of Knockout Deletions in Caenorhabditis elegans. G3 Bethesda Md 9, 135–144. https://doi.org/10.1534/g3.118.200778

Banga I, Szent-Györgyi A. 1942. Preparation and properties of myosin A and B. Basel, New York, Budapest: S. Karger, R. Gergely.

Bao, Z., Zhao, Z., Boyle, T.J., Murray, J.I., Waterston, R.H., 2008. Control of Cell Cycle Timing during C. elegans Embryogenesis. Dev. Biol. 318, 65–72. https://doi.org/10.1016/j.ydbio.2008.02.054

Baraitser, M., Winter, R.M., 1988. Iris coloboma, ptosis, hypertelorism, and mental retardation: a new syndrome. J. Med. Genet. 25, 41–43. https://doi.org/10.1136/jmg.25.1.41

Baranwal, S., Naydenov, N.G., Harris, G., Dugina, V., Morgan, K.G., Chaponnier, C., Ivanov, A.I., 2012. Nonredundant roles of cytoplasmic β- and γ-actin isoforms in regulation of epithelial apical junctions. Mol. Biol. Cell 23, 3542–3553. https://doi.org/10.1091/mbc.E12-02-0162

Bauer, J., Poupart, V., Goupil, E., Nguyen, K.C.Q., Hall, D.H., Labbé, J.-C., 2021. The initial expansion of the C. elegans syncytial germ line is coupled to incomplete primordial germ cell cytokinesis. Development 148, dev199633. https://doi.org/10.1242/dev.199633

Belyantseva, I.A., Perrin, B.J., Sonnemann, K.J., Zhu, M., Stepanyan, R., McGee, J., Frolenkov, G.I., Walsh, E.J., Friderici, K.H., Friedman, T.B., Ervasti, J.M., 2009. Gamma-actin is required for cytoskeletal maintenance but not development. Proc. Natl. Acad. Sci. U. S. A. 106, 9703–9708. https://doi.org/10.1073/pnas.0900221106

Belyy, A., Merino, F., Sitsel, O., Raunser, S., 2020. Structure of the Lifeact–F-actin complex. PLoS Biol. 18, e3000925. https://doi.org/10.1371/journal.pbio.3000925

Benjamini, Y., Hochberg, Y., 1995. Controlling the false discovery rate: a practical and powerful approach to multiple testing. J. R. Stat. Soc. Ser. B Methodol. 57, 289–300.

Bergeron, S.E., Zhu, M., Thiem, S.M., Friderici, K.H., Rubenstein, P.A., 2010. Ion-dependent Polymerization Differences between Mammalian β- and γ-Nonmuscle Actin Isoforms*. J. Biol. Chem. 285, 16087–16095. https://doi.org/10.1074/jbc.M110.110130

Bertrand, V., 2016. β-catenin-driven binary cell fate decisions in animal development. Wiley Interdiscip. Rev. Dev. Biol. 5, 377–388. https://doi.org/10.1002/wdev.228

Bertrand, V., Bisso, P., Poole, R.J., Hobert, O., 2011. Notch-dependent induction of left/right asymmetry in C. elegans interneurons and motoneurons. Curr. Biol. CB 21, 1225–1231. https://doi.org/10.1016/j.cub.2011.06.016

Betapudi, V., 2014. Life without double-headed non-muscle myosin II motor proteins. Front. Chem. 2, 45. https://doi.org/10.3389/fchem.2014.00045

Blanchoin, L., Boujemaa-Paterski, R., Sykes, C., Plastino, J., 2014. Actin Dynamics, Architecture, and Mechanics in Cell Motility. Physiol. Rev. 94, 235–263. https://doi.org/10.1152/physrev.00018.2013

Blanchoin, L., Pollard, T.D., 2002. Hydrolysis of ATP by polymerized actin depends on the bound divalent cation but not profilin. Biochemistry 41, 597–602. https://doi.org/10.1021/bi011214b

Boiero Sanders, M., Toret, C.P., Guillotin, A., Antkowiak, A., Vannier, T., Robinson, R.C., Michelot, A., 2022. Specialization of actin isoforms derived from the loss of key interactions with regulatory factors. EMBO J. 41, e107982. https://doi.org/10.15252/embj.2021107982

Bonnycastle, K., Davenport, E.C., Cousin, M.A., 2021. Presynaptic dysfunction in neurodevelopmental disorders: Insights from the synaptic vesicle life cycle. J. Neurochem. 157, 179–207. https://doi.org/10.1111/jnc.15035

Borisy, G., Heald, R., Howard, J., Janke, C., Musacchio, A., Nogales, E., 2016. Microtubules: 50 years on from the discovery of tubulin. Nat. Rev. Mol. Cell Biol. 17, 322–328. https://doi.org/10.1038/nrm.2016.45

Boxer, L.A., Hedley-Whyte, E.T., Stossel, T.P., 1974. Neutrophil Actin Dysfunction and Abnormal Neutrophil Behavior [WWW Document]. N. Engl. J. Med. https://doi.org/10.1056/NEJM197411212912101

Brault, V., Sauder, U., Reedy, M.C., Aebi, U., Schoenenberger, C.A., 1999. Differential epitope tagging of actin in transformed Drosophila produces distinct effects on myofibril assembly and function of the indirect flight muscle. Mol. Biol. Cell 10, 135–149. https://doi.org/10.1091/mbc.10.1.135

Brenner, S., 1974. The genetics of Caenorhabditis elegans. Genetics 77, 71–94. https://doi.org/10.1093/genetics/77.1.71

Bridges, A.A., Gladfelter, A.S., 2015. Septin Form and Function at the Cell Cortex. J. Biol. Chem. 290, 17173–17180. https://doi.org/10.1074/jbc.R114.634444

Brockmann, C., Huarte, J., Dugina, V., Challet, L., Rey, E., Conne, B., Swetloff, A., Nef, S., Chaponnier, C., Vassalli, J.-D., 2011. Beta- and Gamma-Cytoplasmic Actins Are Required for Meiosis in Mouse Oocytes1. Biol. Reprod. 85, 1025–1039. https://doi.org/10.1095/biolreprod.111.091736

Brogna, S., Wen, J., 2009. Nonsense-mediated mRNA decay (NMD) mechanisms. Nat. Struct. Mol. Biol. 16, 107–113. https://doi.org/10.1038/nsmb.1550

Brown, A.. 2002. John Sulston interview: One man and his worm. The Guardian.

Bunnell, T.M., Burbach, B.J., Shimizu, Y., Ervasti, J.M., 2011. β-Actin specifically controls cell growth, migration, and the G-actin pool. Mol. Biol. Cell 22, 4047–4058. https://doi.org/10.1091/mbc.E11-06-0582

Bunnell, T.M., Ervasti, J.M., 2010. Delayed embryonic development and impaired cell growth and survival in Actg1 null mice. Cytoskelet. Hoboken NJ 67, 564–572. https://doi.org/10.1002/cm.20467

C. elegans Sequencing Consortium, 1998. Genome sequence of the nematode C. elegans: a platform for investigating biology. Science 282, 2012–2018. https://doi.org/10.1126/science.282.5396.2012

Cai, E.D., Sun, B.K., Chiang, A., Rogers, A., Bernet, L., Cheng, B., Teng, J., Rieger, K.E., Sarin, K.Y., 2017. Postzygotic Mutations in Beta-Actin Are Associated with Becker's Nevus and Becker's Nevus Syndrome. J. Invest. Dermatol. 137, 1795–1798. https://doi.org/10.1016/j.jid.2017.03.017

Carvalho, A., Olson, S.K., Gutierrez, E., Zhang, K., Noble, L.B., Zanin, E., Desai, A., Groisman, A., Oegema, K., 2011. Acute drug treatment in the early C. elegans embryo. PloS One 6, e24656. https://doi.org/10.1371/journal.pone.0024656

Chai, Y., Tian, D., Zhu, Z., Jiang, Y., Huang, S., Wu, D., Ou, G., Li, W., 2022. Wnt signaling polarizes cortical actin polymerization to increase daughter cell asymmetry. Cell Discov. 8, 1–13. https://doi.org/10.1038/s41421-022-00376-4

Chalfie, M., Tu, Y., Euskirchen, G., Ward, W.W., Prasher, D.C., 1994. Green Fluorescent Protein as a Marker for Gene Expression. Science 263, 802–805. https://doi.org/10.1126/science.8303295

Chalut, K.J., Paluch, E.K., 2016. The Actin Cortex: A Bridge between Cell Shape and Function. Dev. Cell 38, 571–573. https://doi.org/10.1016/j.devcel.2016.09.011

Chan, F.-Y., Silva, A.M., Saramago, J., Pereira-Sousa, J., Brighton, H.E., Pereira, M., Oegema, K., Gassmann, R., Carvalho, A.X., 2019. The ARP2/3 complex prevents excessive formin activity during cytokinesis. Mol. Biol. Cell 30, 96–107. https://doi.org/10.1091/mbc.E18-07-0471

Charest, J., Daniele, T., Wang, J., Bykov, A., Mandlbauer, A., Asparuhova, M., Röhsner, J., Gutiérrez-Pérez, P., Cochella, L., 2020. Combinatorial Action of Temporally Segregated Transcription Factors. Dev. Cell 55, 483-499.e7. https://doi.org/10.1016/j.devcel.2020.09.002

Chihara, D., Nance, J., 2012. An E-cadherin-mediated hitchhiking mechanism for C. elegans germ cell internalization during gastrulation. Dev. Camb. Engl. 139, 2547–2556. https://doi.org/10.1242/dev.079863

Chisholm, A.D., Hardin, J., 2005. Epidermal morphogenesis, in: WormBook: The Online Review of C. Elegans Biology [Internet]. WormBook.

Chisholm, A.D., Hsiao, T.I., 2012. The C. elegans epidermis as a model skin. I: development, patterning, and growth. Wiley Interdiscip. Rev. Dev. Biol. 1, 861–878. https://doi.org/10.1002/wdev.79

Chugh, P., Paluch, E.K., 2018. The actin cortex at a glance. J. Cell Sci. 131, jcs186254. https://doi.org/10.1242/jcs.186254

Conboy, E., Vairo, F., Waggoner, D., Ober, C., Das, S., Dhamija, R., Klee, E.W., Pichurin, P., 2017. Pathogenic Variant in ACTB, p.Arg183Trp, Causes Juvenile-Onset Dystonia, Hearing Loss, and Developmental Delay without Midline Malformation. Case Rep. Genet. 2017, 9184265. https://doi.org/10.1155/2017/9184265

Condeelis, J., Singer, R.H., 2005. How and why does beta-actin mRNA target? Biol. Cell 97, 97–110. https://doi.org/10.1042/BC20040063

Costa, C.F., Rommelaere, H., Waterschoot, D., Sethi, K.K., Nowak, K.J., Laing, N.G., Ampe, C., Machesky, L.M., 2004. Myopathy mutations in α-skeletal-muscle actin cause a range of molecular defects. J. Cell Sci. 117, 3367–3377. https://doi.org/10.1242/jcs.01172

Cuentas-Condori, A., Chen, S., Krout, M., Gallik, K.L., Tipps, J., Gailey, C., Flautt, L., Kim, H., Mulcahy, B., Zhen, M., Richmond, J.E., Miller, D.M., 2023. The epithelial Na+ channel UNC-8 promotes an endocytic mechanism that recycles presynaptic components to new boutons in remodeling neurons. Cell Rep. 42, 113327. https://doi.org/10.1016/j.celrep.2023.113327

Cuvertino, S., Stuart, H.M., Chandler, K.E., Roberts, N.A., Armstrong, R., Bernardini, L., Bhaskar, S., Callewaert, B., Clayton-Smith, J., Davalillo, C.H., Deshpande, C., Devriendt, K., Digilio, M.C., Dixit, A., Edwards, M., Friedman, J.M., Gonzalez-Meneses, A., Joss, S., Kerr, B., Lampe, A.K., Langlois, S., Lennon, R., Loget, P., Ma, D.Y.T., McGowan, R., Des Medt, M., O'Sullivan, J., Odent, S., Parker, M.J., Pebrel-Richard, C., Petit, F., Stark, Z., Stockler-Ipsiroglu, S., Tinschert, S., Vasudevan, P., Villa, O., White, S.M., Zahir, F.R., DDD Study, Woolf, A.S., Banka, S., 2017. ACTB Loss-of-Function Mutations Result in a Pleiotropic Developmental Disorder. Am. J. Hum. Genet. 101, 1021–1033. https://doi.org/10.1016/j.ajhg.2017.11.006

D, S., Cp, D., X, M., J, B., M, H., M, L., V, S., E, K., R, K., K, B., B, L., B, K., M, M., 2005. Strong and ubiquitous expression of transgenes targeted into the beta-actin locus by Cre/lox cassette replacement. Genes. N. Y. N 2000 42. https://doi.org/10.1002/gene.20135

Dai, A., Ben Amar, M., 2024. Cyclic muscle contractions reinforce the actomyosin motors and mediate the full elongation of C. elegans embryo. eLife 12, RP90505. https://doi.org/10.7554/eLife.90505

Davies, T., Jordan, S.N., Chand, V., Sees, J.A., Laband, K., Carvalho, A.X., Shirasu-Hiza, M., Kovar, D.R., Dumont, J., Canman, J.C., 2014. High-Resolution Temporal Analysis Reveals a Functional Timeline for the Molecular Regulation of Cytokinesis. Dev. Cell 30, 209–223. https://doi.org/10.1016/j.devcel.2014.05.009

Davis, L., Radman, I., Goutou, A., Tynan, A., Baxter, K., Xi, Z., O'Shea, J.M., Chin, J.W., Greiss, S., 2021. Precise optical control of gene expression in C elegans using improved genetic code expansion and Cre recombinase. eLife 10, e67075. https://doi.org/10.7554/eLife.67075

De Simone, A., Spahr, A., Busso, C., Gönczy, P., 2018. Uncovering the balance of forces driving microtubule aster migration in C. elegans zygotes. Nat. Commun. 9, 938. https://doi.org/10.1038/s41467-018-03118-x

Di Donato, N., NMA Consortium., Thom, A., Rump, A., Greve, J N., Kropp, M., Cadiñanos, J., Calabro, S., Cathey, S., Chung, B., Cope, H., Costales, M., Cuvertino, S., Dinkel, P., Erripi, K., Fry, A E., Garavelli, L., Guan, K., Hoffjan, S., Janzarik, W G., Koenig, M., Kreimer, I., Kuenzel, K., Mancini, G., Purificacion Marin-Reina, Meinhardt, A., Niehaus, I., Pilz, D., Ricca, I., Santos Simarro, F., Schrock, E., Marquardt, A., Taft, M H., Tezcan, K., Thunström, S., Verhagen, J., Verloes, A., Wollnik, B., Krawitz, P., Hsieh, T-C., Zeef, L., Seifert, M., Heide, M., Lawrence, C B., Roberts, N., Manstein, D., Woolf, A S., Banka, S. 2024. Genomic and biological panoramas of non-muscle actinopathies. medRxiv.08.21.24310320; doi: https://doi.org/10.1101/2024.08.21.24310320

Dimov, I., Maduro, M.F., 2019. The C. elegans intestine: organogenesis, digestion, and physiology. Cell Tissue Res. 377, 383–396. https://doi.org/10.1007/s00441-019-03036-4

Dorn, J.F., Zhang, L., Paradis, V., Edoh-Bedi, D., Jusu, S., Maddox, P.S., Maddox, A.S., 2010. Actomyosin tube formation in polar body cytokinesis requires Anillin in C. elegans. Curr. Biol. CB 20, 2046–2051. https://doi.org/10.1016/j.cub.2010.10.030

Drummond, D.R., Hennessey, E.S., Sparrow, J.C., 1992. The binding of mutant actins to profilin, ATP and DNase I. Eur. J. Biochem. 209, 171–179. https://doi.org/10.1111/j.1432-1033.1992.tb17274.x

Dugina, V., Zwaenepoel, I., Gabbiani, G., Clément, S., Chaponnier, C., 2009. β- and γ-cytoplasmic actins display distinct distribution and functional diversity. J. Cell Sci. 122, 2980–2988. https://doi.org/10.1242/jcs.041970

Dulyaninova, N.G., Bresnick, A.R., 2013. The heavy chain has its day: regulation of myosin-II assembly. Bioarchitecture 3, 77–85. https://doi.org/10.4161/bioa.26133

Eggink, H., van Egmond, M.E., Verschuuren-Bemelmans, C.C., Schönherr, M.C., de Koning, T.J., Oterdoom, D.L.M., van Dijk, J.M.C., Tijssen, M.A.J., 2017. Dystonia-deafness syndrome caused by a β-actin gene mutation and response to deep brain stimulation. Mov. Disord. 32, 162–165. https://doi.org/10.1002/mds.26842

Ellis, H.M., Horvitz, H.R., 1986. Genetic control of programmed cell death in the nematode C. elegans. Cell 44, 817–829. https://doi.org/10.1016/0092-8674(86)90004-8

Eom, T., Antar, L.N., Singer, R.H., Bassell, G.J., 2003. Localization of a β-Actin Messenger Ribonucleoprotein Complex with Zipcode-Binding Protein Modulates the Density of Dendritic Filopodia and Filopodial Synapses. J. Neurosci. 23, 10433–10444. https://doi.org/10.1523/JNEUROSCI.23-32-10433.2003

Eriksson, J.E., Dechat, T., Grin, B., Helfand, B., Mendez, M., Pallari, H.-M., Goldman, R.D., 2009. Introducing intermediate filaments: from discovery to disease. J. Clin. Invest. 119, 1763–1771. https://doi.org/10.1172/JCI38339

Estes, K.A., Szumowski, S.C., Troemel, E.R., 2011. Non-Lytic, Actin-Based Exit of Intracellular Parasites from C. elegans Intestinal Cells. PLOS Pathog. 7, e1002227. https://doi.org/10.1371/journal.ppat.1002227

Fabritius, A.S., Flynn, J.R., McNally, F.J., 2011. Initial diameter of the polar body contractile ring is minimized by the centralspindlin complex. Dev. Biol. 359, 137–148. https://doi.org/10.1016/j.ydbio.2011.08.013

Feng, G., Yi, P., Yang, Y., Chai, Y., Tian, D., Zhu, Z., Liu, J., Zhou, F., Cheng, Z., Wang, X., Li, W., Ou, G., 2013. Developmental stage-dependent transcriptional regulatory pathways control neuroblast lineage progression. Development 140, 3838–3847. https://doi.org/10.1242/dev.098723

Finsterer, J., 2003. Ptosis: Causes, Presentation, and Management. Aesthetic Plast. Surg. 27, 193–204. https://doi.org/10.1007/s00266-003-0127-5

Fire, A., Xu, S., Montgomery, M.K., Kostas, S.A., Driver, S.E., Mello, C.C., 1998. Potent and specific genetic interference by double-stranded RNA in Caenorhabditis elegans. Nature 391, 806–811. https://doi.org/10.1038/35888

Fregoso, F.E., Boczkowska, M., Rebowski, G., Carman, P.J., van Eeuwen, T., Dominguez, R., 2023. Mechanism of synergistic activation of Arp2/3 complex by cortactin and WASP-family proteins. Nat. Commun. 14, 6894. https://doi.org/10.1038/s41467-023-42229-y

Freitas, J.L., Vale, T.C., Barsottini, O.G.P., Pedroso, J.L., 2020. Expanding the Phenotype of Dystonia-Deafness Syndrome Caused by ACTB Gene Mutation. Mov. Disord. Clin. Pract. 7, 86–87. https://doi.org/10.1002/mdc3.12854

Gally, C., Wissler, F., Zahreddine, H., Quintin, S., Landmann, F., Labouesse, M., 2009. Myosin II regulation during C. elegans embryonic elongation:LET-502/ROCK, MRCK-1 and PAK-1, three kinases with different roles. Development 136, 3109–3119. https://doi.org/10.1242/dev.039412

Gautreau, A.M., Fregoso, F.E., Simanov, G., Dominguez, R., 2022. Nucleation, Stabilization and Disassembly of Branched Actin Networks. Trends Cell Biol. 32, 421–432. https://doi.org/10.1016/j.tcb.2021.10.006

Gearing, M., Juncos, J.L., Procaccio, V., Gutekunst, C.-A., Marino-Rodriguez, E.M., Gyure, K.A., Ono, S., Santoianni, R., Krawiecki, N.S., Wallace, D.C., Wainer, B.H., 2002. Aggregation of actin and cofilin in identical twins with juvenile-onset dystonia. Ann. Neurol. 52, 465–476. https://doi.org/10.1002/ana.10319

Gerhold, A.R., Labbé, J.-C., Singh, R., 2022. Uncoupling cell division and cytokinesis during germline development in metazoans. Front. Cell Dev. Biol. 10. https://doi.org/10.3389/fcell.2022.1001689

Gibieža, P., Petrikaitė, V., 2021a. The regulation of actin dynamics during cell division and malignancy. Am. J. Cancer Res. 11, 4050–4069.

Gibieža, P., Petrikaitė, V., 2021b. The regulation of actin dynamics during cell division and malignancy. Am. J. Cancer Res. 11, 4050–4069.

Gillard, G., Nicolle, O., Brugière, T., Prigent, S., Pinot, M., Michaux, G., 2019. Force Transmission between Three Tissues Controls Bipolar Planar Polarity Establishment and Morphogenesis. Curr. Biol. 29, 1360-1368.e4. https://doi.org/10.1016/j.cub.2019.02.059

Glotzer, M., 2005. The Molecular Requirements for Cytokinesis. Science 307, 1735–1739. https://doi.org/10.1126/science.1096896

Goldstein, B., Nance, J., 2020. Caenorhabditis elegans Gastrulation: A Model for Understanding How Cells Polarize, Change Shape, and Journey Toward the Center of an Embryo. Genetics 214, 265–277. https://doi.org/10.1534/genetics.119.300240

Gönczy, P., Echeverri, C., Oegema, K., Coulson, A., Jones, S.J.M., Copley, R.R., Duperon, J., Oegema, J., Brehm, M., Cassin, E., Hannak, E., Kirkham, M., Pichler, S., Flohrs, K., Goessen, A., Leidel, S., Alleaume, A.-M., Martin, C., Özlü, N., Bork, P., Hyman, A.A., 2000. Functional genomic analysis of cell division in C. elegans using RNAi of genes on chromosome III. Nature 408, 331–336. https://doi.org/10.1038/35042526

Green, R.A., Audhya, A., Pozniakovsky, A., Dammermann, A., Pemble, H., Monen, J., Portier, N., Hyman, A., Desai, A., Oegema, K., 2008. Expression and imaging of fluorescent proteins in the C. elegans gonad and early embryo. Methods Cell Biol. 85, 179–218. https://doi.org/10.1016/S0091-679X(08)85009-1

Green, R.A., Kao, H.-L., Audhya, A., Arur, S., Mayers, J.R., Fridolfsson, H.N., Schulman, M., Schloissnig, S., Niessen, S., Laband, K., Wang, S., Starr, D.A., Hyman, A.A., Schedl, T., Desai, A., Piano, F., Gunsalus, K.C., Oegema, K., 2011. A High-Resolution C. elegans Essential Gene Network Based on Phenotypic Profiling of a Complex Tissue. Cell 145, 470–482. https://doi.org/10.1016/j.cell.2011.03.037

Greve, J N., Manstein D J. 2024. Baraitser–Winter Syndrome Hotspot Mutation R196H in Cytoskeletal β–actin Reduces F–actin Stability and Perturbs Interaction with the Arp2/3 Complex. bioRxiv.03.20.585892; doi: https://doi.org/10.1101/2024.03.20.585892

Greve, Johannes N, Marquardt, A., Heiringhoff, R., Reindl, T., Thiel, C., Di Donato, N., Taft, M.H., Manstein, D.J., 2024. The non-muscle actinopathy-associated mutation E334Q in cytoskeletal γ-actin perturbs interaction of actin filaments with myosin and ADF/cofilin family proteins. eLife 12, RP93013. https://doi.org/10.7554/eLife.93013

Greve, J.N., Schwäbe, F.V., Pokrant, T., Faix, J., Di Donato, N., Taft, M.H., Manstein, D.J., 2022. Frameshift mutation S368fs in the gene encoding cytoskeletal β-actin leads to ACTB-associated syndromic thrombocytopenia by impairing actin dynamics. Eur. J. Cell Biol. 101, 151216. https://doi.org/10.1016/j.ejcb.2022.151216

Greve, Johannes N., Schwäbe, F.V., Taft, M.H., Manstein, D.J., 2024. Biochemical characterization of cardiac α-actin mutations A21V and D26N implicated in hypertrophic cardiomyopathy. Cytoskelet. Hoboken NJ. https://doi.org/10.1002/cm.21852

Gudimchuk, N.B., McIntosh, J.R., 2021. Regulation of microtubule dynamics, mechanics and function through the growing tip. Nat. Rev. Mol. Cell Biol. 22, 777–795. https://doi.org/10.1038/s41580-021-00399-x

Hall, D.H., Herndon, L.A. and Altun, Z. 2017. Introduction to C. elegans Embryo Anatomy. In WormAtlas. doi:10.3908/wormatlas.4.1

Hammarlund, M., Hobert, O., Miller, D.M., Sestan, N., 2018. The CeNGEN Project: The Complete Gene Expression Map of an Entire Nervous System. Neuron 99, 430–433. https://doi.org/10.1016/j.neuron.2018.07.042

Harari, S., Humbert, M., 2020. Ultra-rare disease: an European perspective. Eur. Respir. Rev. Off. J. Eur. Respir. Soc. 29, 200195. https://doi.org/10.1183/16000617.0195-2020

Hayashi, Y., Ono, K., Ono, S., 2019. Mutations in Caenorhabditis elegans actin, which are equivalent to human cardiomyopathy mutations, cause abnormal actin aggregation in nematode striated muscle. F1000Research 8, 279. https://doi.org/10.12688/f1000research.18476.1

Hecquet, T., Arbogast, N., Suhner, D., Goetz, A., Amann, G., Yürekli, S., Marangoni, F., Greve, J N., Di Donato, N., Reymann, A-C. 2024. Classification of human actin pathological variants using C. elegans CRISPR-generated models. bioRxiv.07.22.604239; doi: https://doi.org/10.1101/2024.07.22.604239

Heer, N.C., Martin, A.C., 2017. Tension, contraction and tissue morphogenesis. Dev. Camb. Engl. 144, 4249–4260. https://doi.org/10.1242/dev.151282

Heissler, S.M., Chinthalapudi, K., n.d. Structural and functional mechanisms of actin isoforms. FEBS J. n/a. https://doi.org/10.1111/febs.17153

Heissler, S.M., Sellers, J.R., 2015. Myosin light chains: Teaching old dogs new tricks. Bioarchitecture 4, 169–188. https://doi.org/10.1080/19490992.2015.1054092

Hillers, K.J., 2017. Meiosis. WormBook 1–43. https://doi.org/10.1895/wormbook.1.178.1

Hirani, N., Illukkumbura, R., Bland, T., Mathonnet, G., Suhner, D., Reymann, A.-C., Goehring, N.W., 2019. Anterior-enriched filopodia create the appearance of asymmetric membrane microdomains in polarizing C. elegans zygotes. J. Cell Sci. 132, jcs230714. https://doi.org/10.1242/jcs.230714

Hitchcock-DeGregori, S.E., Barua, B., 2017. Tropomyosin Structure, Function, and Interactions: A Dynamic Regulator, in: Parry, D.A.D., Squire, J.M. (Eds.), Fibrous Proteins: Structures and Mechanisms. Springer International Publishing, Cham, pp. 253–284. https://doi.org/10.1007/978-3-319-49674-0_9

Hobert, O., 2010. Neurogenesis in the nematode Caenorhabditis elegans. WormBook. https://doi.org/10.1895/wormbook.1.12.2
Honda, H., 1925. Experimental and cytological studies on bisexual and hermaphrodite free-living nematodes, with special reference to problems of sex. J. Morphol. 40, 191–233. https://doi.org/10.1002/jmor.1050400202
Horvitz, H.R., 1999. Genetic control of programmed cell death in the nematode Caenorhabditis elegans. Cancer Res. 59, 1701s–1706s.
Hsu, C.R., Sangha, G., Fan, W., Zheng, J., Sugioka, K., 2023. Contractile ring mechanosensation and its anillin-dependent tuning during early embryogenesis. Nat. Commun. 14, 8138. https://doi.org/10.1038/s41467-023-43996-4
Hu, P.J., 2018. Dauer, in: WormBook: The Online Review of C. Elegans Biology [Internet]. WormBook.
Huang, Y., Zhang, S., Park, J.-I., 2022. Nuclear Actin Dynamics in Gene Expression, DNA Repair, and Cancer. Results Probl. Cell Differ. 70, 625–663. https://doi.org/10.1007/978-3-031-06573-6_23
Hundt, N., Preller, M., Swolski, O., Ang, A.M., Mannherz, H.G., Manstein, D.J., Müller, M., 2014. Molecular mechanisms of disease-related human β-actin mutations p.R183W and p.E364K. FEBS J. 281, 5279–5291. https://doi.org/10.1111/febs.13068
Hunter, M.V., Fernandez-Gonzalez, R., 2013. Gastrulation: cell polarity comes full circle. Curr. Biol. CB 23, R845-848. https://doi.org/10.1016/j.cub.2013.08.003
Hurd, D.D., 2018. Tubulins in C. elegans, in: WormBook: The Online Review of C. Elegans Biology [Internet]. WormBook.
Hurlock, M.E., Čavka, I., Kursel, L.E., Haversat, J., Wooten, M., Nizami, Z., Turniansky, R., Hoess, P., Ries, J., Gall, J.G., Rog, O., Köhler, S., Kim, Y., 2020. Identification of novel synaptonemal complex components in C. elegans. J. Cell Biol. 219, e201910043. https://doi.org/10.1083/jcb.201910043
Ilkovski, B., Nowak, K.J., Domazetovska, A., Maxwell, A.L., Clement, S., Davies, K.E., Laing, N.G., North, K.N., Cooper, S.T., 2004. Evidence for a dominant-negative effect in ACTA1 nemaline myopathy caused by abnormal folding, aggregation and altered polymerization of mutant actin isoforms. Hum. Mol. Genet. 13, 1727–1743. https://doi.org/10.1093/hmg/ddh185
Innocenti, M., 2018. New insights into the formation and the function of lamellipodia and ruffles in mesenchymal cell migration. Cell Adhes. Migr. 12, 401–416. https://doi.org/10.1080/19336918.2018.1448352
Iwasaki, K., McCarter, J., Francis, R., Schedl, T., 1996. emo-1, a Caenorhabditis elegans Sec61p gamma homologue, is required for oocyte development and ovulation. J. Cell Biol. 134, 699–714. https://doi.org/10.1083/jcb.134.3.699
Izadi, M., Hou, W., Qualmann, B., Kessels, M.M., 2018. Direct effects of Ca2+/calmodulin on actin filament formation. Biochem. Biophys. Res. Commun. 506, 355–360. https://doi.org/10.1016/j.bbrc.2018.07.159
Jafari, M., Ansari-Pour, N., 2019. Why, When and How to Adjust Your P Values? Cell J. Yakhteh 20, 604–607. https://doi.org/10.22074/cellj.2019.5992
Janke, C., Magiera, M.M., 2020. The tubulin code and its role in controlling microtubule properties and functions. Nat. Rev. Mol. Cell Biol. 21, 307–326. https://doi.org/10.1038/s41580-020-0214-3
Jarriault, S., Schwab, Y., Greenwald, I., 2008. A Caenorhabditis elegans model for epithelial-neuronal transdifferentiation. Proc. Natl. Acad. Sci. U. S. A. 105, 3790–3795. https://doi.org/10.1073/pnas.0712159105
Jiang, Z., El-Brolosy, M.A., Serobyan, V., Welker, J.M., Retzer, N., Dooley, C.M., Jakutis, G., Juan, T., Fukuda, N., Maischein, H.-M., Balciunas, D., Stainier, D.Y.R., 2022. Parental mutations influence wild-type offspring via transcriptional adaptation. Sci. Adv. 8, eabj2029. https://doi.org/10.1126/sciadv.abj2029
Johnston, W.L., Krizus, A., Dennis, J.W., 2010. Eggshell Chitin and Chitin-Interacting Proteins Prevent Polyspermy in C. elegans. Curr. Biol. 20, 1932–1937. https://doi.org/10.1016/j.cub.2010.09.059

Johnston, W.L., Krizus, A., Dennis, J.W., 2006. The eggshell is required for meiotic fidelity, polar-body extrusion and polarization of the C. elegansembryo. BMC Biol. 4, 35. https://doi.org/10.1186/1741-7007-4-35

Kashina, A.S., 2020. Regulation of actin isoforms in cellular and developmental processes. Semin. Cell Dev. Biol., SI: Actin_15 June 2019 102, 113–121. https://doi.org/10.1016/j.semcdb.2019.12.003

Kattuoa, M. l, Das, J.M., 2024. Lissencephaly, in: StatPearls. StatPearls Publishing, Treasure Island (FL).

Kelkar, M., Bohec, P., Charras, G., 2020. Mechanics of the cellular actin cortex: From signalling to shape change. Curr. Opin. Cell Biol., Cell Dynamics 66, 69–78. https://doi.org/10.1016/j.ceb.2020.05.008

Kelly, J.J., Tranter, D., Pardon, E., Chi, G., Kramer, H., Happonen, L., Knee, K.M., Janz, J.M., Steyaert, J., Bulawa, C., Paavilainen, V.O., Huiskonen, J.T., Yue, W.W., 2022. Snapshots of actin and tubulin folding inside the TRiC chaperonin. Nat. Struct. Mol. Biol. 29, 420–429. https://doi.org/10.1038/s41594-022-00755-1

Kelpsch, D.J., Tootle, T.L., 2018. Nuclear Actin: From Discovery to Function. Anat. Rec. Hoboken NJ 2007 301, 1999–2013. https://doi.org/10.1002/ar.23959

Kim, S., Spike, C., Greenstein, D., 2013. Control of Oocyte Growth and Meiotic Maturation in C. elegans. Adv. Exp. Med. Biol. 757, 10.1007/978-1-4614-4015–4_10. https://doi.org/10.1007/978-1-4614-4015-4_10

Kislauskis, E.H., Li, Z., Singer, R.H., Taneja, K.L., 1993. Isoform-specific 3'-untranslated sequences sort alpha-cardiac and beta-cytoplasmic actin messenger RNAs to different cytoplasmic compartments. J. Cell Biol. 123, 165–172. https://doi.org/10.1083/jcb.123.1.165

Kloc, M., Chanana, P., Vaughn, N., Uosef, A., Kubiak, J.Z., Ghobrial, R.M., 2021. New Insights into Cellular Functions of Nuclear Actin. Biology 10, 304. https://doi.org/10.3390/biology10040304

Krause, M., Gautreau, A., 2014. Steering cell migration: lamellipodium dynamics and the regulation of directional persistence. Nat. Rev. Mol. Cell Biol. 15, 577–590. https://doi.org/10.1038/nrm3861

Lacoste, J., Haghighi, M., Haider, S., Reno, C., Lin, Z.-Y., Segal, D., Qian, W.W., Xiong, X., Teelucksingh, T., Miglietta, E., Shafqat-Abbasi, H., Ryder, P.V., Senft, R., Cimini, B.A., Murray, R.R., Nyirakanani, C., Hao, T., McClain, G.G., Roth, F.P., Calderwood, M.A., Hill, D.E., Vidal, M., Yi, S.S., Sahni, N., Peng, J., Gingras, A.-C., Singh, S., Carpenter, A.E., Taipale, M., 2024. Pervasive mislocalization of pathogenic coding variants underlying human disorders. Cell 0. https://doi.org/10.1016/j.cell.2024.09.003

Lai, W.-F., Wong, W.-T., 2020. Roles of the actin cytoskeleton in aging and age-associated diseases. Ageing Res. Rev. 58, 101021. https://doi.org/10.1016/j.arr.2020.101021

Lambert, J., Lloret-Fernández, C., Laplane, L., Poole, R.J., Jarriault, S., 2021. On the origins and conceptual frameworks of natural plasticity—Lessons from single-cell models in *C. elegans*, in: Jarriault, S., Podbilewicz, B. (Eds.), Current Topics in Developmental Biology, Nematode Models of Development and Disease. Academic Press, pp. 111–159. https://doi.org/10.1016/bs.ctdb.2021.03.004

Lang, C.F., Munro, E., 2017. The PAR proteins: from molecular circuits to dynamic self-stabilizing cell polarity. Development 144, 3405–3416. https://doi.org/10.1242/dev.139063

Lardennois, A., Pásti, G., Ferraro, T., Llense, F., Mahou, P., Pontabry, J., Rodriguez, D., Kim, S., Ono, S., Beaurepaire, E., Gally, C., Labouesse, M., 2019. An actin-based viscoplastic lock ensures progressive body-axis elongation. Nature 573, 266–270. https://doi.org/10.1038/s41586-019-1509-4

Latham, S.L., Ehmke, N., Reinke, P.Y.A., Taft, M.H., Eicke, D., Reindl, T., Stenzel, W., Lyons, M.J., Friez, M.J., Lee, J.A., Hecker, R., Frühwald, M.C., Becker, K., Neuhann, T.M., Horn, D., Schrock, E., Niehaus, I., Sarnow, K., Grützmann, K., Gawehn, L., Klink, B., Rump, A., Chaponnier, C., Figueiredo, C., Knöfler, R., Manstein, D.J., Di Donato, N., 2018. Variants in exons 5 and 6 of ACTB cause syndromic thrombocytopenia. Nat. Commun. 9, 4250. https://doi.org/10.1038/s41467-018-06713-0

Lebedev, M., Chan, F.-Y., Lochner, A., Bellessem, J., Osório, D.S., Rackles, E., Mikeladze-Dvali, T., Carvalho, A.X., Zanin, E., 2023. Anillin forms linear structures and facilitates furrow ingression after septin and formin depletion. Cell Rep. 42. https://doi.org/10.1016/j.celrep.2023.113076

Leduc, C., Etienne-Manneville, S., 2015. Intermediate filaments in cell migration and invasion: the unusual suspects. Curr. Opin. Cell Biol., Cell architecture 32, 102–112. https://doi.org/10.1016/j.ceb.2015.01.005

Lee, I., Lehner, B., Crombie, C., Wong, W., Fraser, A.G., Marcotte, E.M., 2008. A single gene network accurately predicts phenotypic effects of gene perturbation in Caenorhabditis elegans. Nat. Genet. 40, 181–188. https://doi.org/10.1038/ng.2007.70

Lee, J.-Y., Goldstein, B., 2003. Mechanisms of cell positioning during C. elegans gastrulation. Dev. Camb. Engl. 130, 307–320. https://doi.org/10.1242/dev.00211

Lee, R.C., Feinbaum, R.L., Ambros, V., 1993. The C. elegans heterochronic gene lin-4 encodes small RNAs with antisense complementarity to lin-14. Cell 75, 843–854. https://doi.org/10.1016/0092-8674(93)90529-y

Lehman, W., Craig, R., Vibert, P., 1994. Ca2+-induced tropomyosin movement in Limulus thin filaments revealed by three-dimensional reconstruction. Nature 368, 65–67. https://doi.org/10.1038/368065a0

Lembo, S., Strauss, L., Cheng, D., Vermeil, J., Siggel, M., Toro-Nahuelpan, M., Jou Chan, C., Kosinski, J., Piel, M., Du Roure, O., Heuvingh, J., Mahamid, J., Diz-Muñoz, A. 2023. The distance between the plasma membrane and the actomyosin cortex acts as a nanogate to control cell surface mechanics. bioRxiv.01.31.526409; doi: https://doi.org/10.1101/2023.01.31.526409

Lints, R. and Hall, D.H. 2009. Reproductive system, germ line. In WormAtlas. doi:10.3908/wormatlas.1.23

Lozano, E., Sáez, A.G., Flemming, A.J., Cunha, A., Leroi, A.M., 2006. Regulation of growth by ploidy in Caenorhabditis elegans. Curr. Biol. CB 16, 493–498. https://doi.org/10.1016/j.cub.2006.01.048

MacQueen, A.J., Baggett, J.J., Perumov, N., Bauer, R.A., Januszewski, T., Schriefer, L., Waddle, J.A., 2005. ACT-5 is an essential Caenorhabditis elegans actin required for intestinal microvilli formation. Mol. Biol. Cell 16, 3247–3259. https://doi.org/10.1091/mbc.e04-12-1061

Maddox, A.S., Habermann, B., Desai, A., Oegema, K., 2005. Distinct roles for two C. elegans anillins in the gonad and early embryo. Development 132, 2837–2848. https://doi.org/10.1242/dev.01828

Madl, J.E., Herman, R.K., 1979. Polyploids and Sex Determination in CAENORHABDITIS ELEGANS. Genetics 93, 393–402.

Markaki, M., Tavernarakis, N., 2020. Caenorhabditis elegans as a model system for human diseases. Curr. Opin. Biotechnol. 63, 118–125. https://doi.org/10.1016/j.copbio.2019.12.011

Martin, E., Suzanne, M., 2022. Functions of Arp2/3 Complex in the Dynamics of Epithelial Tissues. Front. Cell Dev. Biol. 10. https://doi.org/10.3389/fcell.2022.886288

Maruyama, R., Velarde, N.V., Klancer, R., Gordon, S., Kadandale, P., Parry, J.M., Hang, J.S., Rubin, J., Stewart-Michaelis, A., Schweinsberg, P., Grant, B.D., Piano, F., Sugimoto, A., Singson, A., 2007. EGG-3 Regulates Cell-Surface and Cortex Rearrangements during Egg Activation in *Caenorhabditis elegans*. Curr. Biol. 17, 1555–1560. https://doi.org/10.1016/j.cub.2007.08.011

Masters, T.A., Kendrick-Jones, J., Buss, F., 2017. Myosins: Domain Organisation, Motor Properties, Physiological Roles and Cellular Functions. Handb. Exp. Pharmacol. 235, 77–122. https://doi.org/10.1007/164_2016_29

Mattila, P.K., Lappalainen, P., 2008. Filopodia: molecular architecture and cellular functions. Nat. Rev. Mol. Cell Biol. 9, 446–454. https://doi.org/10.1038/nrm2406

Maupas, E. 1899. La mue et l'enkystement chez les nématodes. Arch. Zool. Exp. Gen. 7, 563-628.

Maupas, E. 1900. Modes et formes de reproduction des nématodes. Arch. Zool. Exp. Gen. 8, 463-624.

Martin AC, Goldstein B., 2014. Apical constriction: themes and variations on a cellular mechanism driving morphogenesis. Development. May;141(10):1987-98. doi: 10.1242/dev.102228.
Meaders, J.L., Burgess, D.R., 2020. Microtubule-Based Mechanisms of Pronuclear Positioning. Cells 9, 505. https://doi.org/10.3390/cells9020505
Meenakshi S, I., Rao, M., Mayor, S., Sowdhamini, R., 2023. A census of actin-associated proteins in humans. Front. Cell Dev. Biol. 11. https://doi.org/10.3389/fcell.2023.1168050
Melak, M., Plessner, M., Grosse, R., 2017. Actin visualization at a glance. J. Cell Sci. 130, 525–530. https://doi.org/10.1242/jcs.189068
Mendes Pinto, I., Rubinstein, B., Kucharavy, A., Unruh, J.R., Li, R., 2012. Actin Depolymerization Drives Actomyosin Ring Contraction during Budding Yeast Cytokinesis. Dev. Cell 22, 1247–1260. https://doi.org/10.1016/j.devcel.2012.04.015
Michel, A.M., Fox, G., M. Kiran, A., De Bo, C., O'Connor, P.B.F., Heaphy, S.M., Mullan, J.P.A., Donohue, C.A., Higgins, D.G., Baranov, P.V., 2014. GWIPS-viz: development of a ribo-seq genome browser. Nucleic Acids Res. 42, D859–D864. https://doi.org/10.1093/nar/gkt1035
Migocka-Patrzałek, M., Makowiecka, A., Nowak, D., Mazur, A.J., Hofmann, W.A., Malicka-Błaszkiewicz, M., 2015. β- and γ-Actins in the nucleus of human melanoma A375 cells. Histochem. Cell Biol. 144, 417–428. https://doi.org/10.1007/s00418-015-1349-8
Misare, K.R., Ampolini, E.A., Gonzalez, H.C., Sullivan, K.A., Li, X., Miller, C., Sosseh, B., Dunne, J.B., Voelkel-Johnson, C., Gordon, K.L., Hartman, J.H., 2023. The consequences of tetraploidy on Caenorhabditis elegans physiology and sensitivity to chemotherapeutics. Sci. Rep. 13, 18125. https://doi.org/10.1038/s41598-023-45225-w
Mokin, Y.I., Povarova, O.I., Antifeeva, I.A., Artemov, A.V., Uversky, V.N., Turoverov, K.K., Kuznetsova, I.M., Fonin, A.V., 2024. Bioinformatics Analysis of Actin Interactome: Characterization of the Nuclear and Cytoplasmic Actin-Binding Proteins. Protein J. 43, 675–682. https://doi.org/10.1007/s10930-024-10207-y
Müller, M., Diensthuber, R.P., Chizhov, I., Claus, P., Heissler, S.M., Preller, M., Taft, M.H., Manstein, D.J., 2013. Distinct Functional Interactions between Actin Isoforms and Nonsarcomeric Myosins. PLoS ONE 8, e70636. https://doi.org/10.1371/journal.pone.0070636
Müller, M., Mazur, A.J., Behrmann, E., Diensthuber, R.P., Radke, M.B., Qu, Z., Littwitz, C., Raunser, S., Schoenenberger, C.-A., Manstein, D.J., Mannherz, H.G., 2012. Functional characterization of the human α-cardiac actin mutations Y166C and M305L involved in hypertrophic cardiomyopathy. Cell. Mol. Life Sci. CMLS 69, 3457–3479. https://doi.org/10.1007/s00018-012-1030-5
Naganathan, S.R., Fürthauer, S., Rodriguez, J., Fievet, B.T., Jülicher, F., Ahringer, J., Cannistraci, C.V., Grill, S.W., 2018. Morphogenetic degeneracies in the actomyosin cortex. eLife 7, e37677. https://doi.org/10.7554/eLife.37677
Nance, J., Priess, J.R., 2002. Cell polarity and gastrulation in C. elegans. Development 129, 387–397. https://doi.org/10.1242/dev.129.2.387
Nance, J. et al. Gastrulation in C. elegans. 2005, WormBook, ed. The C. elegans Research Community, WormBook, doi/10.1895/wormbook.1.23.1, http://www.wormbook.org.
Nazockdast, E., Rahimian, A., Needleman, D., Shelley, M., 2017. Cytoplasmic flows as signatures for the mechanics of mitotic positioning. Mol. Biol. Cell 28, 3261–3270. https://doi.org/10.1091/mbc.E16-02-0108
Nietmann, P., Kaub, K., Suchenko, A., Stenz, S., Warnecke, C., Balasubramanian, M.K., Janshoff, A., 2023. Cytosolic actin isoforms form networks with different rheological properties that indicate specific biological function. Nat. Commun. 14, 7989. https://doi.org/10.1038/s41467-023-43653-w
Nigon, V. 1943. Le déterminisme du sexe chez un nématode libre hermaphrodite (Rhabditis elegans Maupas). C. R. Soc. Biol. 137, 40-41.
Nigon, V. 1951. Polyploïdie expérimentale chez un nématode libre, Rhabditis elegans Maupas. Bull. Biol. Fr. Belg. 85, 187-225.
Nigon, V.M., Félix, M.-A., 2017. History of research on C. elegans and other free-living nematodes as model organisms. WormBook Online Rev. C Elegans Biol. 2017, 1–84. https://doi.org/10.1895/wormbook.1.181.1

Nobel Prize in Physiology or Medicine 2002. NobelPrize.org. Nobel Prize Outreach AB 2024. Thu. 10 Oct 2024. https://www.nobelprize.org/prizes/medicine/2002/summary

Nobel Prize in Physiology or Medicine 2006. NobelPrize.org. Nobel Prize Outreach AB 2024. Thu. 10 Oct 2024. https://www.nobelprize.org/prizes/medicine/2006/summary/

Nobel Prize in Chemistry 2008. NobelPrize.org. Nobel Prize Outreach AB 2024. Thu. 10 Oct 2024. https://www.nobelprize.org/prizes/chemistry/2008/summary/

Nobel Prize in Physiology or Medicine 2024. Advanced information. NobelPrize.org. Nobel Prize Outreach AB 2024. Thu. 10 Oct 2024. https://www.nobelprize.org/prizes/medicine/2024/advanced-information/

Nunoi, H., Yamazaki, T., Tsuchiya, H., Kato, S., Malech, H.L., Matsuda, I., Kanegasaki, S., 1999. A heterozygous mutation of β-actin associated with neutrophil dysfunction and recurrent infection. Proc. Natl. Acad. Sci. U. S. A. 96, 8693–8698.

O'Keefe, M., 2017. Chapter 39 - Pediatric iris disorders, in: Lambert, S.R., Lyons, C.J. (Eds.), Taylor and Hoyt's Pediatric Ophthalmology and Strabismus (Fifth Edition). Elsevier, London, pp. 378–384. https://doi.org/10.1016/B978-0-7020-6616-0.00039-6

Ono, K., Ono, S., 2004. Tropomyosin and Troponin Are Required for Ovarian Contraction in the Caenorhabditis elegans Reproductive System. Mol. Biol. Cell 15, 2782–2793. https://doi.org/10.1091/mbc.e04-03-0179

Ono, S., 1999. Purification and biochemical characterization of actin from Caenorhabditis elegans: Its difference from rabbit muscle actin in the interaction with nematode ADF/cofilin. Cell Motil. 43, 128–136. https://doi.org/10.1002/(SICI)1097-0169(1999)43:2<128::AID-CM4>3.0.CO;2-C

Oosterheert, W., Klink, B.U., Belyy, A., Pospich, S., Raunser, S., 2022. Structural basis of actin filament assembly and aging. Nature 611, 374–379. https://doi.org/10.1038/s41586-022-05241-8

Ou, G., Stuurman, N., D'Ambrosio, M., Vale, R.D., 2010. Polarized Myosin Produces Unequal-Size Daughters During Asymmetric Cell Division. Science 330, 677–680. https://doi.org/10.1126/science.1196112

Pacquelet A. 2017. Asymmetric Cell Division in the One-Cell C. elegans Embryo: Multiple Steps to Generate Cell Size Asymmetry. Results and problems in cell differentiation, 61, 115–140. https://doi.org/10.1007/978-3-319-53150-2_5

Pacquelet, A., Jousseaume, M., Etienne, J., Michaux, G., 2019. Simultaneous Regulation of Cytokinetic Furrow and Nucleus Positions by Cortical Tension Contributes to Proper DNA Segregation during Late Mitosis. Curr. Biol. 29, 3766-3777.e4. https://doi.org/10.1016/j.cub.2019.09.013

Palmer, N.J., Barrie, K.R., Dominguez, R., 2024. Mechanisms of actin filament severing and elongation by formins. Nature 632, 437–442. https://doi.org/10.1038/s41586-024-07637-0

Paluch, E.K., Raz, E., 2013. The role and regulation of blebs in cell migration. Curr. Opin. Cell Biol. 25, 582–590. https://doi.org/10.1016/j.ceb.2013.05.005

Panzica, M.T., Marin, H.C., Reymann, A.-C., McNally, F.J., 2017. F-actin prevents interaction between sperm DNA and the oocyte meiotic spindle in C. elegans. J. Cell Biol. 216, 2273–2282. https://doi.org/10.1083/jcb.201702020

Parker, F., Baboolal, T.G., Peckham, M., 2020. Actin Mutations and Their Role in Disease. Int. J. Mol. Sci. 21, 3371. https://doi.org/10.3390/ijms21093371

Peng, Y.-J., Geng, J., Wu, Y., Pinales, C., Langen, J., Chang, Y.-C., Buser, C., Chang, K.T., 2021. Minibrain kinase and calcineurin coordinate activity-dependent bulk endocytosis through synaptojanin. J. Cell Biol. 220, e202011028. https://doi.org/10.1083/jcb.202011028

Piekny, A.J., Mains, P.E., 2002. Rho-binding kinase (LET-502) and myosin phosphatase (MEL-11) regulate cytokinesis in the early Caenorhabditis elegans embryo. J. Cell Sci. 115, 2271–2282. https://doi.org/10.1242/jcs.115.11.2271

Pimm, M.L., Henty-Ridilla, J.L., 2021. New twists in actin–microtubule interactions. Mol. Biol. Cell 32, 211–217. https://doi.org/10.1091/mbc.E19-09-0491

Pollard, T.D., 2016. Actin and Actin-Binding Proteins. Cold Spring Harb. Perspect. Biol. 8, a018226. https://doi.org/10.1101/cshperspect.a018226
Pollard, T.D., Blanchoin, L., Mullins, R.D., 2000. Molecular Mechanisms Controlling Actin Filament Dynamics in Nonmuscle Cells. Annu. Rev. Biophys. Biomol. Struct. 29, 545–576. https://doi.org/10.1146/annurev.biophys.29.1.545
Pollard, T.D., Goldman, R.D., 2018. Overview of the Cytoskeleton from an Evolutionary Perspective. Cold Spring Harb. Perspect. Biol. 10, a030288. https://doi.org/10.1101/cshperspect.a030288
Poole, R.J., Flames, N., Cochella, L., 2024. Neurogenesis in Caenorhabditis elegans. Genetics 228, iyae116. https://doi.org/10.1093/genetics/iyae116
Pradeau-Phélut, L., Etienne-Manneville, S., 2024. Cytoskeletal crosstalk: A focus on intermediate filaments. Curr. Opin. Cell Biol. 87, 102325. https://doi.org/10.1016/j.ceb.2024.102325
Priess, J.R., Hirsh, D.I., 1986. *Caenorhabditis elegans* morphogenesis: The role of the cytoskeleton in elongation of the embryo. Dev. Biol. 117, 156–173. https://doi.org/10.1016/0012-1606(86)90358-1
Priti, A., Ong, H.T., Toyama, Y., Padmanabhan, A., Dasgupta, S., Krajnc, M., Zaidel-Bar, R., 2018a. Syncytial germline architecture is actively maintained by contraction of an internal actomyosin corset. Nat. Commun. 9, 4694. https://doi.org/10.1038/s41467-018-07149-2
Priti, A., Ong, H.T., Toyama, Y., Padmanabhan, A., Dasgupta, S., Krajnc, M., Zaidel-Bar, R., 2018b. Syncytial germline architecture is actively maintained by contraction of an internal actomyosin corset. Nat. Commun. 9, 4694. https://doi.org/10.1038/s41467-018-07149-2
Procaccio, V., Salazar, G., Ono, S., Styers, M.L., Gearing, M., Davila, A., Jimenez, R., Juncos, J., Gutekunst, C.-A., Meroni, G., Fontanella, B., Sontag, E., Sontag, J.M., Faundez, V., Wainer, B.H., 2006. A Mutation of β-Actin That Alters Depolymerization Dynamics Is Associated with Autosomal Dominant Developmental Malformations, Deafness, and Dystonia. Am. J. Hum. Genet. 78, 947–960. https://doi.org/10.1086/504271
Quintin, S., Charvin, G., 2022. Left-right asymmetry in oxidative stress sensing neurons in C. elegans. MicroPublication Biol. https://doi.org/10.17912/micropub.biology.000652
Rajan, S., Kudryashov, D.S., Reisler, E., 2023. Actin Bundles Dynamics and Architecture. Biomolecules 13, 450. https://doi.org/10.3390/biom13030450
Ramazi, S., Zahiri, J., 2021. Posttranslational modifications in proteins: resources, tools and prediction methods. Database J. Biol. Databases Curation 2021, baab012. https://doi.org/10.1093/database/baab012
Ray, S., Agarwal, P., Nitzan, A., Nédélec, F., Zaidel-Bar, R., 2023a. Actin-capping protein regulates actomyosin contractility to maintain germline architecture in C. elegans. Development 150, dev201099. https://doi.org/10.1242/dev.201099
Ray, S., Agarwal, P., Nitzan, A., Nédélec, F., Zaidel-Bar, R., 2023b. Actin-capping protein regulates actomyosin contractility to maintain germline architecture in C. elegans. Dev. Camb. Engl. 150, dev201099. https://doi.org/10.1242/dev.201099
Rella, L., Fernandes Póvoa, E.E., Korswagen, H.C., 2016. The Caenorhabditis elegans Q neuroblasts: A powerful system to study cell migration at single-cell resolution in vivo. genesis 54, 198–211. https://doi.org/10.1002/dvg.22931
Reymann, A.-C., Staniscia, F., Erzberger, A., Salbreux, G., Grill, S.W., 2016. Cortical flow aligns actin filaments to form a furrow. eLife 5, e17807. https://doi.org/10.7554/eLife.17807
Rivière, J.-B., van Bon, B.W.M., Hoischen, A., Kholmanskikh, S.S., O'Roak, B.J., Gilissen, C., Gijsen, S., Sullivan, C.T., Christian, S.L., Abdul-Rahman, O.A., Atkin, J.F., Chassaing, N., Drouin-Garraud, V., Fry, A.E., Fryns, J.-P., Gripp, K.W., Kempers, M., Kleefstra, T., Mancini, G.M.S., Nowaczyk, M.J.M., van Ravenswaaij-Arts, C.M.A., Roscioli, T., Marble, M., Rosenfeld, J.A., Siu, V.M., de Vries, B.B.A., Shendure, J., Verloes, A., Veltman, J.A., Brunner, H.G., Ross, M.E., Pilz, D.T., Dobyns, W.B., 2012. De novo mutations in the actin genes ACTB and ACTG1 cause Baraitser-Winter syndrome. Nat. Genet. 44, 440–444, S1-2. https://doi.org/10.1038/ng.1091
Robinson, J., Teuliere, J., Yoo, S., Garriga, G., 2024. NMY-2, TOE-2 and PIG-1 regulate Caenorhabditis elegans asymmetric cell divisions. PLOS ONE 19, e0304064. https://doi.org/10.1371/journal.pone.0304064

Rodriguez, A., Kashina, A., 2018. Posttranscriptional and Posttranslational Regulation of Actin. Anat. Rec. Hoboken NJ 2007 301, 1991–1998. https://doi.org/10.1002/ar.23958
Roh-Johnson, M., Goldstein, B., 2009. In vivo roles for Arp2/3 in cortical actin organization during C. elegans gastrulation. J. Cell Sci. 122, 3983–3993. https://doi.org/10.1242/jcs.057562
Sakamoto, R., Murrell, M.P., 2024. Active tension and membrane friction mediate cortical flows and blebbing in a model actomyosin cortex. Phys. Rev. Res. 6, 033024. https://doi.org/10.1103/PhysRevResearch.6.033024
Samandar Eweis, D., Plastino, J., 2020. Roles of Actin in the Morphogenesis of the Early Caenorhabditis elegans Embryo. Int. J. Mol. Sci. 21, 3652. https://doi.org/10.3390/ijms21103652
Schierenberg, E., Junkersdorf, B., 1992. The role of eggshell and underlying vitelline membrane for normal pattern formation in the early C. elegans embryo. Rouxs Arch. Dev. Biol. Off. Organ EDBO 202, 10–16. https://doi.org/10.1007/BF00364592
Schröder, J.M., Durling, H., Laing, N., 2004. Actin myopathy with nemaline bodies, intranuclear rods, and a heterozygous mutation in ACTA1 (Asp154Asn). Acta Neuropathol. (Berl.) 108, 250–256. https://doi.org/10.1007/s00401-004-0888-1
Schwayer, C., Sikora, M., Slováková, J., Kardos, R., Heisenberg, C.-P., 2016. Actin Rings of Power. Dev. Cell 37, 493–506. https://doi.org/10.1016/j.devcel.2016.05.024
Serobyan, V., Kontarakis, Z., El-Brolosy, M.A., Welker, J.M., Tolstenkov, O., Saadeldein, A.M., Retzer, N., Gottschalk, A., Wehman, A.M., Stainier, D.Y., 2020. Transcriptional adaptation in Caenorhabditis elegans. eLife 9, e50014. https://doi.org/10.7554/eLife.50014
Severson, A.F., Baillie, D.L., Bowerman, B., 2002. A Formin Homology Protein and a Profilin Are Required for Cytokinesis and Arp2/3-Independent Assembly of Cortical Microfilaments in *C. elegans*. Curr. Biol. 12, 2066–2075. https://doi.org/10.1016/S0960-9822(02)01355-6
Sferra, A., Nicita, F., Bertini, E., 2020. Microtubule Dysfunction: A Common Feature of Neurodegenerative Diseases. Int. J. Mol. Sci. 21, 7354. https://doi.org/10.3390/ijms21197354
Shagieva, G.S., Domnina, L.V., Chipysheva, T.A., Ermilova, V.D., Chaponnier, C., Dugina, V.B., 2012. Actin isoforms and reorganization of adhesion junctions in epithelial-to-mesenchymal transition of cervical carcinoma cells. Biochem. Mosc. 77, 1266–1276. https://doi.org/10.1134/S0006297912110053
Shaham, S., 2015. Glial Development and Function in the Nervous System of Caenorhabditis elegans. Cold Spring Harb. Perspect. Biol. 7, a020578. https://doi.org/10.1101/cshperspect.a020578
Sharma, R.K., 2014. Hypertelorism. Indian J. Plast. Surg. Off. Publ. Assoc. Plast. Surg. India 47, 284–292. https://doi.org/10.4103/0970-0358.146572
Shawlot, W., Deng, J.M., Fohn, L.E., Behringer, R.R., 1998. Restricted beta-galactosidase expression of a hygromycin-lacZ gene targeted to the beta-actin locus and embryonic lethality of beta-actin mutant mice. Transgenic Res. 7, 95–103. https://doi.org/10.1023/a:1008816308171
Shi, R., Kramer, D.A., Chen, B., Shen, K., 2021. A two-step actin polymerization mechanism drives dendrite branching. Neural Develop. 16, 3. https://doi.org/10.1186/s13064-021-00154-0
Simiczyjew, A., Mazur, A.J., Popow-Woźniak, A., Malicka-Błaszkiewicz, M., Nowak, D., 2014. Effect of overexpression of β- and γ-actin isoforms on actin cytoskeleton organization and migration of human colon cancer cells. Histochem. Cell Biol. 142, 307–322. https://doi.org/10.1007/s00418-014-1199-9
Singson, M.R.M.& A., 2010. Fertilization and the oocyte-to-embryo transition in C. elegans. BMB Rep. 43, 389–399.
Skogseid, I.M., Røsby, O., Konglund, A., Connelly, J.P., Nedregaard, B., Jablonski, G.E., Kvernmo, N., Stray-Pedersen, A., Glover, J.C., 2018. Dystonia-deafness syndrome caused by ACTB p.Arg183Trp heterozygosity shows striatal dopaminergic dysfunction and response to pallidal stimulation. J. Neurodev. Disord. 10, 17. https://doi.org/10.1186/s11689-018-9235-z
Smith, C.J., Watson, J.D., Spencer, W.C., O'Brien, T., Cha, B., Albeg, A., Treinin, M., Miller, D.M., 2010. Time-lapse imaging and cell-specific expression profiling reveal dynamic branching and molecular determinants of a multi-dendritic nociceptor in C. elegans. Dev. Biol. 345, 18–33. https://doi.org/10.1016/j.ydbio.2010.05.502

Sobo, J.M., Alagna, N.S., Sun, S.X., Wilson, K.L., Reddy, K.L., 2024. Lamins: The backbone of the nucleocytoskeleton interface. Curr. Opin. Cell Biol. 86, 102313. https://doi.org/10.1016/j.ceb.2023.102313

Sönnichsen, B., Koski, L.B., Walsh, A., Marschall, P., Neumann, B., Brehm, M., Alleaume, A.-M., Artelt, J., Bettencourt, P., Cassin, E., Hewitson, M., Holz, C., Khan, M., Lazik, S., Martin, C., Nitzsche, B., Ruer, M., Stamford, J., Winzi, M., Heinkel, R., Röder, M., Finell, J., Häntsch, H., Jones, S.J.M., Jones, M., Piano, F., Gunsalus, K.C., Oegema, K., Gönczy, P., Coulson, A., Hyman, A.A., Echeverri, C.J., 2005. Full-genome RNAi profiling of early embryogenesis in Caenorhabditis elegans. Nature 434, 462–469. https://doi.org/10.1038/nature03353

Stein, K.K., 2018. The C. elegans eggshell. WormBook 1–36. https://doi.org/10.1895/wormbook.1.179.1

Sternberg, P.W., Van Auken, K., Wang, Q., Wright, A., Yook, K., Zarowiecki, M., Arnaboldi, V., Becerra, A., Brown, S., Cain, S., Chan, J., Chen, W.J., Cho, J., Davis, P., Diamantakis, S., Dyer, S., Grigoriadis, D., Grove, C.A., Harris, T., Howe, K., Kishore, R., Lee, R., Longden, I., Luypaert, M., Müller, H.-M., Nuin, P., Quinton-Tulloch, M., Raciti, D., Schedl, T., Schindelman, G., Stein, L., 2024. WormBase 2024: status and transitioning to Alliance infrastructure. Genetics 227, iyae050. https://doi.org/10.1093/genetics/iyae050

Stone, S., Shaw, J.E., 1993. A *Caenorhabditis elegans act-4::lacZ* fusion: use as a transformation marker and analysis of tissue-specific expression. Gene 131, 167–173. https://doi.org/10.1016/0378-1119(93)90290-J

Straub F. 1942. Actin. New York, Budapest: S. Karger Basel, R. Gergely

Straub F. 1943. Actin II. New York, Budapest: S. Karger Basel, R. Gergely

Sulston, J.E., Schierenberg, E., White, J.G., Thomson, J.N., 1983. The embryonic cell lineage of the nematode Caenorhabditis elegans. Dev. Biol. 100, 64–119. https://doi.org/10.1016/0012-1606(83)90201-4

Sundby, L.J., Southern, W.M., Hawbaker, K.M., Trujillo, J.M., Perrin, B.J., Ervasti, J.M., 2022. Nucleotide- and Protein-Dependent Functions of Actg1. Mol. Biol. Cell 33, ar77. https://doi.org/10.1091/mbc.E22-02-0054

Sundby, L.J., Southern, W.M., Sun, J., Patrinostro, X., Zhang, W., Yong, J., Ervasti, J.M., 2024. Deletion of exons 2 and 3 from Actb and cell immortalization lead to widespread, β-actin independent alterations in gene expression associated with cell cycle control. Eur. J. Cell Biol. 103, 151397. https://doi.org/10.1016/j.ejcb.2024.151397

Svanström, A., Grantham, J., 2016. The molecular chaperone CCT modulates the activity of the actin filament severing and capping protein gelsolin in vitro. Cell Stress Chaperones 21, 55–62. https://doi.org/10.1007/s12192-015-0637-5

Svitkina, T.M., 2020. Actin Cell Cortex: Structure and Molecular Organization. Trends Cell Biol. 30, 556–565. https://doi.org/10.1016/j.tcb.2020.03.005

Syamaladevi, D.P., Spudich, J.A., Sowdhamini, R., 2012. Structural and Functional Insights on the Myosin Superfamily. Bioinforma. Biol. Insights 6, 11–21. https://doi.org/10.4137/BBI.S8451

Takenawa, T., Suetsugu, S., 2007. The WASP–WAVE protein network: connecting the membrane to the cytoskeleton. Nat. Rev. Mol. Cell Biol. 8, 37–48. https://doi.org/10.1038/nrm2069

Taylor, S.R., Santpere, G., Weinreb, A., Barrett, A., Reilly, M.B., Xu, C., Varol, E., Oikonomou, P., Glenwinkel, L., McWhirter, R., Poff, A., Basavaraju, M., Rafi, I., Yemini, E., Cook, S.J., Abrams, A., Vidal, B., Cros, C., Tavazoie, S., Sestan, N., Hammarlund, M., Hobert, O., Miller, D.M., 2021. Molecular topography of an entire nervous system. Cell 184, 4329-4347.e23. https://doi.org/10.1016/j.cell.2021.06.023

Terman, J.R., Kashina, A., 2013. Post-translational modification and regulation of actin. Curr. Opin. Cell Biol., Cell architecture 25, 30–38. https://doi.org/10.1016/j.ceb.2012.10.009

Terry, S.J., Donà, F., Osenberg, P., Carlton, J.G., Eggert, U.S., 2018. Capping protein regulates actin dynamics during cytokinetic midbody maturation. Proc. Natl. Acad. Sci. 115, 2138–2143. https://doi.org/10.1073/pnas.1722281115

The human cell in actin filaments - The Human Protein Atlas. Thul PJ et al. (2017) “A subcellular map of the human proteome” Science 356 (6340): aal332. https://www.proteinatlas.org/humanproteome/subcellular/actin+filaments

Tondeleir, D., Lambrechts, A., Müller, M., Jonckheere, V., Doll, T., Vandamme, D., Bakkali, K., Waterschoot, D., Lemaistre, M., Debeir, O., Decaestecker, C., Hinz, B., Staes, A., Timmerman, E., Colaert, N., Gevaert, K., Vandekerckhove, J., Ampe, C., 2012. Cells lacking β-actin are genetically reprogrammed and maintain conditional migratory capacity. Mol. Cell. Proteomics MCP 11, 255–271. https://doi.org/10.1074/mcp.M111.015099

Tsujimoto, T., Ou, Y., Suzuki, M., Murata, Y., Inubushi, T., Nagata, M., Ishihara, Y., Yonei, A., Miyashita, Y., Asano, Y., Sakai, N., Sakata, Y., Ogino, H., Yamashiro, T., Kurosaka, H. 2024. Compromised actin dynamics underlie the orofacial cleft in Baraitser-Winter Cerebrofrontofacial Syndrome with a variant in *ACTB*. *bioRxiv.04.04.587685; doi: https://doi.org/10.1101/2024.04.04.587685*

Vallin, J., Grantham, J., 2019. The role of the molecular chaperone CCT in protein folding and mediation of cytoskeleton-associated processes: implications for cancer cell biology. Cell Stress Chaperones 24, 17–27. https://doi.org/10.1007/s12192-018-0949-3

van der Voet, M., Berends, C.W.H., Perreault, A., Nguyen-Ngoc, T., Gönczy, P., Vidal, M., Boxem, M., van den Heuvel, S., 2009. NuMA-related LIN-5, ASPM-1, calmodulin and dynein promote meiotic spindle rotation independently of cortical LIN-5/GPR/Gα. Nat. Cell Biol. 11, 269–277. https://doi.org/10.1038/ncb1834

van Zwam, M.C., Dhar, A., Bosman, W., van Straaten, W., Weijers, S., Seta, E., Joosten, B., van Haren, J., Palani, S., van den Dries, K., 2024. IntAct: A nondisruptive internal tagging strategy to study the organization and function of actin isoforms. PLoS Biol. 22, e3002551. https://doi.org/10.1371/journal.pbio.3002551

Vandekerckhove, J., Weber, K., 1981. Actin Typing on Total Cellular Extracts. Eur. J. Biochem. 113, 595–603. https://doi.org/10.1111/j.1432-1033.1981.tb05104.x

Vang, S., Corydon, T.J., Børglum, A.D., Scott, M.D., Frydman, J., Mogensen, J., Gregersen, N., Bross, P., 2005. Actin mutations in hypertrophic and dilated cardiomyopathy cause inefficient protein folding and perturbed filament formation. FEBS J. 272, 2037–2049. https://doi.org/10.1111/j.1742-4658.2005.04630.x

Vanslembrouck, B., Ampe, C., van Hengel, J., 2020. Time for rethinking the different β-actin transgenic mouse models? Cytoskeleton 77, 527–543. https://doi.org/10.1002/cm.21647

Varland, S., Vandekerckhove, J., Drazic, A., 2019. Actin Post-translational Modifications: The Cinderella of Cytoskeletal Control. Trends Biochem. Sci. 44, 502–516. https://doi.org/10.1016/j.tibs.2018.11.010

Vedula, P., Kashina, A., 2018. The makings of the “actin code”: regulation of actin’s biological function at the amino acid and nucleotide level. J. Cell Sci. 131, jcs215509. https://doi.org/10.1242/jcs.215509

Vedula, P., Kurosaka, S., Leu, N.A., Wolf, Y.I., Shabalina, S.A., Wang, J., Sterling, S., Dong, D.W., Kashina, A., 2017. Diverse functions of homologous actin isoforms are defined by their nucleotide, rather than their amino acid sequence [WWW Document]. eLife. https://doi.org/10.7554/eLife.31661

Velarde, N., Gunsalus, K.C., Piano, F., 2007. Diverse roles of actin in C. elegans early embryogenesis. BMC Dev. Biol. 7, 142. https://doi.org/10.1186/1471-213X-7-142

Velle, K.B., Swafford, A.J.M., Garner, E., Fritz-Laylin, L.K., 2024. Actin network evolution as a key driver of eukaryotic diversification. J. Cell Sci. 137, jcs261660. https://doi.org/10.1242/jcs.261660

Verloes, A., Di Donato, N., Masliah-Planchon, J., Jongmans, M., Abdul-Raman, O.A., Albrecht, B., Allanson, J., Brunner, H., Bertola, D., Chassaing, N., David, A., Devriendt, K., Eftekhari, P., Drouin-Garraud, V., Faravelli, F., Faivre, L., Giuliano, F., Guion Almeida, L., Juncos, J., Kempers, M., Eker, H.K., Lacombe, D., Lin, A., Mancini, G., Melis, D., Lourenço, C.M., Siu, V.M., Morin, G., Nezarati, M., Nowaczyk, M.J.M., Ramer, J.C., Osimani, S., Philip, N., Pierpont, M.E., Procaccio, V., Roseli, Z.-S., Rossi, M., Rusu, C., Sznajer, Y., Templin, L., Uliana, V., Klaus, M., Van Bon, B., Van Ravenswaaij, C., Wainer, B., Fry, A.E., Rump, A., Hoischen, A., Drunat, S.,

Rivière, J.-B., Dobyns, W.B., Pilz, D.T., 2015. Baraitser-Winter cerebrofrontofacial syndrome: delineation of the spectrum in 42 cases. Eur. J. Hum. Genet. EJHG 23, 292–301. https://doi.org/10.1038/ejhg.2014.95

Verloes, A., Drunat, S., Pilz, D., Di Donato, N., 1993. Baraitser-Winter Cerebrofrontofacial Syndrome, in: Adam, M.P., Feldman, J., Mirzaa, G.M., Pagon, R.A., Wallace, S.E., Amemiya, A. (Eds.), GeneReviews®. University of Washington, Seattle, Seattle (WA).

Verloes A, Drunat S, Pilz D, et al. Baraitser-Winter Cerebrofrontofacial Syndrome. 2015 Nov 19 [Updated 2022 Mar 24]. In: Adam MP, Feldman J, Mirzaa GM, et al., editors. GeneReviews® [Internet]. Seattle (WA): University of Washington, Seattle; 1993-2024. Available from: https://www.ncbi.nlm.nih.gov/books/NBK327153/

Vuong-Brender, T.T.K., Ben Amar, M., Pontabry, J., Labouesse, M., 2017. The interplay of stiffness and force anisotropies drives embryo elongation. eLife 6, e23866. https://doi.org/10.7554/eLife.23866

Vuong-Brender, T.T.K., Yang, X., Labouesse, M., 2016. *C. elegans* Embryonic Morphogenesis, in: Wassarman, P.M. (Ed.), Current Topics in Developmental Biology, Essays on Developmental Biology, Part A. Academic Press, pp. 597–616. https://doi.org/10.1016/bs.ctdb.2015.11.012

Wagner, J., Carvajal, A.I., Bracher, A., Beck, F., Wan, W., Bohn, S., Körner, R., Baumeister, W., Fernandez-Busnadiego, R., Hartl, F.U., 2024. Visualizing chaperonin function in situ by cryo-electron tomography. Nature 633, 459–464. https://doi.org/10.1038/s41586-024-07843-w

Walck-Shannon, E., Hardin, J., 2016. Another morphogenetic movement on the map: Charting dorsal intercalation in C. elegans. Worm 5, e1176664. https://doi.org/10.1080/21624054.2016.1176664

Welker, J.M., Serobyan, V., Zaker Esfahani, E., Stainier, D.Y.R., 2023. Partial sequence identity in a 25-nucleotide long element is sufficient for transcriptional adaptation in the Caenorhabditis elegans act-5/act-3 model. PLoS Genet. 19, e1010806. https://doi.org/10.1371/journal.pgen.1010806

White, J.G., Southgate, E., Thomson, J.N., Brenner, S., 1986. The structure of the nervous system of the nematode Caenorhabditis elegans. Philos. Trans. R. Soc. Lond. B. Biol. Sci. 314, 1–340. https://doi.org/10.1098/rstb.1986.0056

Wickstead, B., Gull, K., 2011. The evolution of the cytoskeleton. J. Cell Biol. 194, 513–525. https://doi.org/10.1083/jcb.201102065

Wightman, B., Ha, I., Ruvkun, G., 1993. Posttranscriptional regulation of the heterochronic gene *lin-14* by *lin-4* mediates temporal pattern formation in C. elegans. Cell 75, 855–862. https://doi.org/10.1016/0092-8674(93)90530-4

Willis, J.H., Munro, E., Lyczak, R., Bowerman, B., 2006. Conditional Dominant Mutations in the Caenorhabditis elegans Gene act-2 Identify Cytoplasmic and Muscle Roles for a Redundant Actin Isoform. Mol. Biol. Cell 17, 1051–1064. https://doi.org/10.1091/mbc.e05-09-0886

Wioland, H., Jegou, A., Romet-Lemonne, G., 2019. Torsional stress generated by ADF/cofilin on cross-linked actin filaments boosts their severing. Proc. Natl. Acad. Sci. 116, 2595–2602. https://doi.org/10.1073/pnas.1812053116

Withee, J., Galligan, B., Hawkins, N., Garriga, G., 2004. Caenorhabditis elegans WASP and Ena/VASP Proteins Play Compensatory Roles in Morphogenesis and Neuronal Cell Migration. Genetics 167, 1165–1176. https://doi.org/10.1534/genetics.103.025676

Wood., W.B., 1988. *The Nematode Caenorhabditis elegans*. Appendix “Genetics”. Cold Spring Harbor Laboratory Press, Cold Spring Harbor, New York.

Xiong, H., Mohler, W.A., Soto, M.C., 2011. The branched actin nucleator Arp2/3 promotes nuclear migrations and cell polarity in the C. elegans zygote. Dev. Biol. 357, 356–369. https://doi.org/10.1016/j.ydbio.2011.07.008

Yamamoto, K., Kimura, A., 2017. An asymmetric attraction model for the diversity and robustness of cell arrangement in nematodes. Development 144, 4437–4449. https://doi.org/10.1242/dev.154609

Yang, X., Ferraro, T., Molnar, K., Pontabry, J., Malanda, S-R., Maghelli, N., Royer, L., Grill, S W., Myers, G., Grigolon, S., Labouesse, M. 2024. Repeated extrinsic and anisotropic mechanical inputs

promote polarized adherens junction elongation. bioRxiv.07.09.602689; doi: https://doi.org/10.1101/2024.07.09.602689

Yaniv, K., Fainsod, A., Kalcheim, C., Yisraeli, J.K., 2003. The RNA-binding protein Vg1 RBP is required for cell migration during early neural development. Development 130, 5649–5661. https://doi.org/10.1242/dev.00810

Yemini, E., Lin, A., Nejatbakhsh, A., Varol, E., Sun, R., Mena, G.E., Samuel, A.D.T., Paninski, L., Venkatachalam, V., Hobert, O., 2021. NeuroPAL: A Multicolor Atlas for Whole-Brain Neuronal Identification in C. elegans. Cell 184, 272-288.e11. https://doi.org/10.1016/j.cell.2020.12.012

Zech, M., Jech, R., Wagner, M., Mantel, T., Boesch, S., Nocker, M., Jochim, A., Berutti, R., Havránková, P., Fečíková, A., Kemlink, D., Roth, J., Strom, T.M., Poewe, W., Růžička, E., Haslinger, B., Winkelmann, J., 2017. Molecular diversity of combined and complex dystonia: insights from diagnostic exome sequencing. neurogenetics 18, 195–205. https://doi.org/10.1007/s10048-017-0521-9

Zhang, H., Landmann, F., Zahreddine, H., Rodriguez, D., Koch, M., Labouesse, M., 2011. A tension-induced mechanotransduction pathway promotes epithelial morphogenesis. Nature 471, 99–103. https://doi.org/10.1038/nature09765

Zhang, P., Medwig-Kinney, T.N., Goldstein, B., 2023. Architecture of the cortical actomyosin network driving apical constriction in C. elegans. J. Cell Biol. 222, e202302102. https://doi.org/10.1083/jcb.202302102

Zhong, W., Sternberg, P.W., 2006. Genome-Wide Prediction of C. elegans Genetic Interactions. Science 311, 1481–1484. https://doi.org/10.1126/science.1123287

Zuela, N., Gruenbaum, Y., 2016. Intermediate Filaments in *Caenorhabditis elegans*, in: Omary, M.B., Liem, R.K.H. (Eds.), Methods in Enzymology, Intermediate Filament Proteins. Academic Press, pp. 661–679. https://doi.org/10.1016/bs.mie.2015.09.020

Zumdieck, A., Kruse, K., Bringmann, H., Hyman, A.A., Jülicher, F., 2007. Stress Generation and Filament Turnover during Actin Ring Constriction. PLoS ONE 2, e696. https://doi.org/10.1371/journal.pone.0000696

Résumé en français

Introduction

L'actine

L'actine fait partie du cytosquelette, un réseau complexe de filaments à l'intérieur de chaque cellule dans les trois domaines de la vie (Eubactéries, Archées et Eucaryotes) (Wickstead and Gull, 2011). L'actine est une protéine essentielle, ubiquitaire et fortement conservée (Pollard and Goldman, 2018). Celle-ci est produite sous forme monomérique qui a la capacité de polymériser en filaments. Les filaments d'actine forment des réseaux hautement dynamiques régulés par de nombreuses « Protéines se Liant à l'Actine » (PLA) qui peuvent catalyser ou empêcher la polymérisation de filaments. Les PLA peuvent également dépolymériser les filaments, les associer ou permettre la formation de « branches » sur un filament préexistant. Grâce à cela, les réseaux d'actine ont la capacité de s'adapter aux signaux mécaniques et/ou chimiques que la cellule reçoit, permettant la formation de structures spécialisées dans certaines fonctions (Blanchoin et al., 2014). En effet, de façon non exhaustive, l'actine est impliquée dans la contraction musculaire, dans le maintien de la forme de la cellule, de sa division, dans son interaction avec l'environnement, mais est également nécessaire lors de la réparation de l'ADN et dans le maintien de l'intégrité génomique (Blanchoin et al., 2014; Viita and Vartiainen, 2017).

Chez la plupart des eucaryotes, l'actine n'est pas produite par un seul gène. Chez l'Homme, six isotypes d'actine sont produits. Bien que ces protéines soient très similaires dans leurs séquences et structures, les isotypes d'actine ne sont pas exprimés au même niveau dans différents types cellulaires et même au sein de différentes structures subcellulaires. Par conséquent, ces isotypes ont des rôles différents. Quatre isotypes Humains sont dits musculaires, car presque exclusivement présents dans certains types musculaires. Parmi eux, *ACTC1* est principalement exprimé dans les muscles cardiaques, *ACTA1* dans les muscles squelettiques, et *ACTA2* ainsi que *ACTG1* dans le muscles lisses. Les deux gènes restants : *ACTB* et *ACTG1* sont appelées cytoplasmiques, car exprimées de façon ubiquitaire dans tous les types cellulaires (Parker et al., 2020).

Les Actinopathies Non-Musculaires

De par la pléiotropie de l'actine, il n'est pas surprenant que celle-ci soit associée à des maladies lorsqu'elle est défectueuse. Les travaux de ma thèse se sont concentrés sur la compréhension d'un ensemble de maladies appelées Actinopathies Non-Musculaires (ANMs), causées par des variants pathologiques des gènes ACTB et ACTG1 (Di Donato et al., 2024). Les ANMs, sont causées majoritairement par des mutations ponctuelles de substitution faux-sens mais également par des mutations non-sens (Di Donato et al., 2024). Les ANMs sont des maladies rares ; seulement 290 patients associés à 157 variants uniques ont été décrits (Di Donato et al., 2024). Les patients ont une variabilité clinique élevée selon les différents variants, avec des symptômes allant de bénins à sévères pouvant mener à la mort prénatale de l'individu. De façon non-exhaustive, les symptômes peuvent inclure des retards neurodéveloppementaux, de la déficience intellectuelle, de l'épilepsie, de la surdité, ou des malformations faciales. C'est pourquoi, il est aujourd'hui difficile de prédire la sévérité et les conséquences de variants d'actine cytoplasmique.

Pour tenter de déchiffrer les mécanismes physiopathologiques de variants causant des ANMs, de précédentes études ont majoritairement utilisé des cultures cellulaires *in vitro*, des protéines purifiées pour analyses biochimiques, ainsi que des études biophysiques ou de la modélisation *in silico*. Aujourd'hui, une seule étude utilisant des modèles animaux modélisant un variant (S348L) a été publiée (Tsujimoto et al., 2024), en plus de la mention d'un modèle murin non viable récapitulant le variant T120I (Di Donato et al., 2024) et d'études concernant des mutations perte de fonction d'actine cytoplasmique (Belyantseva et al., 2009; Vedula et al., 2017). Il y a donc un manque de connaissances concernant l'effet de mutations causant des ANMs dans un organisme modèle, où l'actine est soumise à différents environnements et contextes cellulaires difficilement reproduits *in vitro*.

Pour combler cette lacune, le laboratoire d'Anne-Cécile Reymann a reproduit 9 variants faux-sens pathologiques associés à différentes ANMs de sévérités variables dans le locus endogène codant pour l'actine *act-2* du nématode *Caenorhabditis elegans* (*C. elegans*) (**Figure 1**). Le gène *act-2* code pour l'un des 5 isotypes d'actine de *C. elegans* et est cytoplasmique (Willis et al., 2006). De plus, ACT-2 a une séquence protéique 98% similaire à ACTB et 97% à ACTG1, faisant de lui un candidat de choix pour y reproduire des variants associés à des ANM.

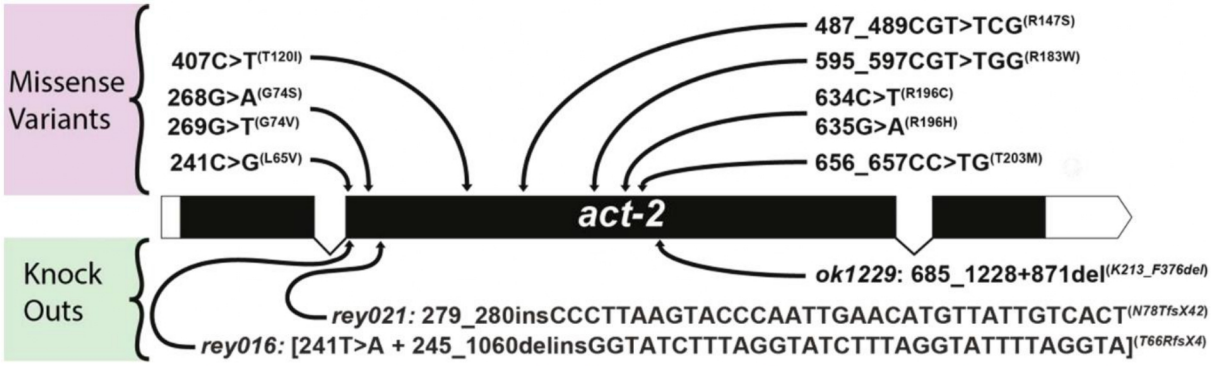

Figure 1 : Représentation schématique du gène *act-2* et des variations faux-sens obtenues grâce à CRISPR-Cas9. (Adapté de http://wormweb.org/exonintron). Trois allèles non-sens sont également annotés: *rey016*, *rey021* and *ok1229* (Willis et al., 2006). Il est à noter que les positions de variations protéiques sont données avec la nomenclature Humaine des gènes ACTB et ACTG1. Il faut ainsi considérer un acide aminé de plus pour la variation avec la nomenclature de *C. elegans*. Figure et légende extraite de Hecquet et al., 2024, Biorχiv.

Mes travaux de thèse se sont appuyés sur l'exceptionnelle reproductibilité et transparence de *C. elegans* afin d'effectuer une caractérisation multi-échelle et comparative de ces souches. La question principale de mon étude était de savoir si *C. elegans* modélise fidèlement les ANM. Cela implique les sous-questions suivantes : Ces variants humains sont-ils pathologiques chez *C. elegans* ? Et si oui, quels sont leurs impacts ? Deuxièmement, pouvons-nous identifier certains mécanismes physiopathologiques de ces variants ? Ceci permettrait une meilleure compréhension des conséquences moléculaires et fonctionnelles des variants, ainsi qu'une compréhension plus fondamentale des rôles spécifiques de certains acides aminés de l'actine. Enfin, nous nous sommes demandé si les modèles *C. elegans* d'ANM pouvaient aider au pronostic médical, notamment dans le cas d'un variant de signification inconnue identifié pendant la grossesse.

Résultats

Au cours de ma thèse, j'ai étudié 9 variants faux-sens ainsi que des mutations perte de fonction (PoF) du gène *act-2*.

J'ai pu observer que ces souches ont une viabilité variable selon le variant associé. En effet, nous avons observé que les animaux possédants les variants R147S et T203M à l'état homozygote se développent en adultes incapables de produire une descendance viable. Les animaux possédant le variant G74V ne produisent aucune progéniture viable, même lorsque cette mutation est présente à l'état hétérozygote. Les autres variants (L65V, G74S, T120I, R183W, R196C, R196H et PoF) sont viables aussi bien à l'état hétérozygote qu'homozygote. Ces résultats démontrent que ces variants identifiés chez l'Homme sont également pathologiques chez *C. elegans*.

Après cette observation initiale, j'ai étudié à différentes échelles certains aspects du développement de *C. elegans* afin de décrire les impacts qu'ont chaque variant. A l'échelle de l'organisme, j'ai mesuré le nombre d'œufs pondus et d'œufs éclos au cours de la vie de *C. elegans* pour chaque souche. J'ai notamment observé une importante baisse de fécondité associée à une hausse de la léthalité embryonnaire pour les variants R147S et T203M. Celle-ci est plus sévère que pour les variants PoF, indiquant une possible toxicité de ces variants au sein de la cellule. Les autres variants sont tous associés à une mortalité embryonnaire accrue, excepté pour les variants G74S et R183W qui semblent non-affectés.

A l'échelle de l'organisme, j'ai également caractérisé la motilité des animaux, ainsi que l'organisation de leur système nerveux et de leurs gonades. Ensuite, j'ai cherché à déterminer la cause de la mortalité embryonnaire que j'ai pu observer. Pour cela, j'ai étudié le développement embryonnaire d'animaux mutants. J'ai pu observer la mort des embryons à différentes étape précises de leur développement ; lors de la première division cellulaire, de la gastrulation, de la fermeture ventrale et de l'élongation. De façon intéressante, chacune de ces étapes est actine-dépendante et ces arrêts du développement ont une fréquence différente pour chaque variant. Comme les rôles de l'actine à l'échelle cellulaire sont hautement étudiés lors de ces processus (Eweis and Plastino, 2020; Lardennois et al., 2019; Roh-Johnson and Goldstein, 2009; Vuong-Brender et al., 2016), ils peuvent révéler des indices quant aux

possibles effets moléculaires dérégulés pour ces variants d'*act-2*, ce dont je discute dans ma thèse.

J'ai ensuite utilisé des PLA, ainsi qu'une sonde se liant à l'actine, couplées à des fluorophores pour observer à l'échelle moléculaire la dynamique *in vivo* du réseau d'actine du zygote jusqu'à sa première division. Ceci n'a pas révélé de défaut majeur dans l'organisation du réseau d'actine dans de nombreux embryons précoces. Néanmoins, j'ai pu observer des phénotypes normalement absents comme des défauts de cytocinèse, de méiose, et la formation de blebs – excroissances transitoires protrusives et anormales du cortex et de la membrane plasmique (PALUCH AND RAZ, 2013). Ces phénotypes sont présents à différentes fréquences chez les variants, indiquant encore une fois des différences spécifiques à chaque variant d'actine.

Enfin, j'ai cherché à utiliser l'ensemble de mes résultats afin de proposer une classification des variants que j'ai étudié. Pour cela, j'ai utilisé une analyse en composantes principales (ACP) (**FIGURE 2**) en utilisant mes résultats comme variables. Cette représentation m'a permis de grouper les variants en différentes classes selon la sévérité de leurs phénotypes. Cette classification se rapproche de la classification Humaine et sous-entend que *C. elegans* est un bon modèle pour l'étude des ANMs. L'ensemble de ces résultats forment un article actuellement en cours de révision dans le journal iScience.

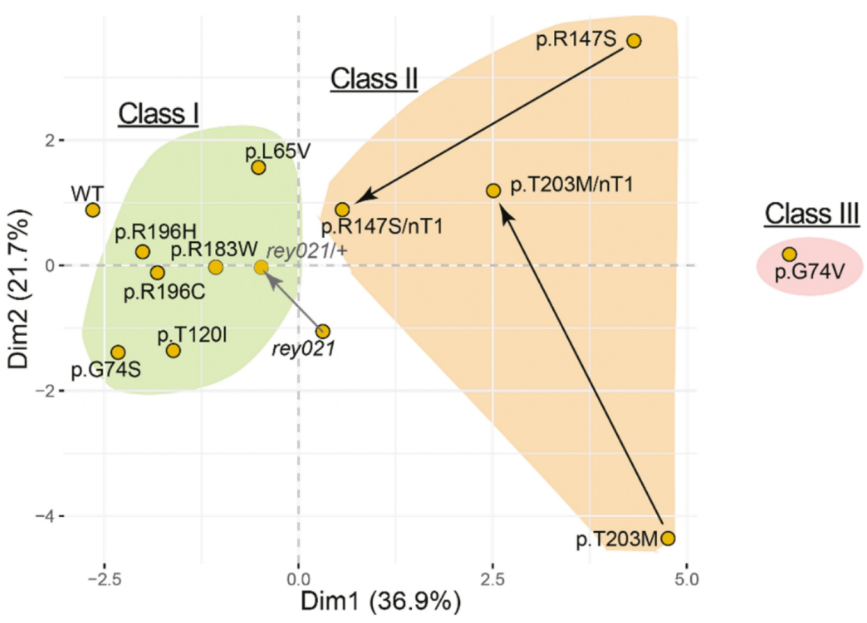

Figure 2 : Analyse en Composantes Principales des variants étudiés. « p.G74V » a été rajouté manuellement car nous n'avons pas pu obtenir de données le concernant de par sa létalité. Les flèches relient les homozygotes à leurs hétérozygotes respectifs. Figure et légende extraite de Hecquet et al., 2024, Biorχiv.

Comme les ANMs sont associées à des problèmes neurodéveloppementaux, nous nous sommes demandé si les variants d'actine pouvaient altérer l'expression de rapporteurs neuronaux chez *C. elegans*, ce qui pourrait sous-entendre des défauts neurodéveloppementaux. Pour cela, j'ai quantifié les valeurs d'intensité des trois « couleurs » exprimées dans NeuroPAL (mTagBFP2 comme « bleu », CyOFP1 comme « vert », et mNeptune2.5 comme « rouge »). Le transgène NeuroPAL comprend 41 rapporteurs neuronaux associés à trois fluorophores, en plus d'un rapporteur panneural. Ainsi, plusieurs gènes expriment le même fluorophore (YEMINI ET AL., 2021). Néanmoins, chaque neurone exprime une combinaison invariante de rapporteurs, permettant d'identifier et d'extraire les intensités d'expressions des rapporteurs de presque tous les neurones de *C. elegans*. Grâce à cette méthode, j'ai pu observer que les variants L65V et R196C ne modifie pas le niveau d'expression de rapporteurs neuronaux en comparaison avec la souche de référence. A l'inverse, j'ai pu observer que les variants T120I et R196H altèrent largement le patron d'expression de marqueurs neuronaux, et notamment pour les motoneurones. De façon intéressante, la comparaison des résultats de ces deux variants entre eux ne montre aucune différence, ce qui sous-entend que ces deux variants modifient le patron d'expression des marqueurs neuronaux de la même façon et que celle-ci ne soit pas faite de manière aléatoire.

Conclusion :

En conclusion, j'ai réalisé une caractérisation de 9 variants d'actine cytoplasmique identifiés chez l'Homme en utilisant l'organisme modèle *C. elegans*. La viabilité générale des souches corrèle avec la sévérité des patients humains, démontrant que *C. elegans* modélise fidèlement les ANMs. Mes résultats montrent la présence de défauts à différentes échelles ; moléculaire, cellulaire et tissulaire, présents à fréquence variable selon le variant étudié. Cela nous donne des pistes quant aux mécanismes pathophysiologiques de ceux-ci. Nos résultats concernant le variant R196H corrèlent avec la récente étude proposant que cette variation impacte l'association de l'actine avec le complexe Arp2/3, une PLA permettant la formation de branches sur le filament d'actine (Greve and Mannstein, 2024, Biorxiv). De par mes résultats, je fais l'hypothèse que le variant R147S pourrait impacter la fonction du complexe chaperon, que les variants T203M et T120I impactent la contractilité du réseau d'actomyosine via différents mécanismes, et que le variant L65V impacte la régulation de l'actine par la calmoduline. Enfin, notre analyse comparative a permis la création d'une ACP qui pourrait permettre d'aider la prédiction de la sévérité clinique de variants à signification inconnue identifiés chez l'Homme.

Références

Belyantseva, I.A., Perrin, B.J., Sonnemann, K.J., Zhu, M., Stepanyan, R., McGee, J., Frolenkov, G.I., Walsh, E.J., Friderici, K.H., Friedman, T.B., Ervasti, J.M., 2009. γ-Actin is required for cytoskeletal maintenance but not development. Proc. Natl. Acad. Sci. 106, 9703–9708. https://doi.org/10.1073/pnas.0900221106

Blanchoin, L., Boujemaa-Paterski, R., Sykes, C., Plastino, J., 2014. Actin Dynamics, Architecture, and Mechanics in Cell Motility. Physiol. Rev. 94, 235–263. https://doi.org/10.1152/physrev.00018.2013

Di Donato, N., NMA Consortium., Thom, A., Rump, A., Greve, J N., Kropp, M., Cadiñanos, J., Calabro, S., Cathey, S., Chung, B., Cope, H., Costales, M., Cuvertino, S., Dinkel, P., Erripi, K., Fry, A E., Garavelli, L., Guan, K., Hoffjan, S., Janzarik, W G., Koenig, M., Kreimer, I., Kuenzel, K., Mancini, G., Purificacion Marin-Reina, Meinhardt, A., Niehaus, I., Pilz, D., Ricca, I., Santos Simarro, F., Schrock, E., Marquardt, A., Taft, M H., Tezcan, K., Thunström, S., Verhagen, J., Verloes, A., Wollnik, B., Krawitz, P., Hsieh, T-C., Zeef, L., Seifert, M., Heide, M., Lawrence, C B., Roberts, N., Manstein, D., Woolf, A S., Banka, S. 2024. Genomic and biological panoramas of non-muscle actinopathies. medRxiv.08.21.24310320; doi: https://doi.org/10.1101/2024.08.21.24310320

Eweis, D.S., Plastino, J., 2020. Roles of Actin in the Morphogenesis of the Early Caenorhabditis elegans Embryo. Int. J. Mol. Sci. 21, 3652. https://doi.org/10.3390/ijms21103652

Greve, J N., Manstein D J. 2024. Baraitser–Winter Syndrome Hotspot Mutation R196H in Cytoskeletal β–actin Reduces F–actin Stability and Perturbs Interaction with the Arp2/3 Complex. bioRxiv.03.20.585892; doi: https://doi.org/10.1101/2024.03.20.585892

Hecquet, T., Arbogast, N., Suhner, D., Goetz, A., Amann, G., Yürekli, S., Marangoni, F., Greve, J N., Di Donato, N., Reymann, A-C. 2024. Classification of human actin pathological variants using C. elegans CRISPR-generated models. bioRxiv.07.22.604239; doi: https://doi.org/10.1101/2024.07.22.604239

Lardennois, A., Pásti, G., Ferraro, T., Llense, F., Mahou, P., Pontabry, J., Rodriguez, D., Kim, S., Ono, S., Beaurepaire, E., Gally, C., Labouesse, M., 2019. An actin-based viscoplastic lock ensures progressive body-axis elongation. Nature 573, 266–270. https://doi.org/10.1038/s41586-019-1509-4

Paluch, E.K., Raz, E., 2013. The role and regulation of blebs in cell migration. Curr. Opin. Cell Biol. 25, 582–590. https://doi.org/10.1016/j.ceb.2013.05.005

Parker, F., Baboolal, T.G., Peckham, M., 2020. Actin Mutations and Their Role in Disease. Int. J. Mol. Sci. 21, 3371. https://doi.org/10.3390/ijms21093371

Pollard, T.D., Goldman, R.D., 2018. Overview of the Cytoskeleton from an Evolutionary Perspective. Cold Spring Harb. Perspect. Biol. 10, a030288. https://doi.org/10.1101/cshperspect.a030288

Roh-Johnson, M., Goldstein, B., 2009. In vivo roles for Arp2/3 in cortical actin organization during C. elegans gastrulation. J. Cell Sci. 122, 3983. https://doi.org/10.1242/jcs.057562

Tsujimoto, T., Ou, Y., Suzuki, M., Murata, Y., Inubushi, T., Nagata, M., Ishihara, Y., Yonei, A., Miyashita, Y., Asano, Y., Sakai, N., Sakata, Y., Ogino, H., Yamashiro, T., Kurosaka, H. 2024. Compromised actin dynamics underlie the orofacial cleft in Baraitser-Winter Cerebrofrontofacial Syndrome with a variant in ACTB. bioRxiv.04.04.587685; doi: https://doi.org/10.1101/2024.04.04.587685

Vedula, P., Kurosaka, S., Leu, N.A., Wolf, Y.I., Shabalina, S.A., Wang, J., Sterling, S., Dong, D.W., Kashina, A., 2017. Diverse functions of homologous actin isoforms are defined by their nucleotide, rather than their amino acid sequence. eLife 6, e31661. https://doi.org/10.7554/eLife.31661

Viita, T., Vartiainen, M.K., 2017. From Cytoskeleton to Gene Expression: Actin in the Nucleus, in: Jockusch, B.M. (Ed.), The Actin Cytoskeleton. Springer International Publishing, Cham, pp. 311–329. https://doi.org/10.1007/164_2016_27

Vuong-Brender, T.T.K., Yang, X., Labouesse, M., 2016. C. elegans Embryonic Morphogenesis. Curr. Top. Dev. Biol. 116, 597–616. https://doi.org/10.1016/bs.ctdb.2015.11.012

Wickstead, B., Gull, K., 2011. The evolution of the cytoskeleton. J. Cell Biol. 194, 513–525. https://doi.org/10.1083/jcb.201102065

Willis, J.H., Munro, E., Lyczak, R., Bowerman, B., 2006. Conditional Dominant Mutations in the Caenorhabditis elegans Gene act-2 Identify Cytoplasmic and Muscle Roles for a Redundant Actin Isoform. Mol. Biol. Cell 17, 1051–1064. https://doi.org/10.1091/mbc.e05-09-0886

Yemini, E., Lin, A., Nejatbakhsh, A., Varol, E., Sun, R., Mena, G.E., Samuel, A.D.T., Paninski, L., Venkatachalam, V., Hobert, O., 2021. NeuroPAL: A Multicolor Atlas for Whole-Brain Neuronal Identification in C. elegans. Cell 184, 272-288.e11. https://doi.org/10.1016/j.cell.2020.12.012

Université de Strasbourg

Théo HECQUET

École Doctorale des Sciences de la Vie et de la Santé STRASBOURG

Multiscale characterization of *Caenorhabditis elegans* models of Human cytoplasmic actin variants hints at their pathophysiological mechanisms

Résumé :

L'actine est une protéine qui s'auto-assemble en réseaux dynamiques essentiels à de nombreux processus physiologiques tels que la migration ou la division cellulaire. Des mutations ponctuelles *de novo*, ainsi que des mutations perte de fonction dans les gènes codant pour l'actine cytoplasmique humaine ACTB et ACTG1 mènent à des maladies rares appelées Actinopathies Non Musculaires (ANM). Les ANM provoquent un large éventail de symptômes allant de légers à graves, incluant des malformations faciales, un déficit intellectuel et de la surdité.

À ce jour, aucune corrélation définitive entre le génotype des ANM et le phénotype observé n'a été établie. De plus, les mécanismes fonctionnels de ces variants d'actine restent vagues. Pour combler cette lacune, nous avons utilisé *Caenorhabditis elegans*. Ce nématode permet d'accéder facilement à toutes les échelles biologiques, de la condition physique générale de l'animal à son développement stéréotypé jusqu'à l'observation des dynamiques moléculaires. À l'aide de nombreuses techniques, nous avons évalué les conséquences à plusieurs échelles de neuf variants d'actine identifiés chez des patients atteints d'ANM que nous avons reproduits dans un gène codant pour l'actine chez *C. elegans*. Nous avons observé une diversité de perturbations variant-spécifiques, incluant des défauts du cytosquelette d'actine, des anomalies à l'échelle cellulaire et lors de la morphogenèse, ainsi que des défauts de la neurogenèse.

La gravité des variants Humains correspond bien à celle des variants reproduits chez *C. elegans*, et laisse entrevoir leurs mécanismes physiopathologiques. Nous concluons que *C. elegans* est un modèle prometteur pour l'étude des variations de l'actine associées aux l'ANM et de leur pronostic.

Mots clés : *Caenorhabditis elegans*, actine cytoplasmique, Actinopathie Non-Musculaire

Summary:

Actin is a protein that self-assembles into dynamic networks essential for physiological processes such as cell migration or division. Single point *de novo* mutations, as well as loss of function mutations in the human cytoplasmic actin coding genes ACTB and ACTG1 lead to ultra-rare disorders, termed Non-Muscle Actinopathies (NMA). NMAs cause a broad spectrum of symptoms ranging from mild to severe including facial malformations, intellectual disorders, and deafness.

To date, a definitive genotype-to-phenotype correlation within the NMA field has yet to emerge, and the functional mechanisms underlying symptoms in patients remain elusive. To fill this gap, we used *Caenorhabditis elegans*. This well-studied nematode allows one to easily access all biologically relevant scales, from general animal fitness to stereotypical organization and development, as well as cell-scale events or molecular dynamics. Using various techniques, we assessed the multiscale consequences of nine actin variants identified in NMA patients that we reproduced in a *C. elegans'* actin coding gene. We observed a diversity of variant-specific perturbations including actin cytoskeleton network defects, cell-scale abnormalities, morphogenesis failure, and neurogenesis defects.

Overall, the severity of Human variants correlates well with that of *C. elegans* variants and hints at their pathophysiological mechanisms. We conclude that *C. elegans* is a promising model for studying NMA-associated actin variations and could serve in the future patients' medical prognosis.

Keywords: *Caenorhabditis elegans*, cytoplasmic actin, Non-Muscle Actinopathy